TRANSPORTATION RESEARCH
RECORD

No. 1436

Materials and Construction

Asphalt Concrete Mix Materials

A peer-reviewed publication of the Transportation Research Board

TRANSPORTATION RESEARCH BOARD
NATIONAL RESEARCH COUNCIL

NATIONAL ACADEMY PRESS
WASHINGTON, D.C. 1994

Transportation Research Record 1436
ISSN 0361-1981
ISBN 0-309-05513-X
Price: $29.00

Subscriber Category
IIIB materials and construction

Printed in the United States of America

Sponsorship of Transportation Research Record 1436

GROUP 2—DESIGN AND CONSTRUCTION OF TRANSPORTATION FACILITIES
Chairman: Charles T. Edson, Greenman Pederson, Inc.

Bituminous Section
Chairman: Harold R. Paul, Louisiana Transportation Research Center

Committee on Characteristics of Bituminous Materials
Chairman: Leonard E. Wood, Purdue University
David A. Anderson, Chris A. Bell, S. W. Bishara, Joe W. Button, Brian H. Chollar, Eileen Connolly, John J. Emery, Claude P. Fevre, Norman W. Garrick, Eric E. Harm, Paul W. Jennings, Prithvi S. Kandhal, Gayle N. King, Dean A. Maurer, Thomas B. Nelson, Tinh Nguyen, Larry F. Ostermeyer, Charles F. Potts, Raymond E. Robertson, Bernard A. Vallerga, John S. Youtcheff, Ludo Zanzotto, Michael Zupanick

Committee on Characteristics of Nonbituminous Components of Bituminous Paving Mixtures
Chairman: N. Paul Khosla, North Carolina State University
Secretary: H. Barry Takallou, TAK Consulting Engineers
Rod Birdsall, Joe W. Button, Douglas M. Colwill, Ervin L. Dukatz, Jr., Frank Fee, John M. Heggen, Richard H. Howe, L. S. Ingram, Ilan Ishai, Prithvi S. Kandhal, Kang-Won Wayne Lee, Kamyar Mahboub, Roger P. Northwood, John W. H. Oliver, Roger C. Olson, Gale C. Page, J. Claine Petersen, Michael W. Rouse, Russell H. Schnormeier, Scott Shuler, Anne Stonex, Ronald L. Terrel, Jack L. Van Kirk

Transportation Research Board Staff
Robert E. Spicher, Director, Technical Activities
Frederick D. Hejl, Engineer of Materials and Construction
Nancy A. Ackerman, Director, Reports and Editorial Services
Norman Solomon, Editor

Sponsorship is indicated by a footnote at the end of each paper. The organizational units, officers, and members are as of December 31, 1993.

Transportation Research Record 1436

Contents

Foreword

The papers in this volume, dealing with various facets of the materials in asphalt concrete mixtures, should be of interest to state and local construction, design, materials, and research engineers as well as contractors and material producers.

The first four papers address the relationship between asphalt physical and chemical properties and field performance. Stoffels et al. report on their empirical approach to validate the proposed Strategic Highway Research Program (SHRP) binder specification for thermal cracking. Their efforts, along with other work, resulted in an alteration of the binder specification. Bouldin et al. compare the performance of the West Coast Asphalt Cement PBA-7 desert specification with conventional AC-40. The binders and the mixes were characterized using SHRP's performance-related test techniques. The researchers found that the PBA-7 binder was much more susceptible to permanent deformation than a conventional AC-40. De La Roche et al. describe a research project conducted in France to study the fatigue behavior of asphalt mixes made with different asphalts using the circular test track of the Laboratoire Central des Ponts et Chaussées. Corté et al. describe their observations made in an investigation to determine what effect axle-loading configurations and binder type have on rutting of asphalt surface layers.

The next five papers discuss recent developments in asphalt binders. Peterson et al. report on work to determine the effect of metals, asphaltenes, and paraffins content on the properties of recycled aged asphalts. They report that highly aromatic recycling agents yielded material superior in the measured properties to the original asphalts. Burr et al. discuss the softening of asphalts in dilute solutions at primary distillation conditions. Lee and Hesp discuss the mechanisms by which the addition of polyethylene improves the low-temperature properties of asphalt binders. Chiu et al. describe a laboratory investigation to evaluate a variety of aging processes used for simulating the long-term aging of asphalt binders. Little et al. report on a study to identify the important chemical aspects of an asphalt molecule that are related to the deformation properties of asphalt.

The following three papers report on experiences with crumb rubber in asphalt mixes. Hui et al. discuss a Canadian investigation to determine the effectiveness of crumb rubber tire and devulcanized rubber tire in improving low-temperature asphalt binder performance. Fager presents preliminary conclusions on the use of rubber in asphalt pavements in Kansas. Hanson et al. discuss the evaluation of a rubber-modified hot mix asphalt pavement constructed in Mississippi 2 years ago.

The last three papers discuss liquid antistrip additives, natural sands, and olive husks in asphalt mixes. Won and Ho describe a study to investigate the effect of liquid antistrip additives on the properties of polymer-modified asphalt binders and mixtures as related to rutting and moisture damage. They concluded that lower dosages of liquid antistrip additives should be used for polymer-modified asphalts than would be required for straight asphalts. Stuart and Mogawer report on an investigation to determine whether good-performing natural sands could be distinguished from poor-performing natural sands. Performance was based on the effects of the sands on asphalt pavement rutting. Al-Masaeid et al. summarize the results of a study undertaken in Jordan to evaluate the effects of olive husk material on the properties of both asphalt cement binder and asphalt concrete mixtures.

Evaluation and Field Validation of Proposed Strategic Highway Research Program Binder Specification for Thermal Cracking

SHELLEY M. STOFFELS, REYNALDO ROQUE, AND TARIQ FARWANA

An empirical approach is used to validate the proposed Strategic Highway Research Program (SHRP) binder specification for thermal cracking. Binders extracted from the SHRP A-005 General Pavement Study sections are used to validate the proposed binder specification. The specification parameters at the required test temperatures were generated from the aged binders' master stiffness curves. Although the proposed specification parameters [creep stiffness (S) and slope of the binder stiffness curve (m) at 60-sec loading time] appear to be reasonable, the temperature ranges defined in Version 7G of the specifications are clearly too broad and result in a specification that is too restrictive. The defined limits on S and m are also too restrictive. Alternative limits are suggested for a specification with narrower temperature ranges. The binder specification was subsequently altered as a result of this and other work. The revised specification is also evaluated. The new specification structure and limits appear to be more effective.

The binder specification parameters that have been forwarded as those controlling thermal cracking potential are the creep stiffness (S) and the slope of the binder stiffness curve (m) at 60-sec loading time. The temperature at which the two parameters are obtained, referred to as test temperature, is selected on the basis of the lowest pavement service temperature. The binder specification structure is shown in Figure 1. The validation and evaluation of the binder specification is described in the following sections and is based on Strategic Highway Research Program (SHRP) Binder Specification Draft 7G, as developed under SHRP Contract A-002. The specification is designed for test properties for pressure aging vessel-aged materials.

APPROACH

Binders extracted from the SHRP A-005 General Pavement Study (GPS) sections were used to validate the proposed binder specification. These sections were selected to represent a range of thermal cracking performance (*1*). The sections used are given in Table 1. Both the SHRP code and the code used as a random blind at the Pennsylvania Transportation Institute (PTI) are indicated. The PTI code is used as the section reference throughout this paper. An empirical approach was used to validate the proposed binder specifications. Existing performance models require mixture properties that cannot be determined directly from the binder with existing relationships. First, the specification was applied as forwarded to binder properties obtained from aged field specimens and related to field performance of those sections. Second, the reasons for any discrepancies were examined. The suitability of the specimen parameters was evaluated. Finally, recommendations for changing the specification ranges and limits were formulated to reduce discrepancies between the specification and observed performance.

In this analysis, direct measurements of the specification parameters at the appropriate test temperatures were not available. Therefore, the parameters for the test temperatures were generated from the binders' master stiffness curves and shift functions, using the time-temperature superposition principle.

PERFORMANCE DATA

A consistent measure of low-temperature cracking performance was needed for each section for the validation. Because of a number of changes and differences in interpretation of the Long-Term Pavement Performance data collection method, the visual surveys could not be directly compared. Reported cracking comparisons between sections and between years on a single section were not consistent. Therefore, the pavement condition data collected by the PASCO video imaging device were used; the data were obtained directly from PCS Law, Inc., where the data were reduced and interpreted.

To correlate field cracking measurements with predicted cracking, a number of assumptions were necessary. All visible cracks were assumed to extend the full depth of the pavement surface; there was no way to differentiate on the basis of the available data. All sections were original pavements; it was assumed that there was no reflective cracking. Cracks were differentiated on the basis of severity in the data, but this information was not directly used in the analysis. The mechanism by which cracks progress from low to high severity also involves mechanisms other than low-temperature contraction. Deteriorative factors include moisture and drainage characteristics, asphalt and mixture properties, and traffic.

Cracking was considered at only one point in time; no cracking versus time data were available because of the changes in data collected and delays in reduction and availability of the PASCO data. The PASCO data were assumed to have picked up all low-temperature cracking and not to have imaged any cracks that were not present. These assumptions regarding the reliability of the

The Pennsylvania State University, The Pennsylvania Transportation Institute, 201 Research Office Building, University Park, Pa. 16802.

Performance Grade	PG 1-		PG 2-					PG 3-					PG 4-	
	4	5	1	2	3	4	5	1	2	3	4	5	1	2
Average 7-day Maximum Pavement Temperature, °C*	<45		<55					<65					<75	
Minimum Pavement Service Temperature, °C*	>-30	>-40	>0	>-10	>-20	>-30	>-40	>0	>-10	>-20	>-30	>-40	>0	>-10
Original Binder														
Flash Point Temp, ASTM D 92: Minimum, °C	230													
Viscosity, ASTM D 4402 (Brookfield):[b] Max, 2 Pa • s (2000 cSt) Test Temp, °C	165													
Dynamic Shear, SHRP B-003: G*/sin δ, Min, 1.0 kPa (0.145 psi) Test Temp @ 10 rad/s, °C	45		55					65					75	
Rolling Thin Film Oven Test (AASHTO T 240; ASTM D 2872) Residue[c]														
Max Loss, Max, percent	1.00													
Dynamic Shear, SHRP B-003: G*/sin δ, Min, 2.0 kPa (0.290 psi) Test Temp @ 10 rad/s, °C	45		55					65					75	
Pressure Aging Vessel Residue (SHRP B-005)*														
PAV Aging Temperature, °C	90		100					100					110	
Dynamic Shear, SHRP B-003: G* sin δ, Max, 3000 kPa (435 psi) Test Temp @ 10 rad/s, °C	10	5	30	25	20	15	10	35	30	25	20	15	40	35
Creep Stiffness, SHRP B-002:[d] S, Max, 2 x 10^5 kpa, (29000 psi) m-value, Min, 0.35 Test Temp @ 60s, °C	-20	-30	10	0	-10	-20	-30	10	0	-10	-20	-30	10	0
Direct Tension, SHRP B-006: Failure Strain, Min, 1.0% Test Temp @ 1.0 mm/min, °C	-20	-30	10	0	-10	-20	-30	10	0	-10	-20	-30	10	0

Notes: * Pavement temperatures determined from air temperatures using algorithm contained in SUPERPAVE program.

[b] AASHTO T 2020, (ASTM D 2171) may be used in lieu of (ASTM D 4402), however, ASTM D 4402 is considered reference method. A second viscosity measurement (145 °C) may be required for reporting purposes to develop viscosity-temperature relationship for estimating mixing and compaction temperatures.

[c] TFOT AASHTO T 179 (ASTM D 1754) may be used in lieu of AASHTO T 240, (ASTM D 2872) is considered reference method.

[d] S is stiffness after 60 seconds loading time and m is the slope of the log stiffness versus log time curve at 60 seconds loading time.

Comments: 1. Tenderness is related to the values of G*/sin δ before and after RTFOT.
2. Rutting is related to the value of G*/sin δ after RTFOT.
3. Fatigue is related to the value of G* sin δ and direct tension strain-to-failure after PAV.
4. Low-temperature thermal cracking is related to S, m, and direct tension strain-to-failure after PAV.
5. Rheological type is controlled by m.

FIGURE 1 SHRP Binder Specification Draft 7G.

PASCO data were discussed with PCS Law personnel who reduced the data and are consistent with the digitizing criteria.

The PASCO data were received in a digitized format, including a summary of pavement distresses for each section. Observation of the crack maps indicated that the amount of cracking was misrepresented by looking only at the number of feet of cracking. The cracking pattern and likelihood that the cracks were caused by low-temperature stresses are also important. All of the transverse and longitudinal cracking is not due to low-temperature cracking; for example, low-severity longitudinal cracking in the wheelpath is probably early-stage fatigue cracking. Other small "stray" cracks were also not considered to be due to low-temperature distress.

A rational attempt was made to estimate the amount of cracking caused by thermal stresses using the available data. The following observations and assumptions were made:

- It appeared more rational to estimate the amount of thermal cracking by multiplying the number of complete or near complete transverse cracks by the width of the lane [generally 3.65 m (12 ft)] than by using the linear sum of all cracking recorded in the PASCO data.
- It was also observed that the pavement sections could be grouped into one of four categories of thermal cracking (zero, low, medium, or high), within which it was difficult to distinguish between the thermal cracking performance of the sections. On the basis of the range in amount of cracking observed within each category, the following system was established to categorize the pavement section with respect to thermal cracking performance: zero cracking, 0 to 7.6 m (25 ft) of cracking per 152-m (500-ft) section [less than one crack per 76 m (250 ft)]; low cracking, 7.6 to 22.9 m (25 to 75 ft) of cracking per 152-m (500-ft) section [from one crack per 76 m (250 ft) to one crack per 25.9 m (85

ft)]; medium cracking, 22.9 to 45.7 m (75 to 150 ft) of cracking per 152-m (500-ft) section [from one crack per 25.9 m (85 ft) to one crack per 12.2 m (40 ft)]; and high cracking, greater than 45.7 m (150 ft) of cracking per 152-m (500-ft) section [more than one crack per 12.2 m (40 ft)].

SERVICE TEMPERATURES

Weather data were obtained from the National Climatic Data Center (NCDC) and from the SHRP A-001 contractor. The greatest emphasis was placed on obtaining reliable daily temperatures for each section. The temperatures were obtained for the closest available weather station with relatively complete data for the years since the pavement was placed. For cases in which several weather stations were approximately equidistant and the temperature information for those stations was different, additional evaluation was completed to select the most appropriate weather station. Topographic maps were consulted and the pavement section and weather stations located. Elevations for the sites were compared, and any intervening topographic features were noted. The most appropriate station was then identified, as given in Table 1.

The minimum pavement surface temperatures of these sections are between −11°C and −31°C, which represents a broad range of service temperatures. The minimum pavement service temperatures were determined using actual air temperatures from NCDC weather stations near the pavement sections for analysis with the FHWA Integrated Environmental Effects Model. The FHWA model was developed for FHWA's Office of Engineering and Highway Operations Research and Development by the Texas Transportation Institute, Texas A&M University (*2*). The use of this model for determining minimum pavement service temperatures for low-temperature cracking predictions has been demonstrated (*3*).

TABLE 1 GPS Sections and Weather Stations Used

State	PTI Code	SHRP Code	Weather Station	Station ID
AZ	2	41022	Hackberry	9158
CO	18	81047	Rangely	6832
ID	12	161001	Coeur D Alene	1956
ID	11	161010	Idaho Falls	4457
IN	32	181028	Huntingburg	7724
IN	36	181037	Bonneville	2731
KS	7	201005	Ottawa	6128
KY	21	211034	Glasgow	3246
ME	33	231026	Farmington	2765
MD	23	241634	Berlin	335
MN	38	271028	Frazee	2142
MN	37	271087	Farmington	5435
MO	28	291010	Waynesville	8777
NB	13	311030	Edison	640
NV	6	322027	Oasis	2573
NJ	27	341011	Trenton	3951
OK	1	404086	Chickasha	1750
OK	22	404088	Ponca City	7201
PA	31	421597	Lawrenceville	5408
SC	26	451008	Salem	8887
TX	3	481183	Southland	7206
UT	16	491008	Marysvale	3514
WY	17	561007	Cody	1840

SELECTION AND EXTRACTION OF BINDER SPECIMEN

The asphalt cement from each of the 23 GPS sites used in this study was extracted from the tested cores and analyzed to determine its linear viscoelastic properties. The extraction procedure used in this project was developed by the SHRP binder study group. To properly characterize each of the field sections used in this study, it was necessary to slice each of the field cores according to their individual cross-sectional characteristics. Figure 2 shows the basic approach used to obtain representative materials for testing from the field cores. In many cases, more than one mixture was present in the cross section. The approach taken was to test the binder from the mixture that predominantly controls the thermal cracking performance of a particular cross section. Obviously, detailed testing at multiple levels of all materials present in the cross section would have been desirable. However, constraints in terms of both time and resources did not allow for such a comprehensive testing program. Three cases were identified and slices were obtained for extractions as indicated in Figure 2.

DEVELOPMENT OF BINDER MASTER CURVES

The extracted material was characterized according to its linear viscoelastic parameters as recommended by SHRP A-002. Two test devices were used to obtain the data required to characterize the different asphalt cements obtained from the tested cores. The first was a bending beam rheometer test (*4*). This test provided the flexural creep stiffness, S, and the log-log slope of the creep curve, m, at −15°C and 120 sec. The second device was a dynamic shear rheometer. From this test, the complex modulus, G^*, at 15°C, 25°C, 45°C, and 60°C was determined for frequencies, f, of 15, 8, 5, 3, 1.5, 0.8, 0.5, 0.3, and 0.15 Hz.

The test results from both testing devices and each of the five temperatures were combined into a master stiffness curve that characterizes the viscoelastic properties of the material using the procedure recommended by Christensen and Anderson (*5,6*). The first step consisted of transforming the magnitude of the complex modulus, G^*, into creep stiffness, S. An exact transformation between these two material responses would require complicated numerical transformation. For practical purposes, it was decided to use a simple and very common approach of assuming that both variables are related at any given frequency by Poisson's ratio, μ, as follows:

$$E = 2(1 + \mu)G^* \quad (1)$$

If it is assumed that the asphalt cement is incompressible and thus has a Poisson's ratio of 0.50, the following conversion is obtained:

$$E = 3G^* \quad (2)$$

This conversion, although not exact, is considered a very reasonable approximation by most researchers. It is reported to be sufficiently accurate for engineering calculations with a maximum error of less than 15 percent (*5*).

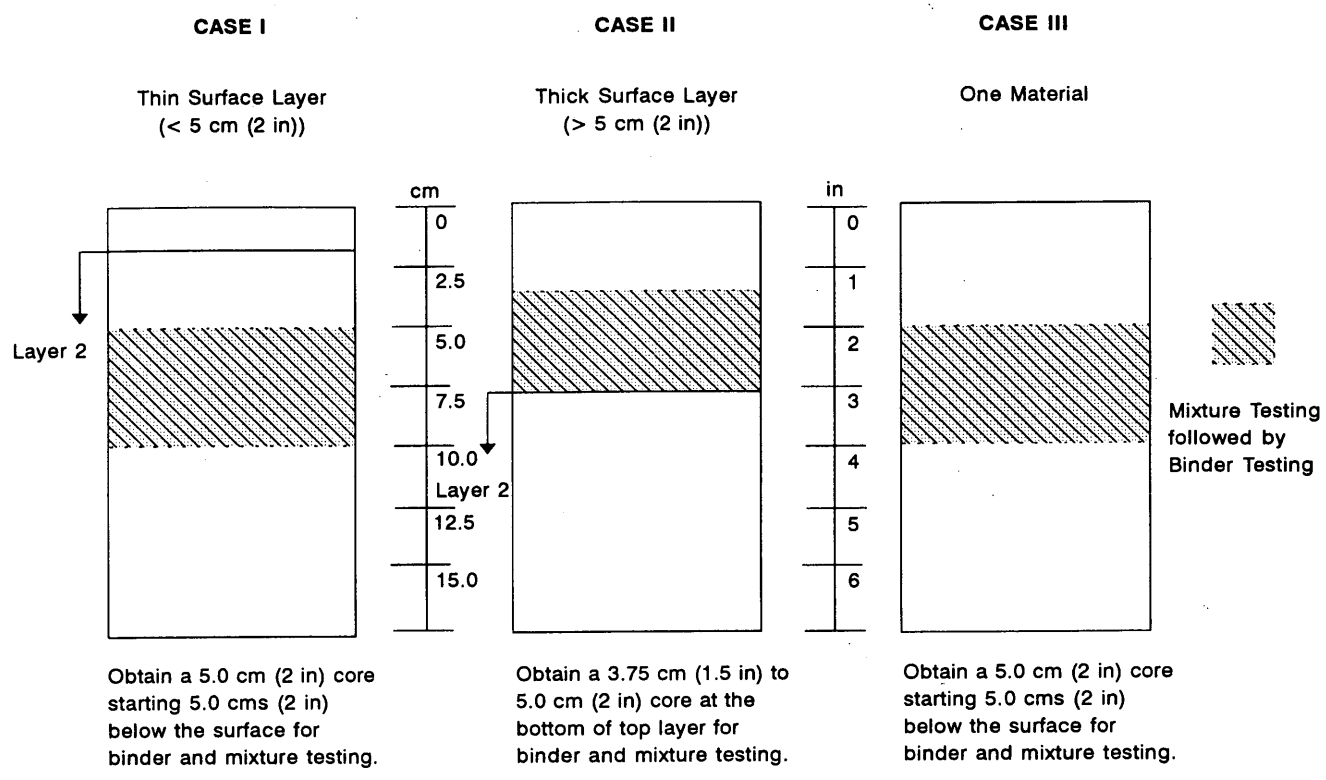

FIGURE 2 Selection of binder specimen.

The test frequencies were converted to loading time using the following formula:

$$t = 1/(2\pi f) \tag{3}$$

Once all the conversions were made, a nonlinear regression routine was performed to fit the data into the following equation proposed by Christensen (*6*):

$$S_{(t,T)} = S_g\left[1 + \left(\frac{t_r}{t_0}\right)^{\frac{\log 2}{R}}\right]^{-\frac{R}{\log 2}} \tag{4}$$

where

$S_{(t,T)}$ = stiffness at loading time t and reference temperature T;
S_g = glassy stiffness, assumed to be 3 GPa for all asphalt cements;
t_r = reduced time (sec);
t_0 = crossover time (sec) (this value is very close to the point at which the viscous asymptote crosses the glassy stiffness and is considered a hardness parameter); and
R = rheological index, defined as the difference between the glassy stiffness and the stiffness at the crossover time.

The reduced time, t_r, and the loading time, t, are related by the time temperature superposition shift factors, a_T, as follows:

$$t_r = t^* (a_T/a_{T\text{ref}}) \tag{5}$$

where $a_T/a_{T\text{ref}}$ is the shift of the time t at temperature T to the reference temperature T_{ref}. The shift factors were represented using two equations. The first of these equations, the Williams-Landel-Ferry (WLF) equation, is used above the defining temperature T_d:

$$\log \frac{a_T}{a_{T\text{ref}}} = \frac{-C_1(T - T_{\text{ref}})}{C_2 + T - T_{\text{ref}}} \tag{6}$$

where C_1 and C_2 are empirically determined constants that were fixed as 19 and 92, respectively. In the regression, to ease numerical computations, the reference temperature T_{ref} was assumed to be the defining temperature T_d.

The second equation is an Arhennius function, which is used to describe the shift factors as a function of temperature below the defining temperature T_d:

$$\log \frac{a_T}{a_{T\text{ref}}} = \frac{H_a}{2.303R}\left(\frac{1}{T} - \frac{1}{T_{\text{ref}}}\right) \tag{7}$$

where H_a is the activation energy for flow below T_d, fixed as 250 KJ/mol, and R is the ideal gas constant, 8.34 J/mol-°K.

A detailed explanation of these models and the meaning of each of the parameters used is given by Christensen (*6*).

The regressed coefficients for the binders extracted from each of the 23 GPS sections are presented in Table 2. The resulting master stiffness curves were plotted; an example is shown as Figure 3. The binder specification parameters were obtained from these master stiffness curves.

TABLE 2 Regressed Coefficients for Extracted Binders

PTI Code	Model Fitting Results at T_d			
	S_g (Pa)	Log t_0 (sec)	R	T_d (°C)
1	3.00 x 10^9	2.52	1.36	-14.55
2	3.00 x 10^9	2.03	0.89	-13.90
6	3.00 x 10^9	2.12	1.42	-15.00
7	3.00 x 10^9	5.27	2.98	-12.90
11	3.00 x 10^9	2.93	1.54	-15.00
12	3.00 x 10^9	3.06	1.82	-12.85
13	3.00 x 10^9	2.90	2.49	-13.23
16	3.00 x 10^9	2.19	1.33	-13.12
17	3.00 x 10^9	2.20	1.41	-15.02
18	3.00 x 10^9	2.36	1.23	-14.97
21	3.00 x 10^9	2.26	1.77	-12.15
22	3.00 x 10^9	3.23	2.26	-12.68
23	3.00 x 10^9	3.31	1.90	-14.04
26	3.00 x 10^9	4.56	1.94	-14.90
27	3.00 x 10^9	2.38	1.62	-14.38
28	3.00 x 10^9	2.16	1.05	-13.47
31	3.00 x 10^9	3.19	1.71	-12.85
32	3.00 x 10^9	2.52	1.74	-13.46
33	3.00 x 10^9	2.07	1.74	-14.33
36	3.00 x 10^9	2.42	1.39	-14.71
37	3.00 x 10^9	2.57	1.67	-14.38
38	3.00 x 10^9	3.70	1.73	-14.61

VALIDATION OF BINDER SPECIFICATION VERSION 7G

An empirical approach was used to validate the proposed binder specifications. The parameters S and m at 60-sec loading time and the appropriate test temperatures were obtained for the 22 GPS sections used in this project. Those properties were compared with the specification limits proposed for thermal cracking. The failed and passed sections, as determined by the specifications, were then compared with the actual cracking observed in the field. Table 3 gives the comparisons between observed cracking and the potential for cracking as predicted by the binder specifications.

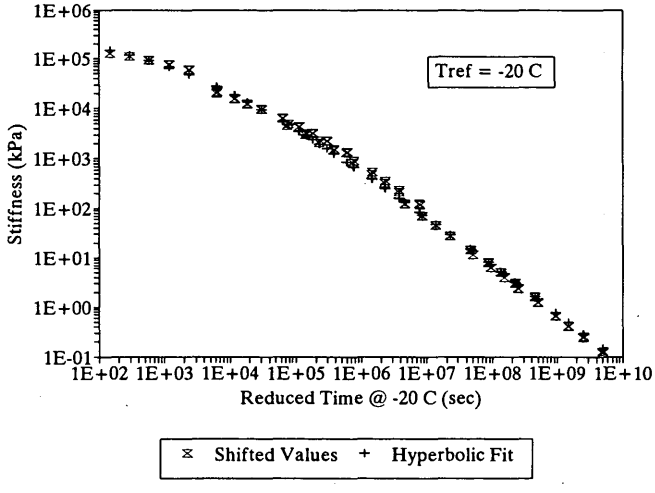

FIGURE 3 Example binder master stiffness curve.

Table 3 indicates that only four of the 22 binders passed the specification requirements. Further examination indicates that the actual cracking observations in the field do not agree with the specification findings. Some binders used in sections with medium observed cracking passed the specification requirements. Conversely, sections with zero and low observed cracking had binder properties that failed the specification. In fact, 7 of the 18 binders that failed the specifications were in sections where either zero or low cracking was observed in the field. All sections with observed high cracking failed the specification. These observations warranted further evaluation and investigation of the proposed specification.

EVALUATION OF THE SPECIFICATION FORMAT

Additional work was performed to investigate the specification limits and temperature ranges proposed in the specifications. The sections were categorized into four groups on the basis of S and m values as determined by the specifications to check for a relationship between failure in either of the specification parameters and cracking potential. The four categories were established on the basis of magnitudes of S and m at the test temperature relative to the specification limits for S and m. The specification limits have been established as a maximum of 2×10^5 kPA (29,000 psi) for S and a minimum of 0.35 for m. The following four categories are indicated in Table 4:

- Sections with binders that have S less than 2×10^5 kPA and m more than 0.35,
- Sections with binders that have S more than 2×10^5 kPA and m more than 0.35 (no sections),
- Sections with binders that have S less than 2×10^5 kPA and m less than 0.35, and
- Sections with binders that have S more than 2×10^5 kPA and m less than 0.35.

Table 4 indicates that almost all the sections rejected by the specification did not meet the specification limits for both S and m. On the other hand, none of the sections was rejected on the basis of the S requirement alone. Table 4 also indicates that two sections did not pass the specification requirement for m only.

All the binders used in the remaining GPS sections not passing the specifications failed to meet both the S and the m limits; neither parameter is solely responsible for rejecting these binders. The data reported in Table 4 indicate that there is no clear correlation between adherence to either of the specification limits and the observed cracking in the field.

A key observation was made with respect to the test temperatures at which these parameters were obtained; it can be clearly seen that binders with test temperatures of -10°C passed the specifications. Section 26 is the only exception to this statement; however, this section is very close to passing the limits. On the other hand, all sections with parameters obtained at test temperatures of -20°C or -30°C failed to meet the specification limits. The outcome of the specification, in its current format, is primarily driven by the test temperature. It appears that the current specification structure is not as sensitive to differences between different binder properties as it is to differences between test temperatures.

TABLE 3 Evaluation of Binders Extracted from GPS Sections with SHRP Binder Specifications, Draft 7G

Specification Result	PTI Code	Minimum Pavement Temperature (°C)	Test (Evaluation) Temperature (°C)	Stiffness @ 60 sec (kPa)	m @ 60 sec	Observed Thermal Cracking (Field)		
						Level of Cracking	(m/152 m)	(ft/500 ft)
PASS	1	-19	-10	109351	0.48	Medium	29	96
	2	-19	-10	199738	0.55	Zero	0	0
	22	-19	-10	43873	0.41	Medium	29	96
	23	-14	-10	82986	0.41	Zero	0	0
FAIL	6	-27	-20	41556	0.31	High	>61	>200
	7	-24	-20	191637	0.23	High	>61	>200
	11	-34	-30	1488327	0.12	High	>61	>200
	12	-21	-20	470746	0.24	Zero	>61	>200
	13	-28	-20	102530	0.32	Low	11	36
	16	-27	-20	684663	0.26	High	>61	>200
	17	-32	-30	1401117	0.13	High	>61	>200
	18	-27	-20	737556	0.26	High	>61	>200
	21	-20	-20	334899	0.29	Zero	0	0
	26	-14	-10	200479	0.32	Medium	29	96
	27	-20	-20	364195	0.30	Low	11	36
	28	-25	-20	1106451	0.22	Medium	37	120
	31	-24	-20	624240	0.22	Low	7	24
	32	-23	-20	358349	0.29	Low	4	12
	33	-28	-20	222508	0.34	Low	4	12
	36	-21	-20	575941	0.27	High	>61	>200
	37	-29	-20	377666	0.29	High	40	132
	38	-34	-30	1492515	0.10	High	>61	>200

TABLE 4 Consideration of Limiting Binder Specification Criteria

Category	PTI Code	Minimum Pavement Temperature (°C)	Test (Evaluation) Temperature (°C)	Stiffness @ 60 sec (kPA)	m @ 60 sec	Observed Thermal Cracking (Field)	Age (years)	Thickness (cm)
Low S	1	-19	-10	109354	0.48	Medium	19	41.9
High m	2	-19	-10	199738	0.55	Zero	13	41.9
	22	-19	-10	43873	0.41	Medium	20	31.8
	23	-14	-10	82986	0.41	Zero	14	8.9
Low S	7	-24	-20	191637	0.23	High	17	33.0
Low m	13	-28	-20	102530	0.32	Low	8	19.1
High S	6	-27	-20	415566	0.31	High	13	23.5
Low m	11	-34	-30	1488327	0.12	High	19	27.3
	12	-21	-20	470746	0.24	Zero	15	8.9
	16	-27	-20	684663	0.26	High	16	23.5
	17	-32	-30	1401117	0.13	High	9	8.9
	18	-27	-20	737556	0.26	High	7	10.2
	21	-20	-20	334899	0.29	Zero	18	36.2
	26	-14	-10	200479	0.32	Medium	20	12.1
	27	-20	-20	364609	0.30	Low	20	23.5
	28	-25	-20	1106451	0.22	Medium	10	33.0
	31	-24	-20	624240	0.22	Low	10	15.9
	32	-23	-20	358349	0.29	Low	15	38.1
	33	-28	-20	222508	0.34	Low	17	15.9
	36	-21	-20	575941	0.27	High	15	35.6
	37	-29	-20	377666	0.29	High	11	40.6
	38	-34	-30	1492515	0.10	High	18	24.1

TABLE 5 Evaluation of Binders Extracted from GPS Sections with SHRP Binder Specification Draft 7G, with Temperature Intervals Reduced to 1°C

Category	PTI Code	Minimum Pavement Temperature (°C)	Test (Evaluation) Temperature (°C)	Stiffness @ 60 sec (kPA)	m @ 60 sec	Observed Thermal Cracking (Field)	Age (years)	Thickness (cm)
Low S	1	-19	-9	95246	0.50	Medium	19	41.9
High m	2	-19	-9	141695	0.59	Zero	13	41.9
	12	-21	-11	110725	0.40	Zero	15	8.9
	21	-20	-10	53155	0.47	Zero	18	36.2
	22	-19	-9	38134	0.42	Medium	20	31.8
	23	-14	-4	23090	0.51	Zero	14	8.9
	26	-14	-4	81505	0.40	Medium	20	12.1
	27	-20	-10	51475	0.50	Low	20	23.5
	32	-23	-13	107162	0.41	Low	15	38.1
	33	-28	-18	156212	0.37	Low	17	15.9
	36	-21	-11	97743	0.49	High	15	35.6
High m								
High S	6	-27	-17	262416	0.37	High	13	23.5
Low S	7	-24	-14	96446	0.28	High	17	33.0
Low m	13	-28	-18	77739	0.34	Low	8	19.1
High S	11	-34	-24	885773	0.19	High	19	27.3
Low m	16	-27	-17	425262	0.33	High	16	23.5
	17	-32	-22	636645	0.26	High	9	8.9
	18	-27	-17	490611	0.32	High	7	10.2
	28	-25	-15	551378	0.34	Medium	10	33.0
	31	-24	-14	287370	0.31	Low	10	15.9
	37	-29	-19	317016	0.31	High	11	40.6
	38	-34	-24	935777	0.17	High	18	24.1

TABLE 6 Sensitivity of Binder Specification Criteria to Evaluation Temperature

	Test Temperature							
	@ -10 °C (From MSC & a_T)		@ -15 °C (Measured)		@ -20 °C (From MSC & a_T)			
PTI Code	Stiffness @ 60 sec (kPa)	m @ 60 sec	Stiffness @ 60 sec (kPa)	m @ 60 sec	Stiffness @ 60 sec (kPa)	m @ 60 sec	Minimum Pavement Temperature (°C)	Observed Thermal Cracking
1	109351	0.48	304579	0.36	667978	0.26	-16	Medium
2	199741	0.55	643705	0.47	1319084	0.21	-11	Zero
6	51718	0.54	146379	0.41	415568	0.31	-20	High
7	51387	0.32	129073	0.32	191640	0.23	-21	High
11	105117	0.45	227179	0.30	576691	0.25	-30	High
12	97409	0.41	N/A	N/A	470746	0.24	-18	Zero
13	16513	0.45	61443	0.41	102532	0.32	-22	Low
16	109275	0.49	160865	0.38	684663	0.26	-21	High
17	58502	0.53	157469	0.45	450359	0.30	-25	High
18	109730	0.52	250004	0.34	737553	0.26	-22	High
21	53827	0.47	123327	0.44	334899	0.29	-18	Zero
22	43871	0.41	80252	0.40	225852	0.27	-17	Medium
23	82985	0.41	228834	0.40	408521	0.25	-11	Zero
26	200479	0.32	362413	0.23	685180	0.19	-12	Medium
27	52800	0.50	168618	0.40	364609	0.30	-15	Low
28	184028	0.51	558806	0.32	1106450	0.22	-21	Medium
31	141880	0.39	233881	0.36	624238	0.22	-20	Low
32	58019	0.47	98912	0.37	358348	0.29	-21	Low
33	27558	0.53	103790	0.49	222508	0.34	-23	Low
36	87170	0.50	238965	0.33	575940	0.27	-18	High
37	59026	0.48	173338	0.37	377667	0.29	-23	High
38	159752	0.37	340074	0.26	660207	0.21	-31	High

The temperature ranges used in the specification were examined to determine whether the sensitivity to differences in binder properties can be improved. The S and m parameters were obtained at the lowest pavement temperature plus 10°C. This represents temperature ranges of 1°C. This approach resulted in acceptance of most of the binders used in sections with observed low cracking as indicated in Table 5. Seven of the 11 field test sections composed of binders with $S < 2 \times 10^5$ kPA (29,000 psi) and $m > 0.35$ were zero or low cracking sections in the field. Three were medium cracking and one was high cracking. Nine of the 11 field test sections exceeding the specification limits [$S > 2 \times 10^5$ kPA (29,000 psi) or $m < 0.35$] were either medium or high cracking sections in the field. Two were low cracking sections. Considering mixture effects, which may result in variance in performance for a single binder, this indicates that S and m are reasonable parameters.

Table 6 provides additional evidence on the effects of test temperature. Binders from each section were evaluated at −10°C, −15°C, and −20°C. Almost all binders passed at −10°C, and all binders failed at −20°C. Large changes in S and m were observed with a 5°C change in test temperature. Furthermore, Binder Specification 7G indicates that no asphalt can be used in service temperatures below −20°C, whereas available performance data indicate that many of the binders were adequate.

CONCLUSIONS

The empirical correlations performed in this study indicate that the binder specification limits and temperature ranges are inadequate. The primary conclusions regarding Binder Specification 7G are as follows:

- S and m appear to be reasonable binder parameters for controlling thermal cracking.
- It appears that the specification is too restrictive.
- The defined limits on S and m [$S < 2 \times 10^5$ kPA (29,000 psi) and $m > 0.35$] are too restrictive.
- It appears that the temperature ranges (−10°C) used to define different asphalt grades are too broad.
- Thermal cracking performance of a particular binder is mixture dependent and cannot be controlled from binder properties alone.

RECOMMENDATIONS

The philosophy of the binder specification needs to be clearly established. Low-temperature properties can be mixture dependent. Mixture properties such as aggregate type, VMA, compaction, and coefficient of thermal contraction have strong effects on thermal performance. Two mixtures with the same binder may have very different low-temperature properties and resulting thermal cracking performance. The best one can hope for from a binder specification is to reject only those binders that have no chance of performing well regardless of what mixture they are used with. Conversely, the specification should accept binders that have a reasonable chance of performing well with a suitable mixture design. It is, however, very difficult to evaluate the binder specifications given the confounding of the mixture effects.

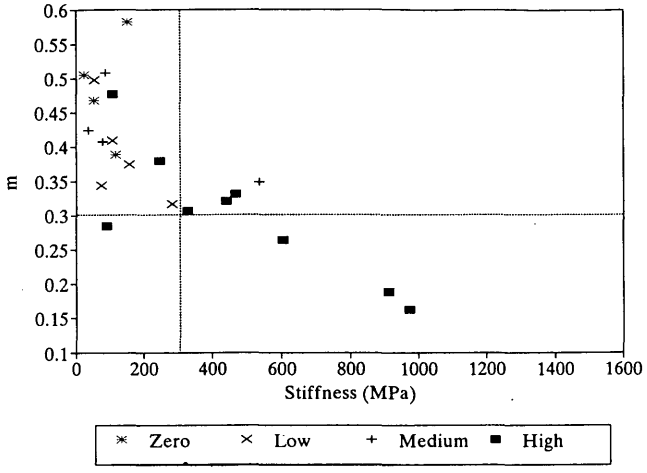

FIGURE 4 Proposed binder specification limits compared with thermal cracking performance of GPS sections for temperature ranges of 1°C.

Although S and m appear to be reasonable, the temperature ranges (−10°C) defined in Version 7G of the binder specifications are clearly too broad and result in a specification that appears to be far too restrictive. These limits should be reduced to as narrow a range as practical, but should probably be no greater than 5°C.

The defined limits on S and m [$S < 2 \times 10^5$ kPA (29,000 psi) and $m > 0.35$] are too restrictive. On the basis of the data obtained in this investigation and as shown in Figure 4, the following limits are recommended: $S < 3.2 \times 10^5$ kPA (45,000 psi) and $m > 0.30$, for temperature ranges of 1°C. Broader temperature ranges may require even less restrictive specification limits. These proposed new limits are consistent with the binder philosophy recommended above.

Further investigations beyond the scope of this project are recommended to verify that S and m are appropriate specification parameters. Such investigations should use mechanistic prediction models to isolate their effects from the effects of other factors such as mix design and pavement geometry. Then the specification structure and corresponding limits could be examined by using performance prediction models.

REVISED SPECIFICATION

As a result of examination of the proposed specification, including the work described in this paper, the binder specification was revised. The temperature ranges for grades were reduced to 6°C; the limits were changed to a maximum stiffness of 300 MPa and a minimum m of 0.30. The revised specification is shown in Figure 5.

Stiffnesses and m values were generated for each of the binders at the temperatures required by the revised specification. Ten binders passed the specification requirements; 12 did not. As shown in Figure 6, two binders from high-cracking sections passed the specification; one binder from a zero-cracking section and three from low-cracking sections failed. The revised specification represents a significant improvement. Although narrower temperature ranges might produce better results, the difficulty of accurately

PERFORMANCE GRADE	PG 52-							PG 58-					PG 64-					PG 70-			
	10	16	22	28	34	40	46	16	22	28	34	40	16	22	28	34	40	10	16	22	28
Average 7-day Maximum Pavement Design Temperature, °C[a]	<52							<58					<64					<70			
Minimum Pavement Design Temperature, °C[a]	>-10	>-16	>-22	>-28	>-34	>-40	>-46	>-16	>-22	>-28	>-34	>-40	>-16	>-22	>-28	>-34	>-40	>-10	>-16	>-22	>-28
ORIGINAL BINDER																					
Flash Point Temp, T48: Minimum °C	230																				
Viscosity, ASTM D 4402:[b] Maximum, 3 Pa • s, Test Temp, °C	135																				
Dynamic Shear, TP5:[c] G*/sinδ, Minimum, 1.0 kPa Test Temp @ 10 rad/s, °C	52							58					64					70			
Physical Hardening Index[d], h	Report																				
ROLLING THIN FILM OVEN RESIDUE (T240)																					
Max Loss, Maximum, percent	1.00																				
Dynamic Shear, TP5: G*/sinδ, Minimum, 2.2 kPa Test Temp @ 10 rad/s, °C	52							58					64					70			
PRESSURE AGING VESSEL RESIDUE (PP1)																					
PAV Aging Temperature, °C	90							100					100					100(110)[e]			
Dynamic Shear, TP5: G*sinδ, Maximum, 5000 kPa Test Temp @ 10 rad/s, °C	25	22	19	16	13	10	7	25	22	19	16	13	28	25	22	19	16	34	31	28	25
Creep Stiffness, TP1:[f] S, Maximum, 300 MPa, m-value, Minimum, 0.30 Test Temp @ 60s, °C	0	-6	-12	-18	-24	-30	-36	-6	-12	-18	-24	-30	-6	-12	-18	-24	-30	0	-6	-12	-18
Direct Tension, TP3:[f] Failure Strain, Minimum, 1.0% Test Temp @ 1.0 mm/min, °C	0	-6	-12	-18	-24	-30	-36	-6	-12	-18	-24	-30	-6	-12	-18	-24	-30	0	-6	-12	-18

[a] Pavement temperatures are estimated from air temperatures using an algorithm contained in the SUPERPAVE software program or may be provided by the specifying agency.

[b] This requirement may be waived at the discretion of the specifying agency if the supplier warrants that the asphalt binder can be adequately pumped and mixed at temperatures that meet all applicable safety standards.

[c] For quality control of unmodified asphalt cement production, measurement of the viscosity of the orignal asphalt cement may be substituted for dynamic shear measurements of G*/sinδ at test temperatures where the asphalt is a Newtonian fluid (generally above 55°C). Any suitable standard means of viscosity measurement may be used, including capillary or rotational viscometry.

[d] The physical hardening index h accounts for physical hardening and is calculated by $h=(\frac{S_{24}}{S_1})^{\frac{m_1}{m_{24}}}$ where 1 and 24 indicate 1 and 24 hours of conditioning of the tank asphalt. Conditioning and testing is conducted at the designated test temperature. Values should be calculated and reported. S is the creep stiffness after 60 seconds loading time and m is the slope of the log creep stiffness versus log time curve after 60 seconds loading time.

[e] The PAV aging temperature is 100°C, except in desert climates, where it is 110°C.

[f] If the creep stiffness is below 300 MPa, the direct tension test is not required. If the creep stiffness is between 300 and 600 MPa the direct tension failure strain requirement can be used in lieu of the creep stiffness requirement. The m-value requirement must be satisfied in both cases.

FIGURE 5 Revised SHRP binder specification, May 1993.

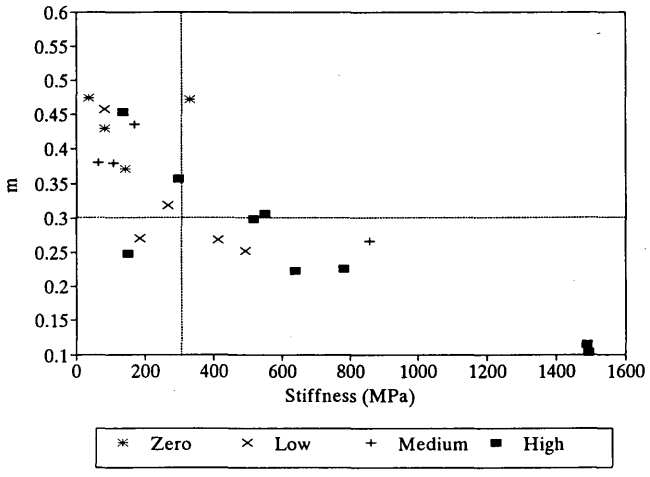

FIGURE 6 Evaluation of binder extracted from GPS sections with revised SHRP binder specification, May 1993.

predicting expected minimum service temperatures may make narrower ranges impractical.

ACKNOWLEDGMENTS

The work described in this paper was the result of the efforts of a team of faculty and student researchers at The Pennsylvania State University. The authors gratefully acknowledge the efforts of the following individuals who made the successful completion of this work possible: D. R. Hiltunen, S. A. Arnold, M. G. Sharma, William G. Buttlar, Namho Kim, Kevin Knechtel, Wendy Lauritzen, Srinivas Reddy, Pedro Romero, Nader Tabatabaee, and Vivek Tandon. A comprehensive description of the work performed by this team can be found in the final report by Lytton et al. (*1*). Financial support for this work was provided by SHRP. The authors gratefully acknowledge this support.

REFERENCES

1. Lytton, R. L., R. Roque, J. Uzan, D. R. Hiltunen, E. Fernando, and S. M. Stoffels. *Development and Validation of Performance Prediction Models and Specifications for Asphalt Binders and Paving Mixes.* SHRP-A-357. Strategic Highway Research Program, National Research Council, 1993.
2. Lytton, R. L., D. E. Pufahl, C. H. Michalak, H. S. Liang, and B. J. Dempsey. *An Integrated Model of the Climatic Effects on Pavements.* Report 033. Texas Transportation Institute, Texas A&M University, 1993.
3. Stoffels, S. M., W. R. Lauritzen, and R. Roque. Estimation of Asphalt Concrete Pavement Temperatures for the Prediction of Low-Temperature Cracking. In *Transportation Research Record 1417*, TRB, National Research Council, Washington, D.C., 1993, pp. 160–169.
4. Bahia, H. U., D. A. Anderson, and D. W. Christensen. The Bending Beam Rheometer; A Simple Device for Measuring Low-Temperature Rheology of Asphalt Binders. *Journal of the Association of Asphalt Paving Technologists*, Vol. 61, 1992, pp. 117–153.
5. Christensen, D. W., and D. A. Anderson. Interpretation of Dynamic Mechanical Test Data for Paving Grade Asphalt Cements. *Journal of the Association of Asphalt Paving Technologists*, Vol. 61, 1992, pp. 67–116.
6. Christensen, D. W. *Mechanical Modeling of the Linear Viscoelastic Behavior of Asphalt Cements.* Ph.D. dissertation. The Pennsylvania State University, University Park, 1992.

Publication of this paper sponsored by Committee on Characteristics of Bituminous Materials.

Designing Asphalt Pavements for Extreme Climates

MARK G. BOULDIN, GEORGE WAY, AND G. M. ROWE

Three test sections were placed in the Arizona low desert in 1992 to test the use of the West Coast Asphalt Cement PBA-7 desert specification. After a short hot spell the material exhibited significant rutting compared with the conventional AC-40. The binders and mixes were characterized using performance-related test techniques that were developed within the Strategic Highway Research Program (SHRP). The results indicated that the PBA-7 binder was much more susceptible to permanent deformation in marginal mixes than a conventional AC-40. However, both the rheological characterization of the binder and repetitive creep on the appropriate SHRP PG grade indicated superior performance over both traditional binders both at high and low temperatures and over the PBA-7 at high temperatures.

The extremely high temperatures of the southwestern United States present a unique challenge for hot mix asphalt (HMA) pavements and can lead to accelerated aging of the asphalt binder. Reese and Predoehl observed that the viscosity of the base asphalt may increase by a factor of 40 within 2 to 4 years (*1*). This aging causes the pavement to embrittle and consequently to fatigue crack (*2*). In some cases the effect can be so serious that the pavements may need to be resurfaced within 2 to 5 years because of severe alligator cracking. On the other hand the high pavement temperatures of up to 170°F coupled with high traffic loading may result in premature failure due to rutting. Consequently, the major issue under these climatic conditions is to balance durability versus rut resistance, as shown in Figure 1. Depending on the quality of the HMA and the structural design, a window of acceptable performance may not exist for conventional unmodified asphalts.

To overcome these problems, Caltrans developed an experimental polymer-modified asphalt (PMA) grade, which was placed on the Needles test section in the Mojave Desert. The performance of the test sections was monitored and compared with a straight AR4000 and a more conventional PMA. After 4 years the experimental grade showed essentially no fatigue cracking and a much lesser degree of aging than the control sections (*1*). Thus, this experimental system appeared to offer an opportunity to balance rut resistance and durability in a comprehensive manner (see "ideal asphalt" in Figure 1). On the basis of this experience the West Coast User Producer Conference (WCUP) adopted a desert specification that was descriptive of the material used in Needles test sections into their performance-based asphalt cement specification (PBA) as a PBA-7 (Table 1).

In this paper we will discuss the results of test sections that were placed in early 1992 on I-10 about 50 mi west of Phoenix, Arizona, near Tonopah. In this test section a PBA-7 was compared with a conventional AC-40 and another PMA. The field performance data will be compared with SHRP binder tests and performance-related mix testing, specifically high-temperature repetitive creep.

M. G. Bouldin, Applied Paving Technology, 1339 Allston, Houston, Tex. 77008. G. Way, Arizona Department of Transportation, 206 South 17th Avenue, Phoenix, Ariz. 85009. G. M. Rowe, SWK Pavement Engineering, Stonehouse Road, Millington, N.J. 07946.

CONSTRUCTION OF THE TONOPAH TEST SECTION

To test the pavement performance value of the PBA-7 grade of asphalt, an Interstate overlay project near Tonopah, Arizona, approximately 55 mi west of Phoenix, was selected and several test sections built. The project was 4.72 mi (7.87 km) long and in a hot desert climate. The project selected, Tonopah (FIR-10-2 (141), consisted of a 3-in. (76.2-mm) full-width overlay with an AC-40 base mix. On top of the overlay, an open-graded ½-in. (12.7-mm) finishing course was placed on the driving (high traffic lane) and passing lanes. The PBA-7 test sections consisted of two ½-mi (0.83-km) overlay test sections, built back to back from Mileposts 90 to 91 in both the eastbound and westbound directions. The test section overlays covered both the high traffic travel lane and the right distress lane. The passing lane and median shoulder were overlaid with the AC-40 base mix. Before overlaying, the existing badly cracked and rutted pavement was milled to a depth of 4 in. (101.6 mm) in the high traffic driving lane and 3 in. (76.2 mm) in the passing lane. The milled trenches were inlaid with AC-40 base mix.

Project construction started in March 1992. Before construction, mix design testing was conducted by the contractor's materials consulting laboratory, the Arizona Department of Transportation (ADOT), the PBA-7 supplier, and Shell. Results of this mix design testing indicated that the PBA-7 mix could be tender and prone to rutting. The Marshall stability of the AC-40 base mix was 3,106 which exceeded the minimum required value of 3,000. The PBA-7 mix Marshall stability was 1,867. Repetitive creep testing carried out at Shell indicated the chance of hot-weather rutting. It was decided to build the PBA-7 test sections with 0.5 percent less asphalt to help improve the stability.

Construction occurred on March 25 and 26, 1992. The PBA-7 mix was very tender, and it was allowed to cure for a considerable time before traffic was allowed on it. The westbound section needed a 6-hr traffic-free period, and the eastbound section needed an overnight traffic-free period to allow the mix to cure.

BINDER RHEOLOGY

Recent research has shown that the major contributions to rut resistance and fatigue resistance come from the mix properties (*3*). However, estimates made within the SHRP contract put the binder

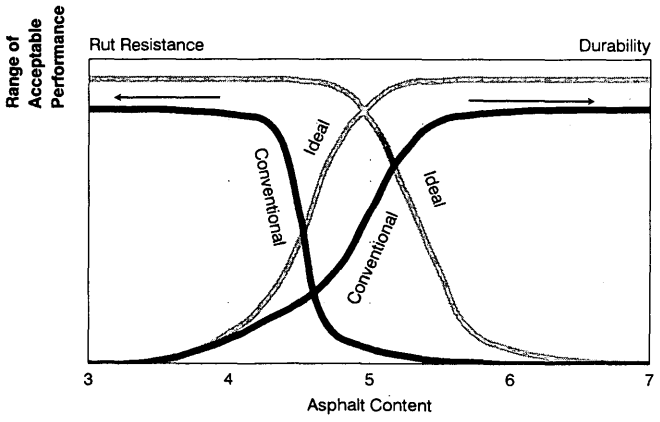

FIGURE 1 Durability versus rut resistance.

contribution at about 20 to 40 percent. This has been substantiated by wheel tracking experiments (*4*) and fatigue experiments (*5*), which showed significantly different performance levels in the same mix when different binders were used. These differences have also been found to be mirrored in field performance evaluations (*1,6*). The SHRP researchers had also based the SHRP performance grade asphalt cement specification on the presumption that the binder plays an important role in preventing rutting (*7*). They proposed using the inverse shear loss compliance, $1/J''$ (see Equation 1), as a measure of the ability of the binder to resist permanent deformation. This is a novel and intriguing approach because it captures both the stiffness and elastic behavior of the binder in one parameter via the complex modulus, G^*, and the phase angle. It also accounts for the rate dependency of the material functions because the moduli are a function of the angular velocity.

$$1/J'' = \frac{(G^*)^2}{G''} \frac{G^*}{\sin \delta} \quad (1)$$

In the case of an ideally elastic material the phase angle is 0, and hence $1/J''$ is infinite. In this case no permanent deformation should occur. Consequently, in an ideally viscous material the phase angle is 90 degrees and $1/J''$ is proportional to the viscosity of the binder. In fact, most straight unmodified asphalts have purely viscous behavior at elevated temperatures (T > 60°C) (*8,9*). The larger $1/J''$, the better the binder should be in mitigating permanent deformation. The rut resistance is considered to be a function of this parameter, as indicated in Equation 2. To ensure a certain rut resistance, the final SHRP specification calls for a minimum value of $1/J''$ of 2.2 kPa (RTFO residue) at 10 rad/sec.

$$\text{rut rate} = f\left(\frac{1}{J''_\omega}\right) \quad (2)$$

The three binders that were used in Tonopah were rheologically characterized at ADOT using a Rheometrics RAA, and $1/J''$ was measured over a relatively wide temperature range to determine whether the three binders met the SHRP specification requirements and to determine how the three materials ranked in performance. The results are given in Table 2. At the temperature of 70°C that the SHRP specification calls for, none of the binders placed meet the 2.2-kPa requirement. However, the PBA-7 material has a value of $1/J''$ of 0.9 kPa, which is only 40 percent of the minimum value required by the SHRP specification. This is in traditional terms equivalent to placing an AC-16 where an AC-40 was called for. Consequently, one would not expect the material to exhibit good rut resistance in marginal mixes. With regard to rut resistance, one would expect the following relative ranking according to $1/J''$:

AC-40 > PMA6/7 > PBA-7

As previously mentioned, the intent of the PBA-7 specification was to obtain fatigue-resistant binders. From the dissipated energy concept (*10*) it follows that in the case of a strain-controlled pavement structure the fatigue resistance should be a function of the loss modulus, G'' [i.e., the softer and more elastic a material the less prone it should be to fail because of fatigue cracking (*11*)]. However, this ranking by G'' will only hold true in the very same mix with the very same structural design and foundation. One cannot obtain any correlation when comparing different pavements' fatigue performances on the basis of the binders' G''. In this case the situation becomes significantly more complicated, and viscoelastic pavement analysis programs such as PACE are required to obtain fatigue resistance predictions (*12*). The SHRP binder specification calls for a maximum value of 5 MPa for G'' at a 34°C after rolling thin film oven (RTFO) and subsequent pressure aging vessel (PAV) aging for a PG70-10, which should have been placed in this climatic region according to the SHRP binder specification and SUPERPAVE (*13*). The G'' values are shown for two of the three test binders in Table 2. The PBA-7 and the PMA6/7 exhibit relatively small values of G'' and, therefore, the materials are expected to exhibit excellent fatigue resistance compared with the AC-40. The relative performance would probably be even more in favor of the PMA after a few years of aging in the field (*2*). With regard to fatigue resistance we obtained the following relative ranking: PBA-7 > AC-40.

MIX RHEOLOGY

Current research has shown that the Marshall stability test does not capture the true performance of HMA (*9*). This is especially true for ground tire rubber or polymer-modified systems, which tend to exhibit pronounced elastic recoil. The most widely accepted performance-related method to evaluate the rut resistance of mixes is the repetitive creep test. In this test a specimen is subjected to a pulse load and then allowed to relax. The load period can be chosen to best fit the loading conditions in the field [i.e., if the loading is slow (e.g., slow-moving truck) a long load is applied and if the load application is fast (transient traffic) a load pulse a short duration is applied (*9*)]. As previously mentioned, the pulse is followed by a relaxation time, which allows the material to recover elastically. This is of special importance for modified mixes, which may exhibit elastic recovery in excess of 90 percent (*14*). The relative performance of the mixes in preventing rutting is measured using the strain accumulation rate in the linear range, ϵ'. The strain accumulation rates of the three mixes are given in Table 2. (The testing was carried out on mix that went through the hot mix plant and not on virgin materials.) As predicted by the binder rheology, the AC-40 performs the best, followed by the PMA6/7. The PBA-7 exhibits about a five times

TABLE 1 WCUP PBA-7 Desert Specification

PBA-7	Binder Test	AASHTO Test Method	Very Hot Climate $T_- > -10F$ $T_+ > 100F$
High Ambient Temperature Mix Stability	Absolute Viscosity @ 140F, P		
	Original Binder	T-202	
	RTFO Binder	T-202	1100+
Consistency During Construction.	Kinematic Viscosity @ 275F, cSt		3000+
- Pumpability	Original Binder	T-201	
- Mix Tenderness	RTFO Binder	T-201	
Hardening During Hot Mix Paving Operation	Absolute Viscosity Ratio μ_{RTFO}/μ_{ORG}		2000-
			275+
			4.0-
Severe Climate Aging.	Pen @ 77F (100g, 5s), dmm		
	CATOD Residue	T-49	30+
Severe Climate Aging.	Ductility @ 77F (5cm/min), cm		
	CATOD Residue	T-51	40+
Severe Climate Aging.	Absolute Viscosity @ 140F, P		
	CATOD Residue	T-202	50,000-
Safe Handling.	Flash Point (COC), F		
	Original Binder	T-48	450+
Environmental Impact.	Mass Loss after RTFO, %	T-240	Report
Asphalt Binder Purity.	Solubility in Trichlorethylene, %		
	Original Binder	T-44	Report
Asphalt Cement Internal Compatibility.	Ductility @ 77F (5cm/min), cm		
	RTFO Binder	T-51	75+

TABLE 2 Rheological Properties of the Binders Used in the Tonopah Test Sections

Rut Resistance of the Binder	**1/J", KPa @60C**	**1/J", KPa @70C**	
AC-40			
Org.	6.5	1.3	
RTFO	14.8	4.2	
Extracted[1]	58.6	11.7	
PMA 6/7			
Org.	1.2	0.5	
RTFO	2.1	0.7	
Extracted[1]	3.2	1.1	
PBA-7			
Org.	1.7	0.7	
RTFO	2.1	0.9	
Extracted[1]	2.8	0.9	
Fatigue Resitance of the Binder	**G", MPA @ 10 C**	**G", MPA @ 20 C**	**G", MPA @ 30 C**
AC-40			
Org.	8.7	2.25	0.38
RTFO	7.5	2.54	0.58
Extracted[1]	25.8	----	----
PBA 7			
RTFO	5.8	0.55	0.069
Extracted	15.7	2.82 (@17.8 C)	----
', in/in/cycle @ 60 C			
AC-40			
PMA 6/7	4.5		
PBA-7	5.8		
	25		

[1] Interpolated value.

TABLE 3 Air Temperatures Measured in Tonopah, Arizona, During Time Period in Which Pavement Rutted and the Hot Spell in June 1990

Date, July 1992	**T_{max}, F**	**T_{min}, F**	**Date, June 1990**	**T_{max}, F**	**T_{min}, F**
9	105	79	19	107	69
10	105	72	20	111	71
11	101	75	21	111	70
12	104	72	22	110	76
13	106	76	23	112	79
14	109	72	24	112	80
15	113	74	25	118	85
16	112	75	26	121	83
17	109	75	27	115	76
18	109	82	28	115	84
19	106	82	29	106	87
20	106	79	30	111	87
Average	107	76	Average	113	79

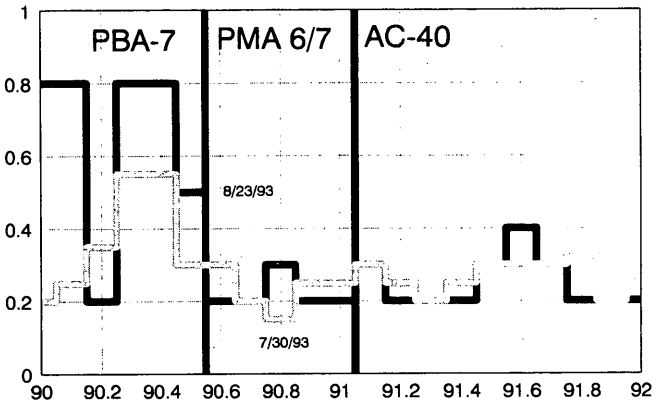

FIGURE 2 Rut depths in the various test sections.

higher strain accumulation rate, which indicates that this mix will not perform well in preventing permanent deformation.

FIELD PERFORMANCE

After construction, the test sections were closely observed. In June 1992 the daily high temperatures were consistently higher than 100°F (38°C). Starting about June 16, 1992, the air temperature reached and subsequently exceeded 109°F (43°C) as indicated in Table 3. On June 22, 1992, significant rutting was observed in both the eastbound and westbound PBA-7 test sections. Rutting continued to worsen during the summer. The measured rut depths for the eastbound lane are shown for all test section in Figure 2 (the results are randomly replicated in the westbound lane). The average number of ESALs in the high traffic lane is approximately 1,550,000 per year. During the first measurement period (April 1992 to August 1992) the high traffic lane experienced about 644,000 ESALs. In the subsequent measurement period (August 1992 to August 1993) the pavement was trafficked by another 1,550,000 ESALs. However, in fall 1992, maintenance removed the high side portions of the rut. Consequently, the measured rut depths in the second period would have been even higher. Subsequent to this, it was agreed that the high traffic lane would be removed and replaced with the next construction project scheduled for summer 1993.

PAVEMENT TEMPERATURE

To properly evaluate the performance of the binders and mixes used in this test section, it is important to have information on the pavement temperature. In this case we used both the "simple" SHRP temperature depth approximation, which is a part of SUPERPAVE, and a sophisticated heat flux finite element program (HiRoad) (*15*) to calculate the temperature depth profiles on the basis of the 12 hottest days during which the rutting occurred. The air temperatures are given in Table 3. The calculated pavement temperatures of the hottest day are given in Table 4. The analysis shows a clear discrepancy between the SHRP method and the finite element program. This probably stems from the fact that the SHRP algorithm cannot take the heat history into account and therefore will underpredict the absolute highs. Nonetheless the

TABLE 4 Calculated Temperature Depth Profiles for Tonopah, Arizona (Temperature Data Are for Hottest Case During Respective Periods)

Depth, in	HiRoad, 7/92	SUPER-PAVE, 7/92	HiRoad, 6/90	SUPER-PAVE, 6/90
surface	160	150	171	155.5
1	150	141.5	164	146.5
2	144	134.5	155.5	139.5
4	131.5	125	142.5	129.5

results clearly show that the binder needs to exhibit good rut resistance up to pavement temperatures of 150°F to 160°F (65.6°C to 71°C). Historical data indicate that to rule out premature rutting it would be best to have a material that will perform up to temperatures as high as 170°F (77°C) to cover extreme hot spells, as experienced during June 1990 (Tables 3 and 4). Consequently, the binder should probably meet a PG76 or even a PG82 grade to perform in the Arizona low desert. Where slow or standing traffic is prevalent, even higher PG grades would be required to mitigate permanent deformation.

COMPARISON OF CONVENTIONAL BINDERS WITH SHRP BINDERS

To evaluate whether the proposed SHRP binders will help mitigate permanent deformation, a PG76-10 was formulated. The binder was rheologically characterized and its rut resistance evaluated using repetitive creep. The mix testing was carried out with the same mix design and aggregate that was used in the Tonopah test road. The results of the rheological characterization and the strain accumulation rates are given in Table 5. The mix containing the

TABLE 5 Rheological Characteristics of a PG76-10 Binder Formulated for Repetitive Creep Testing in Tonopah Mix

Property	Spec Limit	PG76-10 Binder
Original Binder		
1/J", KPa @ 76 C	1.00+	1.37
RTFO Binder		
1/J", KPa @ 76 C	2.20+	2.24
PAV Residue, T_{PAV} =110 C		
G", MPa @ 34 C	5.00-	2.33
S(60s), MPa @ 0 C	300-	159
m-value @ 0 C	0.30+	0.37
γ', μin/in/cycle	---	2.2

PG76-10 clearly outperforms all the materials used in the Tonopah test road by a wide margin. It is worth noting that the mix of the PG76-10 has only half the strain accumulation rate of the AC-40 (ϵ' = 2.2 μin./in./cycle versus 4.5 μin./in./cycle). The most astounding fact is that the strain accumulation rate in the linear range is about 10 smaller than that of the PBA-7. Thus, this binder specification appears to provide a material that can resist thermal cracking and fatigue cracking without becoming unnecessarily soft at elevated temperatures.

CONCLUSIONS

1. The PBA-7 evaluated tended to be relatively tender and required significantly more attention during placement than conventional asphalts or even standard PMAs. In fact, the traffic could not be released on the PBA-7 pavement for more than 12 hr to prevent immediate rutting of the fresh pavement.
2. The PBA-7 specification provides binders with excellent aging and fatigue cracking resistance. However, the material does not provide good rut resistance and can lead to catastrophic failure when used with average to mediocre mixes. In excellent mixes it can, however, perform well.
3. The PG76-10 binder resulted in a mix that combined good cracking resistance with superior rut resistance. The repetitive creep data appear to substantiate the SHRP findings and lead us to believe that the PG76-10 provides a binder with a better balance of properties than the PBA-7 binder.

REFERENCES

1. Reese, R. and N. Predoehl. *Evaluation of Modified Asphalt Binders.* Caltrans Report 65324-633383. Sacramento, Calif., 1989.
2. Bouldin, M. G., and M. A. Berggren. *The Use of PBA Materials in Severe Climates: Predictive Tests.* Technical Bulletin. Shell Development Co., Houston, Tex., 1991.
3. Hicks, R. G., F. N. Finn, C. L. Monismith, and R. B. Leahy. Validation of SHRP Binder Specification Through Mix Testing. *AAPT*, Vol. 62, 1993.
4. Bouldin, M. G., and J. H. Collins. Influence of Binder Rheology on Rut Resistance of Polymer Modified and Unmodified Hot Mix Asphalt. In *Polymer Modified Asphalt Binders, ASTM STP 1108* (K. R. Wardlaw and S. Shuler, eds.), Philadelphia, Pa., 1992.
5. Goodrich, J. L. Asphaltic Binder Rheology, Asphalt Concrete Rheology and Asphalt Concrete Mix Properties. *AAPT*, Vol. 60, 1991.
6. Fleckenstein, J., K. C. Mahboub, and D. L. Allen. Performance of Polymer Modified Asphalt Mixes in Kentucky. In *Polymer Modified Asphalt Binders, ASTM STP 1108* (K. R. Wardlaw and S. Shuler, eds.), Philadelphia, Pa., 1992.
7. Anderson, D. A., and T. W. Kennedy. Development of SHRP Binder Specifications. *AAPT*, Vol. 62, 1993.
8. Bouldin, M. G., J. H. Collins, and A. Berker. Rheology and Microstructure of Polymer/Asphalt Blends. *Rubber Chem. Tech.*, Vol. 64, 1991.
9. Bouldin, M. G., G. M. Rowe, J. B. Sousa, and M. J. Sharrock. Repetitive Creep as a Tool to Determine the Mix Rheology of Hot Mix Asphalt. *AAPT* (submitted for publication).
10. Van Dijk, W. Practical Fatigue Characterization of Bituminous Mixes. *AAPT*, Vol. 44, 1991.
11. Rowe, G. M. Performance of Asphalt Mixtures in the Trapezoidal Fatigue Test. *AAPT*, Vol. 62, 1993.
12. Rowe, G. M. M. S. Sharrock, and M. G. Bouldin. A Visco-Elastic Analysis of Hot Mix Asphalt Pavement Structures. *AAPT* (submitted for publication).
13. Huber, G. A. SUPERPAVE Software: A Tool for Mixture Design. *AAPT*, Vol. 62, 1993.
14. Bouldin, M. G. *Results of Repetitive Creep Experiments Carried Out on Polymer Modified Hot Mix Asphalts Used on the Mesquite Nevada Job.* Technical Bulletin. Shell Development Co., Houston, Tex., 1991.
15. Rowe, G. M., M. S. Sharrock, L. Pierce, M. G. Bouldin, and N. Jackson. The Effect of Climate and Traffic on the Performance of HMA Pavements. *Proc., 4th International Conference on Bearing Capacity of Roads and Airfields* (in preparation).

Publication of this paper sponsored by Committee on Characteristics of Bituminous Materials.

Study of the Fatigue of Asphalt Mixes Using the Circular Test Track of the Laboratoire Central des Ponts et Chaussées in Nantes, France

CHANTAL DE LA ROCHE, HUGUES ODÉON, JEAN-PIERRE SIMONCELLI, AND ALEXANDRA SPERNOL

The conventional French fatigue test has yielded significantly different results for two asphalt materials with the same grade of pure asphalt. A research program was begun to study the influence of the asphalt nature on the fatigue behavior of asphalt materials. The program included full-scale experimentation on the circular test track of the Laboratoire Central des Ponts et Chaussées, laboratory tests, and mechanical analysis. Four asphalt mixes with pure asphalt were tested on the experimental pavement: two asphalt concretes with asphalts 50/70 of A and B origin, a high-modulus asphalt mix (bitumen 10/20), and a classical asphalt road base (bitumen A). The asphalt materials were fatigue tested in the laboratory according to several procedures: two-point bending fatigue tests on trapezoidal samples, with controlled strain, with and without rest periods, and with controlled stress, without rest periods; and three-point bending fatigue tests on parallelepiped-like samples, with controlled stress, with and without rest periods. The ranking of the materials according to their laboratory fatigue behavior depends strongly on the test procedure. The mechanical analysis carried out on the basis of the laboratory test results and the behaviors observed on the test track indicate that the controlled stress fatigue tests lead to results closer to the test track behavior and that the shift factor to be applied to the high-modulus asphalt mix should be 1. All these results have to be confirmed by a repetition of this experiment still in progress.

Differences in results found between two asphalt mixes made with pure asphalt of the same grade in the usual laboratory fatigue test, that of French Standard NF P 98-261-1 (controlled strain two-point bending on trapezoidal specimen, with no rest periods), led to a study of the pertinence of this fatigue test with respect to the influence of the type of asphalt. The absence of rest periods and the dissipative heating that can be observed in the course of the test are two phenomena not found with actual traffic that might tend to shorten the life and affect differently the various types of asphalt.

Accordingly, a research program was set up to

- Compare the classification obtained from fatigue tests (conventional or with rest periods, with controlled stress or strain) with the ranking obtained on an experimental pavement tested on the circular fatigue test track of the Laboratoire Central des Ponts et Chaussées (LCPC);
- Identify the most pertinent laboratory test for the type of structure concerned; and
- Compare the life predictions for asphalt structures according to the French pavement design method with the results obtained on the test track.

In addition, the design of high-modulus asphalt pavement structures was compared with the classical asphalt road base design.

This research program was conceived in the context of the technical cooperation between the USAP (toll motorways companies) and the LCPC, which financed the experiment on the test track. The Shell Company was associated with the laboratory experiments at the start of this project and performed impulse fatigue tests at the Shell-KSLA laboratory (Amsterdam).

C. de La Roche and H. Odéon, Laboratoire Central des Ponts et Chaussées, Centre de Nantes, BP 19, 44340 Bouguenais, France. J.-P. Simoncelli, Société des Pétroles Shell, Direction Bitumes, 89 Boulevard Franklin Roosevelt, 92564 Rueil Malmaison Cedex, France. A. Spernol, Scétauroute-USAP, 23 Avenue du Centre, 78286 Saint-Quentin en Yvelines, France.

EXPERIMENT ON LCPC'S CIRCULAR FATIGUE TEST TRACK

The experiment presented here lasted from October 1990 to July 1991, during which 2,730,000 loadings were applied, leading to significant damage to the various pavement sectors tested (*1*).

Experimental Conditions

Four 0/14 mm asphalt mix formulas were tested on four sectors arranged as shown in Figure 1:

- Sector I—an asphalt concrete made with 50/70 asphalt from Source B (AC B);
- Sector II—an asphalt concrete made with 50/70 asphalt from Source A (AC A);
- Sector III—a high-modulus asphalt mix (made with hard 10/20 asphalt) (EME); and
- Sector IV—a classical asphalt road base made with 50/70 asphalt from Source A (GB A).

These layers, built on a well-graded untreated granular material (GRH), were designed to yield, according to the usual design method, a service life on the order of 2 million cycles while com-

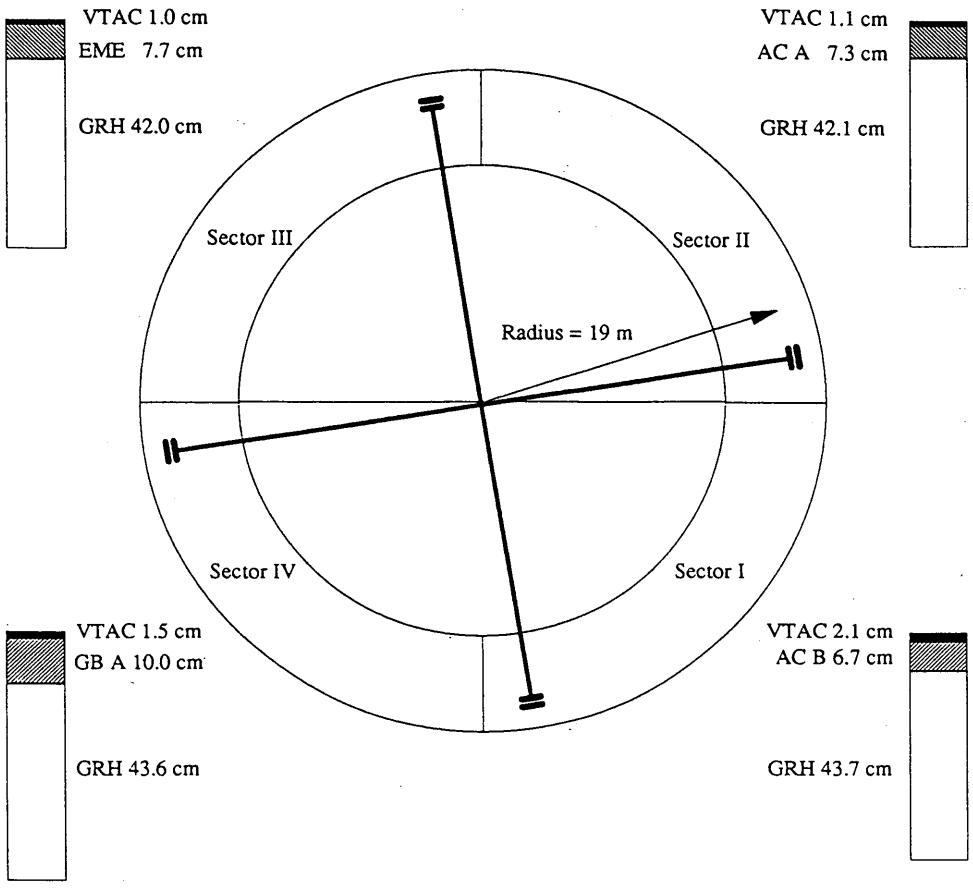

Sector	I	II	III	IV
Asphaltic binder	B 60/70	A 60/70	10/20	A 60/70
Content (%)	5.4	5.4	6.2	4.6

Grading curve of granular material used in the asphaltic mixes

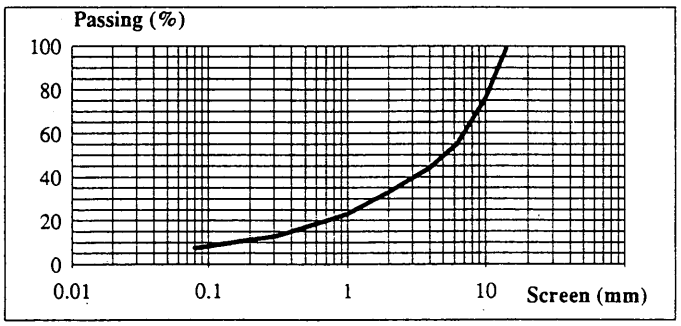

FIGURE 1 Experimental structures.

plying with the usual thicknesses of placement of these materials. The thickness of the asphalt road base was determined by the usual design method to yield the same calculated life as the high-modulus asphalt mix. All of the structures were covered with a wearing course of very thin asphalt concrete (VTAC) (20 to 25 mm theoretical thickness). The topographical surveys revealed thicknesses of asphalt materials (Figure 1) that were, on the average, less than the theoretical values (8 cm for AC B, AC A, and EME and 12 cm for GB A). The "foundation soil" was a clayey 0/10 sand, 2.80 m thick, on clayey silt.

The experiment was performed with the following configuration of the circular test track: load, 65 kN per dual wheel (half French legal axle) with transverse sweep over 1.60 m; speed, 10 rpm (70 kph linear at the mean radius of 19 m); and tires, Dunlop SP 321 inflated to 0.8 MPa.

During construction, the structures were equipped with strain gauges, pressure sensors, and thermocouples. There were also measurements of quasi-static deflection and of radius of curvature, surveys of the longitudinal and transverse profiles, and cracking surveys.

Course of Experiment and Main Results

This experiment was performed during two periods: one "cold" (90 percent of loadings between 0°C and 15°C), which included 1,165,000 loadings and resulted in the appearance of the first cracks in Sectors I and II; and one "warm" (80 percent of loadings between 15°C and 20°C), which included 1,565,000 additional loadings until significant cracking developed in all four sectors.

Initialization of Measurements (Zero Point)

The data presented in Table 1 correspond to the measurements made at the start of the experiment, before damage to the structures. The measured deflections are rather homogeneous, and the observed variations seem to depend only on the variations of thickness of the asphalt layers. On the whole, the deflection values are high, which indicates a low soil bearing capacity. The values of the radii of curvature are consistent with the measured deflections and thicknesses. The strains at the base of the asphalt layers of Sectors I and II are of the same order of magnitude. The same is true of Sectors III and IV.

Results at End of Cold Period

Increases in deflections are comparable and moderate for Sectors I and III. Deflections increase a little more in Sector II and less in Sector IV (Figure 2).

The first cracks are observed at the surface of the pavements after 1,165,000 loadings (end of cold period), following heavy rains. Core drillings confirmed that they were in fact structural cracks through the bound layers. The presence of VTAC probably masked the appearance of the first cracks in the pavement base. The extent of cracking measured at the end of the cold period is indicated in Figure 3.

Whereas the extent of cracking is locally large on Sectors I and II at the end of this first period of traffic, the cracks are fine and the pavements cannot be regarded as destroyed. For Sector III, the cracks appeared in a zone of underthickness and are therefore not significant. As for Sector IV, no crack was recorded. Consequently, it was decided to continue the experiment without maintenance a few months later (warm period).

Results at End of Warm Period

A reduction of the deflections was noted between the last measurements of the previous period and the first measurements of the new period; it may have resulted from a change in the moisture condition of the foundation soil. With the traffic and the increase of cracking, the deflections increased regularly on Sectors I and II. On Sector III the deflection measurements increased substantially with the total traffic, whereas Sector IV measurements increased very little (Figure 2).

Cracking evolved in a way that varied from one structure to another during the warm period. Whereas it developed similarly in Sectors I and II, it appears that the onset of cracking in Sector III occurred later during the cold period, and a comparable subsequent development was observed. On the other hand, the cracking of Sector IV appeared late during the warm period but then developed faster than on the other sectors (Figure 3).

At the end of the experiment, Sector I (AC B) exhibited the most damage and had a high density of cracks. Sector II (AC A) had a lower average cracking density with a large area that was preserved (this zone corresponds to a slight local overthickness of the layer of asphalt concrete). Sector III (EME) has areas of dense cracking along with a few longitudinal cracks. Other areas have transverse cracking only. The extent of cracking at the end of the experiment was close to those of Sectors I and II. The extent of cracking of Sector IV (GB A) reached only 47 percent at the end of the experiment.

Since none of the sectors was totally destroyed at the end of the experiment, the strengths of the various structures were compared at the same percentage extent of cracking—50 percent (which is the final value reached on Sector IV). The number of axle loads for 50 percent cracking, denoted N 50, is 1,250,000

TABLE 1 Measurements on Test Track at Zero Point

Sectors Materials	I AC B	II AC A	III EME	IV GB A
Mean deflection (0.01 mm) *Measurement temperature 26°C*	96	111	91	90
Mean radius of curvature (m) *Measurement température 21°C*	111	91	161	158
Order of magnitude of the strains at the base of the asphaltic layers (μstrains)				
Longitudinal strains	134 *(3)*	122 *(4)*	87 *(1)*	95 *(4)*
Transverse strains	131 *(1)*	120 *(1)*	42 *(1)*	111 *(1)*
Measurement temperature in °C	19.5	19	19	17.5

(*) The italicized figure in parentheses is the number of gauges on which the mean was determined to calculate the order of magnitude of the strains.

(**) The longitudinal and transverse strains (base of asphaltic layer) were measured with speed of 10 rpm and load of 6.5 T; one of the wheels of the pair directly above the gauges, at the zero point.

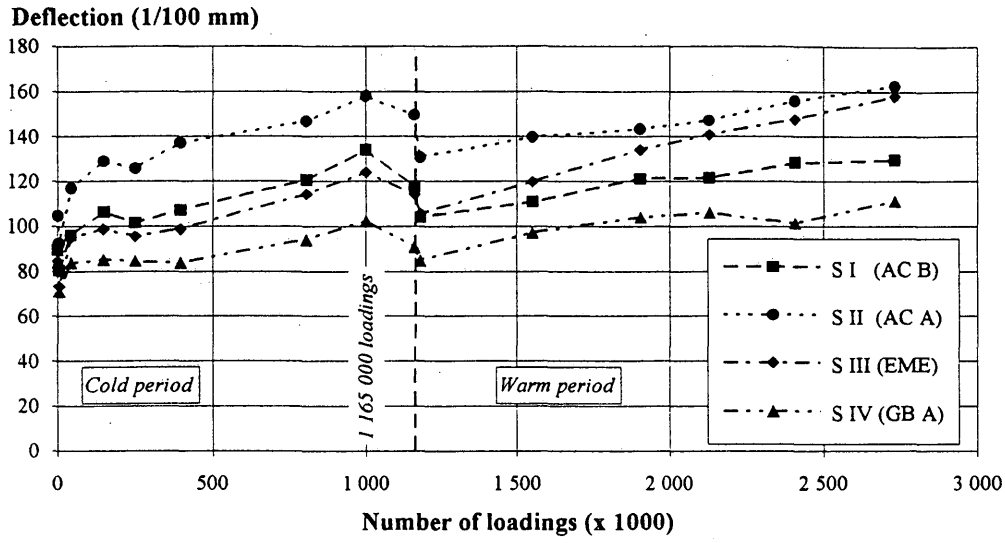

	Number of loadings	Sector I AC B	Sector II AC A	Sector III EME	Sector IV GB A
Deflections	40,000	96	117	95	84
1/100 mm	1,165,000	118	150	114	91
(20°C)	2,700,000	129	163	158	111

FIGURE 2 Deflections referred to 20°C.

loadings for Sector I, 1,750,000 loadings for Sectors II and III, and 2,750,000 loadings for Sector IV.

Conclusions Concerning Behavior on Circular Test Track

The following main conclusions can be drawn from these full-scale tests:

- With the actual thicknesses, on foundation soils having the same bearing capacity, it takes approximately 1.5 times as many loadings to obtain the same extent of damage on Sector II (AC A) as on Sector I (AC B). This difference must be considered in light of the differences in the thicknesses of the AC and of the VTAC on these two sectors.
- The comparison of GB A, 10 cm thick, and EME, 7.5 cm thick, on a foundation liable to deformation (not the usual conditions of use of such a material) clearly favors GB A.
- Cracking appears to start in EME substantially later than in both conventional asphalt mixes at similar thicknesses of placement, but the evolution of this cracking, once started, appears faster.

LABORATORY TESTS

Tests on Binders

The original binders were sampled when the pavements of the circular test track were built and the recovered binders were extracted from slabs cut from the test track. They underwent conventional tests (Table 2) and complex modulus tests [Figure 4 (top)], which indicate the following (*2*):

- All binders are within the specifications. Asphalt B shows a large evolution after RTFOT.
- Generally, Asphalt A exhibits more thermal and kinetic sensitivity than Asphalt B; its Black's curve (logarithm of modulus of complex modulus versus phase angle) evolves faster, and its isothermals are steeper. It is also less structured.
- Asphalt B and the hard asphalt have very different rigidities and thermal sensitivities but similar kinetic sensitivities.

On the whole, the results of the recovered binders give the same trends.

Tests on Asphalt Mixes

All tests performed on the four asphalt mixes presented here were performed on specimens cut from slabs of materials sampled in place. These slabs were taken in the untraveled areas of the circular test track, before rotation.

Measurements of Complex Modulus

Complex modulus tests (*3*) on trapezoidal specimens, in accordance with French standard NFP 98-260-2, were performed by the Bordeaux LRPC. The corresponding Black's curves (logarithm of modulus of the complex modulus versus phase angle) are given in Figure 4 (bottom). Modulus measurements were also made in all the other laboratories at the beginning of the fatigue test, either on trapezoidal specimens in two-point bending or in three-point bending on beams (Table 3).

The results obtained by each of the laboratories are consistent, taking into account the temperature and frequency influences. This

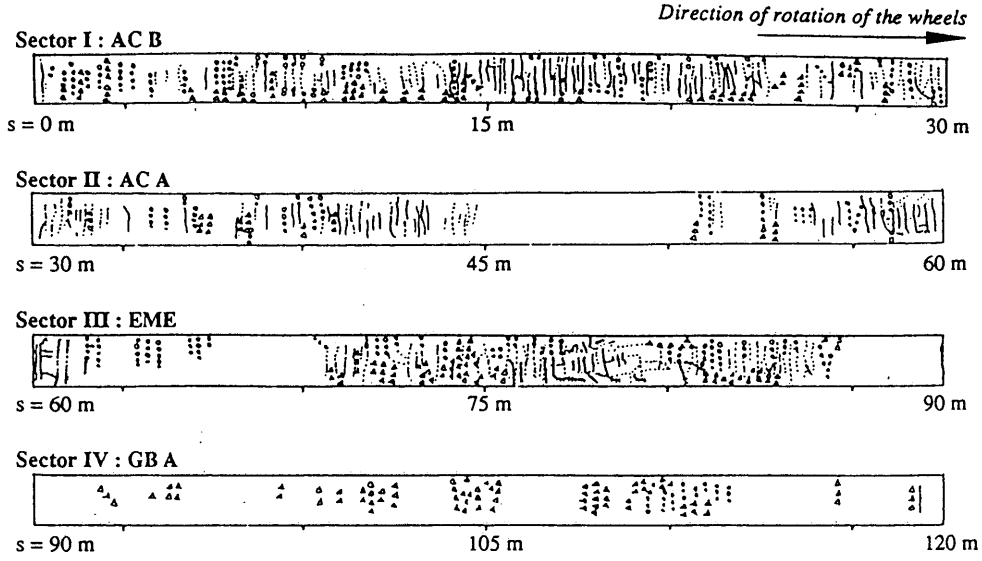

Note: cracking after

1,165,000 loadings
1,902,000 loadings
2,124,000 loadings
2,300,000 loadings
2,665,000 loadings

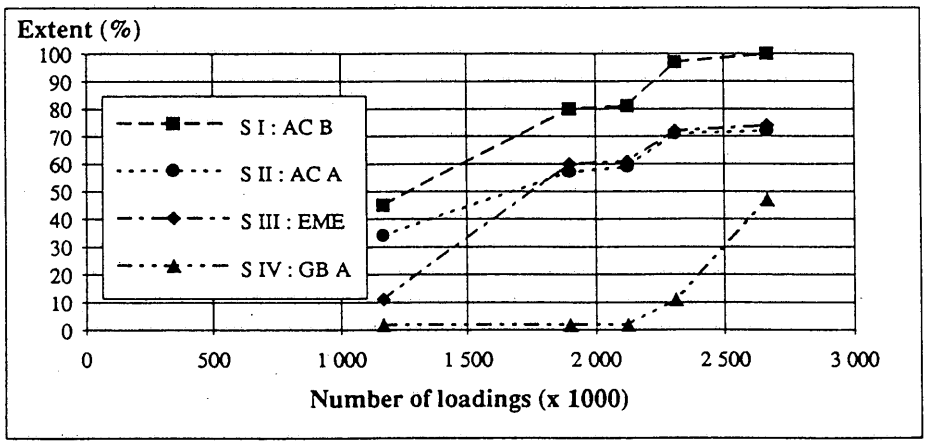

Sector	I	II	III	IV
Cracking (%) after				
1,165,000 loadings	45	34	11	0
2,665,000 loadings	100	72	74	47

FIGURE 3 Cracking.

is an important first conclusion given the multiplicity of apparatuses and methods used.

Fatigue Tests

The conditions of the fatigue tests are given in Table 4.

Controlled Strain Fatigue Tests

The four asphalt mixes were tested in continuous fatigue with controlled strain by Procedures 1, 2, and 3. The results are given in terms of ϵ_6 and the slope of the fatigue line in Table 3. ϵ_6 is the strain corresponding to conventional failure (i.e., reduction of the force at the top by half) of the specimen at 1 million loadings. The fatigue line is obtained by a regression of the form

$$\ln(\text{number of cycles}) = a - \text{slope} \times \ln \epsilon$$

on the individual results.

These results confirm that with respect to the two-point bending fatigue test on trapezoidal specimens in the continuous mode, Asphalts A and B lead to very different values of ϵ_6 between AC B

TABLE 2 Characteristics of Binders—Original, After RTFOT, and Extracted

Bitumen	50/70 B			50/70 A			10/20		
Tests results	Pen	RB	PfI	Pen	RB	PfI	Pen	RB	PfI
Original binder	61	51	-0.5	65	48	-1.1	16	69.5	0.3
After RTFOT	37	59	0.1	42	53	-0.9	13	75	0.8
Extracted binder	44	56	-0.1	39	53.5	-0.9	13	75	0.8

Note: Pen: Penetration at 25°C (mm x 0.1)
RB: Ring and Ball Temperature (°C)
PfI: Pfeiffer penetration index

and AC A (*4*). The results from the different laboratories, in terms of ϵ_6, rank the asphalt mixes as follows, for all test procedures: AC B ≈ EME > AC A ≈ GB A. The results by Procedures 1 and 2 show that AC B is a little more sensitive to temperature than AC A in terms of fatigue performance. Similarly, EME is more sensitive to temperature than GB A.

Controlled Stress Fatigue Tests

Controlled stress fatigue tests were performed by Procedure 4 for the four materials and by Procedures 6 and 7 for AC A, AC B, and EME only. This makes it possible to compare the stresses σ_6 and the slopes of the fatigue lines (Table 3). σ_6 is the stress corresponding to conventional failure (doubling of the displacement at the top) of the specimen at 1 million loadings. The fatigue line is obtained by a regression of the form

$$\ln(\text{number of cycles}) = a - \text{slope} \times \ln \sigma$$

on the individual results.

The results obtained rank the asphalt mixes as follows: EME >> GB A ≈ AC B > AC A in the continuous mode and EME >> AC A ≈ AC B in the discontinuous mode.

The values of σ_6 determined by Procedure 6 (three-point bending) are higher than those measured by Procedure 4 (two-point bending).

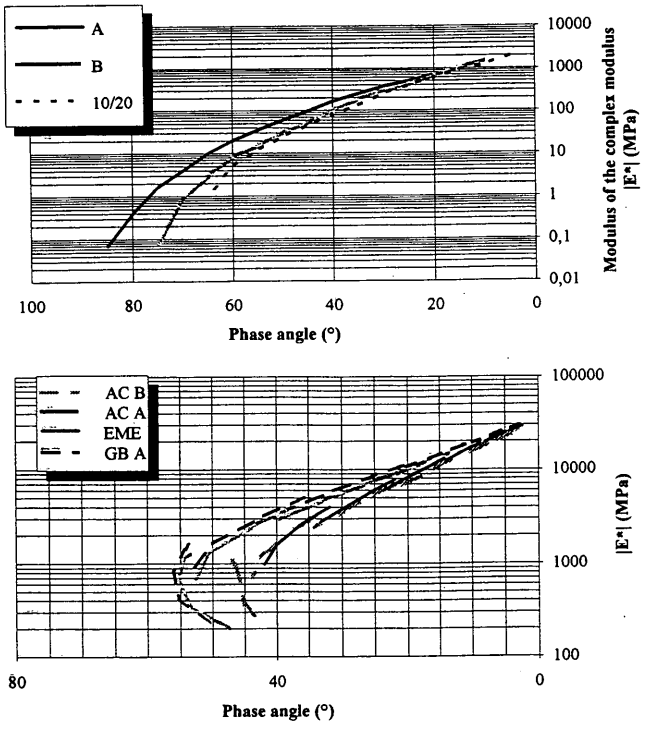

FIGURE 4 Complex modulus curves in the Black space: *top*, Black curves of the original binders; *bottom*, Black curves of the asphalt mixes.

Continuous and Discontinuous Fatigue

To quantify the influence of the rest period on fatigue behavior, tests with and without rest periods were performed in two ways: by Procedure 5, for which trapezoidal specimens were loaded at the top in strain (two-point bending) and by Procedures 6 and 7, for which rectangular specimens are loaded in stress at midpoint (three-point bending).

The controlled strain tests were performed in continuous and discontinuous fatigue for only one level of strain of the specimen, 200 μstrains. This strain level was considered representative of the strains obtained on the circular fatigue test track at the base of the layer of asphalt mix. This analysis leads to the following ratios of life durations (continuous/discontinuous): 4 for AC B, 2 for AC A, 3 for EME, and 1 for GBA.

The results of the continuous and discontinuous controlled stress tests were analyzed in terms of initial stress: for a stress level of 2 MPa, the corresponding lives in the continuous and discontinuous modes are deduced from the fatigue line of the test. This leads to the following ratios of life durations (continuous/discontinuous): 7 for AC B, 8 for ACA, and 2 for EME.

For the two asphalt concretes, it is found that the incidence of the rest periods differs between the controlled stress test (AC A and AC B benefit from the rest periods in the same way whichever analysis is performed) and the controlled strain test (AC B then performs better). However, the discontinuous tests were performed according to different procedures: the controlled strain test is a test with bursts of loading (8 sec or 320 loading cycles, 80 sec of rest), whereas the controlled stress test is in pulses (one loading cycle; five cycles of rest).

EME gives ratios of numbers of cycles that are of the same order as those of the asphalt concretes in the tests with bursts of

TABLE 3 Results of Laboratory Tests on Asphalt Mixes

Sectors Materials		I AC B	II AC A	III EME	IV GB A
MODULI OF THE ASPHALT MATERIALS					
Moduli of the complex modulus measured in LRPC Bordeaux					
10°C, 10 Hz		10,280	12,374	15,024	13,486
20 °C, 10 Hz		5,110	5,876	9,788	7,097
10 °C, 30 Hz		12,425	14,991	17,037	15,831
20 °C, 30 Hz		6,892	8,102	11,750	9,342
Moduli measured in the laboratory at the beginning of the fatigue tests					
LCPC (10°C, 25 Hz - 2 point)		12,000	14,200	16,600	15,000
LPC Ang (10°C, 25 Hz - 2 point)		12,500	16,000	18,300	17,500
LCPC (20°C, 25 Hz - 2 point)		6,900	8,000	11,000	9,600
Shell (20°C, 40 Hz - 3-point)		6,900	9,300	11,400	-
FATIGUE TESTS RESULTS*					
Controlled strain fatigue tests					
Procedure 1	ε_6 (μstrain)	140 ± 10	90 ± 5	140 ± 6	88 ± 11
10°C, 25 Hz in air	slope	6.3	5.2	5.3	4.3
Procedure 2	ε_6 (μstrain)	169 ± 11	104 ± 8	159 ± 13	91 ± 9
20°C, 25 Hz in air	slope	6.0	5.2	5.7	4.1
Procedure 3	ε_6 (μstrain)	143 ± 10	92 ± 6	136 ± 6	91 ± 6
10°C, 25 Hz in water	slope	3.7	4.5	5.9	5.7
Controlled stress fatigue tests					
Procedure 4	σ_6 (MPa)	0.67 ± 0.06	0.52 ± 0.11	1.38 ± 0.06	0.67 ± 0.04
20°C, 25 Hz continuous	slope	5.5	4.4	6.2	7.0
Procedure 6	σ_6 (MPa)	1.19 ± 0.18	1.13 ± 0.05	1.91 ± 0.11	-
20°C, 40 Hz continuous	slope	6.1	6.2	5.9	-
Procedure 7	σ_6 (MPa)	1.68 **	1.70 **	2.20 **	-
20°C, 40 Hz discontin.	slope	6.9	9.0	3.4	-

** The results of the fatigue tests are given in terms of values of ε_6 and σ_6, with the associated 95% confidence interval and of the slope of the fatigue line.*

*** 95% confidence interval not calculated because total number of values less than 5.*

-material not tested

loading (controlled strain) but performs much more poorly than these same asphalt concretes in the pulsed tests (controlled stress).

GB A seems not to be improved by the introduction of a rest period, but this remark applies only to the test with bursts of loading (controlled strain).

Conclusions Concerning the Laboratory Tests

The four asphalt mixes were tested under different conditions and by different laboratories. The results lead to the following conclusions:

- The modulus values measured by the different laboratories are consistent.
- The results of the fatigue tests and the corresponding classification of the asphalt mixes depend on the test conditions.

For both asphalt mixes with 50/70 asphalt, the following conclusions are drawn:

- ϵ_6 of AC B is substantially greater than ϵ_6 of AC A with controlled strain.
- σ_6 of AC B is slightly greater than σ_6 of AC A with controlled stress without rest periods.
- σ_6 of AC B is equal to σ_6 of AC A with controlled stress with rest periods.
- The life ratios between the continuous and discontinuous tests are close for AC A and AC B in the pulsed tests (with controlled stress) and favor AC B in the tests with bursts of loading (with controlled strain).

For EME and GB A, the following observations are made:

- The fatigue performance level of EME is substantially greater than that of GB A.
- The fatigue characteristics of GB A are not improved by the introduction of rest periods in a controlled strain test with bursts of loadings.

TABLE 4 Conditions of Fatigue Test

Procedure	Laboratory	θ (°C)	f (Hz)	Loading
1	LCPC	10	25	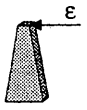 3 levels of strain 8 specimens per level
2	LCPC	20	25	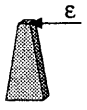 3 levels of strain 8 specimens per level
3	LPC Angers	20 (in water)	25	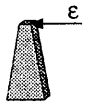 3 levels of strain 8 specimens per level
4	LPC Bordeaux	20	40	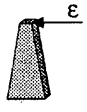 3 levels of strain 8 specimens per level
5	LPC Bordeaux	20	40	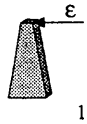 and 8:80 (1) 1 level of strain (200 mstrain) 8 specimens
6	KSLA	20	40	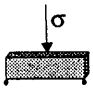 6 to 8 specimens (stress sweep)
7	KSLA	20	40	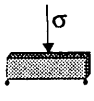 1:5 (2) 2 to 4 specimens (stress sweep)

Note : (1) 8 s or 320 loading cycles, 80 s without loading
(2) one loading cycle, then 5 without loading

• EME has a life ratio between the continuous and discontinuous tests that is of the same order of magnitude as those of the two asphalt mixes in the controlled strain tests with bursts of loading and much smaller than those of the two asphalt mixes in the controlled stress pulsed tests.

MODELING OF THE BEHAVIOR OF THE STRUCTURES

The French design method for road pavement structures is a rational method (*5*). The strains (and stresses) engendered in the structure by a 65-kN pair are first determined, using the Alizé software, on the basis of the multilayer static linear elastic model of Burmister. On the basis of the initial characteristics of the structure, allowable strains (and stresses) are then calculated for each of the layers for a specified probability of failure, according to the fatigue behavior of the material (with reference to the controlled strain fatigue test—Procedure 1), the traffic, and the bearing capacity of the foundation soil. The structure will perform correctly if the calculated strain and stress values are less than or equal to the allowable values.

A shift factor corrects for the differences between the strain values derived from the model and those deduced from observation of the behavior of actual pavements. A shift factor value is assigned to each family of materials.

Determination of Structure of Calculation Model

The foundation soil is represented with two layers: the substratum, treated as a half-space having a Young's modulus of 400 MPa,

and a 2.8-m-thick clayey sand layer. Deflection measurements made at the surface of this layer allowed backcalculation of a mean modulus of 35 MPa for this material.

The moduli of the two layers of GRH (200 MPa and 250 MPa) are backcalculated from quasi-static deflection measurements made by Benkelman beam and measurements of the radius of curvature made at the beginning of the experiment at the surface of the VTAC.

The fit obtained is not as good for the deflection measurements on Structures III and IV: the calculated values are, respectively, 24 and 19 percent greater than the measured values. Since identical characteristics were selected for the foundation soil of the four sectors, the fit is not equally good everywhere. This is due to the difference in stiffness of the four structures and to the nonlinear character of the foundation soil, which was not represented here.

Mechanical Analysis

First of all, it is interesting to compare the strain values derived from the calculation with those measured in the bound layers for identical temperature and frequency conditions (15°C, 10 Hz).

The description of these structures is completed by considering the dynamic modulus values of the asphalt materials measured in the laboratory. The pavements, which exhibit variations of thickness, are divided into zones of uniform thickness on which the extent of cracking is recalculated.

Analysis of Strains on Passage of an Axle

Table 5 gives three series of values (referred to 15°C and 10 Hz):

1. The strain values, based on strain gauge measurements (these values are derived from filtered signals, corrected for temperature and frequency);
2. The strain values computed with the Alizé software in which the half axle load is represented as a double circular area (contact pressure 0.662 MPa, loading radius 125 m); and
3. The strain values from a finite-element calculation on a three-dimensional static elastic model (César-LCPC software), to evaluate the influence of the load geometry. In this model, the half axle load is represented by two 0.18- × 0.33-m rectangular areas at a uniform pressure of 0.542 MPa, which is closer to the imprint recorded for the wheels of the pair.

Several conclusions can be drawn from these values:

1. The calculated strains in the asphalt material are systematically greater than the measured values.
2. At the base of the asphalt layers, the longitudinal strains are generally greater than the transverse strains. This finding is corroborated by the appearance of transverse cracks in the wheelpath on the structures of the circular test track.
3. The strain values obtained by the calculation with César-LCPC are generally closer to the measured values than those given by the Alizé model. It is therefore apparent that, on thin structures, the shape of the imprint has a decisive impact on the values of the maximum strains at the base of the bound layers.
4. Finally, large differences in the strains between the sections of different thicknesses of Sectors III and IV indicate the significant effect of thickness of the asphalt layer.

Life Prediction

From the strains calculated by the Alizé and César-LCPC software for 15°C and 10 Hz, it is possible to determine the allowable numbers of loading cycles for each structure using the fatigue characteristics determined by the usual test (Procedure 1) and the fatigue characteristics determined in controlled stress tests (Procedures 4, 6, and 7) and to compare them with those based on the observations on the circular test track.

Use of the Fatigue Characteristics of the Usual Fatigue Test

According to the design method, the number of cycles N for which fatigue failure of the asphalt material occurs with a probability of 50 percent is

$$N = 10^6 \left[\frac{\epsilon_{cal}}{k\epsilon_6(\theta)} \right]^{1/b}$$

where

ϵ_{cal} = calculated maximum tensile strain under a passage of an axle,
$\epsilon_6(\theta)$ = strain for which there is failure at 10^6 loadings in the bending fatigue test at a constant temperature of θ,
k = shift factor reflecting the difference between the calculation approach and observation of the behavior of actual pavements, and
$1/b$ = slope of the fatigue line of the material.

The usual fatigue test is performed at 10°C and 25 Hz (Procedure 1); the value of ϵ_6 is corrected in temperature to be referred to 15°C according to the following equation:

$$\epsilon_6(\theta) \sqrt{E(\theta)} = C^{ste}$$

The tensile strain value, derived from the calculations performed by Alizé and César-LCPC and used to determine the number of loading cycles, is the maximum of the longitudinal and transverse strains; it is generally the longitudinal strain. All of these characteristics are summarized in Table 5.

The number of cycles Nz at which the structure fails because of excessive permanent strain in the unbound layers (GRH and foundation soil) is determined by the criterion $\epsilon_z = 22{,}500 Nz^{-1/4.1}$. This criterion was not critical in this study. The analysis indicates that the pavements should fail first by fatigue of the asphalt layers, a result in agreement with the findings on the pavements of the circular test track.

To compare calculation results with the observations of pavement behavior on the circular test track, an assumption must be made. It will be assumed that 50 percent cracking observed on the circular test track is associated with the 50 percent risk of failure.

A search is then made for the coefficients k to be associated with each of the sectors so that the number of loadings leading

TABLE 5 Characteristics for Calculations of Modeling and Results

Materials			AC B	AC A	EME		GB A	
Sectors			I	II	III		IV	
					min	max	min	max
Distance along curve (m)			5 to 30	30 to 48 52 to 60	77 to 87	60 to 77 87 to 90	90 to 108	108 to 120
Thicknesses (m)								
Asph. mat.			0.081	0.080	0.073	0.089	0.101	0.128
GRH 1			0.218	0.210	0.207	0.211	0.225	0.204
GRH 2			0.218	0.210	0.207	0.211	0.225	0.204
Number of cycles on the circular test track for 50% cracking (x 1,000)			1,100	1,450	1,450	2,000	2,700	2,750
Measured strains (μstrain)								
ε long (base of AC)			136	92	107	75	78	79
ε trans (base of AC)			124	89	77	41	87	83
ε vert (top of GRH)			-	935	1419	-	-	829
ε vert (top of soil)			632	554	410	410	691	-
Characteristics for calculation								
E (15°C;10 Hz)		MPa	7,700	9,125	12,400		10,300	
Procedure 1	ε_6	μstrain	140	90	140		88	
	-1/b		6.3	5.2	5.3		4.3	
Procedure 4	σ_6	MPa	0.67	0.52	1.38		0.67	
	-1/b		5.5	4.4	6.2		7.0	
Procedure 6	σ_6	MPa	1.19	1.13	1.91		-	
	-1/b		6.1	6.2	5.9		-	
Procedure 7	σ_6	MPa	1.68	1.70	2.20		-	
	-1/b		6.9	9.0	3.4		-	
Calculated maximum tensile values								
Strain	ε Alizé	μstrain	235	222	205	179	177	149
	ε César	μstrain	172	160	148	137	136	121
Stress	σ Alizé	MPa	2.18	2.46	3.10	2.72	2.22	1.88
	σ César	MPa	1.69	1.84	2.39	2.18	1.79	1.59
Back-calculated shift factor k								
Procedure 1	k	Alizé	1.5	2.3	1.4	1.3	2.2	1.9
		César	1.1	1.6	1.0	1.0	1.7	1.5
	$k / k_{AC\,B}$	Alizé	1	1.5	0.93	0.87	1.47	1.27
		César	1	1.45	0.91	0.91	1.54	1.36
Procedure 4	k	Alizé	2.7	4.1	2.1	2.0	3.2	2.7
	k	César	2.1	3.1	1.6	1.6	2.6	2.3
Procedure 6	k	Alizé	1.5	1.8	1.5	1.4	-	-
	k	César	1.2	1.4	1.2	1.2	-	-
Procedure 7	k	Alizé	1.1	1.2	1.4	1.3	-	-
	k	César	0.8	0.9	1.1	1.1	-	-

to 50 percent cracking on the pavements of the circular test track (values interpolated for Sectors I, II, and III and extrapolated for Sector IV) is equal to the number of cycles associated with 50 percent risk as determined by calculation with Alizé and César-LCPC.

For the calculations done both with Alizé and with César-LCPC, it is found that

1. k determined for AC A is substantially greater than that for AC B (1.6 for AC A against 1.1 for AC B, the usual value of the shift factor for an asphalt concrete);
2. The ratio of coefficients k for GB A and AC B ranges from 1.25 to 1.55. This value is larger than the one normally used (namely 1.3/1.1 = 1.2), but the orders of magnitude are comparable; and
3. k is smaller for EME than for AC B; the ratio between the two coefficients is close to 0.9.

Use of the Fatigue Characteristics Based on the Controlled Stress Tests

The study is repeated here using results of the controlled stress fatigue tests. The σ_6 values are corrected for temperature according to

$$\frac{\sigma_6(\theta)}{\sqrt{E(\theta)}} = C^{ste}$$

and referred to 15°C.

The tensile stress at the base of the asphalt layers determined by the calculations of Alizé and César-LCPC for 15°C and 10 Hz, used to determine the number of loading cycles, is the maximum of the longitudinal and transverse stresses. It is most often the longitudinal stress. These results are given in Table 5.

As previously, the coefficients k are determined (Table 5). When values of k are chosen to duplicate by calculation the life durations observed on the circular test track, some tendencies appear:

1. By Procedure 4, substantially different values of k are found for the two ACs (ratio approximately 1.5). The k found for EME is lower than those of the ACs; that of GB A is higher than that of AC B.
2. By Procedure 6, the k's for the two ACs are closer together (ratio approximately 1.2). For EME, k is of the same order of magnitude as for AC B. There is no value for GB A (no fatigue tests).
3. By Procedure 7, the k's for the ACs are similar. That for EME is slightly greater. No value is available for GB A.

These remarks are valid for the calculations done with Alizé and with César-LCPC.

Conclusions Concerning the Mechanical Analysis

This mechanical analysis points to the following conclusions:

1. When the loads are represented by circular wheel imprints, the calculation model gives strain values substantially different from those measured in the experimental structures. The model is improved by using rectangular imprints.
2. If only the conventional design method is considered, it is found that the large differences in life prediction between Sectors I and II result primarily from the differences in the values of ϵ_6 determined from the controlled strain tests. In addition, analysis of the relative behavior of the structures observed on the circular test track in the course of this first experimental phase appears to indicate that the value of the shift factor usually used for EME (1.1) is too high; a value of 0.9 to 1 appears more appropriate.
3. The results of the controlled stress fatigue tests by Procedures 6 (without rest periods) and 7 (with rest periods) lead, with similar coefficients k, to life durations comparable with those observed on the circular test track. This finding needs to be confirmed by a larger number of tests.

CONCLUSION

This experiment compared the behavior of four asphalt materials (two asphalt concretes made with 60/70 asphalt, one EME, and one asphalt-bound granular material) on the basis of their fatigue resistance as determined in the laboratory by different testing procedures and on the basis of full-scale tests on the circular fatigue test track. It was found that the test procedure strongly influences the ranking of the materials according to their fatigue behavior observed in the laboratory.

Analysis of the behavior of structures on the circular test track, using the design method normally used in France, shows the following:

- The relative behavior of AC B and AC A observed on the circular test track cannot be explained from the values of ϵ_6 determined by the continuous controlled strain fatigue test.
- It appears that the shift factor to be applied to EMEs, in light of the behavior observed on the circular test track, should be less than for asphalt concretes. The new proposed value is 1.
- The controlled stress fatigue tests give results for the two asphalt concretes AC A and AC B that appear to be in better agreement with the observed behavior of the pavements tested on the circular test track.

This experiment also served to determine the economic utility of solutions using high-modulus asphalt mixes (EME) in base courses, by comparison with conventional approaches using asphalt-bound granular materials. These are the lessons learned by Scétauroute, which will include new solutions including EMEs in the next issue of the Motorway Pavement Design Manual.

To confirm some conclusions and refine the analysis, it was decided to repeat the same experiment on the circular fatigue test track with the same materials. This experiment was run on the circular test track between October 1991 and January 1992, and the laboratory studies are still in progress (1993). The corresponding results and the comparison with the first experiment will be published later.

ACKNOWLEDGMENTS

This research program involved the participation of several organizations: for LCPC, the Circular Fatigue Test Track section, the Pavement Materials Laboratory section, the Pavement Design section, and the Road Binders section. The LRPC of Angers and Bordeaux have also been involved in the laboratory tests. For Shell, the research laboratories of Grand-Couronne (Rouen, France) and KSLA (Amsterdam, the Netherlands) participated.

REFERENCES

1. Autret, P., A. Baucheron de Boissoudy, and J.-C. Gramsammer. The Circular Test Track of the Laboratoire Central des Ponts et Chaussées—Nantes, First Results. Conférence internationale sur le dimensionnement des chaussées souples, Ann Arbor, Mich., July 1987.
2. Ramond, G., B. Dupeyrray, M. Pastor, and C. Such. Relation Between the Composition of Bitumens and Their Rheological Properties. *Proc., 11th International Congress on Rheology,* Elsevier Science Publishers BV, 1992.
3. Francken, L. Module complexe des mélanges bitumineux. Bull liaison Labo. P. et CH., spéc. V, Bitumes et enrobés bitumineux, 1977, pp. 181–198.
4. Moutier, F. Etude statistique de l'effet de la composition des enrobés bitumineux sur leur comportement en fatigue et leur module complexe. Bull liaison Labo. P. et CH., No. 172, March–April 1991, pp. 33–41.
5. Autret, P., A. de Boissoudy, and J.-P. Marchand. Alizé III, Practice. Fifth International Conference on the Structural Design of Asphalt Pavements, Delft University of Technology, the Netherlands, 1982, pp. 174–191.

Publication of this paper sponsored by Committee on Characteristics of Bituminous Materials.

Investigation of Rutting of Asphalt Surface Layers: Influence of Binder and Axle Loading Configuration

JEAN-FRANÇOIS CORTÉ, YVES BROSSEAUD, JEAN-PIERRE SIMONCELLI, AND GILBERT CAROFF

The increasing proportion of trucks with wide single-wheel axles makes asphalt pavements more vulnerable to creeping of the surface layers. Experiments on the circular test track of the Laboratoire Central des Ponts et Chaussées (LCPC) and laboratory tests focused on the effect of the type of binder [three asphalt-coated materials (a straight-run, conventional 50/70 grade bitumen; an SBS-polymer-modified bitumen; and the Shell Multigrade bitumen) and a very thin asphalt layer on a high-modulus coated material (hard bitumen 10/20 grade) were compared], the effect of the axle loading configuration (a wide single-wheel axle versus a traditional dual-wheel axle), and the capability of various laboratory tests (LCPC wheel tracking rutting test, static and dynamic creep tests) to rank the materials according to their resistance to rutting as observed on the test track. The observations made on the asphalt pavements and the results of the tests on the binders and the asphalt-coated materials are described. The higher aggressiveness of the wide single-wheel axles on the test track is discussed.

Truck traffic is growing substantially on French interurban routes, particularly motorways (a threefold increase in 15 years). Over the past 5 years, there has also been a change in the truck types, and on motorways 50 to 60 percent of trucks now have five axles with single-wide wheels. These changes have led to larger effects on asphaltic materials (*1*).

To better understand the effects of these changes, a major research program was begun in 1992 combining experiments using the circular test track of the Laboratoire Central des Ponts et Chaussées (LCPC) at Nantes and laboratory tests. This investigation was conducted as a joint study grouping LCPC, the Shell Company, and motorway operating companies under the aegis of the Union des Sociétés des Autoroutes à Péage, represented by Scétauroute.

OBJECTIVES OF THE STUDY

The experiment focuses on the study of permanent deformation of the surface course. The following aspects are considered: the binder effect on the rutting resistance of the wearing course with an asphaltic material sensitive to deformation, the incidence of the axle load configuration (the effect of wide single wheels is compared with that of dual wheels), selective or predictive character of the laboratory tests performed on the binder (usual tests and complex modulus) and on the asphalt mixtures (LPC rutting tester and static and dynamic creep tests) by a direct comparison of the indicators yielded by these tests with the behavior observed on the circular test track, and the procurement of reference data for a later evaluation of rutting calculation models using the results of laboratory tests. With regard to the first item, the parameters of the four pavement sectors of the circular fatigue test track (thickness, density, and composition) were identical except for the type of binder. The comparison was made between an SBS-modified asphalt, a Shell Multigrade (MG) asphalt having a low temperature sensitivity, a hard class 10/20 asphalt, and a standard class 50/70 pure asphalt taken as a reference.

J.-F. Corté and Y. Brosseaud, Laboratoire Central des Ponts et Chaussées, BP 19, 44340 Bouguenais, France. J.-P. Simoncelli, Société des Pétroles Shell, Direction Bitumes, 89 Boulevard Franklin Roosevelt, 92564 Rueil Malmaison Cedex, France. G. Caroff, Scétauroute-USAP, 23 Avenue du Centre, 78286 Saint-Quentin en Yvelines, France.

MATERIALS

Asphaltic Binders

The binders were chosen more or less in accordance with current practice for high-traffic pavements: for the asphalt base, a grade 35/50; and for the wearing course, the following:

- A 50/70 asphalt for the reference material (Sector I) even though current practice is tending toward grade 35/50;
- The Shell MG asphalt (*2*), recently developed to increase the rutting resistance of asphalt mixes while maintaining good behavior at low temperatures (Sector II);
- A hard asphalt traditionally used for high-modulus asphalt concretes (EME) (Sector III); and
- A binder modified by SBS, representative of an "average" product for this type of modified binder (3.8 percent of Cariflex type polymer as determined by infrared spectrometry) (Sector IV).

The binder identification tests were performed on the original binders before coating and after artificial aging in the laboratory (RTFOT), on the binders recovered by dissolution in trichloroethylene from asphalt mixes made in the plant before placement, and on the asphalt mixes sampled on the track after the experiment. The results of the tests are given in Table 1.

Complex moduli were determined on these binders. Figure 1, which deals only with the original binders, shows (*a*) curves in Black's space (phase angle versus modulus in logarithmic coordinates) for a frequency of 7.8 Hz and (*b*) isotherms (modulus versus frequency in log/log coordinates) at 25°C (mean tempera-

TABLE 1 Summary of Characteristics of Binders—Original Condition, After Passage Through Plant, Recovered After the Experiment, Artificially Aged in RTFOT

	Pure asphalt, class 50/70	Shell Multigrade binder	Hard asphalt, grade 10/20	SBS-modified asphalt
Sector	**I**	**II**	**III**	**IV**
Origin				
Pen 25°C (1/10 mm)	63	52	15.5	55.5
RBT (°C)	50.5	60.5	70.5	58.5
LCPC PI	- 0.2	+ 1.1	+ 1.1	+ 0.1
PFEIFFER PI	- 0.5	+ 1.2	+ 0.4	+ 0.8
After production in plant	*	*	*	*
Pen 25 °C	45	36	13	46
Residual pen (%)	(71)	(69)	(84)	(83)
RBT	53	61.5	75.5	57
Δ RBT (°C)	(+ 2.5)	(+ 1)	(+ 5)	(≃ 0)
LCPC PI	-	-	-	-
PFEIFFER PI	- 0.7	+ 0.5	+ 0.8	+ 0.2
After recovery at end of experiment				
Pen 25°C	47	41.5	14.5	44
Residual pen (%)	(75)	(79)	(94)	(85)
RBT	55.5	60.5	76.5	58.5
Δ RBT (°C)	(+ 5)	(0)	(+ 6)	(0)
LCPC PI	+ 0.1	+ 1.5	+ 2.1	+ 0.9
PFEIFFER PI	- 0.1	+ 0.7	+ 1.2	+ 0.4
After RTFOT				
Pen 25°C	37	31.5	13	38.5
Residual pen (%)	(61)	(58)	(81)	(75)
RBT	59	70.5	75	61.5
Δ RBT (°C)	(+ 8.5)	(+ 10)	(+ 4.5)	(+ 3)
LCPC PI	+ 0.7	+ 2.0	+ 1.2	+ 0.2
PFEIFFER PI	+ 0.1	+ 1.8	+ 0.8	+ 0.7

* Shell tests

ture of the experiment), 40°C (approximately the maximum ambient temperature in the test track experiment, temperature of the creep tests), and 60°C (temperature of the tests with the LPC rutting tester).

In Black's diagram, the Shell MG binder appears as the most structured of the pure asphalts (Sectors I, II, and III). The SBS-modified asphalt exhibits a curve that is characteristic of this type of binder: at high moduli (high frequency or low temperature) the character of the basic asphalt is preponderant and the curve corresponds to a fairly unstructured binder, whereas at low moduli (low frequencies or high temperatures) the phase angle exhibits a plateau shape reflecting the lower sensitivity of the polymer binder.

Whereas there is little or no difference between the binders of Sectors I, II, and IV for the isotherm at 25°C, differences in behavior start to appear at 40°C. These differences are accentuated at 60°C, at which temperature the 50/70 asphalt exhibits the lowest modulus values.

The lower kinetic sensitivity found at 40°C for the MG binder in relation to that of the SBS-modified asphalt is confirmed at 60°C; its modulus of rigidity is also higher. However, the differences between these two binders are not very pronounced.

The hard asphalt (Sector III) exhibits the highest moduli in all cases. As an illustration, a modulus of 0.1 MPa at a frequency close to 10 Hz corresponds to a temperature of 55°C for the 50/70 asphalt (Sector I), 60°C for the SBS-modified asphalt (Sector IV), 62°C for the MG binder (Sector II), and 80°C for the hard asphalt (Sector III).

This gives a classification of the four binders in terms of increasing sensitivity to the combined effects of temperature and loading time.

Aggregates

The aggregates come from Cusset, the sand of which is produced by grinding. The rock is a rhyolitic tuff. The main mechanical and production properties of these aggregates are as follows: Los Angeles coefficient, 10 to 13; wet Micro-Deval coefficient, 4 to 9; and flatness coefficient (2/6 and 10/14 fractions), 15 and 13, respectively. These characteristics comply with the specifications for the production of asphalt mixes and exhibit no singularity.

The ground sand is produced in a bar mill from a 0/2 mm sand containing 13 percent fines. The mill yields a sand having a high fines content of 18 to 20 percent, but with grain edges that are particularly blunted and rounded. This is reflected by the sand flow test (standard NF P 18-564): ground Cusset sand, 35 s; crushed Cusset sand, 41 s (repeatability r = 1.2 s).

The fines produced by grinding have less "stiffening power" on the asphaltic mastic (increase of RBT due to the incorporation of 6 percent fines) than those produced by crushing (+14°C to 16°C for the ground sand, +19°C to 20°C for the crushed sand).

Composition of the Asphalt Mixes

The design of the mix of asphaltic materials was primarily based on the results of the LPC rutting tester. The objective was to define (*a*) for the road base, an asphalt concrete having a very good rutting resistance (no deformation of this layer was actually observed on the circular test track) and (*b*) a reference wearing course asphalt mix (Sector I) particularly sensitive to rutting. The mixture selected at the end of the preliminary tests was a 0/14 densely graded Cusset asphalt concrete with 32 percent ground sand including 1.5 percent added fines (total fines 7.5 percent) and 5.7 percent Class 50/70 asphalt. The corresponding rutting in the LPC rutting test was 11 percent after 3,000 cycles, whereas the standard for thick-layer asphalt concrete calls for less than 10 percent rutting after 30,000 cycles.

This mix is analogous to the case of a motorway site where a rut depth of 1.5 to 2 cm was observed after 2 to 3 years of traffic with a corresponding result of 12 percent rutting after 4,000 cycles with the LPC rutting tester.

Only the type of binder was changed for Sectors II and IV. For Sector III the proportion of hard 10/20 asphalt was raised to 6.0 percent since the wearing course consisted of a very thin asphalt concrete (VTAC, 2 cm) having a usual composition: 0/10 with 2/6 gap, crushed La Noubleau aggregates, with 25 percent sand and 6.0 percent SBS-modified asphalt.

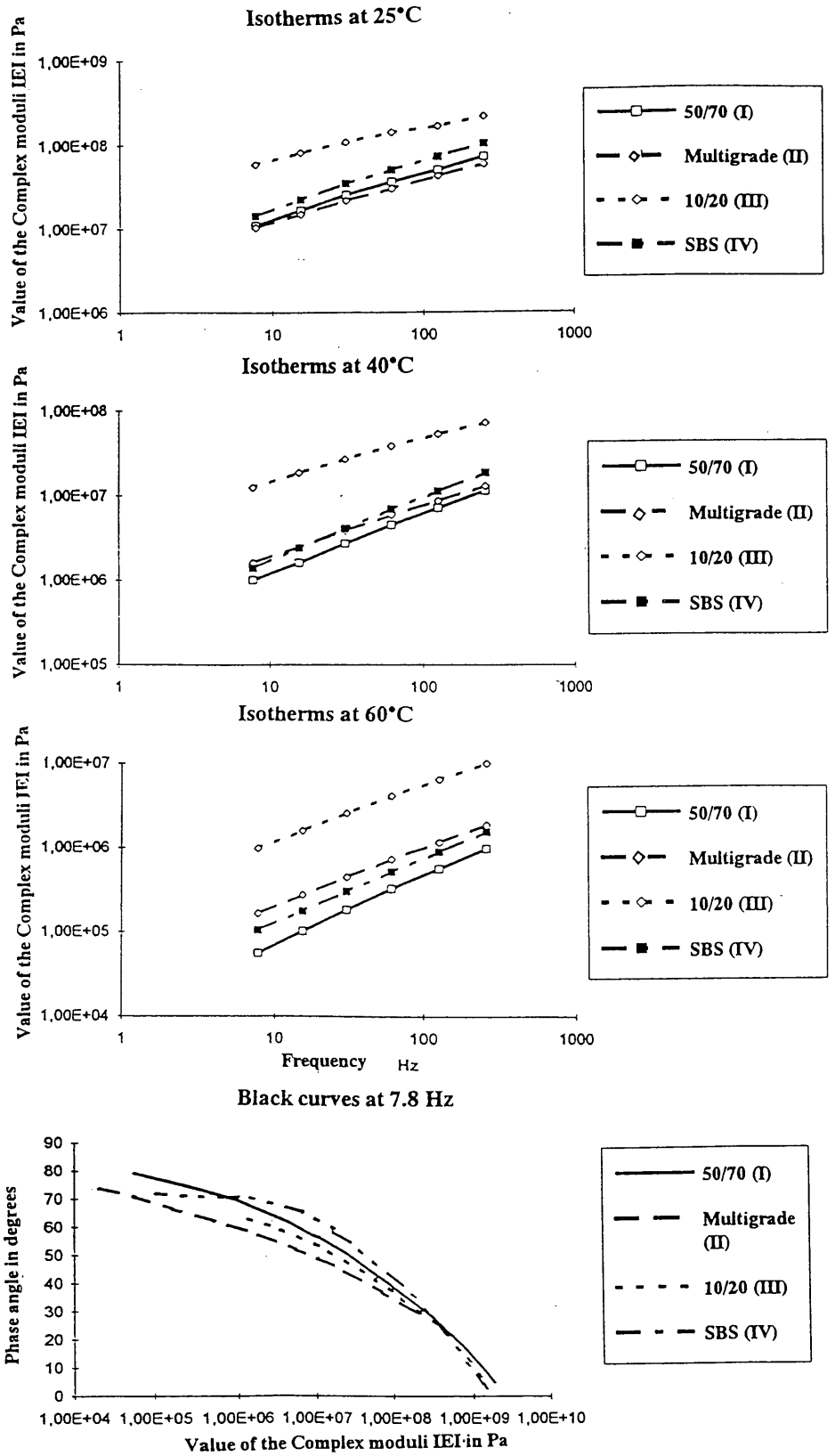

FIGURE 1 Isotherms of the binders' complex moduli at 25°C, 40°C, and 60°C and Black curves.

The gyratory shear press tests (standard NF P 98–252) confirm the high workability and compactibility of the materials due to the ground sand. Between 28 and 36 percent ground sand the voids content at 80 gyrations varies only from 4.7 to 4 percent. The rutting tests are performed at a voids content of 4 percent, which is the value also obtained for the pavements of the circular test track.

LABORATORY TESTS ON THE ASPHALT MIXES

Results with LPC Rutting Tester

In this standard test (NF P 98-253-1) performed at a temperature of 60°C, a slab of asphalt mix (10 cm thick here) is subjected to the passage of a rolling load (tire inflation pressure 0.6 MPa, load 5000 N) at a rate of one forward and return cycle per second. The graph, on log/log coordinates of the percentage of rutting versus the number of cycles, is generally a straight line for a material that is properly resistant to rutting. This test is an integral part of the French methodology for investigating asphalt mixes (*3*). The effect of the various parameters of the composition is determined on the 0/14 Cusset reference formulation with pure 50/70 asphalt.

Grading

Figure 2 shows the effect of the percentage of ground sand in the range 28 to 36 percent. It appears that below a threshold of 30 percent the mix exhibits good rutting resistance, since the test continued to 30,000 cycles with less than 10 percent rutting.

If the 2/10 Cusset coarse aggregates are replaced by La Noubleau aggregates, the rut depths are unchanged for the same proportions of ground sand. It is therefore the nature of the ground sand that results in the poor rutting resistance beyond a certain percentage of ground sand (30 percent) (*4*).

Binder

The type of binder is preponderant, as is shown by Figure 3, which gives the results for the four formulas tested on the circular test track. The SBS-modified, hard, and MG binders clearly improve the rutting resistance of the asphalt mixes. Whereas there is no difference between the SBS-modified asphalt and the MG binder up to 3,000 cycles, beyond this the SBS-modified asphalt exhibits a rut that grows rapidly. No decisive explanation has yet been found for this change of behavior.

Creep Tests on the Asphalt Mixes

Static Creep Test

This test consists of applying a static axial stress of 0.1 MPa on the upper part of a cylindrical specimen kept in water at a temperature of 40°C. The axial strain of the sample is recorded as a function of time (Figure 4). For conventional asphalts, a correlation has been found between rutting performance (measured using a laboratory test track developed by Amsterdam Shell Laboratory, KSLA) and two parameters drawn from this Smix/Sbit curve (slope and intercept).

Dynamic Creep Test

Since the static creep test presents some drawbacks for various types of mixes, a dynamic creep test was developed to take into account the recovery of the strain when the load is no longer applied. The principle of this dynamic creep test consists of applying a series of 0.1-MPa loads for 0.2 sec followed by rest periods of 1.8 sec. The test is typically performed at 40°C. The cumulative residual strain is recorded as a function of time (Figure 5).

EXPERIMENT ON LCPC'S CIRCULAR TEST TRACK

Description of Experiment

The experiment on LCPC's circular test track (*5*) was carried out on a pavement consisting of four sectors, the structures of which

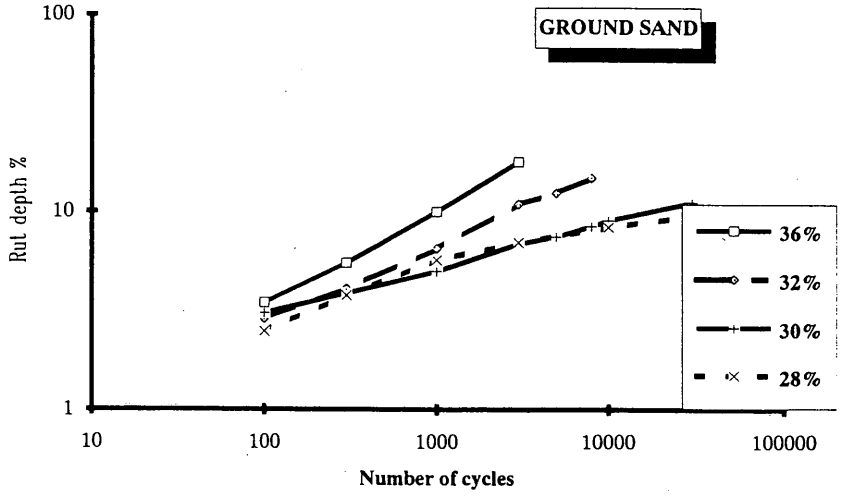

FIGURE 2 Influence of the percentage of ground sand on the rut depth (LCPC wheel tracking rutting tester).

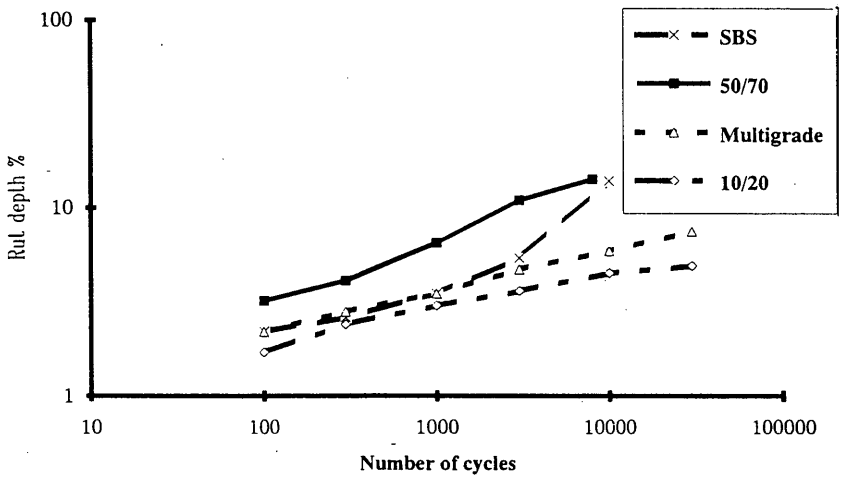

FIGURE 3 Influence of type of binder on rut depth (LCPC wheel tracking rutting tester).

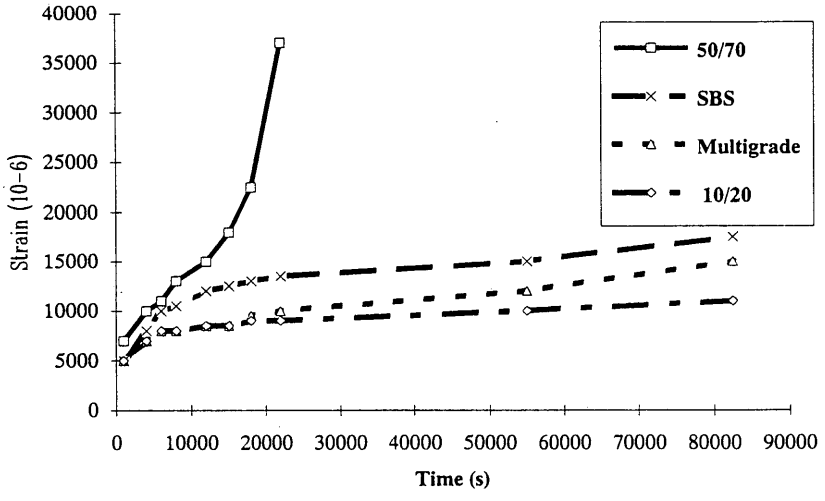

FIGURE 4 Results of static creep tests (Shell method).

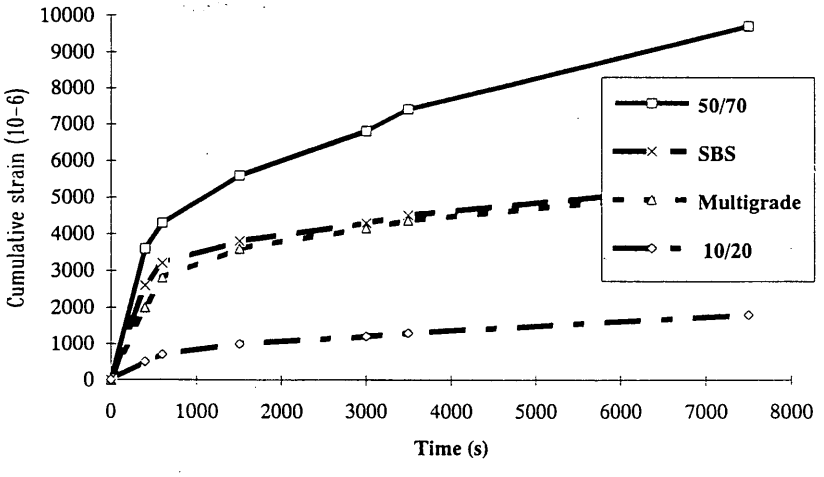

FIGURE 5 Results of dynamic creep tests (Shell method).

are shown in Figure 6. The experiment was conducted in two phases with two different configurations of the loading arms. For the first phase (202,000 loading cycles), the four axles traveling different paths had the following configuration: single wheels at radii of 16.5 and 19.5 m and dual wheels at radii of 15.5 and 18.5 m. The purpose of this arrangement was to judge the effect of the difference in traffic speed imposed by the simultaneous application of two loading arrangements.

For the second phase (from 202,000 to 250,000 loading cycles), the two axles equipped with wide single wheels were placed at the same radius of 19.50 m, and the two dual wheels at 18.50 m. The loads were 42.5 kN for the wide single wheel and 65 kN for the pair. The tire inflation pressure was 0.85 MPa. Under these conditions the imprint survey indicated the following: for the wide single wheel, a contact area of 636 cm^2 (mean contact pressure, 0.67 MPa); for the dual wheels, a contact area of 567 cm^2 per tire (mean pressure, 0.57 MPa).

For the first phase, the speed of rotation of the circular test track was fixed at 6.5 rpm. The tangential speed therefore varied from 38 km/hr at a radius of 15.5 m to 48 km/hr at 19.5 m. The width of the rolling strip swept was 0.75 m for the single wheel and 1.0 m for the dual wheels. For the second phase, the experiment was continued with the loads channeled and the speed of rotation reduced to 3 rpm.

Temperatures During the Experiment

The ambient temperature and temperatures at the surface and at various depths were monitored hour by hour for the duration of the experiment. Figure 7 shows the ambient temperature during the first phase versus the number of passages. There were fewer than 2,000 revolutions at more than 30°C ambient; the mean temperature was in the vicinity of 21°C. For the second phase, the temperatures were lower, always below 30°C, with a mean value of the order of 19°C. Values recorded at the surface were higher than the ambient temperature, up to 55°C.

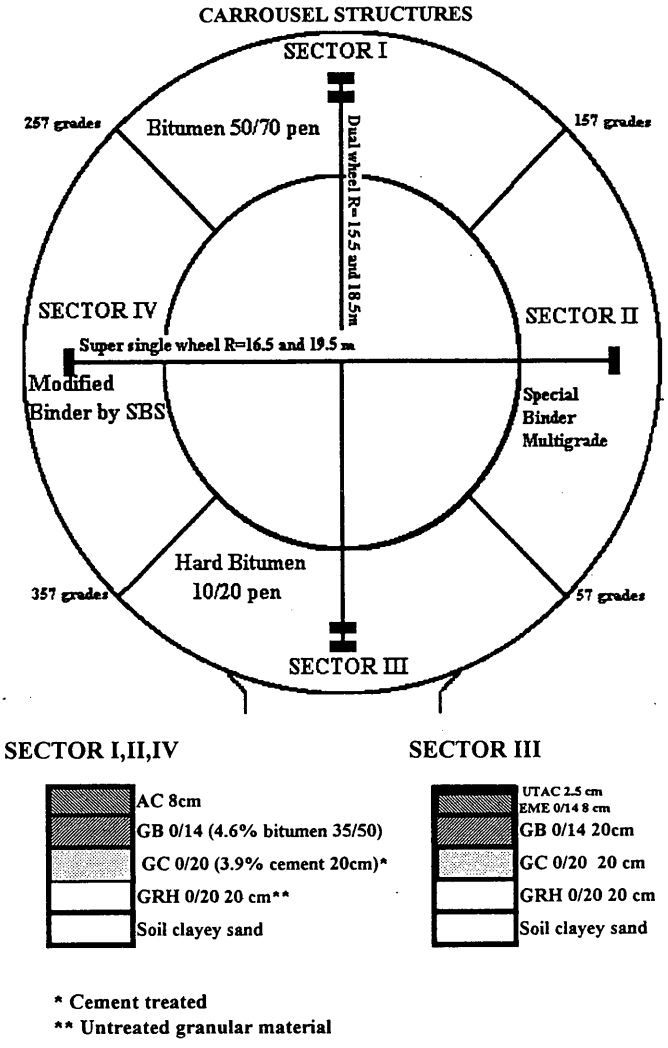

FIGURE 6 Description of pavement sectors.

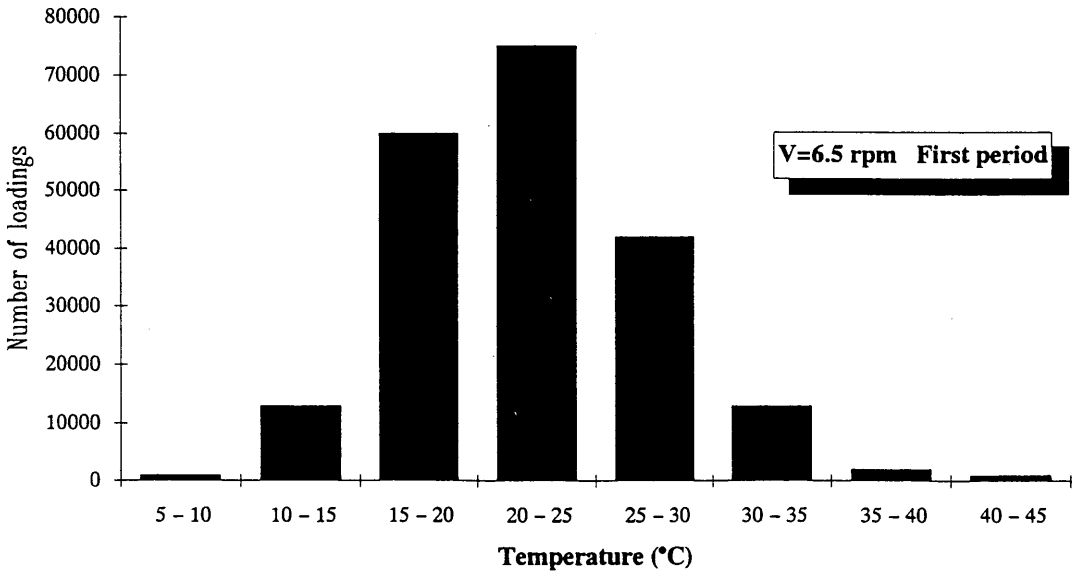

FIGURE 7 Description of ambient temperature.

Figure 8 shows when during the experiment the temperature at the middle of the asphalt mixes of the wearing course of Sector I exceeded 40°C. There were few such periods, for 1,000 passages toward 20,000 cycles and for 10,000 passages between 50,000 and 90,000 cycles total traffic.

Evolution of Rut Depth

Figure 9 shows, for the four sectors, the evolution of maximum rut depth (mean value of the maxima recorded on five transverse profiles per sector) for the wheelpath at the mean radius of 16.5 m (wide single wheel). Figure 10 shows the results for Sector I.

Table 2 gathers the rutting values for the four sectors and the four wheelpaths at the end of the first phase of the experiment.

The rate of increase of rut depth is greatest for the period between 20,000 and 91,000 loadings, which corresponds to the period of the highest temperatures. In the second phase, although the loads were channeled and the speed cut in half, there was practically no rut depth evolution. These two findings reveal the essential incidence of temperature.

First Analysis of Experiment Results

The foregoing data show that the rut depth depends on the configuration of the axle and on the radius of the path and does not increase regularly with the number of loadings (nonuniform temperature conditions over the duration of the experiment).

Since the temperature, the speed of translation of loads, and the axle configuration act in combination, it is difficult to make direct term-by-term comparisons without a global explanatory model. In a first analysis, an attempt is made here to isolate some tendencies by introducing several simplifying assumptions.

Comparison Between Sectors

The ranking of the sectors with reference to the rut depth is the same for all wheelpaths. Sector I, with pure 60/70 asphalt, exhibits the largest deformations, more than 12 mm. At the opposite extreme is the EME + VTAC solution, which exhibits the smallest deformations, between 3 and 5 mm. Sector II, with the Shell MG binder, and Sector IV, with the SBS-modified asphalt, exhibit similar intermediate performance, with deformations between 5 and 7 mm.

Influence of Loading Speed

Between 19,000 and 91,000 cycles, the increase of rut depth and speed vary roughly in inverse proportion for the materials of Sectors II, III, and IV. In the case of Sector I, for which the influence of the speed is more marked, the results may have been affected by the segregation recorded along the transverse profile when the asphalt mix was placed.

Influence of Axle Configuration

The 42.5-kN wide single-wheel axle turns out to be more aggressive than the 65-kN axle with dual wheels. The mean contact pressure of the former is 0.67 MPa, whereas for the latter it is 0.57 MPa.

To refine the comparison, it is first necessary to correct the observations for the influence of speed, because the paths are not the same. The period between 19,000 and 91,000 cycles will be considered here by interpolating, for each axle configuration, a rut depth for a radius of 17.5 m (traffic speed of 43 km/hr).

Table 3 indicates that the effect of the axle configuration depends on the material. The greater the aggressiveness of the wide single wheel in relation to that of the pair, the more sensitive the mix is to rutting. For the same number of axle loads, the ratio of rut depths ranges here from 1.1 to 1.6.

In a first analysis, the mean contact pressure is compared with the rutting depth by a relation such as the following:

$$(q/q_0)^{\alpha} = d/d_0$$

where

q = 0.67 MPa is the mean contact pressure of the single wheel,

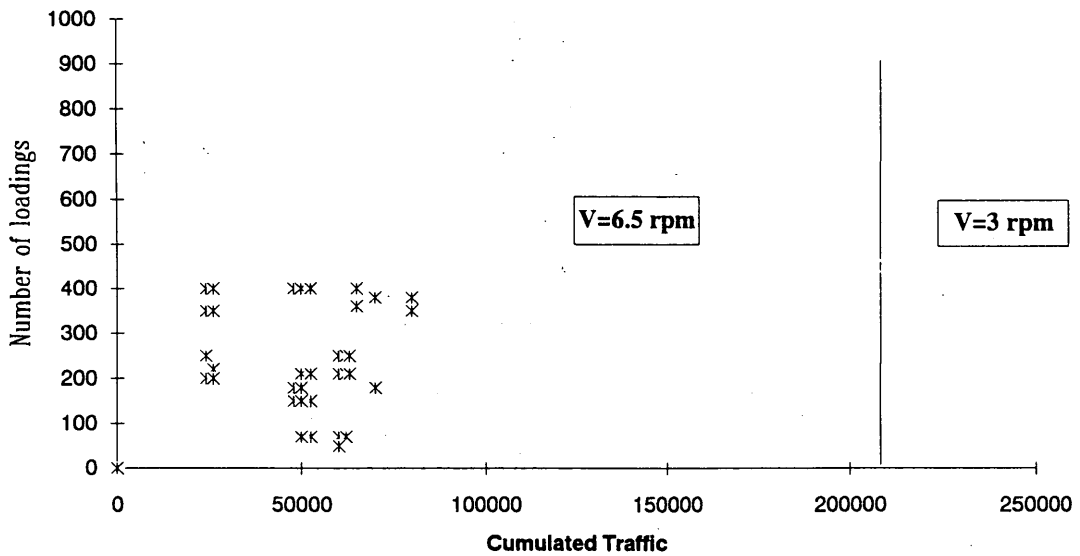

FIGURE 8 Period of test corresponding to asphalt concrete temperature higher than 40°C.

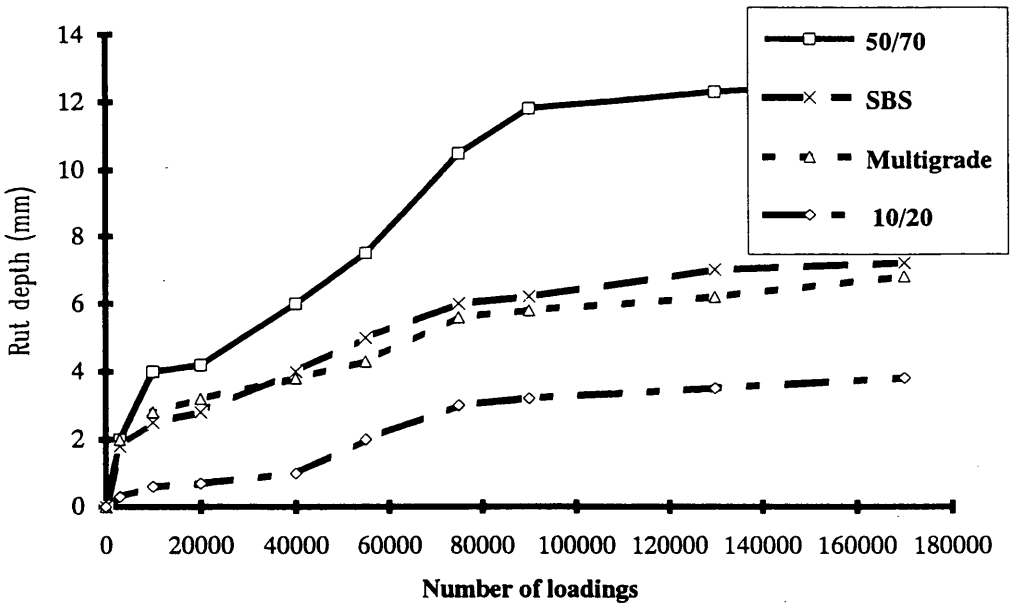

FIGURE 9 Test track results: rut depth evolution on the four sectors (wide single wheel, r = 16.5 m, V = 40 km/hr).

q_0 = 0.57 MPa is the mean contact pressure under a wheel of the pair,
d = rut depth produced by the single wheel, and
d_0 = rut depth produced by the dual wheels.

Hence α ranges from approximately 1 for asphalt mixes made with hard or modified binders to 3 for the mix made with 50/70 asphalt on Sector I.

Comparing the aggressiveness in terms of rutting of a 210-kN road trailer on a tridem axle with wide single wheels with that of the same load carried by a tandem axle with twin wheels, with α = 2 to be representative of common asphaltic materials, we find that the tridem axle is roughly 1.5 times as aggressive as the tandem axle (for the temperature conditions of the fatigue test track experiment).

COMPARISON OF RESULTS OF LABORATORY TESTS AND TEST TRACK EXPERIMENT

There is good agreement between the qualitative rankings yielded by the different laboratory tests on the binders and the asphalt

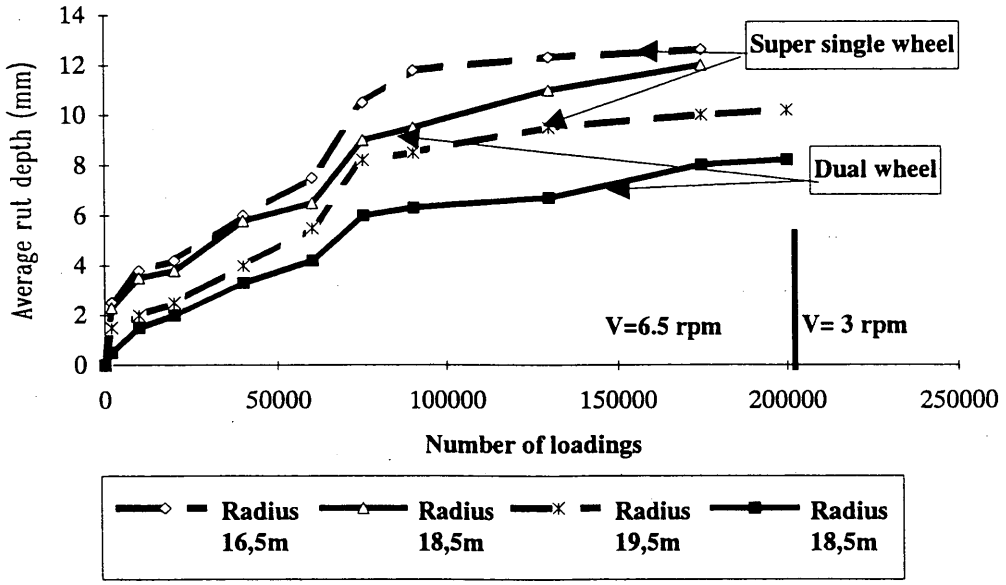

FIGURE 10 Rut depth evolution for Sector I.

TABLE 2 Rut Depths (mm) After 202,000 Loadings

	radius 15.5m J	radius 16.5m RS	radius 18.5m J	radius 19.5m RS
sector I 60/70 asphalt	11.8	12.6	8.2	10.2
sector IV SBS asphalt	6.7	7.2	5.6	6.9
sector II Multigrade	5.8	7.2	4.2	5.1
sector III EME + VTAC	4.9	3.7	2.9	4.7

J: dual wheels RS: wide single wheel

mixes and those corresponding to the deformations obtained on the test track. It is more difficult to judge the results of the tests in quantitative terms, since there are still only a limited number of observations.

Tests on Binders

In a first analysis with the pure asphalts (50/70, 10/20, and MG binder), the RBT turns out to be a good indicator of sensitivity to rutting, but it is not sufficient (*6,7*). Complementary tests measuring the complex modulus provide information about the structured character of the binder (or otherwise) and its temperature and kinetic sensitivity. For the four binders tested, classification by the isotherm at 40°C or 50°C at various frequencies agrees with the classification of the asphalt mixes on the test track.

Tests Using the LPC Rutting Tester

The classification correctly matches the behavior of the asphalt mixes made with pure asphalt of Sectors I, II, and III for all of the rutting curve. The asphalt mix of Sector IV including the SBS-modified asphalt, however, is difficult to characterize because its behavior changes during the test.

Creep Tests

As expected, the dynamic creep test appears to be more representative of what happens in the field. Indeed, a good correlation has been achieved (compare Figures 5 and 9). Thus, we can consider that this dynamic creep test shows promise for predicting the rutting performance of the types of mixes considered in the study.

TABLE 3 Estimated Rut Depths for a Single Path Radius of 17.50 m

Sector	I	II	III	IV
Dual wheels (J)	3.8	2.2	2.5	3.2
Wide single wheel (RS)	6.1	2.6	2.7	3.6
RS/J	1.60	1.18	1.08	1.12

CONCLUSIONS

This study has yielded useful knowledge of factors influencing rutting:

- The type of binder affects the improvement of the rutting resistance of an unstable granular mix. The use of a hard asphalt (grade 10/20) in an approach combining high-modulus asphalt mixes with wearing courses of VTAC is confirmed as very effective. It is routinely used on French motorways when the surface layer is also expected to make a structural contribution to the pavement. The use of an asphalt modified by SBS polymers or of the Shell MG asphalt gives the wearing course better rutting resistance than a pure asphalt of the same penetration class (50/70).
- The means of production of the sand is important to rutting resistance. A ground sand has many rounded edges and makes the asphalt mixes more workable. Above a certain proportion of ground sand, the asphalt mixes containing a "standard" asphalt of average grade (50/70) have a poor rutting resistance. The fines of this sand generally have a rather low stiffening power, and the mastic is more sensitive to temperature variations.
- Axles with wide single wheels are more aggressive than dual wheels. The rutting as a result of this effect also depends on the type of asphalt mix, and the more sensitive the asphalt mix is to rutting, the more pronounced the effect seems to be. However, it is still difficult to isolate from this single experiment a law of load aggressiveness.
- Use of the LPC rutting tester is valuable in ensuring that a mix will have a good rutting behavior insofar as it satisfies the standard specifications. It turns out that this test can also be used for determining the influence of the compositional factors of the asphalt mixes on rutting resistance. The test seems satisfactory for classifying asphalt mixes according to their sensitivity to rutting on site.
- The dynamic creep test, in which the loading cycle includes a rest period, is useful in establishing a ranking of asphalt mixes similar to what was observed on the circular test track.
- Characterization of binders by the complex moduli that reflect the combined effects of loading rate and temperature is useful. The observed tendencies in the sensitivity of the binders here are in agreement with their ranking according to the sensitivity to deformation of the asphalt mixes.

The processing of the results of this experiment is not completed. Tests for determining the rheological properties of asphalt

mixes are still being carrried out. Studies based on the results of laboratory tests and using calculation models will follow, with the results of the experiment on the test track as a reference.

ACKNOWLEDGMENT

This research program was carried out with the participation of several groups: for LCPC, the Circular Fatigue Test Track and Pavement Materials Laboratory Sections of the Pavement Materials and Structures Division and the Road Binders Section; and for Shell, the laboratories of Shell Research Grand-Couronne and KSLA (Amsterdam).

REFERENCES

1. Bertaux, J.-M., J.-P. Simoncelli, and M. Faure. Rutting of Asphaltic Mixtures. *Eurobitume*, Stockholm, Sweden, June 1993 (in French).
2. Robertus, C. Shell Multigrade Bitumen: Binder for High Stability Asphalt. *Eurobitume*, Stockholm, Sweden, June 1993.
3. Brosseaud, Y., J.-L. Delorme, and R. Hiernaux. Use of LPC Wheel-Tracking Rutting Tester To Select Asphalt Pavements Resistant to Rutting. In *Transportation Research Record 1384*, TRB, National Research Council, Washington, D.C., 1993.
4. Panis, A., et al. Stability of Asphaltic Asphalt Mixes for Roadbases or Base Courses Made with More or Less Angular Alluvial Aggregates. *Bulletin de liaison des Laboratoires des Ponts et Chaussées*, No. 174, July 1991 (in French).
5. Gramsammer, J.-C. The LCPC's Circular Test Track and Research. *Revue Générale des Routes et Aérodromes*, June 1991 (in French).
6. Barbé, B. Effect of the Asphalt, Aggregates, and Mixture Composition Factors on the Rutting Resistance of Asphalt Mixes in the Laboratory. *Revue Générale des Routes et Aérodromes*, 1988 (in French).
7. King, G. N., et al. Influence of Asphalt Grade and Polymer Concentration on the High Temperature Performance of Polymer Modified Asphalt. *AAPT*, Vol. 61, 1992.

Publication of this paper sponsored by Committee on Characteristics of Bituminous Materials.

Effect of Composition on Asphalt Recycling Agent Performance

G. D. PETERSON, R. R. DAVISON, C. J. GLOVER, AND J. A. BULLIN

Experiments have been conducted to determine the effect of metals, asphaltenes, and paraffins (oils and waxes) content on the properties of recycled aged asphalts. Recycling agents were produced by using a large Corbett type apparatus to fractionate asphalt fractions that had been previously separated from asphalt by supercritical fractionation. The material was separated into asphaltenes, aromatics, oils, and waxes, which were mixed in different ratios and blended with oxidized asphalts. The blends were then aged to study the composition effects during aging. In general, metals had little effect. Asphaltenes increase the hardening rate but not the oxidation rate. The effect of saturates depended on the asphaltene content. Waxes showed little, if any, effect on the measured properties. In general, highly aromatic recycling agents yielded material superior in the measured properties to the original asphalts.

Recycling of asphalt pavements is a very attractive concept, both environmentally and economically. Currently, about 27 million tons of asphalt binder and half a billion tons of rock are consumed each year in the building and maintenance of the nation's roads. Reuse of a significant portion of this material would eliminate an enormous amount of waste and greatly reduce the cost of our transportation system. Furthermore, if the recycling process could be used to optimize and improve the performance of the pavement, the costs of road maintenance could be reduced, and the general quality of roads could be improved.

During asphalt oxidative aging, the saturates (also known as paraffins) remain the same while the solubilizing aromatics decrease in quantity. The aromatics react with oxygen to produce asphaltenes, which causes the asphaltene content to increase. Because the saturates and asphaltenes are not soluble in one another, the increase in asphaltenes, accompanied by the decrease in solubilizing aromatics, leads to incompatibility. The incompatibility causes sharply increased viscosities and decreased ductility.

The softening agents presently used are often just a soft asphalt, which does little or nothing to improve, and can even exacerbate, the instability within the binder material. Thus, recycling agents that will reestablish the compatibility and performance of the old material on a long-term basis are much needed.

The main objective of this research is to determine what types of materials are suitable for use as asphalt recycling agents. Any material under consideration must of course be low in viscosity, so that the aged material can be blended back to new asphalt viscosity, using the smallest amount of recycling agent possible. Furthermore, the material must be highly aromatic, to replace the aromatic materials that have been consumed by oxidation reactions. It must be low in asphaltenes to maintain low viscosity and because the aged asphalt is already too rich in asphaltenes. Finally, recycle blends should have good aging characteristics.

Texas Transportation Institute, Texas A&M University, College Station, Tex. 77843-3122.

METHODS

To produce recycling agents of specific compositions and measure their effects on the aging properties of reblended asphalts, experiments were designed in which the various components were produced, mixed in controlled amounts, and artificially aged. Typically, the materials used for recycling agents were fractionated using a procedure based loosely on the one developed by Corbett (*1*). The aim of this "Giant Corbett" procedure was to produce similar fractions, but in larger amounts than the Corbett procedure. Tank asphalts were artificially aged and recycling agents were mixed with them, yielding reblended asphalts that could be tested by artificial aging in a pressurized oxygen vessel (POV). The basic properties of interest in these experiments were the zero shear viscosity and the carbonyl area, an indicator of oxidation obtained through infrared spectrometry. These properties were measured on aged and unaged blends. In one experiment it was also necessary to measure the nickel and vanadium content of the samples using atomic absorption. It has been shown that the amount of increase of ln (viscosity) relative to the corresponding increase in carbonyl area is a unique linear function for each asphalt (*2,3*) and is an excellent measure of aging. It is called the hardening susceptibility.

The modified Corbett procedure was a fractionation based on polarity. It was used to separate asphalt into four fractions—asphaltenes, polar aromatics, naphthene aromatics, and paraffins—in analytical amounts. The enlarged version was developed to produce these or similar fractions in larger amounts. Using the Giant Corbett procedure, a sample of up to 250 g may be processed, also yielding four fractions: asphaltenes, which roughly correspond to Corbett's asphaltenes; aromatics, which are basically a mixture of polar and naphthene aromatics; oils; and waxes. The asphaltenes are separated by precipitation, and the aromatics and paraffins are split by adsorption-elution chromatography on an enlarged alumina bed (about 1 kg). The last two fractions come from a further separation of the paraffin fraction based on the procedure described by Hoiberg and Garris (*4*).

The sample to be fractionated, either asphalt or supercritical fraction, is dissolved in 10 mL of hexane per gram of material and vacuum filtered. If asphaltenes are present, they are collected on the filter. The material still dissolved is then recovered using the Abson procedure, ASTM D1856-79, and redissolved in n-heptane. This solution is poured over a bed of activated alumina. A mixture of paraffin and solvent flows into a reboiling flask, where the solvent is boiled away, recondensed, and allowed to flow back into the top of the column and into the alumina bed. Over 3 hr this removes all of the paraffinic material, which, when recovered, resembles petrolatum in appearance and texture.

Once the paraffins have been removed from the bed, the column is drained of heptane. A new solvent composed of 85 percent

trichloroethylene and 15 percent ethanol dissolves the aromatic material adsorbed on the bed. Over another 3 hr this fraction, which contains both the naphthene and polar aromatics, is recovered and reported as aromatics.

The paraffins are dissolved in a solvent composed of two parts dichloromethane and one part acetone. This solution is then chilled to 0°C and vacuum filtered. The solid collected is a white or yellowish wax and is reported as waxes. The material that remains dissolved, when recovered, is a light yellow or brown oil and is reported as oils.

Although the asphaltenes may be slightly different from Corbett's asphaltenes due to the use of hexane rather than heptane for the precipitation, the difference is one of necessity. To ensure that all of the heptane-insolubles, which will plug the alumina column very quickly, are removed, it is necessary either to precipitate the asphaltenes from a highly dilute solution (100 mL solvent per gram of asphalt) or to use a weaker solvent. Corbett analysis of the fractions indicates that the aromatics contain no paraffins and that the paraffins contain no aromatics. However, IR analysis shows some aromatic pressure in the oils.

Supercritical fractions were obtained in a four-stage pilot unit capable of producing kilogram quantities of material (*5*). For this study two runs were made on the asphalt. The first removed asphaltenes and produced a large lower-molecular weight material fraction. This fraction was rerun to produce four more fractions. The lightest of these fractions is designated as Fraction 1 and the next as Fraction 2, and these were used in this study in several experiments.

To produce large amounts of aged material suitable for recycling, tank asphalts from various sources were artificially hardened in the laboratory by bubbling oxygen through molten asphalt at 450°F. Asphalts were also artificially aged in the POV. This was done at 190°F and 300 psia oxygen for some previously determined time period.

Once suitable materials were obtained or created using the preceding procedures, they were blended in controlled ways to test the effect of each fraction on the overall properties. A typical test blend consisted of a recycling agent, either selected from some available material or made up of the various Giant Corbett fractions, which was mixed with an aged asphalt. A series of blends was designed in each experiment to test the various compositional effects and artificially aged in a POV. This procedure is described by Lau et al. (*3*).

A Carri-Med CSL-500 controlled stress rheometer was used to measure the zero-shear complex viscosity of the samples at 60°C.

A Mattson Galaxy Series 5000 FTIR was used to measure the infrared spectra of samples using the attenuated total reflection (ATR) method, in which the IR beam passes though a prism and reflects off the inside of the sample surface (*6*). A slight penetration of the beam into the sample allows measurement of the spectra.

The trace metal content, specifically that of nickel and vanadium, was determined using an atomic absorption method based on the method described by Davison et al. (*7*), but which allowed use of smaller sample size and more efficient sample preparation.

EXPERIMENTAL DESIGN AND RESULTS

To accomplish the goals of the research several experiments were performed. They involved selecting or producing materials, making blends from these materials, and performing POV aging tests on the blends. The experiments were designed to examine the following properties: effect of oils on aging of aromatic fractions; effect of metals and asphaltenes on aging; and effect of oils, waxes, and asphaltenes on reblended asphalt aging.

Some temperature gradient problems made kinetic analysis impossible in several experiments, but this does not affect the hardening susceptibility, which is independent of aging temperature.

Oils and Aromatics (Experiment 1)

On the basis of considerations already discussed, it was decided that the Giant Corbett aromatic fraction would be a good material to use as a recycling agent. However, it was found that aromatic fractions from asphalt had viscosities at 60°C as high as 4000 poise and that even aromatics from light supercritical fractions were a minimum of 100 to 200 poise. To bring the recycling agents into the required range, low-viscosity (typically less than 2-poise) oils could be added, but their effect on aging would have to be examined. To do this, a Fina supercritical fraction #1 was fractionated into four components using the Giant Corbett. From the oils and aromatics, three blends were made. They contained 20, 40, and 60 percent oil, respectively. These blends were POV aged at 180°F and 300 psia along with the pure oil and pure aromatic for periods of 4, 8, 12, and 16 days. Both change in ln viscosity and carbonyl are linear in time, and a plot of ln η versus carbonyl (Figure 1) yields the hardening susceptibility as the slope.

The pure oil fraction experienced little or no aging during the test period. As the oil content of the blends decreased, the viscosity and carbonyl aging rates increased for all of the blends that contained oil. This trend did not apply to the pure aromatic fraction, which had lower aging rates after 4 days than the 20 percent oil blend, but this almost certainly was due to the temperature gradient in the POV together with the hypothesis that the aging rates should actually have been an average of the rates for the pure components. This possibility is supported by the hardening susceptibilities (a property independent of aging temperature) and their linear dependence on oil content as shown in Figure 2. The hardening susceptibility of each blend is actually an average of the hardening susceptibility of its components.

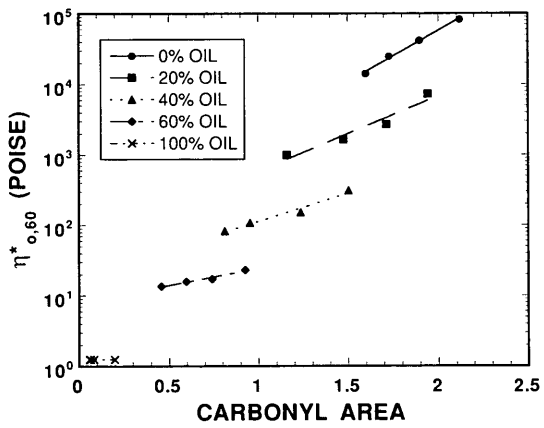

FIGURE 1 Experiment 1: hardening susceptibilities.

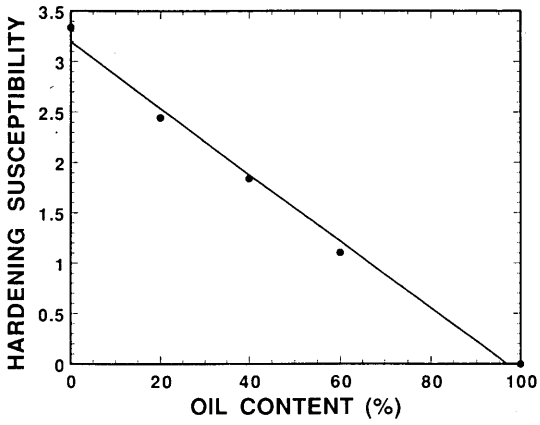

FIGURE 2 Hardening susceptibility versus oil content.

Metals and Asphaltenes (Experiment 2)

This experiment was designed to examine the effects of trace metals and asphaltenes on aging. Jemison (*6*) showed a strong correlation between hardening susceptibility and both metals (nickel and vanadium) and asphaltenes. There was some difficulty deciding how to isolate these two effects, since the asphaltenes typically contain almost all of the metals from the asphalt or fraction. The solution was to use asphaltenes from three different asphalts with different levels of metals. Blending these materials with an aromatic base would yield blends in which the asphaltene and metal contents would not be interdependent.

To perform the experiment, three tank asphalts were fractionated using the Giant Corbett: the McMillan low metal AC-20, the intermediate metals Exxon AC-20, and the Coastal AC-20 high levels. Nickel and vanadium content of the fractions was determined using atomic absorption. To make the asphaltene measurement more consistent, the heptane asphaltenes were measured for the asphaltene and aromatic fractions. (Since the bulk asphaltene precipitation was not a careful analytical separation, there was a significant amount of asphaltene in the aromatic, and vice versa.) These data are presented in Table 1. The aromatic fractions were combined and used as a base, with 15 percent oil added to reduce viscosity. The three types of asphaltenes were blended with this material, producing nine blends with varying levels of metals and asphaltenes. The resulting blend compositions are given in Table 2. These blends were all aged in the POV at 180°F and 300 psia for periods of 4, 8, 11, and 14 days, and the viscosities and carbonyl areas were measured. The results show some scatter because of the temperature gradient problem, but the results are still interesting. Figure 3 shows no effect of metals on hardening susceptibility, whereas Figure 4 shows a definite correlation with asphaltenes. This leads to the surprising result shown in Figure 5 that starting asphaltenes have essentially no effect on the oxidation rate but definitely increase the hardening rate through the adverse effect on hardening susceptibility.

Supercritical Fractions as Recycling Agents

Three sets of experiments were performed using light supercritical fractions directly as recycling agents or they were used after alteration of the oil, wax, and asphaltene content. In the first set of experiments (Experiment 3), two light supercritical fractions were chosen: a Fina fraction #2 and a Coastal fraction #1. In addition, the same fractions were dewaxed using the procedure for the oil and wax separation from the Giant Corbett, and the dewaxed materials were used as two more recycling agents. These four agents were blended with five artificially aged asphalts to make 10 blends. Table 3 gives the composition based on Corbett analysis and the viscosity of each recycling agent, aged asphalt, and reblended asphalt. The hardening susceptibilities are also given in Table 3 except for blends R1, R7, and R8, which either hardened too little or too much because of a temperature control problem. The saturate content was much higher in this experiment than in the other two, and the hardening susceptibilities, as will be shown later, are anomalous.

TABLE 1 Asphaltenes and Metals of Starting Fractions

Material	Starting % Asphaltenes	Nickel (PPM)	Vanadium (PPM)
Coastal Asphaltenes	78.1	142.1	966.7
Coastal Aromatics	2.2	32.1	160.9
Exxon Asphaltenes	80.6	20.5	32.1
Exxon Aromatics	2.8	9.0	13.3
McMillan Asphaltenes	48.1	82.5	288.7
McMillan Aromatics	3.6	22.1	60.7

TABLE 2 Compositions of Blends in Experiment 2

Blend	Base % Aromatic	Starting % Asphaltene	Nickel (PPM)	Vanadium (PPM)
L-10	88.67	11.33	45.3	54.6
L-20	83.21	16.79	22.2	46.8
I-10	89.79	10.21	24.2	88.5
I-20	80.05	19.95	27.6	83.3
I-30	73.15	26.85	26.7	75.1
H-10	89.96	10.04	29.2	137.7
H-20	82.19	17.81	32.7	128.1
H-30	74.37	25.63	36.3	118.5
Aromatic Base	97.38	2.62	16.9	47.3

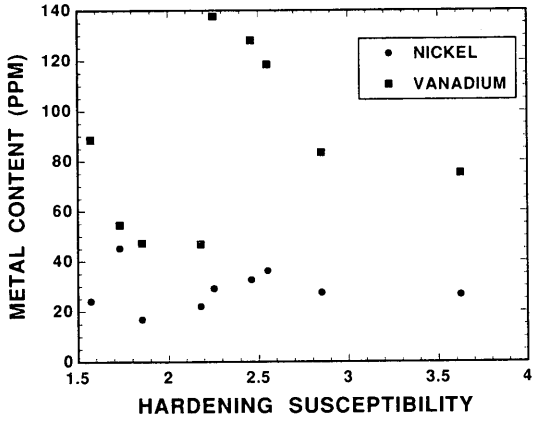

FIGURE 3 Effect of metals on hardening susceptibility.

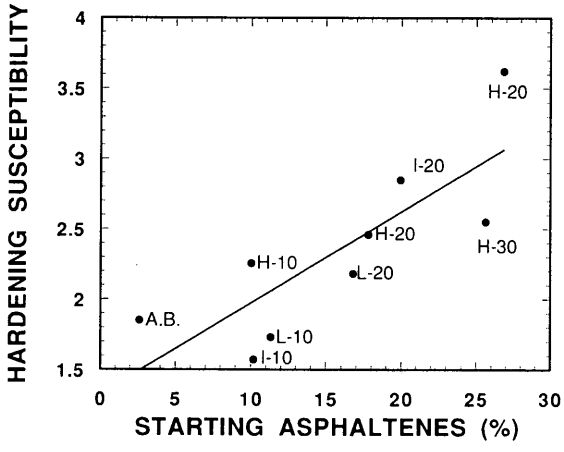

FIGURE 4 Effect of asphaltenes on hardening susceptibilities.

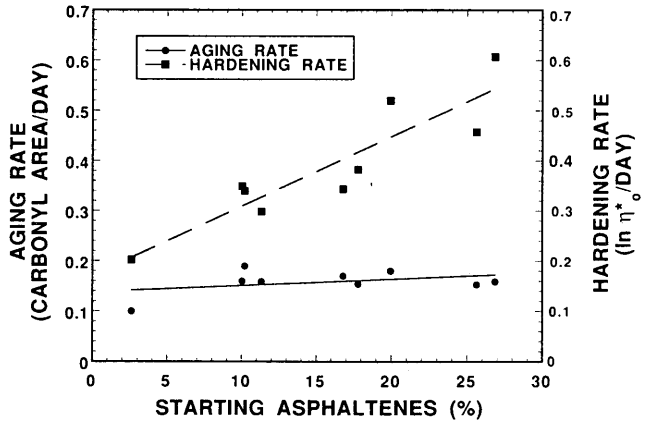

FIGURE 5 Effect of asphaltenes on hardening rate and carbonyl formation rate.

Although the ductility was not measured in this research, there were samples from this experiment that had visibly poor ductility. At viscosities of only several thousand poise, the material from the POV trays would crumble and had the texture of soft cheese. It is thought that the high paraffin content caused incompatibility and the resultant loss in ductility. Evidence of this effect also came from the viscosity data. The frequency sweeps run to determine the zero-shear viscosities tended to become flat very soon in the run, as expected with these low viscosities, but later jump to a higher viscosity and level out again. A typical frequency sweep and one exhibiting this behavior are shown in Figure 6. This effect was especially notable at higher saturate levels and became more pronounced as the blends aged.

In Experiment 4, a Coastal supercritical fraction #1 was fractionated and its oils and aromatics and waxes were used to make four recycling agents. They contained 15.28 percent oil, 8.26 per-

TABLE 3 Compositions and Viscosities of Materials in Experiment 3

Material	Blend Makeup	% Par.	% Orig. Asph.	Mix Ratio %	Hard. Susc.	Viscosity (P)
Coastal SC Fraction 1	NA	20.33	0.33	NA	NM	0.599
FINA SC Fraction 2	NA	33.67	0.67	NA	NM	0.631
DW Coastal SC Fraction	NA	18.04	0.35	NA	NM	1.358
DW FINA SC Fraction	NA	30.21	0.72	NA	NM	1.185
Aged Ampet AC-20 #1	NA	8.33	12.33	NA	NM	83,000
Aged Ampet AC-20 #2	NA	8.33	12.33	NA	NM	260,000
Aged Ampet AC-20 #3	NA	8.33	12.33	NA	NM	160,000
Aged Cosden AC-20	NA	13.00	16.00	NA	NM	105,000
Aged Texaco AC-20	NA	8.22	18.41	NA	NM	230,000
Blend R1	Ampet #2/ Coastal SC	13.57	8.95	56/44	NM	270
Blend R2	Ampet #2/ Fina SC	19.25	9.16	57/43	2.05	265
Blend R3	Ampet #3/ Fina SC	18.47	9.60	59/41	2.09	271
Blend R4	Ampet #3/ DW Coast.	12.07	8.95	61/39	2.25	333
Blend R5	Cosden/ DW Coast.	15.43	10.50	52/48	2.06	130
Blend R6	Cosden/ DW Fina	21.33	10.67	52/48	2.48	261
Blend R7	Texaco/ DW Fina	17.10	12.65	60/40	NM	568
Blend R8	Texaco/ Coastal SC	13.45	12.64	57/43	NM	470
Blend R9	Ampet #1/ Coastal SC	15.58	6.88	37/63	1.41	30.3
Blend R10	Ampet #1/ DW Coast.	14.67	5.09	35/65	1.90	70.2

NA Not Applicable
NM Not Measured

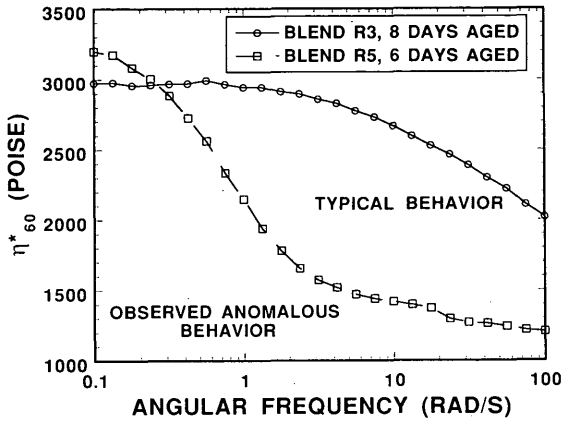

FIGURE 6 Asphalt viscosity frequency sweep.

cent oil, 7.71 percent oil plus 4.09 percent wax, and one with no oil or wax. They were named A, B, C, and D, respectively. They were blended with four aged asphalts to make 11 blends. Table 4 gives the viscosities of the asphalts, agents, and blends and the mixing ratios for each blend and composition.

Unfortunately, continued temperature problems ruined many of the kinetic data from this experiment. However, the hardening susceptibilities of the blends could still be analyzed, and they revealed some important results. Figure 7 shows combined viscosity versus carbonyl curves from all three aging temperatures for the various blends for the aged Coastal asphalt. In addition, the thick line above the blend data shows the viscosity/carbonyl relationship previously measured for the original asphalt. The slopes of these lines, the hardening susceptibilities, are actually lower in every case for the reblended material than for the original asphalt, indicating that the aged asphalt was improved by the recycling agent, at least from the standpoint of this analysis. There was less improvement for the Ampet materials than for the Texaco and Coastal, presumably because the Ampet was originally a better material. The improvements in hardening susceptibilities for the Texaco and Coastal asphalts are significant.

The fifth experiment was very similar to the fourth in that recycling agents were designed to have a specific composition. This time, however, more variation was used in the amount of wax in the blends, and asphaltenes were included. Also, the temperature gradient in the POV had been eliminated. The materials for the recycling agents came from an Exxon Supercritical fraction #1, which was further fractionated by the Giant Corbett. Only one-half of the paraffin fraction was separated into oil and wax; the other was left alone. Six recycling agents containing varying amounts of oils, paraffins, aromatics, and asphaltenes were made from these materials. They were labeled E, F, G, H, I, and J, respectively. The agents were blended with an artificially aged

TABLE 4 Viscosities and Blending Ratios for Experiment 4

Material	Visc. (P)	Mix Ratio (%) (Asph./Agnt.)	Hard. Susc.	Temp. Susc.	% Orig. Asph.	% Sat.
Agent A	20.2	NA	NM	NM	0	15.28
Agent B	47.7	NA	NM	NM	0	8.26
Agent C	37.6	NA	NM	NM	0	11.8 (7.71 oil, 4.09 wax)
Agent D	183	NA	NM	NM	0	0
Ampet AC-20	20,200	NA	NM	NM	12.33	8.33
Coastal AC-20	41,000	NA	NM	NM	19.41	8.91
Texaco AC-20	89,700	NA	NM	NM	18.41	8.22
Blend AA	1230	70/30	2.32	19746	8.63	10.41
Blend AB†	500	63/37	1.79	20597	12.22	8.30
Blend AC	1055	65/35	1.95	19242	8.02	9.54
Blend AA*	615	45/55	2.42	19000	5.55	12.15
Blend CA	750	64/36	2.33	18748	7.89	11.20
Blend CB	495	56/44	2.02	19046	10.87	8.62
Blend CC	535	58/42	2.21	18215	11.26	10.12
Blend CD	518	40/60	1.74	19231	7.76	3.56
Blend TA	436	58/42	1.79	17935	10.67	11.18
Blend TB	445	50/50	1.93	18876	9.21	8.24
Blend TC	450	52/48	1.90	18064	9.57	9.93
Blend TD	555	36/64	1.39	18970	6.63	2.95

(Notation for blends: A_ = Ampet, C_ = Coastal, T_ = Texaco; _A = Agent A, _B = Agent B, _C = Agent C, _D = Agent D; Example: Blend CB contains Coastal AC-20 and Agent B.)

NA Not Applicable

NM Not Measured

† Due to a shortage of material, a more highly aged Ampet asphalt was used for this blend, which had a viscosity of 260,000 Poise.

* Also due to a shortage of material, this blend contains the same recycling agent as blend AA.

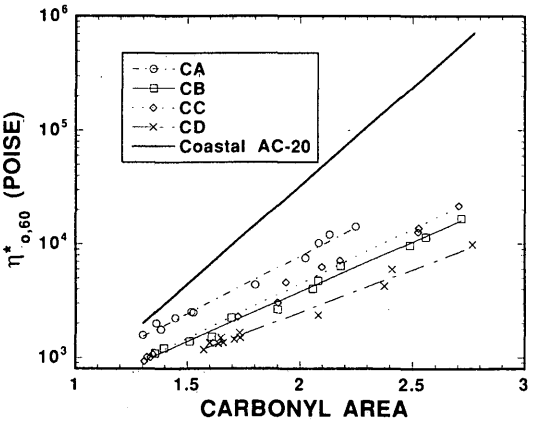

FIGURE 7 Coastal blend hardening susceptibilities.

Texaco asphalt. Table 5 gives the component viscosities, mixing ratios, and resulting viscosities and compositions for each reblend.

These recycled blends were aged in the POV at 300 psia and 160°F for 8, 12, 14, and 16 days; at 175°F for 10, 13, 16, and 19 days; and at 190°F for 4, 6, 8, and 10 days. All of the blends have roughly the same aging rate except for I and J, which contain wax. This behavior was observed at all three temperatures; moreover, at two temperatures the carbonyl growth rate decreased as wax content increased. (The actual wax content was not measured; the reblending agent that contained only paraffins would have approximately twice as much wax as the one containing paraffins and oil.) Examination of the viscosity data reveals similar behavior. This would indicate that, although the aging rates seemed to be lower for the blends with waxes, the hardening susceptibilities should be close to the same. Arrenhius plots indicate no obvious effect of composition on activation energies.

Also of importance are the differences between the aging rates for the original and recycled asphalts. Aging data previously collected for the Texaco AC-20 (*8*) reveal similar rates of carbonyl growth. At 160°F, the asphalt's carbonyl area increased by approximately 0.3 over 10 days, whereas the blends in this experiment displayed increases of approximately 0.25 over 9 days at the same temperature. At the same time, the asphalt's viscosity increased by about half an order of magnitude, whereas the blends only hardened half that much (which is consistent with the hardening susceptibility). Furthermore, the 20-day, 160°F aged asphalt had a viscosity of about 100 000 poise from a tank value of 2500; a typical blend viscosity from a similar aging time was 6000 poise from an initial 600.

TABLE 5 Viscosity and Mixing Data for Experiment 5

Material	% Sat.	% Asph.	Visc(P)	Hard. Susc.	Temp. Susc. ($^*10^{-4}$)	Mixing Ratio % (Asphalt) /Agent)
Agent E	20.4	0	36	NM	NM	NA
Agent F	14.9	0	37	NM	NM	NA
Agent G	10.2	2.8	111	NM	NM	NA
Agent H	9.9	5.4	132	NM	NM	NA
Agent I*	11.2 (6.1 oil, 5.1 paraffin)	0	37	NM	NM	NA
Agent J*	10.6 (all paraffin)	0	63	NM	NM	NA
Aged Texaco AC-20	8.22	18.41	160,000	NM	NM	NA
Blend E	13.1	11.0	358	2.25	1.87	60/40
Blend F	10.9	11.0	579	2.16	1.89	60/40
Blend G	8.9	13.4	945	2.02	1.92	68/32
Blend H	8.2	14.5	1169	1.97	1.97	70/30
Blend I	9.4	11.0	755	1.88	1.9	60/40
Blend J	9.1	11.8	865	2.03	1.93	64/36

NM Not Measured
NA Not Applicable
* Saturates in agent I are part oil and part unseparated paraffin. In agent J, saturates are all paraffin. The wax in these agents is contained in the paraffin.

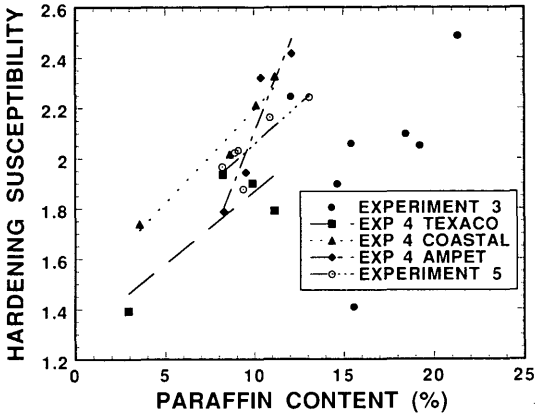

FIGURE 8 Effect of paraffins on hardening susceptibilities.

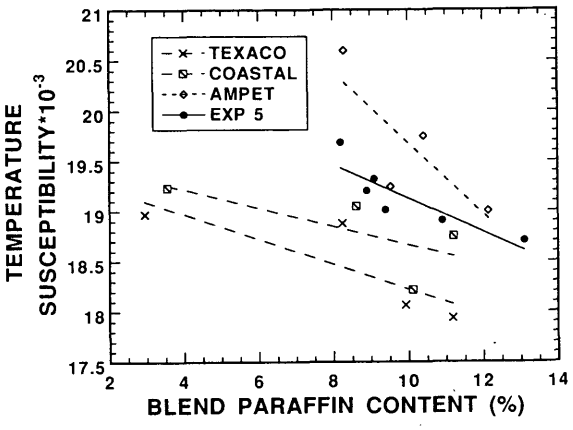

FIGURE 9 Effect of paraffins on temperature susceptibilities.

Effect of Saturates on Hardening Susceptibility and Temperature Susceptibility

In Experiments 3 through 5, hardening susceptibilities were measured for each blend. They are plotted versus saturate content in Figure 8. As expected, there is considerable variation because a variety of aged asphalts and blending agents were used, but in general the hardening susceptibility increases with saturate content. This most clearly is seen in Experiment 5, in which a single aged asphalt and a single recycling agent base stock were used. This result is contrary to the data in Experiment 1, in which oils and aromatics were aged, but confirms the adverse effect of asphaltenes in Experiment 2.

There is no apparent effect of wax in these experiments, which is not surprising since these hardening susceptibilities are based on 60°C viscosities, whereas the detrimental effects of wax are at low temperature.

Most of the Experiment 3 data appear anomalous. There are two possible explanations. The first is that Experiment 3 composites are based on Corbett analysis, whereas in Experiments 4 and 5 they were made by weight. Perhaps there is a systematic error. The other possibility is that the strange frequency sweeps seen in Figure 9 are giving erroneous viscosities as a result of phase separation.

In Experiments 4 and 5 viscosities were run from 0°C to 60°C. The logarithms of viscosities were plotted versus reciprocal absolute temperature to obtain the temperature susceptibility, the slope of these lines (Tables 4 and 5). These values are plotted as a function of saturate content in Figure 9. The property shows no sensitivity to wax but correlates with total saturate content. In all cases, temperature susceptibility decreases with paraffin content. The temperature susceptibilities of the original asphalts are markedly larger than the reblended aged material.

CONCLUSIONS

Recycling agents should be highly aromatic, and if so the recycled pavement can be superior to the original pavement. Both hardening susceptibility and temperature susceptibility were generally improved by adding highly aromatic agents. Saturates reduce the hardening susceptibility of the aromatic fraction in the absence of asphaltenes. In the recycling of aged material containing large amounts of asphaltenes, saturates increase hardening susceptibility but improve temperature susceptibility. Wax had little effect at the small amounts added, but both waxes and saturates almost certainly affect ductility adversely at levels as low as 15 percent, and wax has been reported to affect low-temperature properties.

The metal study indicated that metals appear to have little if any effect on either oxidation rate or hardening susceptibility. The apparent effect often reported probably results from the high correlation between metal content and asphaltenes. The oxidation rate is primarily determined by the reactivity of the aromatic fraction.

ACKNOWLEDGMENTS

Support for this work by the Texas Department of Transportation, in cooperation with the U.S. Department of Transportation, the Federal Highway Administration, and the Advanced Technology Program, is gratefully acknowledged. The technical contributions of Ann Ferry and Stephen Smiley are greatly appreciated.

REFERENCES

1. Corbett, L. W. Composition of Asphalt Based on Generic Fractionation, Using Solvent Deasphaltening, Elution-Adsorption Chromatography, and Densimetric Characterization. *Analytical Chemistry*, Vol. 41, April 1969, pp. 576–579.
2. Martin, K. L., R. R. Davison, C. J. Glover, and J. A. Bullin. Asphalt Aging in Texas Roads and Test Sections. In *Transportation Research Record 1269*, TRB, National Research Council, Washington, D.C., 1990, pp. 9–19.
3. Lau, C. K., K. M. Lunsford, C. J. Glover, R. R. Davison, and J. A. Bullin. Reaction Rates and Hardening Susceptibilities as Determined from POV Aging of Asphalts. In *Transportation Research Record 1342*, TRB, National Research Council, Washington, D.C., 1992, pp. 50–57.
4. Hoiberg, A. J., and W. E. Garris. Analytical Fractionation of Asphalts. *Ind. and Eng. Chem. Analytical Edition*, Vol. 16, 1944, pp. 294–302.
5. Stegeman, J. R., A. L. Kyle, B. L. Burr, H. B. Jemison, R. R. Davison, C. J. Glover, and J. A. Bullin. Compositional and Physical Properties

of Asphalt Fractions Obtained by Supercritical Extraction. *Fuel Science and Technology International*, Vol. 10, 1992, pp. 767–794.
6. Jemison, H. B. *Supercritical Refining of Asphalts.* Ph.D. thesis. Texas A&M University, College Station, 1992.
7. Davison, R. R., J. A. Bullin, C. J. Glover, B. L. Burr, H. B. Jemison, A. L. G. Kyle, and C. A. Cipione. *Development of Gel Permeation Chromatography, Infrared and Other Tests To Characterize Asphalt Cements and Correlate with Field Performance.* Research Report FHWA/TX-90/458-1F. State Department of Highways and Public Transportation, Austin, Tex., 1989.
8. Lau, C. K. *Photo- and Low-Temperature Oxidation Reactions and Their Impacts on the Rheological and Chemical Properties of Asphalt as Pavement Binder.* M.S. thesis. Texas A&M University, College Station, 1991.

Publication of this paper sponsored by Committee on Characteristics of Bituminous Materials.

Softening of Asphalts in Dilute Solutions at Primary Distillation Conditions

B. L. BURR, R. R. DAVISON, C. J. GLOVER, AND J. A. BULLIN

Softening of asphalts in dilute solutions, often by as much as 50 percent, occurred in several instances during experiments using a modified Roto-vap recovery technique. The softening is caused by a mechanism that is characterized by Fourier transform infrared spectroscopy spectral growth near the traditional carbonyl region associated with oxidative hardening, as well as other minor changes. Gel permeation chromatograms of solvent-softened asphalts show formation of one and sometimes two new narrow peaks, suggesting that the reactions produce a very narrow range of products. Reaction rates vary considerably with asphalt source, solvent, and solution conditions. The rates also increase considerably with Roto-vap oil bath temperature from 102°C to 149°C. Reaction rates decrease with concentration, being almost nonexistent at 0.12 g/mL but generally significant at 0.06 g/mL. Reactions proceed faster in more polar extraction solvents, such as trichloroethylene with 15 percent ethanol (TCE/EtOH), than in toluene with 15 percent ethanol. Inhibitors such as butylated hydroxy toluene slow the reactions but do not appear to affect the extent of reaction. Compatible asphalts (such as SHRP AAG-1) react fastest at lower temperatures, whereas incompatible but reactive asphalts (SHRP AAK-1) react fastest at higher temperatures. The reactions appear to be dependent on the solvent's ability to dissolve associated species. However, the reactions have also been detected in dissolved maltene fractions. Care should be taken to avoid exposing asphalts in dilute solutions (below 0.15 g/mL) to temperatures above 93°C, especially in polar solvents such as TCE/EtOH, for extended periods of time.

Recently, several new modifications of the SHRP extraction and recovery method (*1*) have been made that speed the procedure time and reduce the sample size. One of these is an In-can recovery flask, which allows for the recovery of asphalt directly into an asphalt tin. It leaves no asphalt residue on a round-bottom flask and therefore reduces the initial sample size from about 50 to about 25 g. Also, the continuous addition of extract into the Roto-vap during primary distillation stabilizes boiling. This improvement speeds distillation considerably, to about 2.5 L/hr, so long as the oil bath temperature is raised from 100°C to about 121°C to provide the necessary heat. With the advent of the In-can final recovery method, frequent instances of asphalt softening began to occur within this laboratory. During verification of a new extraction and recovery procedure (called the Auto method in this paper), asphalts often had about half the viscosity of other identical asphalts using the SHRP method and ASTM D-2172A (Method A). During calibrations with Method A using portions of Asphalt Materials Reference Library (AMRL) test mixtures, the Auto method yielded much softer asphalts and the Fourier transform infrared (FT-IR) spectra showed a new peak at 1735 cm^{-1} just to the left of the carbonyl peak associated with oxidative hardening (*2*). Large-scale Corbett fractions (*3*) being similarly concentrated from heptane solutions were often soft and had the mysterious FT-IR peak at 1735 cm^{-1}. When these softening phenomena started to appear within a short period of time, it was not clear whether the cause was some sort of contamination through the In-can flask's O-ring seal or a new form of reaction that occurs in solution under In-can recovery conditions.

Department of Chemical Engineering and Texas Transportation Institute, Texas A&M University, College Station, Tex. 77843-3122.

BACKGROUND

In prior studies of different extraction and recovery methods, reactions of asphalts in extraction solvents have been reported; such reactions raise the recovered asphalt viscosities by up to 100 percent. These reactions may occur at different rates in different solvents. Chlorinated extraction solvents were suspected of participating in these reactions (*4*), but it was also shown later that the reactions occur in nonchlorinated solvents with the rates being more a function of a solvent's ability to dissolve an asphalt (*5*). The susceptibility of SHRP asphalts to harden in extraction solvents was shown to correlate reasonably well with RTFO aging. However, the reaction mechanisms are not identical because carbonyl growth does not consistently follow solvent hardening as in oxidative aging (*5*). These solvent hardening reactions occur at temperatures as low as room temperature. The rates increase as the asphalt concentration in solution is lowered from about 0.4 to about 0.1 g/mL. Below 0.1 g/mL, solvent hardening becomes difficult to reproduce (*5*). The SHRP extraction and recovery procedure was designed to avoid solvent hardening by using low recovery temperatures and maintaining high asphalt concentrations (*1*).

The literature has no mention of reactions that soften asphalt while in high temperature or dilute solutions or of the strange FT-IR peaks near the oxidative aging carbonyl region.

EXPERIMENTAL PROCEDURES

Softening Experiments Simulating Solvent Recovery

To find conditions where solvent softening of asphalt occurred during solvent removal, asphalts were dissolved at various concentrations in several solvents and boiled in a 1000-mL round-bottom flask attached to a rotary evaporator. Distillate was continuously drawn and fresh solvent continuously charged to simulate real recovery conditions. Aliquots of solution were re-

moved after each hour for 3 hr. The dissolved hourly samples were measured by FT-IR using a film casting technique. The asphalts in the bulk solution were recovered for subsequent GPC and viscosity analysis.

The temperature of the bulk solution was primarily determined by the solution's boiling point under the applied vacuum of 660 mm Hg. This is about 38°C for trichloroethylene with 15 percent ethanol (TCE/EtOH) and 60°C for toluene with 15 percent ethanol (Tol/EtOH). However, as the temperature of the solution film approaches the oil bath temperatures, the reaction rates are affected, as will be shown later. The reason oil bath temperatures were used in this analysis is that they best describe recovery conditions in which these reactions are pertinent.

Longer-Term Solvent Softening Experiments

Asphalt samples (0.05 g/mL of TCE) were mixed with varying levels of the oxidation inhibitor, butyl-hydroxytoluene (BHT). Solutions were held at 70°C for several days. About 500-mL aliquots were removed after each day and recovered using the In-can procedure. The recovered asphalts were analyzed by viscometry, GPC, and FT-IR.

Property Analyses

FT-IR spectra were obtained using a Mattson Galaxy Series 5000 spectrometer. Most of the recovery simulation samples were still in solution and had to be film-cast onto the prism. The other samples were applied as melts (*6*). In film-casting, a few drops of the asphalt solution are placed on the zinc selenide prism, and the solvent is driven off by evaporation and final drying with a hot air gun. This results in a several-micron layer of asphalt on the prism surface, which is free of solvent. The use of the hot air gun does not appear to affect asphalt properties. Viscosities of recovered samples were taken with the Carri-Med 500 CSL rheometer. GPC analyses were performed on a Waters HPLC system fitted with 1000 and 500 Å Ultrastyragel columns and a 50 Å PL Gel column using tetrahydrofuran flowing at 1 mL/min as the carrier solvent.

Samples and Materials

Exxon AC-20 tank asphalt was used in the recovery simulation tests. Apparently, the Exxon AC-20 used in one series of tests was different from that used in some later experiments because common tests showed extreme differences in reaction rates. Therefore, these asphalts will be designated Exxon 1 and Exxon 2. Unfortunately, reasons for these differences are unknown. SHRP Asphalts AAG-1 and AAK-1 were mixed with the oxidation inhibitor and held at 70°C for longer periods. AMRL Asphalt Concrete Samples 37 and 38 were extracted using the Auto method with TCE/EtOH as the solvent and compared with Method A extractions. Extraction or solvent-softening reaction solvents were toluene and TCE with and without 15 percent ethanol additions. Pure BHT from DuPont Petroleum Chemicals was added in varying levels to solutions aged at 70°C.

RESULTS AND DISCUSSION

AMRL Proficiency Samples

To determine how the Auto extraction method performed against a large sample of extractors nationwide, two AMRL proficiency samples (37 and 38) were extracted. These were 500-g portions of the samples sent to the asphalt materials group at the Texas Transportation Institute. Unfortunately, the viscosities of the Auto extracted samples 37 and 38, respectively, were 5,700 and 3,600 poise (570 and 360 Pa·s), whereas the Method A extracted viscosities were 10,200 and 7,500 poise (1,020 and 750 Pa·s). The FT-IR spectra of the Auto and Method A extracted AMRL 37 asphalts were also quite different, as shown in Figure 1. There are four spectral regions where serious differences arise. From 1697 to 1770 cm^{-1} (Peak 1), just to the left of the carbonyl peak that tracks oxidative aging, is a large, sharp peak. The peak is as large as the carbonyl peaks found in asphalts aged to several million poise. Another range of growth in the spectrum occurs from 1213 to 1329 cm^{-1} (Peak 2). This area contains a region from 1300 to 1329 cm^{-1}, which had previously shown signs of correlating with viscosity and oxidation. Another region that increases during solvent softening is from 1098 to 1150 cm^{-1} (Peak 3). Absorbance in sulfoxide region, from 985 to 1051 cm^{-1}, decreased during solvent softening.

Recovery Simulations with Solvent Softening

After several attempts to detect oil leakage through the In-can recovery flask O-ring, it seemed probable that the new peaks were caused by reactions in solution rather than contamination. If it were a reaction, peak growth rates should change with temperature or asphalt concentration. Exxon 1 (30 g) samples were dissolved in TCE/EtOH to give 0.06 g sample/mL solution and refluxed under 660 mm Hg vacuum (100 mm Hg absolute) at oil bath temperatures of 102°C, 124°C, and 149°C. After each hour of refluxing, a 10-mL aliquot of solution was removed for analysis. After 3 hr, the asphalt was recovered. Figure 2 shows the FT-IR spectra from 700 to 1900 cm^{-1} for the batch run at 149°C. Growth

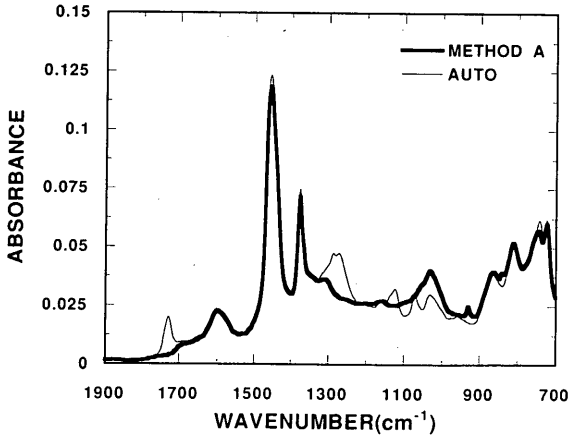

FIGURE 1 Comparison of FT-IR spectra for an asphalt binder extracted and recovered from aggregate by two methods.

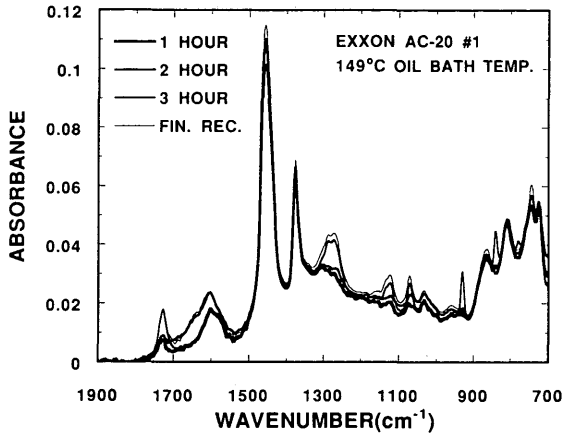

FIGURE 2 Effect of incubation time on the FT-IR spectra of Exxon AC-20 (0.06 g/mL TCE/EtOH, 149°C oil bath).

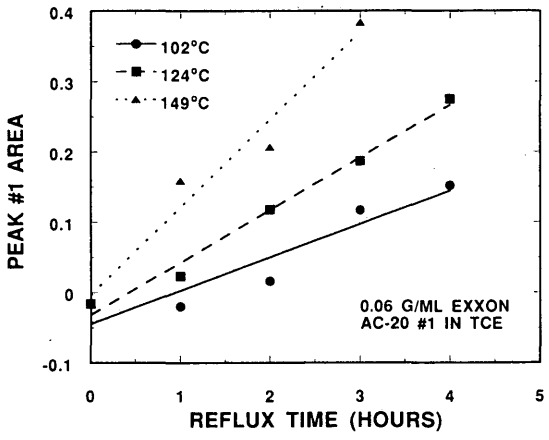

FIGURE 4 Growth of Peak 1 (1770 to 1697 cm^{-1}) in Exxon AC-20 at three oil bath temperatures (0.06 g/mL TCE).

over time is apparent for Peaks 1, 2, and 3, but the sulfoxide region does not show a decrease as in the AMRL samples. However, there was a large amount of initial sulfoxide in the AMRL samples, whereas there was very little in the Exxon AC-20. Sulfoxides may be eliminated in the solvent softening process, but their presence does not appear necessary for the other peaks to form. Figure 3 shows the region from 1500 to 1800 cm^{-1} and growth of Peak 1. Here there is a steady growth during the refluxing stage over time but no real growth during the final recovery step. Figures 4 through 6 show the growth in the peaks of interest (1, 2, and 3) at the three oil bath temperatures for the 0.06-g/mL solutions. For Peaks 1, 2, and 3, the peaks increase with time at each temperature and the growth rates increase with temperature. The sulfoxide region has small and random changes suggesting that there is no significant reaction occurring in this region. The oil bath temperature is not representative of the bulk solution temperature. The solvent and system pressure determine the boiling temperature. The oil bath temperature only affects the boiling rate and the temperature gradient in the solution film near the flask surface. Since there are definite changes in reaction rates due to the oil bath temperature, which is approached only in a small portion of the system, the rates in a true isothermal system at these temperatures are expected to be much higher.

Chemical reactions follow an Arrhenius relationship between reaction temperature and the log of the rate constant. The growth rates can be estimated by calculating the slopes of the curves in Figures 4 through 6. These slopes represent the rate of peak area growth, $d(\text{peak area})/dt$, for each peak at each temperature. The sulfoxide rates exhibited almost random variation and are not shown. The logs of the growth rates are plotted against inverse temperature to form an Arrhenius plot in Figure 7. Peaks 1, 2, and 3 all follow the Arrhenius relationship and have the same slope. Common slopes indicate that they are all participating in the same reaction.

Since growth stopped upon final recovery, the reactions may not occur at higher asphalt concentrations. Several similar batches having asphalt concentrations of 0.12 g/mL were run at 102°C, 124°C, and 149°C. At 124°C, peak growth was only negligible

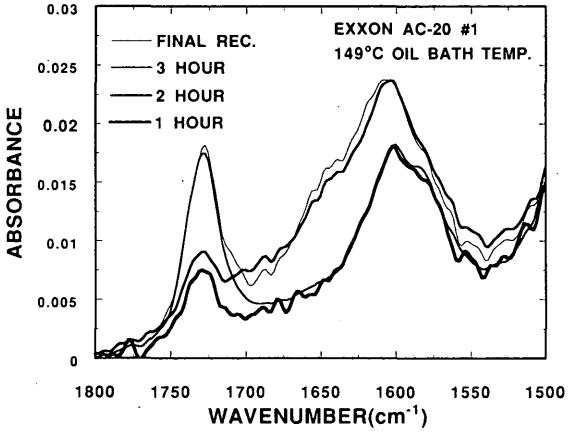

FIGURE 3 Effect of incubation time on the FT-IR carbonyl region of Exxon AC-20 (0.06 g/mL TCE/EtOH, 149°C oil bath).

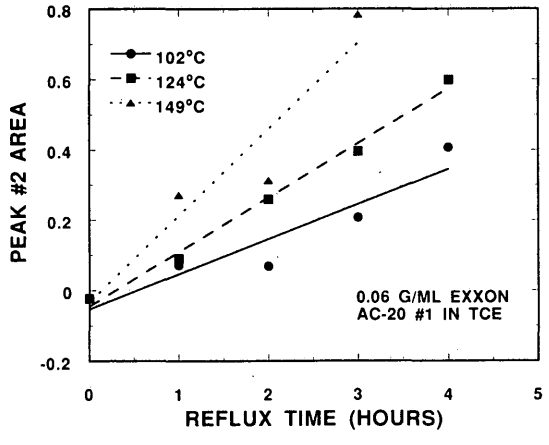

FIGURE 5 Growth of Peak 2 (1329 to 1213 cm^{-1}) in Exxon AC-20 at three oil bath temperatures (0.06 g/mL TCE).

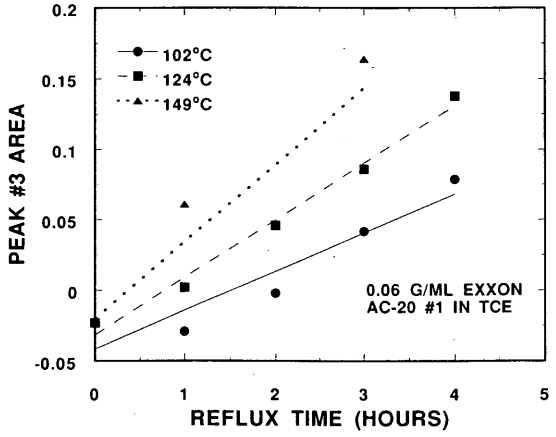

FIGURE 6 Growth of Peak 3 (1150 to 1098 cm^{-1}) in Exxon AC-20 at three oil bath temperatures (0.06 g/mL TCE).

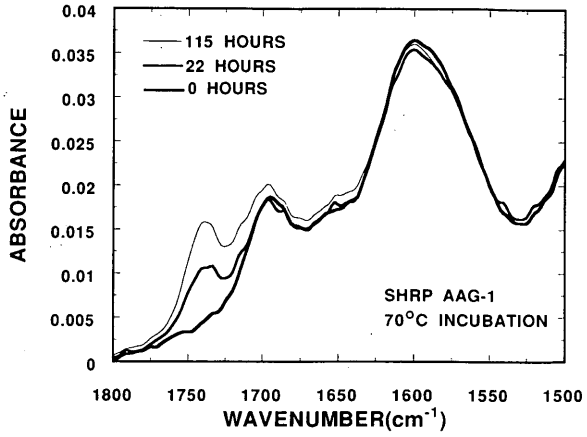

FIGURE 8 Effect of extended incubation times on solvent-softening peak growth for SHRP AAG-1 (0.07 g/mL TCE, 70°C).

after the 4 hr. There was no direct level indication or control in the boiling flask, but evaporative analysis of asphalt concentrations in the aliquots showed variation from 0.10 g/mL for the 3-hr sample to 0.17 g/mL for the 2-hr sample. This poor concentration control leaves the possibility that the concentration dropped low enough to initiate reaction.

In light of these results, it was decided that future extractions would be run such that the boiling flask liquid level was kept at around 150 mL, yielding a concentration at 0.2 g/mL during extraction of a 600-g mixture containing 5 percent asphalt. This is more in line with concentrations found in earlier extraction and recovery methods. However, it makes operation of the Auto method more tedious, since the boiling flask level must be monitored more closely.

Long-Term Solvent Softening with Inhibitor

There were questions whether these reactions would respond to the presence of oxidation inhibitors. This might give some clue as to the nature of the reactions. SHRP AAG-1 and AAK-1 tank asphalts were dissolved in TCE at 0.07 g/mL and spiked with 0, 1, or 2 wt percent BHT. These solutions, about 1000 mL each, were stored at 70°C in an oven for several days. About 200- to 300-mL aliquots were removed after 0, 22, and 115 hr of incubation. Figure 8 shows the carbonyl region (1500 to 1800 cm^{-1}) where Peak 1 grows in the samples having no BHT. This is similar to what is seen in the Exxon AC-20, though it is much slower because the temperature is lower. Figure 9 shows the effect of BHT concentration on the growth of Peak 1 for the 22-hr samples. The effect is less dramatic on the 115-hr samples because, eventually, the BHT-treated samples' peaks reach the same equilibrium level of peak growth that the untreated samples reach. This suggests two things. First, the reaction is a free-radical transfer mechanism (which is what oxidation inhibitors can slow). Second, the peak growth inhibition in the BHT-treated samples is only temporary, since after 115 hr, all samples have comparable softening peaks. This may be due to depletion of softening reactants at the lower temperature or depletion of inhibitor. GPCs of these sam-

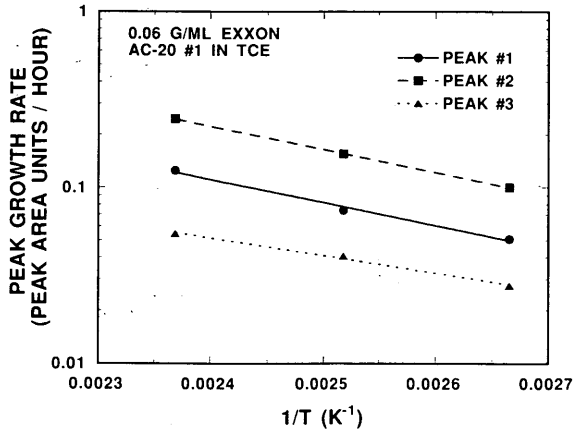

FIGURE 7 Peak 1, 2, and 3 Arrhenius curves for an Exxon AC-20 at three oil bath temperatures (0.06 g/mL TCE).

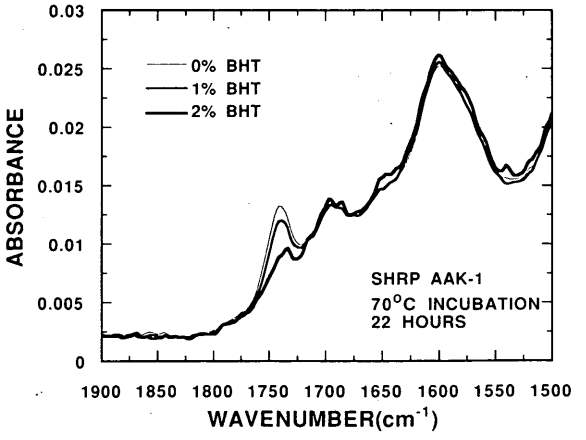

FIGURE 9 Effect of BHT inhibitor on FT-IR spectra changes due to solvent softening of SHRP AAK-1 (0.07 g/mL TCE).

ples show formation of two narrow peaks, one of which is lower in molecular weight than the bulk of the asphalt (Figure 10). Viscosities are strongly affected by solvent softening for SHRP AAG-1 and AAK-1 (Figure 11). SHRP AAG-1 softens considerably at first and somewhat less at later times. More relative softening occurs for the uninhibited sample, as is expected. SHRP AAK-1 softens considerably in the uninhibited material but hardens at later times. Inhibited SHRP AAK-1 just hardens very gradually. It is probable that both hardening and softening reactions are occurring, with softening being most responsive to inhibitors. The softening possibly arises from the presence of the low-molecular-weight reaction product seen on the GPC chromatogram.

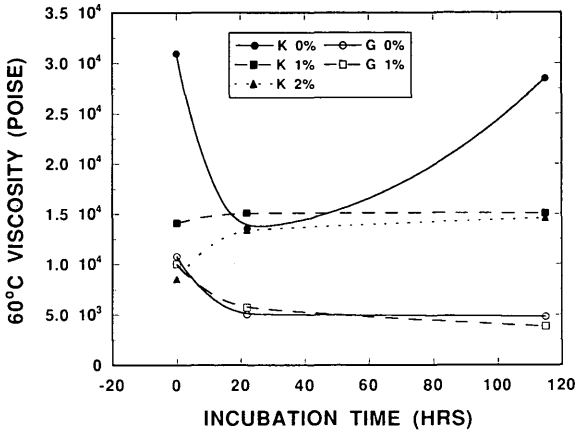

FIGURE 11 Effect of BHT on solvent softening of SHRP AAK-1 and AAG-1 (0.07 g/mL TCE).

Effects of Solvent and Asphalt Source

Solvent softening rates vary considerably with the source of asphalt and extraction solvent. In Figure 12, solvent softening rates for Exxon 1 and 2 in TCE/EtOH and Exxon 2 in Tol/EtOH are shown at several temperatures and concentrations. It is clear that TCE/EtOH promotes solvent softening more than Tol/EtOH. In fact, Tol/EtOH stimulates softening in only the most severe recovery conditions (high temperature and very low concentration). Even though Tol/EtOH is a slightly poorer solvent for extracting strongly adsorbed material from the aggregate (7), its superior resistance to solvent softening makes it the solvent of choice. Also, it can be seen that two asphalts, which were thought to be identical, have very different solvent softening susceptibilities. Exxon 1 has softening rates that are roughly three times that of Exxon 2. Exxon 1, which reacted fastest of all asphalts tested, might have shown signs of softening in Tol/EtOH at typical conditions, but it was depleted by the time those experiments were performed.

Table 1 gives softening rates for Exxon 1, Exxon 2, SHRP AAG-1, and SHRP AAK-1 under identical conditions. Exxon 2 is comparable to SHRP AAK-1 at high temperatures with SHRP AAG-1 being much less reactive. However, at lower temperatures, SHRP AAG-1 is nearly as reactive as SHRP AAK-1. This is not surprising, since this relative rate switching also occurs during oxidative aging for the two asphalts. At low temperatures, the poorer compatibility of SHRP AAK-1 probably keeps it from being as completely dissolved as SHRP AAG-1. This could hinder the reactive sites of SHRP AAK-1 and yield lower rates. SHRP AAK-1 may actually have more reactive sites than SHRP AAG-1 at high temperatures where SHRP AAK-1 is dissolved as completely as SHRP AAG-1.

Solvent Softening Reaction Mechanism

There is not enough information available yet to explain mechanistically the phenomena occurring in these experiments. However, several things are known. First, the FT-IR peaks arise because of some reaction (or reactions) that does not involve dissolved free oxygen, since they occur in refluxing systems saturated with solvent. The reactions also respond to free-radical inhibitors, suggesting that they are initiated by free radicals existing naturally in the asphalt. There has been considerable speculation in the past that TCE reacts with dissolved asphalt. However, the occurrence of these reactions in other solvents like heptane and

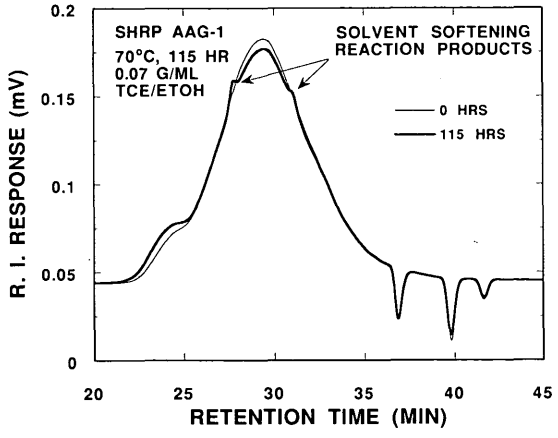

FIGURE 10 Formation of two unique GPC peaks during solvent softening of SHRP AAG-1 without BHT (0.07 g/mL TCE, 115 hr, 70°C).

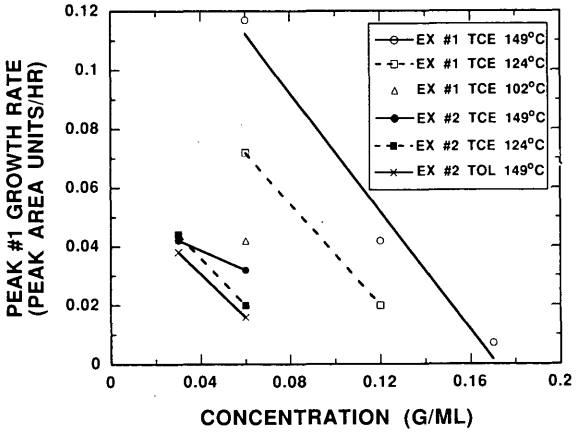

FIGURE 12 Solvent softening rates of Exxon 1 and 2 in TCE/EtOH and Exxon 2 in Tol/EtOH at several solution conditions.

TABLE 1 Comparison of Softening Rates for Several Asphalts Treated Under Identical Conditions

Asphalt	Condition	Softening Rate (Peak #1 Area Units/hr)
SHRP AAG-1	70°C, .07g/mL, TCE	.0057
SHRP AAK-1	70°C, .07g/mL, TCE	.0063
Exxon #1	149°C, .06g/mL, TCE/EtOH	.117
Exxon #2	149°C, .06g/mL, TCE/EtOH	.032
SHRP AAG-1	149°C, .06g/mL, TCE/EtOH	0
SHRP AAK-1	149°C, .06g/mL, TCE/EtOH	.017
Exxon #2	124°C, .03g/mL, TCE/EtOH	.044
SHRP AAG-1	124°C, .03g/mL, TCE/EtOH	.0066
SHRP AAK-1	124°C, .03g/mL, TCE/EtOH	.043

toluene means that the solvent is not participating in, but is merely providing an environment for, the reactions. The increase in reaction rate as concentration decreases means that the rate-limiting step is probably not a second- or higher-order in asphalt species, since this would require multiparticle interactions, which decrease in probability as the asphalt solution gets more dilute. There could be other higher-order steps in the mechanism that are not rate determining. However, with increasing dilution, more dissociation of organized molecular structures in the asphalt occurs. If these structures contain the free radicals, it could be that they are shielded from reaction while in concentrated solutions. The degree of solvation, then, is likely to control the amount of initiator (free radical) available. If this is a rate-controlling step, the Arrhenius plot should reflect something about the degree of solvation. The presence of a narrow molecular weight reaction product makes it appear that a certain functional group is being attacked and clipped from parent molecules. This is also supported by the fact that the reactions diminish as if a certain required species had been consumed. Possibly, these species are shielded from reaction while in concentrated solutions. These reactions have occurred in solutions of maltenes, so the reactants are not found solely in asphaltenes.

In some temperature-concentration ranges, it is difficult to tell whether solvent softening or solvent hardening will occur. There are some temperature-concentration regions where hardening will occur with some asphalts while softening occurs with other asphalts. Apparently, these reactions compete in some boundary regions. Figure 13 shows where hardening and softening have occurred for Exxon 1, SHRP AAG-1, and SHRP AAK-1 with respect to concentration and temperature. In Figure 13 only the presence, and not the degree, of softening or hardening is shown. The first letter in the symbol denotes the hardening (H), softening (S), or occurrences of both hardening and softening (S, H). The second letter indicates the asphalt source. Signs of softening begin to appear at room temperature and at very low concentrations for SHRP AAG-1, which is the most compatible asphalt and also has the lowest amount of asphaltenes. Since the degree of solvation appears to be important, SHRP AAG-1 is expected to be the first asphalt to undergo softening as conditions become more favorable (i.e., temperature is increased or concentration is lowered). This is because, for the more soluble SHRP AAG-1, less severe solvent conditions are required to bring softening initiators into solution. Conversely, SHRP AAK-1 is the least compatible and the least susceptible to solvent softening. Exxon 1 may exhibit severe softening, but its softening zone is not noticeably different from that of SHRP AAK-1.

CONCLUSIONS

Asphalts and maltene undergo softening reactions when they are exposed to high temperature while in dilute solutions. These reactions cause growth of several FT-IR spectral peaks that have not

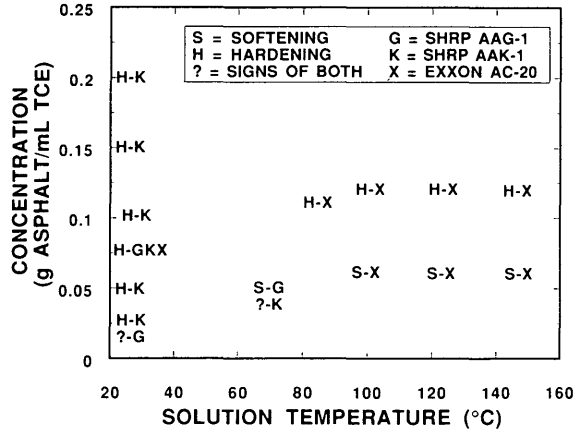

FIGURE 13 Instances of solvent hardening and softening over a range of solution conditions for three asphalts.

been seen in other reactions of asphalt. Also, narrow molecular-weight products are formed during solvent softening. The one having low molecular weight could lower asphalt viscosities. The solvent softening reaction rates increase with recovery oil bath temperature. Within practical temperature ranges, there appear to be threshold asphalt concentrations, above which softening does not occur. In higher asphalt concentrations, solvent hardening dominates. Below threshold concentrations, softening rates increase as asphalt concentration decreases. Softening rates also increase with the strength of the extraction solvent. TCE/EtOH is better at removing strongly adsorbed material from aggregate but also promotes solvent softening more than Tol/EtOH. The softening reactions respond to oxidation inhibitors, suggesting that they are free radical-initiated reactions.

The importance of these reactions is their potential effect on asphalt properties during extraction and recovery. With the advent of new recovery techniques that use lower asphalt concentrations and higher oil bath temperatures during recovery, softening becomes a genuine concern. These reactions are more damaging to asphalt properties than solvent hardening because they can cause a reduction of viscosity of more than 50 percent during a recovery, whereas increases in viscosity due to hardening can easily be held to less than 15 percent. Solution conditions that minimize the risk of solvent softening can be specified. This may be done by using Tol/EtOH rather than TCE/EtOH, keeping oil bath temperatures below 110°C, and ensuring that recovery solutions have asphalt concentrations higher than 0.15 g/mL.

ACKNOWLEDGMENTS

Support for this work by the Texas Department of Transportation, in cooperation with the U.S. Department of Transportation, the Federal Highway Administration, and the Texas Advanced Technology Program, is gratefully acknowledged. The technical contributions of Ann Ferry and Stephen Smiley are greatly appreciated.

REFERENCES

1. Burr, B. L., C. J. Glover, R. R. Davison, and J. A. Bullin. New Apparatus and Procedure for the Extraction and Recovery of Asphalt Binder from Pavement Mixtures. In *Transportation Research Record 1391*, TRB, National Research Council, Washington, D.C., 1993.
2. Lau, C. K., K. M. Lunsford, C. J. Glover, R. R. Davison, and J. A. Bullin. Reaction Rates and Hardening Susceptibilities as Determined from POV Aging of Asphalts. In *Transportation Research Record 1342*, TRB, National Research Council, Washington, D.C., 1992, pp. 50–57.
3. Peterson, G. D. *Relationship Between Composition and Performance of Asphalt Recycling Agents.* M.S. thesis. Texas A&M University, College Station, 1993.
4. Abu-Elgheit, M. A., C. K. Hancock, and R. N. Traxler. Effect of Selected Solvents on the Viscosities and Oxygen Contents of Asphalts. *Analytical Chemistry*, Vol. 41, May 1969, pp. 823–826.
5. Burr, B. L., R. R. Davison, H. B. Jemison, C. J. Glover, and J. A. Bullin. Asphalt Hardening in Extraction Solvents. In *Transportation Research Record 1323*, TRB, National Research Council, Washington, D.C., 1991, pp. 70–76.
6. Jemison, H. B., B. L. Burr, R. R. Davison, J. A. Bullin, and C. J. Glover. Application and Use of the ATR, FT-IR Method to Asphalt Aging Studies. *Fuel Science and Technology International*, Vol. 10, 1992, pp. 795–808.
7. Cipione, C. A., R. R. Davison, B. L. Burr, C. J. Glover, and J. A. Bullin. Evaluation of Solvents for the Extraction of Residual Asphalt from Aggregates. In *Transportation Research Record 1323*, TRB, National Research Council, Washington, D.C., 1991, pp. 47–52.

Publication of this paper sponsored by Committee on Characteristics of Bituminous Materials.

Low-Temperature Fracture Toughness of Polyethylene-Modified Asphalt Binders

NOLAN K. LEE AND SIMON A. M. HESP

One of the key factors that determines the susceptibility of a pavement to thermal cracking is the ability of the binder to withstand or relieve thermal stresses before they reach a critical point where cracks form. The mechanisms by which the addition of polyethylene improves the low-temperature properties of asphalt binders are discussed. Also examined is the degree to which the quality of the additive dispersion influences these mechanisms. Notched bending beam tests conducted at −20°C yielded fracture toughness values for three different polyethylene-asphalt systems. In all systems studied, the fracture toughness was found to increase linearly with the additive content. The chlorinated polyethylene-modified binders produced the toughest samples, followed by the stabilized polyethylene and the unstabilized polyethylene binders, respectively. High-magnification photographs, made with an environmental scanning electron microscope, yielded additional information concerning the nature of the failure mechanisms in these systems. The combined results show that greater toughening occurs with more finely dispersed polymers and with greater compatibility at the interface between the polymer and the asphalt matrix. These observations are consistent with the mechanisms of crack pinning and shear yielding, both of which are regularly found in multiphase thermoplastic materials.

One of the most promising methods of improving asphalt performance at both low and high service temperatures is by using additives. Of the many additives investigated, polymers show the greatest versatility in modifying the structural and adhesive properties of asphalt (*1*). Polymer additives currently available include natural and synthetic rubber latex (*2,3*), ground rubber tire (*4,5*), styrene-butadiene block copolymers (*6,7*), in situ reacted elastomeric polymers (*8,9*), and polyethylene (*10,11*).

Polyethylene has a number of characteristics that distinguish it from the other additives previously mentioned. Being a plastomer rather than an elastomer (rubber or rubberlike polymers), polyethylene remains a semicrystalline solid throughout regular pavement service temperatures and will show greater rigidity and less elasticity (*12*). Polyethylene is not miscible in asphalt and naturally separates into two phases. The quality of the dispersion is dependent on the process and the stabilizer used to emulsify the polyethylene (*13*). Finally, the general availability of recycled polyethylene from waste materials is high, providing a further incentive to study its potential as an additive (*14*).

Polymers alter the bulk viscosity of asphalt, thereby allowing softer asphalt grades to be used without causing adverse performance at higher service temperatures. The lower viscosity of the softer binder is commonly understood to be the key factor that increases the resistance to thermal cracking (*15*). However, other mechanisms of toughening may also exist. Isolating and exploiting these mechanisms could lead to further improvements in low-temperature performance.

Department of Chemistry, Queen's University, Kingston, Ontario, Canada K7L 3N6.

This paper examines the low-temperature toughening mechanisms for different systems of polyethylene dispersed in asphalt. Part of this study included measuring the low-temperature fracture toughness of asphalt binders modified with different quantities of polyethylene. Also examined was the role of the dispersion process and whether the average polyethylene particle size, particle size distribution, or the degree of adhesion to the asphalt matrix significantly affected the resulting fracture toughness. Finally, toughening mechanisms for asphalt at low temperatures based on multiphase toughening of brittle and pseudoductile polymers will be proposed.

BACKGROUND

Toughness and Thermal Stress Cracking

Thermal cracking results from the stresses created by different rates of thermal contraction within an asphalt-aggregate composite. As the temperature decreases, the asphalt will contract at a greater rate and to a greater degree than the base layer. This thermally induced stress condition causes microcracks to form at the pavement surface. As microcracks, they have little or no effect on pavement performance and may eventually "heal" (*16*). However, with repeated thermal cycles and continual vehicle loading, many of these microcracks grow into macrocracks. Rapid deterioration results when macrocracks grow to span the depth of the asphalt concrete, thereby allowing water to penetrate into the base layer (*17*). Therefore it is of great benefit to limit the propagation of cracks at the microscopic level, when the damage is still reversible.

Toughening Mechanisms in Multiphase Materials

For the purposes of this study, toughness is defined as a measurement of the energy expended in fracturing a material. The amount of yielding that takes place during the fracture process greatly influences the toughness. Even in the fracture of a brittle material, some localized yielding, permanent (plastic) deformation that occurs when a material is stressed beyond its recoverable (elastic) limit, always occurs. Enhancing this localized yielding by introducing a dispersed secondary phase into the brittle matrix is the basis of many toughened plastics.

The three main toughening mechanisms that occur in multiphase materials are crack pinning, shear yielding, and crazing. All three involve plastic deformation in the microscopic region sur-

rounding the dispersed phase. With crack pinning, this deformation occurs when the moving crack front encounters a row of dispersed particles (*18*). If these particles have a greater strength than the surrounding matrix, the crack front must travel around the particles to reform as a new fracture surface. Since the plastic flow occurs at the particle-matrix interface, the level of adhesion influences the toughening effect. Interparticle spacing is another important factor, since the formation of each new fracture surface consumes additional energy.

Shear yielding is a constant-volume process and occurs without loss of intermolecular cohesion. Whereas all materials show shear yielding to some degree, its contribution to toughening may be small, as in the case of a brittle, single-phase material. When a dispersed phase has a different elastic modulus from the matrix, it creates conditions of localized stress concentration (*19*). This in turn increases the potential size and effect of the shear-yielded regions and may lead to significant increases in fracture toughness. In materials where shear yielding is the dominant toughening mechanism, the number of dispersed particles governs the overall toughening effect.

Crazing is a toughening mechanism found in high-molecular-weight materials. With crazing, there is a significant change in volume as small voids, called crazes, form within the matrix. Instead of coalescing and propagating as a macrocrack, an interpenetrating network of fibrils stabilizes the voids. The fibrils form when the matrix material becomes highly oriented. The orientation process consumes energy and also makes the fibrils strong enough to stabilize the craze. As with shear yielding, fibril formation is dependent on localized matrix softening resulting from the inclusion of a finely dispersed second phase. Since overcoming the intermolecular cohesion in the region of crazing consumes a significant amount of the fracture energy, the degree of interfacial adhesion is important (*20*). It is also important for there to be a quantity of larger particles that serve to limit the crazes from growing into true cracks. Thus the toughening effect due to crazing will be sensitive to both the degree of adhesion between the particles and the matrix and the particle size distribution.

Measurement of Toughness Using Performance-Based Tests

Performance-based tests do not isolate localized toughening mechanisms from changes in bulk properties. Instead, they measure the effect of many microscopic and macroscopic factors acting together. For example, Joseph et al. (*21*) found thermal shrinkage strains in mixes containing (unstabilized) polyethylene-modified binders that were markedly lower than those made with either the unmodified or ground rubber tire–modified binders. As shown in Figure 1, the temperature versus induced strain curve for the mix containing the polyethylene-modified binder has the smallest slope. In an unstable system, though, coalescence of the polyethylene will occur, and most of the polymer will exist in large (greater than 100-μm) domains. Without an even distribution of finely dispersed particles, the increase in fracture toughness will be limited. Large polyethylene domains, though, may serve to bridge the aggregates and thus reduce thermal shrinkage and failure. In this way unstable polyethylene may be a beneficial additive even though it may not greatly increase the binder toughness.

Binder tests based on failure strain and failure stress were also not intended to measure fracture toughness. Neither the force ductility test nor the direct tension test developed under the Strategic Highway Research Program (SHRP) can distinguish changes in bulk viscosity from effects that occur at the microscopic level. What the newly developed binder tests clearly demonstrate, though, is that the addition of polymer to the binder can significantly alter the thermal cracking properties of an asphalt mix. Using the thermal stress restrained specimen test, Jung and Vinson (*17*) showed that the low-temperature performance of the mix is influenced by the thermal and mechanical properties of the binder. This test was also used to validate the low-temperature binder specification tests developed by the SHRP program. When performed with polymer-modified binders, these tests confirmed that the addition of polymers often improves the low-temperature performance of a given asphalt grade. Such performance-based testing has led to a general conclusion that "different polymers achieve their effects by significantly different mechanisms" (*22*). However, performance-based testing alone cannot provide any additional information concerning the actual mechanisms involved.

Where To Look for Evidence of a Toughening Mechanism in Asphalt

When testing an unstable, polyethylene-asphalt system at low temperatures, Jew and Woodhams (*23*) found that fracture properties were sensitive to polymer concentration. They suggested both shear yielding and crazing as possible explanations for the increase in toughness. Also suggested as having significance were the particle characteristics of the secondary phase. The latter suggestion agrees with observations made in other studies that recognized the importance of achieving fine dispersions in multiphase polymer-asphalt systems (*24,25*). However, to date no one has quantitatively analyzed the results of altering the quality of the dispersion to investigate theories of low-temperature toughening.

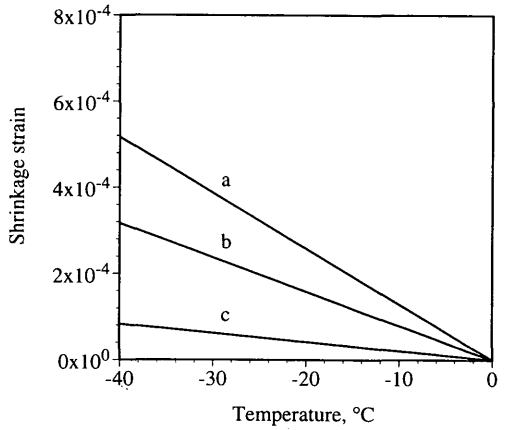

FIGURE 1 Unrestrained shrinkage strain in various asphalt-aggregate mixes (*21*): a = unmodified binder, b = rubber-modified binder, c = unstabilized polyethylene-modified binder.

EXPERIMENTAL

Materials

The base asphalt used for the polyethylene-modified binders was a Bow River 85–100 penetration grade asphalt (SHRP code AAN). An 85–100 and a 200–300 penetration grade asphalt from Venezuela were used as the base asphalt for the samples modified with chlorinated polyethylene.

Stable polyethylene-modified binders were prepared by previously established procedures (*11*), only a brief description of which is given here. In addition to the polyethylene, a low-molecular-weight elastomer was added to heated, molten asphalt. Under high shear mixing at 165°C, the additives react in situ to form micron-sized polyethylene particles surrounded by a layer of elastic, asphalt-grafted polymer. As the elastic interface becomes swollen by the asphalt, it acts to sterically stabilize the polyethylene and prevents coalescence from occurring.

The unstable polyethylene-modified binder was also created using the described procedure except that a coupling agent necessary for the polyethylene-elastomer reaction was not added. As a result, there was no compatibility at the interface between the polyethylene and the asphalt matrix. Coalescence occurred as the test samples cooled down, resulting in a much coarser dispersion.

The chlorinated polyethylene additive (Tyrin 2552 from Dow Chemical of Midland, Michigan) contains 25 wt percent chlorine and is partially soluble in most asphalts. The mixture requires no additional additives to remain thermally stable. High shear mixing at 195°C with an 85–100 pen and 200–300 pen Venezuelan asphalt created modified binders with a very fine dispersion of partially dissolved polymer.

Control samples for the polyethylene-modified systems were created by adding only the elastomeric stabilizer to the base asphalt and reacting it under high shear for 2 hr. Unmodified asphalts served as the control for the chlorinated polyethylene-modified samples.

Fracture Mechanics

Preparing samples for fracture testing involved pouring hot liquid asphalt into a notched silicone rubber mold and cooling the filled mold in a freezer set at the testing temperature of −20°C. After 2 hr, the asphalt bars, measuring 25 mm wide by 12.5 mm deep by 175 mm long, were cold enough to be easily removed from the molds. The cast bars were then returned to the freezer to cool before testing. This cooling period ranged from 18 to 36 hr.

Fracture testing was performed using a three point bend configuration based on ASTM E399–90. Tests were performed on a computer-controlled Sintech 2/G testing frame equipped with an environmental chamber. As shown in Figure 2, each sample bar was cast with a 5-mm-deep, 90-degree starter notch and centered on two supports that were set at a 100-mm span. Immediately before each test, the notch was sharpened with a razor blade. The point of loading was opposite the sharpened notch, and the crosshead speed was set at a constant rate of 0.01 mm/sec. Samples were monotonically loaded until failure. Load and deflection data were measured using a 200-lb load cell, digitally recorded, and stored for later analysis.

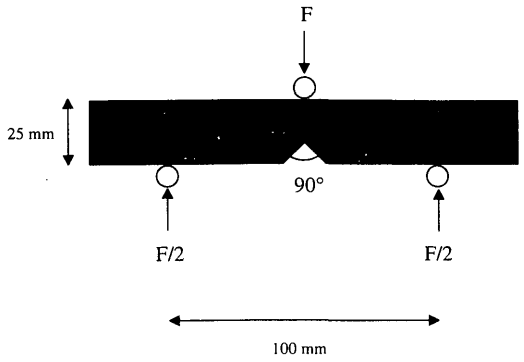

FIGURE 2 Bending beam configuration for low-temperature fracture tests on asphalt binders (test temperature = −20°C and 0.01 mm/sec loading rate).

Brittle fracture studies were completed for 15 samples. Measured data included the failure load and the modulus. Fracture toughness values were calculated according to the following equation (*26*):

$$K_{Ic} = \frac{P_f S}{B W^{3/2}} \times \left\{ \frac{3\left(\frac{a}{W}\right)\left[1.99 - \frac{a}{W}\left(1 - \frac{a}{W}\right)\left(2.15 - 3.93\frac{a}{W} + 2.7\frac{a^2}{W^2}\right)\right]}{2\left(1 + 2\frac{a}{W}\right)\left(1 - \frac{a}{W}\right)^{3/2}} \right\}$$

where

K_{Ic} = critical stress intensity factor or fracture toughness (N m$^{-3/2}$),
P_f = applied failure load (N),
S = loading span (m),
B = specimen depth (m),
W = specimen width (m), and
a = crack length (m).

The two main parameters (the fracture toughness, K_{Ic}, and the stiffness modulus, E) were calculated assuming linear elastic conditions. Creating conditions where the equations are based on linear elastic fracture mechanics (LEFM) avoids the difficulties associated with viscoelastic behavior. LEFM equations are valid when the modulus of the matrix and the added polymer phase vary only slightly with time (*19*). Choosing a low test temperature of −20°C ensured that the asphalt matrix would not exhibit any viscous behavior during testing, even at low strain rates. Selecting a sample thickness that was large compared with the plastic zone size ensured that plane strain conditions existed at the crack tip.

Fracture toughness is a fundamental material parameter that measures the stress intensity at critical conditions. When the stress distribution is uniform throughout the material, the fracture toughness is a measurement of strength. However, with a well-defined stress field, such as in a notched sample under conditions of plane strain, the fracture toughness measures the magnitude and distri-

bution of the stress at the crack tip (*27*). Unlike tests that measure material strength, strain-to-failure, or ductility, the fracture toughness test is directly related to the energy released during crack propagation. For this reason, the fracture toughness of a binder may be a better parameter for measuring its ability to withstand internal stresses before they build up and lead to catastrophic failure.

Morphology

Scanning electron microscope (SEM) photographs yielded particle size distributions for the four asphalt samples containing 6 wt percent polyethylene. Approximately 0.5 g of asphalt was dissolved in 10 mL of tetrahydrofuran (THF), filtered through a Nuclepore polyester membrane filter (0.2-μm pore size and 25-mm diameter) and rinsed twice with additional 10-mL portions of fresh THF. The residue was then gold coated for SEM examination. Using the SEM, the samples were scanned and photographed at 1000X magnification. Particle diameters were measured manually using enlargements of the SEM photographs.

Each particle size distribution is the result of measuring more than 1,000 particle diameters. Distributions are expressed in cumulative wt percent (equivalent to vol percent) to better illustrate the effect of large particles. Particle volumes were calculated using the measured diameters and assuming a spherical geometry. Volumes for each particle size category were divided by the total volume to produce a distribution that approximated a log-normal distribution (*28*). The distributions are defined by two parameters: the mean particle size and the standard deviation of the mean.

RESULTS AND DISCUSSION

Low-temperature fracture results, presented in Table 1, clearly distinguish between regular and polymer-modified binders. With this test, nonbrittle fracture may occur with samples that warm up even slightly, and thus maintaining the test specimen to within 1°C of −20°C was essential to getting consistent test results. Slight inconsistencies in the sharpness of the notch, the geometry of the samples tested, and the point of loading also add to the scatter in results. In the results presented, samples showing bulk yielding, indicated by an inflection point on the stress-strain curve, were discarded.

Test results show different low-temperature modulus values for binders of different penetration grades. For linear-elastic conditions, the slope of the stress-strain curve provides the modulus. It is analogous to the Young's modulus for elastic materials. The base asphalt determines the elastic modulus. At −20°C, the stiffness of the binder is not significantly changed by the addition of up to 8 wt percent polyethylene.

Whereas the addition of polymer did not greatly increase the binder stiffness, it increased the fracture toughness (K_{Ic}) of the material. Compared with their respective control samples, the addition of 6 percent stabilized polyethylene led to a 50 percent increase in the fracture toughness. Adding 5 percent chlorinated polyethylene more than doubled the fracture toughness. Of the three systems studied, the unstabilized polyethylene showed the least increase, approximately 25 percent for 6 percent added polymer.

Shown in Figures 3 and 4 are the fracture toughness values plotted against polymer content for the polyethylene system and the chlorinated polyethylene systems, respectively. In both systems, the relationship was linear with correlation coefficients of 0.94 or greater. Compared with the stable polyethylene system, the slope of the chlorinated polyethylene-modified binder was 30 percent greater.

Figure 5 shows the fracture toughness contribution of 6 percent added polyethylene for the three polymer-modified systems studied. With higher additive contents, the toughening effect becomes markedly different. This observation resembles that of multiphase toughening of a pseudoductile polymer, such as polypropylene, that relieves internal stresses primarily through crack pinning and shear yielding. The number of dispersed particles and the polymer-asphalt interfacial adhesion govern the enhancement of these toughening mechanisms. Since each particle creates a yielded region in the

TABLE 1 Results from Low-Temperature Fracture Testing of Polyethylene-Modified Asphalt Binders

Asphalt Grade (Penetration)	Additive (wt. %)	Modulus (GPa)	Fracture Toughness, K_{Ic} (kN $m^{-1.5}$)
85-100	0% PE[a]	1.4 ± 0.1	79 ± 5
Bow River	3% PE	1.4 ± 0.1	88 ± 5
	4% PE	1.4 ± 0.1	98 ± 6
	6% PE	1.4 ± 0.1	117 ± 9
	7% PE	1.4 ± 0.1	123 ± 6
	8% PE	1.6 ± 0.1	140 ± 9
85-100	0% CPE[b]	1.4 ± 0.1	44 ± 4
Bow River	3% CPE[c]	1.4 ± 0.1	83 ± 6
	5% CPE	1.4 ± 0.1	91 ± 3
200-300	0% CPE	0.45 ± 0.03	50 ± 3
Bow River	3% CPE	0.50 ± 0.08	100 ± 20
	5% CPE	0.42 ± 0.03	155 ± 8

[a] Control sample containing only elastomeric stabilizer.
[b] Control sample containing 100% Bow River Asphalt.
[c] Chlorinated polyethylene (no stabilizer necessary).

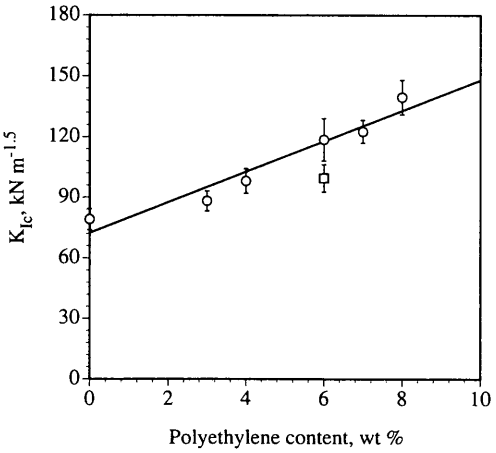

FIGURE 3 Fracture toughness for polyethylene-modified 85-100 Bow River asphalts (○ = sterically stabilized, □ = unstabilized; error bars give 90 percent confidence limits).

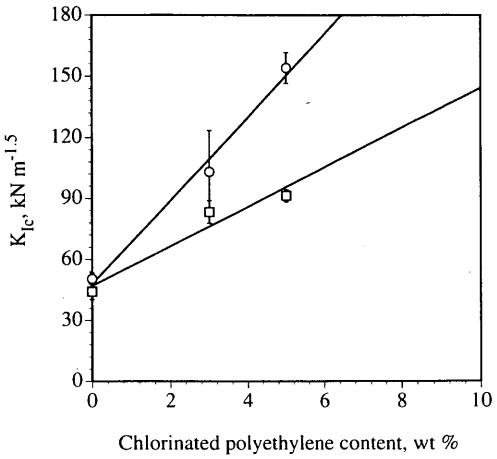

FIGURE 4 Fracture toughness for chlorinated polyethylene-modified 85-100 and 200-300 Bow River asphalts (○ = 200-300 asphalt, □ = 85-100 asphalt; error bars give 90 percent confidence limits).

surrounding matrix material, a greater number of inclusions will necessarily create a greater toughening effect. With rubber-toughened polypropylene (*29*), a transition occurs when the rubber content exceeds roughly 12 wt percent. At that concentration, the shear yielding mechanism contributes to a massive increase in toughening. Yield zones overlap and strong particle interactions lead to a much tougher material. Test results in our asphalt systems show no such transition from brittle to ductile behavior. To achieve such a transition, the additive content would most likely have to exceed 10 wt percent, which is neither cost-effective nor feasible with current processing methods.

With the softer-grade Venezuelan asphalt, the toughening effect due to the addition of chlorinated polyethylene was the most pronounced. Without modification, the 200-300 pen binder shows only a marginal increase in fracture toughness over the 85-100 pen asphalt. When this lower viscosity binder was modified with 5 percent chlorinated polyethylene, though, the fracture toughness increased by more than 300 percent. SEM photographs of the fracture surface show yielded regions in the softer matrix. Apparently there is a synergistic effect in which the added polymer contributes to larger regions of plastic deformation within the lower-viscosity matrix. A low-viscosity binder modified with enough chlorinated polyethylene may even begin to demonstrate pseudoductile behavior. To study the brittle-to-ductile transition, techniques based on elastic plastic fracture mechanics, such as J-integral tests (*18*), are necessary.

For the systems studied in this work, the crazing mechanism is not thought to be of as much importance as crack pinning or shear yielding. First, crazing is highly dependent on the molecular weight of the matrix. Only fibrils formed of high-molecular-weight matrix material have the necessary strength to stabilize crazes. In the case of toughened polystyrene (*19*), significant crazing occurs only when the molecular weight of the matrix exceeds 70 000 g mole^{-1}. As a comparison, an asphalt matrix has a typical number average molecular weight of approximately 1000 g mole^{-1}. Furthermore, usually toughening due to crazing is sensitive to changes in the particle size distribution. As indicated in Table 2 and Figure 6, for the stabilized polyethylene-asphalt systems, fine changes in the particle size distribution did not lead to any difference in the fracture toughness.

TABLE 2 Particle Size Data for 6 percent Polyethylene-Modified Asphalt Binders (Bow River 85/100 Pen)

Sample	Wt. Average Particle Diameter (μm)	Standard Deviation (μm)	Fracture Toughness, K_{Ic} (kN m$^{-1.5}$)
Control[a]	-	-	79 ± 5
A	2.2	1.12	119 ± 9
B	3.5	1.18	115 ± 7
U[b]	10.8	5.12	99 ± 7

[a] Control sample containing only elastomeric stabilizer.
[b] Unstabilized polyethylene

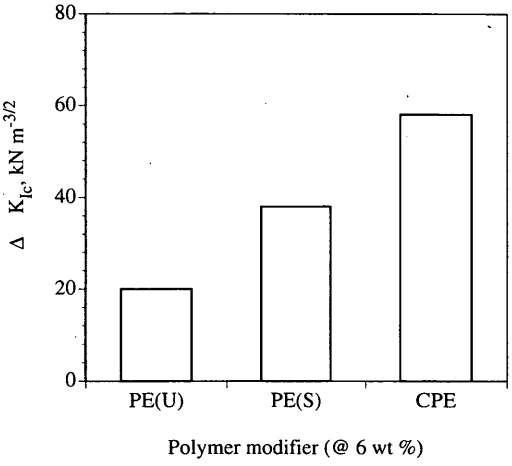

FIGURE 5 Added benefit to low-temperature fracture toughness for different polyethylene modifiers in an 85-100 Bow River binder.

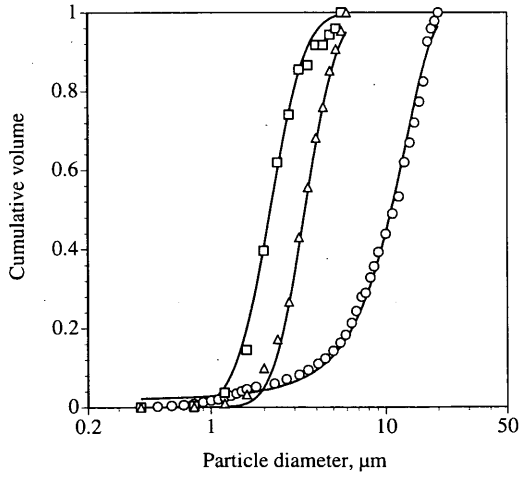

FIGURE 6 Particle size distribution for 6 percent polyethylene-modified samples (□ = Sample A, △ = Sample B, and ○ = Sample U).

Results from this single study do not completely discount the possibility of craze formation in all polymer-modified asphalts. In the chlorinated polyethylene system, where the polymer partially dissolves in the asphalt matrix, enough high-molecular-weight material may be present for crazing to occur. Further investigations using techniques such as volumetric strain measurements (*19*) are necessary before evidence supporting or disproving crazing becomes conclusive.

SUMMARY

1. Low-temperature fracture testing distinguishes between different grades of asphalt binders and between different polyethylene-asphalt binder systems.
2. The addition of polyethylene improves the low-temperature fracture toughness of an asphalt binder without significantly increasing its stiffness at low temperatures.
3. For polyethylene contents below 8 wt percent, the increase in fracture toughness is a linear function of the polymer content. No sudden increase in toughening was seen that would indicate a brittle-to-ductile transition at the chosen test temperature.
4. Finer dispersions of polyethylene contributed to a more pronounced toughening effect.
5. The toughening effect is more pronounced when chlorinated polyethylene was added to a softer matrix.
6. With stabilized and unstabilized polyethylene, the toughening is attributed to a crack pinning mechanism.
7. With the chlorinated polyethylene modifier, there is also evidence of shear yielding at the crack tip.
8. It is unlikely that crazing plays a significant role in any of the systems studied.

ACKNOWLEDGMENTS

The authors gratefully acknowledge the funding provided by Imperial Oil of Canada through the Institute for Chemical Science and Technology. In addition, they thank Helle Hedmark for her work in preparing the stable polyethylene binders and Joseph Hui for his work on the unstabilized polyethylene system. Finally, the authors are highly appreciative of the time donated by Geoffrey Morrison in developing the fracture testing technique and by Rob Evans, who operated the SEM.

REFERENCES

1. Button, J. W. Summary of Asphalt Additive Performance at Selected Sites. In *Transportation Research Record 1342*, TRB, National Research Council, Washington, D.C., 1992, pp. 67–75.
2. Beaty, A. N. S. Latex Modified Bitumen for Improved Resistance to Brittle Fracture. *Highways and Transportation*, Sept. 1992, pp. 32–41.
3. Brown, E. R., F. Parker, Jr., and M. R. Smith. Study of the Effectiveness of Styrene-Butadiene Rubber Latex in Hot Mix Asphalt Mixes. In *Transportation Research Record 1342*, TRB, National Research Council, Washington, D.C., 1992, pp. 85–91.
4. Ciesielski, S. K., and R. J. Collins. Current Nationwide Status of the Use of Waste Materials in Hot Mix Asphalt Mixtures and Pavements. In *Use of Waste Materials in Hot-Mix Asphalt*, ASTM STP 1193, American Society for Testing and Materials, Philadelphia, Pa., 1993.
5. Huffman, J. E. *The Use of Ground Vulcanized Rubber in Asphalt.* ASTM STP 724, American Society for Testing and Materials, Philadelphia, Pa., 1980, pp. 3–12.
6. Berker, A., M. G. Bouldin, and J. H. Collins. Rheological Rationales for Rutting Resistance. *Proc., Association of Asphalt Paving Technologists*, Vol. 59, Albuquerque, N.Mex., Feb. 1990.
7. Carpenter, S. H., and T. Van Dam. Laboratory Performance Comparison of Polymer-Modified and Unmodified Asphalt Concrete Mixtures. In *Transportation Research Record 1115*, TRB, National Research Council, Washington, D.C., 1987, pp. 62–74.
8. King, G. N., H. W. King, O. Harders, P. Chavenot, and J. Planche. Influence of Asphalt Grade and Polymer Concentration on the High Temperature Performance of Polymer Modified Asphalts. *Proc., Association of Asphalt Paving Technologists*, Vol. 61, Charleston, S.C., Feb. 1992.
9. Ali, N., A. T. Papagiannakis, J. S. S. Chan, and A. T. Bergan. Engineering Properties of Two Polymer-Modified Asphalts. *Proc., Canadian Technical Asphalt Association*, Vol. 35, Morin Heights, Quebec, Canada, Nov. 1990.
10. Flynn, L. Recycled Plastic Finds Home in Asphalt Binder. *Roads and Bridges*, March 1993, pp. 41–45.
11. Hesp, S. A. M., Z. Liang, and R. T. Woodhams. U.S. Patent Application 07/767941, 1991.
12. King, G. N., and H. W. King. Polymer Modified Asphalts. In *Solutions for Pavement Rehabilitation*, American Society of Civil Engineering, New York, 1986, pp. 240–254.
13. Hesp, S. A. M., and R. T. Woodhams. Stabilization Mechanism in Polyolefin-Asphalt Emulsions. In *Polymer Modified Asphalt Binders*, ASTM STP 1108, American Society for Testing and Materials, Philadelphia, Pa., 1992, pp. 1–19.
14. Flynn, L. Recycling: Will Roads Become Linear Landfills. *Roads and Bridges*, Oct. 1992, pp. 65–69.
15. Goodrich, J. L. Asphalt and Polymer Modified Asphalt Properties Related to Performance of Hot Asphalt Concrete Mixes. *Proc., Association of Asphalt Paving Technologists*, Vol. 57, Williamsburg, Va., Feb. 1988.
16. Kim, Y. R., D. N. Little, and F. C. Benson. Chemical and Mechanical Evaluation on Healing Mechanism of Asphalt Concrete. *Proc., Association of Asphalt Paving Technologists*, Vol. 60, Seattle, Wash., March 1990.
17. Jung, D., and T. S. Vinson. Statistical Analysis of Low Temperature Thermal Stress Restrained Specimen Test Results. *Proc., Canadian Technical Asphalt Association*, Vol. 37, Victoria, British Columbia, Canada, Nov. 1992.
18. Kinloch, A. J., and R. J. Young. *Fracture Behaviour of Polymers.* Elsevier Applied Science Publishers, Ltd., London, 1985.
19. Bucknall, C. B. *Toughened Plastics.* Applied Science Publishers, Ltd., London, 1977.
20. Könczöl, L., W. Döll, and G. G. Michler. Study of the Toughening Mechanism of Crazing in Rubber Modified Thermoplastics. *Colloid and Polymer Science*, Vol. 270, 1992, pp. 972–981.
21. Joseph, P., J. H. Dickson, and G. Kennepohl. Evaluation of Polymer-Modified Asphalts in Ontario. *Proc., Canadian Technical Asphalt Association*, Vol. 37, Victoria, British Columbia, Canada, Nov. 1992.
22. Stock, A., and W. Arand. Low Temperature Cracking in Polymer Modified Binder. Preprint. Association of Asphalt Paving Technologists, 1993.
23. Jew, P., and R. T. Woodhams. Polyethylene-Modified Bitumen for Paving Applications. *Journal of Applied Polymer Science*, Vol. 31, 1986, pp. 2685–2704.
24. Zanzotto, L., D. Foley, C. E. Rodier, and R. D. Watson. Modified Asphalts—Are You Really Coming? *Proc., Canadian Technical Asphalt Association*, Vol. 32, Toronto, Ontario, Canada, 1987.
25. Molenaar, J. M. M. Polymer Modified Bitumens: Functional Properties and Quality Aspects. *Proc., International Symposium Chemistry of Bitumen*, Vol. 2, Rome, June 1991.
26. Broek, D. *Elementary Engineering Fracture Mechanics* (3rd edition). Martinus Nijdroff, The Hague, Netherlands, 1982.
27. Selvadurai, A. P. S., and M. C. Au. *Transient Effect in Low Temperature-Induced Fracture and Failure of Pavement Structures.* Report PAV-88-02. Research and Development Branch, Ontario Ministry of Transportation, 1988.
28. Stockham, J. D. *Particle Size Analysis.* Ann Arbor Science, Inc., Ann Arbor, Mich., 1977.
29. Jancar, J., A. DiAnselmo, and A. T. Dibenedetto. Ductile-Brittle Transition in Elastomer-Modified Polypropylene. *Polymer Communications*, Vol. 32, No. 12, 1991, pp. 367–369.

Publication of this paper sponsored by Committee on Characteristics of Bituminous Materials.

Investigation of Laboratory Aging Processes of Asphalt Binders Used in Florida

CHUI-TE CHIU, MANG TIA, BYRON E. RUTH, AND GALE C. PAGE

A laboratory investigation was performed to evaluate a variety of aging processes used for simulating the long-term aging of asphalt binders. Four promising methods investigated in this study include an extended thin film oven test (TFOT), an ultraviolet (UV) chamber, the California tilt oven (CTO), and the pressure aging vessel (PAV). A few conventional asphalts commonly used in Florida and a few modified binders were subjected to these aging processes, and their aged residues were tested for comparison of aging severity. Because of the insensitivity of consistency measurements at lower temperatures, the most sensitive parameter for differentiating the aging severity was found to be the aging index at 60°C, which is the ratio of absolute viscosities at 60°C. On the basis of this parameter, the relative aging severities of aging processes were established. Various asphalts were found to exhibit different aging severities when subjected to different aging processes. Asphalts from different sources exhibit differentiable degrees of volatile loss when subjected to the extended TFOT. The UV chamber was found to be effective only in aging the surfaces of the binder samples. Low-viscosity asphalts were found to age more in the CTO process. Whereas low-volatile-loss asphalts show less aging in most aging processes, some high-volatile-loss asphalts could age less in the PAV process.

Asphalts undergo two substantially different aging processes in their service life. They are subjected to high temperatures and a high degree of air exposure during their relatively short production time (short-term aging) and then to the environment at a relatively lower temperature and air void content for a long duration (long-term aging). A variety of methods have been proposed and investigated to simulate the aging effects on asphalt during mixing as well as field service. The purpose of this study was to conduct a laboratory evaluation of different aging processes on typical asphalt binders commonly used in Florida. The aging effects of the conventional aging processes were compared with the newly proposed pressure aging vessel (PAV) process. The effects of a few modifiers on the aging characteristics of the asphalts were also evaluated.

The most important mechanism of age hardening is the change in the chemical composition of asphalt molecules from reaction with atmospheric oxygen. As in most chemical reactions, the contact surface area and temperature dominate the oxidation rate of asphalt. First, substantial oxidation and loss of volatiles occur during mixing. The aging process continues, although at a much slower rate, while the asphalt concrete is processed through a surge or storage silo, transported to the paving site, laid, and compacted. After the asphalt pavement has cooled and been opened to traffic, the age hardening process continues at a significantly slower rate, depending on the air void content and pavement temperature. Corbett and Merz (*1*) showed that the amount of the saturate fraction, which is the potentially volatile component, remained virtually constant during 18 years of service in the well-known Michigan Road Test.

A tabulated review of the laboratory simulation of asphalt aging has been made by Welborn (*2*). Ideally, asphalts hardened by a laboratory aging method should be similar to those aged in actual service environments. Furthermore, the method should be reasonably simple to be used as a routine control test. The sample size of aged residue should be reasonable to allow for necessary tests.

The most successful simulation methods are the thin film oven test (TFOT) and rolling thin film oven test (RTFOT). These two methods are recognized to give the same aging effect and can be used to predict the degree of age hardening of an asphalt cement during conventional hot mixing at 150°C, as indicated by penetration or viscosity measurements. It is believed that some asphalts, especially those refined from heavy crudes, were affected more by mixing than in situ aging, whereas the opposite is true for some other asphalts. Therefore Santucci and Schmidt (*3*) suggested that it might be unreliable to predict long-term durability from short-term hardening characteristics.

In a study by Kemp and Predoehl (*4*), the RTFOT test was modified to heat asphalt at a lower temperature (111°C) for 168 hr with the oven slightly tilted to prevent asphalt buildup. Penetration at 25°C, absolute viscosity at 60°C, and ductility at 25°C were measured on the aged residues as indicators of the durability characteristics of the asphalts after 2 years of exposure to a hot desert environment. Higher-viscosity asphalts tend to roll less during the rolling process in the RTFOT, which might result in a lower oxidation rate. This is one of the possible drawbacks of the California tilt oven (CTO).

Durability studies at the University of Florida showed that it is possible to simulate the effects of aging during service and the hot mixing process by using the TFOT or RTFOT at a higher temperature (*5,6*). The potential advantages of using the TFOT at higher temperatures as compared with other long-term aging tests are that existing standardized equipment could be conveniently used and that the test would require much less time to complete. To determine the aging characteristics of asphalts at a lower temperature, an ultraviolet (UV) chamber, which is maintained at a temperature of 60°C, was used to simulate the effects of heat, UV light, and air on asphalt mixtures.

The PAV has been proposed by SHRP researchers to simulate long-term aging of asphalt binders. By applying a higher oxygen content through increasing air pressure, oxidation of asphalt can be accelerated at a lower temperature, which is closer to the real

C.-T. Chiu, M. Tia, and B. E. Ruth, Department of Civil Engineering, University of Florida, Gainesville, Fla. 32611. G. C. Page, Florida Department of Transportation, P.O. Box 1029, Gainesville, Fla. 32602.

exposure temperature. These proposed methods need to be evaluated and compared with one another before being introduced into the asphalt specifications.

TESTING PROGRAM

Laboratory Aging Processes Used

As indicated in Table 1, four promising laboratory aging methods, including an extended TFOT, UV chamber, CTO, and PAV, were selected for simulating the effect of long-term asphalt aging.

Extended TFOT

The TFOT (ASTM D1754) was extended by using different process temperatures, durations, and film thicknesses, as indicated in Table 1, to obtain eight levels of age hardening.

UV Chamber

A UV chamber, which was built at the University of Florida (*6*), was used in this study. The chamber was made from 3/8-in. plywood in the shape of a trapezoidal box with a rectangular base 4 ft 2 in. × 3 ft 9-1/2in. and a height of 1 ft 10 in. The two sides of the chamber were hinged to permit access into the chamber, and the interiors of these two hinged sides were used to mount four lamp assemblies, each assembly carrying two lamps. The roof of the chamber was used to mount one more lamp assembly carrying two lamps. Ten 40-W fluorescent UV-B lamps (UVB-313) were used in the chamber. Temperature in the chamber was maintained at 60°C through the use of a thermostat, infrared heat lamps, and a circulation fan on the vertical end sides of the chamber. The residues from the conventional TFOT process were reduced to 25-g samples and placed in the same TFOT plates. The TFOT plates containing 25-g residues were then placed in the 60°C UV chamber for durations of 7, 14, and 28 days.

CTO

The rolling thin film oven (ASTM D2872) was positioned so that the horizontal axes of the glass containers are tilted by 1 degree higher in the front of the oven. The RTFOT bottles with 35-g samples were heated at 111°C for 24, 72, and 168 hr. After the process, the RTFOT bottles were put into a 160°C oven for 20 min to obtain sufficient fluidity to pour the aged residues out of the bottles.

PAV

The SHRP-proposed PAV was investigated in this study. In consideration of the convenience of the testing procedure, it was decided to perform the PAV test on TFOT residues (50-g samples transferred directly from TFOT oven) rather than on RTFOT residues. The PAV process was performed under 300 psi for 20 hr at three temperatures (90°C, 100°C, and 110°C).

Asphalt Binders and Evaluation Parameters Used

Five conventional asphalts commonly used in Florida were subjected to the 17 artificial aging processes, and their aged residues were evaluated. Five modifiers, which include fine ground tire rubber (GTR), carbon black (CB), styrene ethylene butylene styrene (SEBS), ethylene vinyl acetate (EVA), and styrene butadiene rubber (SBR), were blended at adequate dosage levels with an AC-30 to produce five blends of modified AC-30 asphalts. The modified asphalts were subjected to the CTO and PAV aging processes, and their aged residues were tested for the effects of modifiers on the aging characteristics of the asphalt binder.

The following tests were performed on both the unaged and aged samples:

1. Penetration at 25°C (ASTM D5),
2. Absolute viscosity at 60°C (ASTM D2171),
3. Schweyer rheometer tests at 25°C and 5°C, and
4. Infrared absorption spectral analysis.

The percent penetration retained, aging indices based on the ratios of viscosity at three temperatures, and carbonyl ratio index, which is the ratio of carbonyl ratio of the aged residue to the carbonyl ratio of original asphalt, were used to measure the severity of age hardening of the various aging processes.

The major concern in evaluating the aging characteristic of an asphalt binder is the potential of thermal cracking of the aged asphalt binder. Stiffness limit temperature concept has been proposed from the study of low-temperature cracking in the field (*7*). A stiffness limit of 300 MPa for a loading time of 2 hr has been used in the recent SHRP specification. Experiences in Florida (*6*) have shown that low-temperature cracking occurs when the constant power viscosity of the binder exceeds 2.6×10^{10} poise. Davis (*8*) suggested a maximum viscosity of 2.1×10^{10} poise for the control of asphalt. The constant stress (1-MPa) viscosity used in this study as described in the following section is smaller than its corresponding constant power (100-W/m^3) viscosity due to the pseudoplastic nature of asphalt at low temperature. A constant stress viscosity limit of 2×10^{10} poise was considered to be adequate and used in this study.

Schweyer Rheometer Tests

A Cannon Schweyer Constant Stress Rheometer was used to characterize low-temperature rheology of the binders in this study. A comprehensive review of the theoretical background of the Schweyer constant stress rheometer and the application of rheological concepts proposed by H. E. Schweyer has been presented by Tia and Ruth (*9*). The rheometer consists of a gas-operated pneumatic cylinder that applied a specified force to the plunger in the sample tube. An LVDT measured the movement of the plunger, and the output voltage was digitized and acquired by a data acquisition and analysis system, which was operated on an IBM PC-compatible computer.

On the basis of the steady-state laminar flow of power law fluid in the capillary tube, the shear stress and shear rate under the applied pressure can be obtained from the movement of the plunger and dimensions of the tube. Tests are usually conducted at a minimum of five stress levels. The shear susceptibility is computed and used to calculate the constant power viscosity at

TABLE 1 Asphalt Binders and Laboratory Aging Processes Investigated

Unmodified Binders		
Refinery Source	Grade	Abbreviation
Coastal	AC-30	CT30
Amoco	AC-30	AM30
Amoco	AC-20	AM20
Mariani	AC-30	MA30
Mariani	AC-20	MA20
Modified Binders (use Coastal AC-30 as base asphalt)		
Modifier	Dosage (%)	Abbreviation
#80 fine ground tire rubber	5	GTR
carbon black	10	CB
styrene ethylene butylene styrene	5	SEBS
ethylene vinyl acetate	5	EVA
styrene butadiene rubber	3.5	SBR
Extended TFOT		Abbreviation
TFOT, 50 g, 140 °C, 5 hours		TL
TFOT, 50 g, 163 °C, 5 hours		TS
TFOT, 50 g, 185 °C, 5 hours		TH
TFOT, 50 g, 163 °C, 10 hours		TF10
TFOT, 50 g, 163 °C, 15 hours		TF15
TFOT, 25 g, 140 °C, 5 hours		TLM
TFOT, 25 g, 163 °C, 5 hours		TSM
TFOT, 25 g, 185 °C, 5 hours		THM
UV Chamber		Abbreviation
reduce TS-residues to 25 g, 60 °C UV, 7 days		UV7
reduce TS-residues to 25 g, 60 °C UV, 14 days		UV14
reduce TS-residues to 25 g, 60 °C UV, 28 days		UV28
California Tilt Oven		Abbreviation
111 °C for 24 hours		C24
111 °C for 72 hours		C72
111 °C for 168 hours		C168
Pressure Aging Vessel		Abbreviation
TS + PAV, 300 psi, 90 °C for 20 hours		P90
TS + PAV, 300 psi, 100 °C for 20 hours		P100
TS + PAV, 300 psi, 110 °C for 20 hours		P110

100 W/m^3. This is the viscosity when the shear stress times the shear rate equals 100 W/m^3. When performed on highly aged residues at 5°C, it was found that the 100-W/m^3 constant power viscosity has to be extrapolated far from the observed data points. To avoid the extrapolating error, an apparent viscosity at a shear stress of 1 MPa (constant stress viscosity), which is close to the average shear stress used in performing the test at 5°C, was used instead. This is the viscosity when the shear stress is at 1 MPa.

Infrared Absorption Spectral Analysis

Infrared spectroscopic technique was used to measure changes in molecular structures of the binders due to aging in terms of the changes in the amount of certain functional groups in them. The infrared absorption spectrum between 1600 and 1900 cm^{-1} is of particular interest, since it contains the absorption bands for the functional groups of carboxylic acids, ketones, and anhydrides (*10*). In previous research by Tia et al. (*5,6*), it was concluded that the carbonyl ratio, which is a ratio of infrared absorbance at 1700 cm^{-1} and 1600 cm^{-1}, can be used to express the level of oxidation in an asphalt binder.

Statistical Model

In the comparison of aging processes, the test results were analyzed as a factorial experiment comprising 5 asphalts (ASPHALT) and 17 aging methods (METHOD). The concern is the specified aging processes and asphalts. Therefore, ASPHALT and METHOD are regarded as fixed effects. The following linear model is assumed for any single parameter in the experiment:

$$Y_{ijk} = \mu + \text{ASPHALT}_i + \text{METHOD}_j + \text{INTERACTION}_{ij} + \epsilon_{ijk} \quad (1)$$

where

Y_{ijk} = response of kth replicate, jth aging method, and ith asphalt;
μ = overall mean;

$ASPHALT_i$ = main effect of ith asphalt;
$METHOD_j$ = main effect of jth aging method;
$INTERACTION_{ij}$ = interaction effect;
ϵ_{ijk} = experimental error;
i = 1 to 5 for the five asphalts;
j = 1 to 17 for the 17 aging methods; and
k = 1 to 2 for two replicates.

The SAS/STAT computer software was used for the statistical analysis.

It is well known that the variation of viscosity measurements is a function of viscosity value. The higher the viscosity, the larger the variation will be. Therefore, the aging index used as the response in the preceding statistical model could not satisfy the constant variance assumption. To solve this problem, a data transformation technique is suggested by most statisticians. The logarithm of the aging index was used as the response variable in the statistical model.

TEST RESULTS

Investigation of Aging Processes

The five conventional asphalts show substantially different weight changes in the extended TFOT process. The weight changes are differentiable by the refinery source of asphalt, as shown in Figure 1. CT asphalt shows the highest weight loss, and AM asphalts show higher weight loss than MA asphalts. Among the 17 aging processes, the high-temperature TFOT (using 50- or 25-g samples) produced large amounts of weight loss. On the other hand, the SHRP-proposed PAV processes produce large amounts of weight gain as shown in Figure 1. However, the PAV-aged residues are not differentiable by refinery source. The difference in the effect of refinery source appears to be enlarged by using a higher exposure temperature in the TFOT and PAV processes.

The results of the absolute viscosity test and the corresponding aging indices at 60°C are given in Table 2. The results of the Schweyer rheometer test at 5°C are given in Table 3. These data are the average values from two replicates. The analysis of variance (ANOVA) was performed according to the two-factor factorial model as described. The results of ANOVA and Duncan's multiple range test at $\alpha = 0.05$ on the five aging severity parameters are summarized in Table 4.

Because of the insensitivity of the consistency measurements at lower temperatures, it was found that the aging index at 60°C is the most sensitive parameter in detecting differences in aging severity. The interaction of asphalt and aging method is seen to have a significant effect on the aging index at 60°C. This means that different aging methods are very likely to produce different aging severities on different asphalts. As an example, in the ranking of aging severity by the CTO process for 168 hr, CT30 is a severely aged asphalt as indicated by its high aging index at 60°C, given in Table 2. However, in the PAV method, it is the least severely aged asphalt no matter what process temperature is used. On the basis of the aging index at 60°C, the AM asphalts show higher aging potential than the MA asphalts in all 17 aging processes.

As seen in Figure 1 and Table 2, asphalts with low volatile loss during the TFOT processes exhibit a lower aging index, particularly at higher process temperatures. This trend is also observed in the TFOT processes using 25-g samples or longer exposure periods.

A close examination of the aging indices at 60°C of different asphalts in the processes of the UV chamber (Table 2) indicates that there was no significant additional hardening of the asphalt residues from 7 to 28 days' exposure in the UV chamber. This might be due to the formation of a thin skin on the surface of the

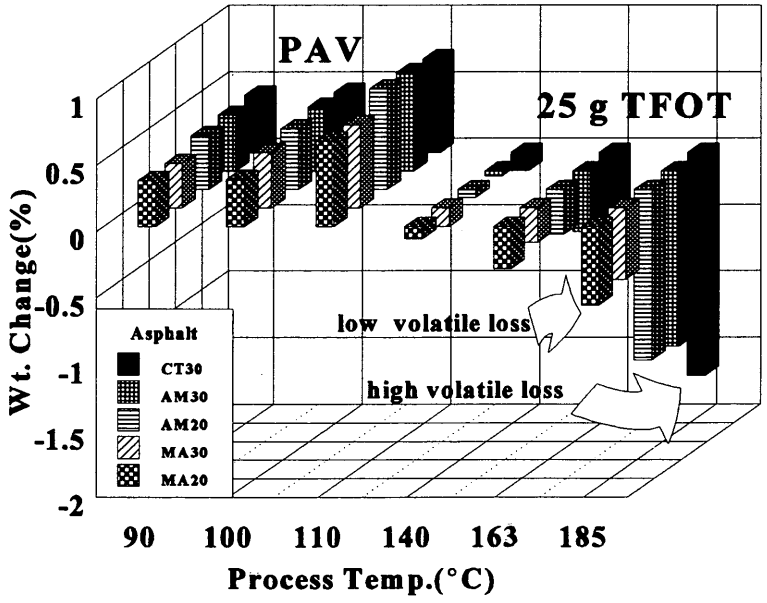

FIGURE 1 Weight change of various asphalts in the processes of PAV and 25-g TFOT at different process temperatures.

TABLE 2 Results of Absolute Viscosity Tests at 60°C and Corresponding Aging Indexes

Laboratory Aging Process	Asphalt Type				
	CT30	AM30	AM20	MA30	MA20
Original	2883	3146	2246	3108	2248
TL	4422*(1.53**)	5034(1.60)	3486(1.55)	4560(1.47)	3142(1.40)
TS	6064(2.10)	7454(2.37)	5266(2.34)	5988(1.93)	4943(2.20)
TH	13390(4.64)	17204(5.47)	11222(5.00)	11434(3.68)	8537(3.80)
TLM	6208(2.15)	7826(2.49)	5312(2.37)	6988(2.25)	4785(2.13)
TSM	11834(4.10)	17457(5.55)	11441(5.09)	13306(4.28)	9314(4.14)
THM	74405(25.81)	141495(44.98)	88590(39.44)	54798(17.63)	31327(13.94)
TF10	13311(4.62)	15600(4.96)	13239(5.89)	13715(4.41)	10235(4.55)
TF15	23450(8.13)	54878(17.44)	23276(10.36)	24578(7.91)	15920(7.08)
UV7	9672(3.35)	14784(4.70)	12754(5.68)	17167(5.52)	9646(4.29)
UV14	11730(4.07)	11558(3.67)	16088(7.16)	15622(5.03)	11412(5.08)
UV28	10344(3.59)	13770(4.38)	11756(5.23)	14790(4.76)	10208(4.54)
C24	12194(4.23)	12872(4.09)	10674(4.75)	15120(4.86)	11230(5.00)
C72	47250(16.39)	45904(14.59)	43014(19.15)	43863(14.11)	38749(17.24)
C168	127756(44.31)	111090(35.31)	103595(46.12)	82702(26.61)	95092(42.30)
P90	18698(6.49)	27166(8.64)	17750(7.90)	23922(7.70)	15500(6.90)
P100	18320(6.35)	34997(11.12)	31358(13.96)	30699(9.88)	20088(8.94)
P110	53796(18.66)	125046(39.75)	82366(36.67)	62216(20.02)	45057(20.04)

Note :

See Table 1 for the meaning of codes.

*: Absolute viscosity in Poises.

**: Aging index.

TABLE 3 Constant Stress Viscosities at 5°C as Measured by Schweyer Rheometer (10^9 poise)

Laboratory Aging Process	Asphalt Type				
	CT30	AM30	AM20	MA30	MA20
Original	1.22	0.88	0.70	0.66	0.40
TL	1.66	0.93	0.77	0.90	0.66
TS	2.68	1.52	1.07	0.97	0.88
TH	6.07	3.00	1.99	2.19	1.60
TLM	2.57	1.64	1.07	1.48	0.79
TSM	5.70	3.65	1.95	2.58	2.59
THM	13.40	6.70	5.08	5.25	3.18
TF10	5.53	2.13	1.85	2.22	1.21
TF15	8.06	2.35	2.37	3.00	1.70
UV7	5.55	2.79	2.26	3.26	1.75
UV14	4.63	2.86	1.91	4.32	1.58
UV28	4.96	2.96	1.72	3.78	1.86
C24	6.56	3.91	2.10	3.36	1.82
C72	24.40	8.33	6.14	8.58	3.32
C168	43.20	28.80	31.80	11.50	14.30
P90	9.77	6.82	3.93	3.61	1.34
P100	13.33	6.74	5.33	5.16	2.17
P110	25.70	26.90	12.18	7.68	3.72

Note:

See Table 1 for the meaning of codes.

TABLE 4 Results of Statistical Analysis in Comparison of Laboratory Aging Processes

Item		Penetration Retained (%)	Carbonyl Ratio Index	Aging Index at60 °C	Aging Index at25 °C	Aging Index at5 °C
R o E f S A U N L O T V S A	Source	Significance	Significance	Significance	Significance	Significance
	A*	Yes	Yes	Yes	Yes	Yes
	M*	Yes	Yes	Yes	Yes	Yes
	I*	No	No	Yes	No	No
Duncan's Grouping on ASPHALT		Grouping ASPHALT A MA30 B A AM30 B A CT30 B C MA20 C AM20	Grouping ASPHALT A AM30 A MA20 B AM20 B MA30 B CT30	Grouping ASPHALT A AM20 A AM30 B MA30 B MA20 B CT30	Grouping ASPHALT A AM30 A CT30 B AM20 B MA30 B MA20	Grouping ASPHALT A CT30 B A MA30 B AM30 B MA20 B AM20
Duncan's Grouping on METHOD		Grouping METHOD A TL B TS B TLM C THM D C UV7 D C UV14 D C C24 D C TF10 D C TSM D E UV28 F E TF15 F P90 G P100 H C72 H THM H P110 I C168	Grouping METHOD A P110 B A C168 B C THM D C P100 D C E C72 D C E TF15 D F E UV7 D F E UV28 G F E P90 G F E TF10 G F UV14 G F C24 G F TSM G TH H TS H TLM H TL	Grouping METHOD A C168 B THM B P110 C C72 D P100 D TF15 E P90 F TF10 F UV14 F TSM F C24 F UV7 F UV28 F TH G TLM G TS H TL	Grouping METHOD A C168 B P110 C B C72 C D THM E D P100 E F P90 G F TF15 G F UV28 G C24 G UV14 G TSM G UV7 G TH G TF10 H TLM H TS I TL	Grouping METHOD A C168 B P110 C B C72 C D THM C D P100 E D P90 E F C24 E F TSM E F TF15 E F UV28 E F UV7 E F UV14 E F TH F TF10 G TLM G TS G TL

Note: See Table 1 for the meaning of codes.
For Duncan's groupings, those with same letter are not significantly different at $\alpha = 0.05$.
*: A= ASPHALT; M= METHOD; I= INTERACTION

asphalt residue during early UV exposure, which might seal the rest of the asphalt residue from further oxidation.

In the CTO processes, AC-20 shows a higher aging index than AC-30. This might be due to the higher mobility of the less viscous AC-20, resulting in a larger exposure surface during the rolling process.

In the PAV processes, CT30, which exhibits high volatile loss in the extended TFOT and CTO tests, shows a low aging index at all three process temperatures. The high pressure and relatively lower temperature limit the volatile loss. However, the asphalts (MA) with low volatile loss show lower aging indexes than those (AM) with relatively higher volatile loss.

The 17 aging processes can be grouped as indicated in Table 4 from most severe aging to minor aging as follows:

1. CTO for 168 hr, with an average aging index of 38;
2. PAV at 110°C and high-temperature (185°C) TFOT using 25-g samples, with an average aging index of 25;
3. CTO for 72 hr, with an average aging index of 16;
4. PAV at 100°C and TFOT for 15 hr, with an average aging index of 9.5;
5. PAV at 90°C, with an average aging index of 7.5;
6. TFOT for 10 hr, using 25-g samples, high-temperature (185°C) TFOT, UV chamber for 7, 14, and 28 days, and CTO for 24 hr, with an average aging index of 4.5;
7. Standard TFOT and low-temperature (140°C) TFOT using 25-g samples, with an average aging index of 2; and
8. Low-temperature TFOT, with an average aging index of 1.5.

The aging severity order on the basis of percent penetration retained is similar to that on the basis of the aging index at 60°C. Because of the lower sensitivity of the penetration test on harder asphalts, low penetration asphalts (AC-30) show a higher percentage of penetration retained than high penetration asphalts (AC-20) as indicated in Table 4. The order of severity among the 17 aging processes as ranked on the basis of carbonyl ratio index, aging index at 25°C, and aging index at 5°C is in general agreement with that ranked by aging index at 60°C. However, the ranking of aging severity could be different if different parameters were used. The high-temperature TFOT process on 25-g samples produces aging severity similar to that of the PAV process at 110°C in terms of aging index at 60°C. In terms of carbonyl ratio index, the PAV process at 110°C produces higher oxidation than the high-temperature TFOT process on 25-g samples.

The temperature susceptibility of the tested binders was evaluated by two parameters, PVN'(25-60) and VTS(60-5), which are defined as follows:

$$PVN'(25\text{-}60) = \frac{-1.5[(6.4890 - 1.59\log(p25) - \log(V60)]}{1.05 - 0.2234\log(p25)} \quad (2)$$

$$VTS(T_1 - T_2) = \frac{\log[\log(V_2)] - \log[\log(V_1)]}{\log(T_1) - \log(T_2)} \quad (3)$$

where

V60 = viscosity (poise) at 60°C,
p25 = penetration in 0.1 mm at 25°C,
T_1, T_2 = temperature (degrees Kelvin), and
V_1, V_2 = viscosity (centipoise) at T_1 and T_2.

Both PVN'(25-60) and VTS(60-5) were found to be substantially reduced by the 17 aging processes as indicated in Table 5. The higher the degree of aging, the lower the temperature susceptibility would become. CT30 is the most temperature susceptible asphalt among the five asphalts used in this study, before or after any of the 17 aging processes.

The major concern with aged asphalt is its low temperature property. The viscosity at 5°C, which was obtained from the Schweyer rheometer test, is given in Table 3. The empirical viscosity limit in avoiding thermal cracking problem is the critical viscosity value of 2×10^{10} poise. As indicated in Table 3, six residues exhibit a viscosity value exceeding this limit at 5°C.

Investigation of Aging Characteristics of Modified Asphalts

The results of tests on modified asphalts that were aged by the CTO and PAV processes are given in Tables 6 and 7, respectively. These two aging processes were performed at similar temperatures. The CTO process provides longer reaction time, and the PAV process provides higher oxygen content through pressurized air. Because different asphalts produce different aging severity in different aging processes, the CTO and PAV data were analyzed separately.

The effects of different modifiers on the aging index at 60°C in the CTO processes are shown in Figure 2. The SBR modified asphalt was not investigated in the CTO process. The same statistical model described earlier was used to analyze the aging indices at 60°C. Because of the significant effect of interaction of

TABLE 5 Temperature Susceptibility Parameters of Unmodified Asphalts and Their Aged Residues

Parameter	PVN'(25-60)					VTS(60-5)				
Method	CT30	AM30	AM20	MA30	MA20	CT30	AM30	AM20	MA30	MA20
Original	-0.57	-0.40	-0.50	-0.52	-0.52	3.92	3.81	3.91	3.76	3.79
TL	-0.41	-0.32	-0.43	-0.38	-0.43	3.80	3.62	3.74	3.66	3.75
TS	-0.38	-0.15	-0.27	-0.32	-0.40	3.77	3.57	3.64	3.56	3.62
TH	-0.18	0.34	0.08	-0.08	-0.10	3.62	3.38	3.46	3.47	3.52
TF10	-0.08	0.20	0.14	-0.01	-0.09	3.61	3.35	3.38	3.40	3.39
TF15	0.27	1.02	0.52	0.36	0.13	3.46	2.90	3.21	3.24	3.29
TLM	-0.32	-0.03	-0.23	-0.29	-0.46	3.75	3.56	3.63	3.59	3.61
TSM	-0.29	0.26	0.09	-0.13	-0.22	3.66	3.41	3.45	3.45	3.59
THM	0.74	1.44	1.04	0.63	0.52	3.15	2.79	2.89	3.07	3.17
UV7	-0.23	0.11	0.07	0.04	-0.11	3.73	3.42	3.44	3.40	3.49
UV14	-0.06	-0.11	0.19	-0.04	-0.08	3.62	3.53	3.31	3.49	3.40
UV28	-0.22	0.04	-0.01	-0.04	-0.14	3.68	3.46	3.41	3.49	3.48
C24	-0.11	0.03	0.03	0.03	-0.05	3.68	3.55	3.49	3.45	3.44
C72	0.43	0.61	0.62	0.51	0.53	3.43	3.22	3.18	3.25	3.10
C168	0.83	1.08	1.02	0.83	0.95	3.19	3.16	3.20	3.08	3.07
P90	-0.05	0.40	0.23	0.17	0.06	3.63	3.44	3.44	3.33	3.24
P100	-0.12	0.50	0.47	0.27	0.13	3.60	3.33	3.39	3.30	3.30
P110	0.54	1.18	1.12	0.66	0.53	3.45	3.30	3.24	3.15	3.1

Note:
PVN'(25-60) calculated by Equation 2 and VTS(T_1-T_2) calculated by Equation 3.
See Table 1 for the meaning of codes.

TABLE 6 Results of Tests on CTO Residues of Modified Asphalts

Process Time	Asphalt Type				
	AC-30	GTR	CB	SEBS	EVA
Penetration at 25 °C (0.01 mm)					
0 hour	56	46	48	24	40
24 hours	30	28	27	21	22
72 hours	19	19	18	16	17
168 hours	14	17	14	14	11
Absolute viscosity at 60 °C (poise)					
0 hour	2883	5922	4600	24944	4880
24 hours	12194	23772	13512	58784	20757
72 hours	47250	53950	36584	83776	92725
168 hours	127756	122240	97678	145675	1909352
Viscosity at 25 ° C (10^6 poise)					
0 hour	3.58	1.84	2.39	22.15	6.38
24 hours	16.10	28.45	17.65	44.70	10.15
72 hours	53.80	38.65	45.10	84.10	24.15
168 hours	178.00	92.35	89.55	154.00	70.50
Viscosity at 5 °C (10^9 poise)					
0 hour	1.22	1.00	0.87	5.30	5.56
24 hours	6.56	6.54	4.18	6.21	8.37
72 hours	24.40	9.29	15.65	13.00	9.90
168 hours	43.20	15.05	39.45	71.45	39.75
Carbonyl Ratio					
0 hour	0.3083	0.3214	-	0.3044	0.3874
24 hours	0.4350	0.4185	-	0.3015	0.4484
72 hours	0.4805	0.5380	-	0.3877	0.5968
168 hours	0.5662	0.5676	-	0.4427	0.7116

Note: See Table 1 for the meaning of codes.

-: Data not available caused by too many peaks in the spectrum.

the two main factors, the Duncan's multiple range test was performed at separate aging levels. The results of statistical analysis are given in Table 8. As indicated in Figure 2 and Table 8, the EVA-modified asphalt showed a high aging index, particularly when the process time is long, as in the 168-hr CTO process.

On the basis of the results of tests on the CTO residues, all three modified asphalts, with the exception of the EVA-modified asphalt, show lower aging severity in terms of lower aging indices at 60°C. Carbon black and fine ground tire rubber used in this study exhibit similar aging indices. The SEBS-modified asphalt exhibits a very low aging index, which might be attributed to the slower movement of the binders in the flasks during the rolling process of the CTO due to its high initial viscosity. This does not necessarily mean that the SEBS-modified asphalt will have a lower thermal cracking potential than the EVA-modified asphalt or the control AC-30. As long as the aged residues have low enough viscosity to prevent the buildup of high thermal stresses, an asphalt with low initial viscosity could be allowed to age to a high degree. As indicated in Table 6, after a 72-hr exposure in the CTO process, all four modified asphalts show lower viscosity at 5°C compared with their base AC-30. However, after a 168-hr exposure in the CTO, only the fine ground tire rubber–modified asphalt shows a significantly lower viscosity at 5°C.

The effects of modifiers on the aging index at 60°C in the PAV processes are plotted in Figure 3. In the PAV process at 90°C, only the SBR- and SEBS-modified asphalts show significantly less severe aging in terms of aging index at 60°C, as indicated in Figure 3 and Table 8. After the PAV process at 100°C, the carbon black- and EVA-modified asphalt show more severe aging than the control AC-30. Although SBR- and SEBS-modified asphalts show less aging after the PAV process at 100°C, the difference is not significant. After the PAV process at 110°C, EVA-, carbon

TABLE 7 Results of Tests on PAV Residues of Modified Asphalts

Process Temperature	Asphalt Type					
	AC-30	GTR	CB	SEBS	EVA	SBR
Penetration at 25 °C (0.01 mm)						
Original	56	46	48	24	40	-
90 °C	24	24	22	24	44	41
100 °C	23	22	20	21	22	42
110 °C	19	18	16	18	20	37
Absolute viscosity at 60 °C (poise)						
Original	2883	5922	4600	24944	4880	7404
90 °C	18699	34476	27540	100950	38392	26411
100 °C	18321	45204	40827	139257	58999	38861
110 °C	53796	88388	87361	278471	195354	56813
Viscosity at 25 ° C (10^6 poise)						
Original	3.58	3.52	2.39	22.15	6.38	1.02
90 °C	21.20	35.05	30.70	115.00	23.00	2.56
100 °C	25.90	40.15	49.60	160.00	19.80	6.32
110 °C	71.30	77.80	84.55	198.00	72.40	10.60
Viscosity at 5 °C (10^9 poise)						
Original	1.22	1.00	0.87	5.30	5.56	3.12
90 °C	9.77	8.74	11.80	17.92	10.63	2.52
100 °C	13.33	16.20	17.85	28.63	11.17	7.85
110 °C	25.70	22.90	32.60	34.71	21.21	11.26
Carbonyl Ratio						
Original	0.3083	0.3214	-	0.3044	0.3874	0.2209
90 °C	0.4502	0.4431	-	0.4120	0.5442	0.3840
100 °C	0.4896	0.4582	-	0.4354	0.5229	0.4678
110 °C	0.5759	0.5437	-	0.4958	0.5828	0.5129

Note: See Table 1 for the meaning of codes.

**: Missing Data. -: Data not available caused by too many peaks in the spectrum.

black-, and ground tire rubber-modified asphalts show a higher aging index at 60°C than the control AC-30. On the other hand, SBR- and SEBS-modified asphalts exhibit a lower aging index at 60°C than their base AC-30. The SBR-modified asphalt exhibits a substantially lower viscosity at 5°C, and the SEBS-modified asphalt shows a substantially higher viscosity at 5°C as indicated in Table 7. If the PAV processes could simulate long-term aging in the field, these results would indicate that the SBR-modified asphalt would probably have a lower thermal cracking potential, whereas the SEBS-modified asphalt would have a higher thermal cracking potential than that of the base asphalt. This observation may not be conclusive since there was great variability in the results of the Schweyer rheometer tests on the SBR-modified asphalts. The great variability of the test results might be due to the high compressibility of the SBR-modified asphalts, which makes the basic assumptions of the Schweyer rheometer test invalid.

SUMMARY

The major findings from this study are as follows:

1. A reasonable laboratory aging process and an adequate evaluation parameter are required in the durability study of asphalt binders. Different asphalts could age differently in different aging processes. The ranking of aging severity for different asphalts could depend on the parameters chosen.
2. Because of the insensitivity of consistency measurements at lower temperatures, the most sensitive parameter for characterizing the aging severity of asphalt binders was found to be the aging index at 60°C, which is the ratio of absolute viscosities at 60°C.
3. For conventional asphalts used in Florida, high-temperature TFOT processes produce higher weight loss and PAV processes produce weight gain. The weight loss in high-temperature TFOT

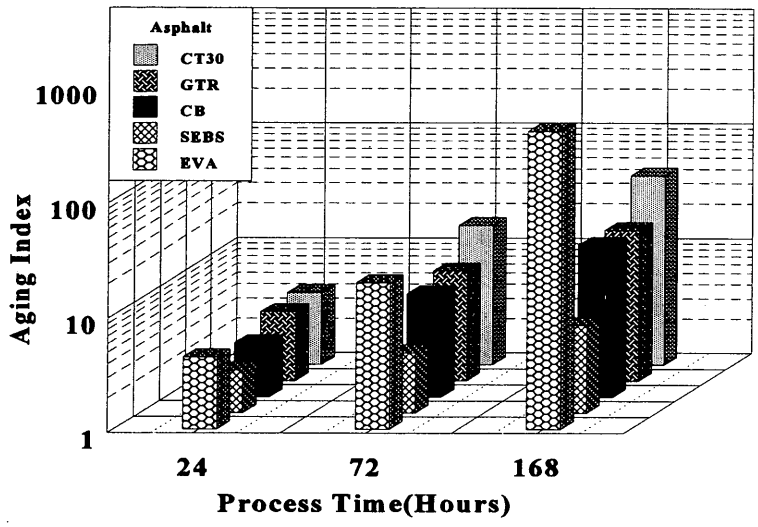

FIGURE 2 Effects of various modifiers on aging index at 60°C in CTO processes.

TABLE 8 Results of ANOVA and Duncan's Grouping on Aging Index at 60°C of CTO and PAV Residues

Item	CTO Process		PAV Process	
Results of ANOVA	Source	Significance	Source	Significance
	ASPHALT	Yes	ASPHALT	Yes
	METHOD	Yes	METHOD	Yes
	INTERACTION	Yes	INTERACTION	Yes
Duncan's Grouping on ASPHALT	Grouping at METHOD=C24 Grouping Mean N ASPHALT A 4.27 2 EVA A 4.23 2 AC-30 A 4.02 2 GTR A 3.01 2 CB A 2.56 2 SEBS Grouping at METHOD=C72 Grouping Mean N ASPHALT A 19.30 2 EVA A 16.39 2 AC-30 B 9.10 2 GTR B 8.14 2 CB C 3.65 2 SEBS Grouping at METHOD=C168 Grouping Mean N ASPHALT A 380.19 2 EVA B 44.36 2 AC-30 C 21.28 2 GTR C 20.65 2 CB D 6.11 2 SEBS		Grouping at METHOD=P90 Grouping Mean N ASPHALT A 7.87 2 EVA B A 6.48 2 AC-30 B 5.99 2 CB B 5.82 2 GTR C 4.05 2 SEBS C 3.57 2 SBR Grouping at METHOD=P100 Grouping Mean N ASPHALT A 12.09 2 EVA B 8.88 2 CB C B 7.63 2 GTR C D 6.35 2 AC-30 D 5.58 2 SEBS D 5.25 2 SBR Grouping at METHOD=P110 Grouping Mean N ASPHALT A 40.03 2 EVA B 18.99 2 CB B 18.65 2 GTR C 14.93 2 AC-30 D 11.16 2 SEBS D 7.67 2 SBR	

Note: See Table 1 for the meaning of codes.
For Duncan's groupings, those with same letter are not significantly different at α = 0.05.

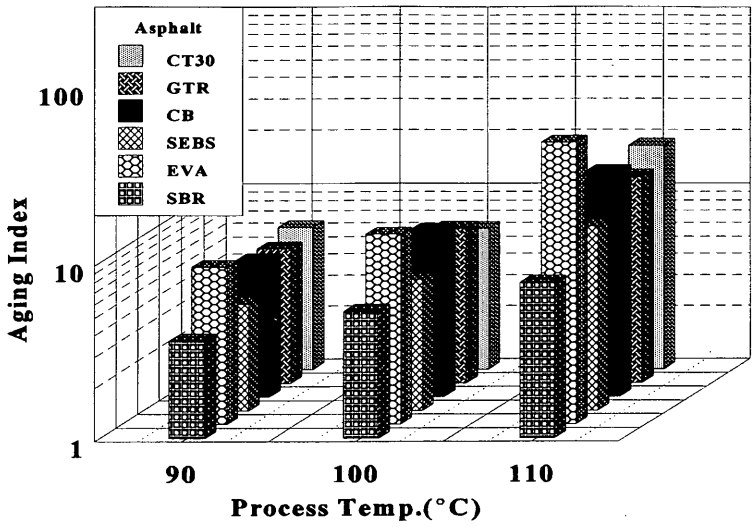

FIGURE 3 Aging index of modified asphalts in PAV processes at 60°C.

is differentiable by refinery source of the asphalt. Whereas asphalts with a low volatile loss show less aging in most aging processes, an asphalt with a high volatile loss could age less in the PAV process.

4. Only the surface of the asphalt samples was aged by the UV light in the UV chamber. Low-viscosity asphalts were found to age more in the CTO process because of a larger contact surface caused by higher mobility in the rolling process.

5. Most of the modified asphalts, except EVA-modified asphalt, show less aging in the CTO process than the control asphalt in terms of aging index at 60°C. All of the modified asphalts show lower viscosity at 5°C than the control asphalt after a 72-hr CTO exposure. However, after a 168-hr CTO exposure, only the ground tire rubber-modified asphalt exhibits a lower viscosity at 5°C than the control asphalt.

6. In terms of the aging index at 60°C, the effect of modifiers on reducing the aging severity of asphalts in the PAV process is different at different process temperatures. At 90°C, SEBS- and SBR-modified asphalts exhibit a lower aging index at 60°C than the control asphalt. When the process temperature was increased to 100°C, no substantial reduction of aging index was found for any of the five modified asphalts compared with the control asphalt. The fine ground tire rubber–, SEBS-, and SBR-modified asphalts exhibit lower aging indexes than the control asphalt at the process temperature of 110°C.

REFERENCES

1. Corbett, L. W., and R. E. Merz. Asphalt Binder Hardening in the Michigan Test Road After 18 Years of Service. In *Transportation Research Record 544*, TRB, National Research Council, Washington, D.C., 1975, pp. 27–34.
2. Welborn, J. Y. Physical Properties as Related to Asphalt Durability: State of the Art. In *Transportation Research Record 999*, TRB, National Research Council, Washington, D.C., 1984, pp. 31–36.
3. Schmidt, R. J., and L. E. Santucci. *Proc., AAPT*, Vol. 38, 1969, p. 39.
4. Kemp, G. R., and N. H. Predoehl. *An Investigation of the Effectiveness of Asphalt Durability Tests.* Final report. FHWA/CA/TL-80/14, 1980.
5. Tia, M., B. E. Ruth, C. T. Chari, J. Shiau, D. Richardson, and J. Williams. *Investigation of Original and In-service Asphalt Properties for the Development of Improved Specifications—Final Phase of Testing and Analysis.* Final report. Department of Civil Engineering, University of Florida, July 1988.
6. Tia, M., B. E. Ruth, J. Shiau, S. Huang, and D. Richardson. *Evaluation of Criteria for Improved Durability of Asphalt.* Final report. Department of Civil Engineering, University of Florida, Dec. 1990.
7. Anderson, D. A., D. W. Christensen, and H. Bahia. Physical Properties of Asphalt Cement and the Development of Performance-Related Specifications. *Journal of AAPT*, Vol. 60.
8. Davis, R. L. Relationship Between the Rheological Properties of Asphalt and the Rheological Properties of Mixtures and Pavements. In *Asphalt Rheology: Relationships to Mixtures*, ASTM STP 941, 1987, pp. 28–50.
9. Tia, M., and B. E. Ruth. Basic Rheology and Rheological Concepts Established by H. E. Schweyer. In *Asphalt Rheology: Relationships to Mixtures*, ASTM STP 941, 1987, pp. 118–145.
10. Petersen, J. C. Chemical Composition of Asphalt as Related to Asphalt Durability: State of the Art. In *Transportation Research Record 999*, TRB, National Research Council, Washington, D.C., 1984, pp. 13–30.

Publication of this paper sponsored by Committee on Characteristics of Bituminous Materials.

Rheological and Rheo-Optical Characterization of Asphalt Cement and Evaluation of Relaxation Properties

DALLAS N. LITTLE, ALAN LETTON, S. PRAPNNACHARI, AND Y. RICHARD KIM

The rheological properties of asphalt depend on its molecular structure and chemical composition. The widely used Corbett fractions provide the composition of asphalt but lack the detailed structure/property relationships needed to accurately design asphalt systems. Depending on the proportions of the generic fractions, an asphalt is either a dispersed type or a solution type. The dispersed type is also termed micellar or colloidal; the solution type is termed "polymer type." The literature is unclear as to which structure accurately represents the mechanical behavior of an asphalt system. Material science tools are used to elucidate the structure of asphalt. In particular, a rheo-optical technique was developed and used to probe changes in molecular vibrations via Fourier transform infrared spectroscopy (FTIR) during shear deformation. The objective is to identify the important chemical aspects of an asphalt molecule that are related to the deformation properties of the asphalt. To clarify this relationship, detailed viscoelastic characterization of the asphalt was conducted to ensure an understanding of the asphalt's rheological properties. The FTIR results suggest an important link between rheological performance and linear structures in the asphalt cement complex. This concept was further probed through small-angle X ray scattering. Fractal analysis was used to determine the Porod scattering dimension, which is a measure of the dimensionality of the tested structure (i.e., whether it is linear or branched, or three-dimensionally branched).

Asphaltenes are proposed to be colloids (or micelles) dispersed in an oily medium peptized by resins. The peptizing ability of resins keeps asphaltenes, the highly associated component of asphalt, dispersed in the oily phase. The asphaltene fraction is the solute, and the other fractions combined (called maltenes) make up the solvent. There is limited consensus among researchers as to whether the asphaltene or the maltene contributes more to the overall physical behavior of an asphalt. Corbett described asphaltenes as solution thickeners that raise the asphalt's viscosity, and the other fractions have been described as being responsible for the ductility and fluidity of asphalt (*1*). Dealy (*2*) found asphaltenes to be the structuring component of asphalt and to play a key role in the rheological behavior of asphalt. Conversely, Boduszynski et. al. (*3*) found that asphaltenes lacked an independent rheological identity. They indicated that, because of the presence of the solvents, asphaltenes conglomerate as a highly associated phase; their study also indicated similarity in the molecular weights of asphaltenes and saturates (*3*). Petersen (*4*), referring to the work of Boduszynski et. al. (*3*), emphasized the role of compatibility among the four generic fractions of an asphalt. Halstead (*5*) reviewed the work of Boduszynski et al. and Petersen and found that it is the intercomponent relationship among the generic fractions that controls the overall physical properties of an asphalt, not simply the quantity of any single component. The functionality and the molecular structure are two main factors that determine the balance among the components of an asphalt (*4*). The microstructural model developed by Strategic Highway Research Program (SHRP) researchers is based on the hypothesis of a dispersed polar fluid (DPF) (*6*).

To predict the long-term performance properties of the asphalt, the microstructure of the whole asphalt, containing all the fractions together, must be known. Monismith (*7*) proposed two physical models to explain the chemical composition of asphalt. The first is the colloid or the micellar model, presented earlier, where the asphaltenes are held as discrete lumps by the peptizing ability of the resins (polar aromatics and naphthene aromatics) in the oil (saturates) medium. In the solution model, it is proposed that asphaltenes are dissolved in the oil-resin phase. The colloidal model has been more popular than the solution model as asphalt has been shown to deviate from true solution behavior (*5*).

Recently, SHRP announced its findings on the microstructure of asphalt studied using nuclear magnetic resonsance (NMR) and chromatography techniques. The DPF model pictures asphalt as a continuous, three-dimensional association of polar molecules dispersed in a fluid of nonpolar or relatively low-polarity molecules. Sulfur, nitrogen, and oxygen are incorporated in asphalt molecular substituents in the form of polar functional groups that are attached to hydrocarbon molecules. Many of the polar functional groups will behave as either acids or bases, and all are capable of forming dipolar, intermolecular bonds of varying strength with functional groups of opposite polarity. In this model, the viscoelastic properties of the asphalt and the response of asphalt to load- and temperature-induced stresses result directly from the making and breaking of bonds between polar molecules or other properties associated with a molecular superstructure. When the asphalt is subjected to stress, these secondary bonds are broken and reformed continuously. (This suggests the existence of a yield stress that could be probed using a stress-controlled rheometer.)

The DPF model proposed by SHRP differs from the older micellar model in several important ways. First, the micellar model postulates that asphalt is a collodial system with particles that are very large on a molecular scale—representing an agglomeration of many individual asphalt substituents (*6*). By contrast, the DPF model postulates no large assemblages. Rather, microstructural interactions depend on the wide variety of polar molecules dispersed

D. N. Little, A. Letton, and S. Prapnnachari, Texas Transportation Institute, Texas A&M University, TTI/CE Building, College Station, Tex. 77843-3135. Y. R. Kim, North Carolina State University, Box 7908, Mann Hall, Raleigh, N.C. 27695.

in the asphalt (*6*). NMR analysis has failed to find any large-scale assemblages.

Second, in the micellar model, colloidal particles are considered to be relatively permanent assemblages suspended in a dispersing medium. Because the electron density should vary between the colloidal and the suspending fluid, X ray scattering should demonstrate the presence of a colloidal system (*6*). The DPF model, conversely, proposes a structure that is continually forming and reforming as energy flows to and from the asphalt through media of external loading and temperature fluctuations (*6*).

Finally, the DPF model stresses the importance of polar asphalt molecules in mediating performance to a larger degree than the micellar model. A major component of the DPF model—producing a major influence over the formation of the molecular matrix—is the amphoteric. These molecules act as both an acid and a base and can thus associate extensively because they can fasten to other molecules at two or more sites instead of one (*6*).

The proposition of a network of molecules floating in a nonpolar fluid was investigated in this study.

VISCOELASTIC CHARACTERIZATION

Overview

Usually, strain-controlled, static tests are used to study the viscoelastic relaxation of a material. This type of test is particularly suitable for materials that are more elastic than viscous. For materials showing considerable viscous behavior, use of a strain-controlled, static test may be limited by extremely short experiment times. Asphalt exhibits both viscous and elastic properties depending on temperature and deformation rate. Dynamic mechanical tests overcome these constraints and, therefore, were used to characterize the asphalts studied here. Interconversions between viscoelastic functions are well documented in the literature and were used in this study to predict time-dependent properties.

To facilitate interconversion between time- and frequency-dependent linear viscoelastic functions, master curves of the storage (G') and loss (G'') moduli were constructed and used to calculate the discrete relaxation spectrum for each asphalt. The discrete function is related to the master curve through the following expressions:

$$G(t) = \sum_{i=1}^{z} G_i \, e^{\frac{-\tau}{\tau_i}}$$

$$G'(\omega) = \sum_{i=1}^{z} \frac{G_i \omega^2 \tau_i^2}{1 + \omega^2 \tau_i^2}$$

$$G''(\omega) = \sum_{i=1}^{z} \frac{G_i \omega \tau_i}{1 + \omega^2 \tau_i^2}$$

The G_i's and corresponding τ_i's make up the discrete relaxation spectra. A nonlinear algorithm is used to calculate a unique set of G_i's and τ_i's. The number of discrete nodes (τ_i values) is selected to provide a good fit to G' and G''. If the G_i's and τ_i's are known from the G' and G'' master curves, $G(t)$, the relaxation modulus, can be calculated straightforwardly. Similarly, the compliance function can be determined using the approximation

$$J_1 = \frac{1}{G_c} \text{ then } J(\tau) = \sum_{i=1}^{z} J_i(1 - e^{-\tau/\tau_i})$$

The relaxed modulus, G_R [$G(t = \infty)$], and the zero shear viscosity, η_0, are synonymous in characterizing the long-term behavior of a material (η_0 is proportional to the longest relaxation time). The relaxed modulus or equilibrium modulus is the stiffness of a material under a sustained deformation at an infinitely long time. The relaxed modulus is indeed the long-term resistance of a material against flow. For the range of frequencies and temperatures used in this study, the asphalt's equilibrium modulus was not obtainable. For this reason, the study of zero shear viscosity was an essential alternative to evaluate the long-term resistance against flow. The zero shear viscosity is approximated as follows:

$$\eta_0 = \sum_{i=1}^{z} G_i \tau_i$$

Prapnnachari (*8*) provides more detailed information about the viscoelastic characterization performed in this study.

Since the procedure for dynamic measurements on the Rheometrics Mechanical Spectrometer (RMS) is well established (*9,10*), it will not be repeated here. The asphalts tested were characterized over temperatures ranging from −25°C to 65°C and at frequencies ranging from 0.1 to 100 rad/sec. Details of the testing procedure are discussed by Little et al. (*11*).

Master curves and discrete relaxation spectra were constructed for each asphalt (*12*). The discrete relaxation spectra were used to calculate steady state or zero shear viscosity. Table 1 summarizes the zero shear viscosity for the asphalts tested.

Asphalts Analyzed

Eleven asphalts representing different sources were tested (*8*) using an RMS. For purposes of simplification in identification of data, asphalts studied are referred to as Type A, B, C, D, E, F, G, H, I, J, and K in lieu of identification by the asphalt's commercial name. The identification key for these asphalts is as follows:

Type	*Identification*
A	SHRP Asphalt AAA (AC-20)
B	SHRP Asphalt AAG (AC-20)
C	SHRP Asphalt AAM (AC-20)
D	Conoco AC-20
E	Frontier AC-20
F	Conoco AC-10
G	Frontier AC-10
H	Sinclair AC-10
I	Exxon AC-20
J	Santa Maria AC-10
K	Coastal AR-4000

MICROSTRUCTURAL MECHANICS BY RHEO-OPTICAL/FOURIER TRANSFORM INFRARED SPECTROSCOPY STUDIES

Overview

Infrared (IR) is widely used to study the influence of mechanical stress on the molecular structure of polymers. This study used IR

TABLE 1 Relaxation Parameter of Zero Shear Viscosity, η_0, as Obtained from the Relaxation Spectra of the 11 Asphalts Tested

Asphalt Type	Zero Shear Viscosity (Poises)
A	2.95e+05
B	9.16e+05
C	1.78e+07
D	3.14e+06
E	4.23e+06
F	1.17e+06
G	1.19e+06
H	2.59e+06
I	1.89e+06
J	0.49e+06
K	3.76e+06

spectroscopy to evaluate the influence of shearing on the molecular structure of asphalt. Although the detailed chemical knowledge of the interconnectivity of asphalt systems is not known and cannot be determined by this technique, information about the importance of specific bond or group types to mechanical properties can be extracted using rheo-optical techniques. The coupling of IR spectroscopy and controlled shear deformation was introduced by Little et al. (*11*). A detailed introduction to and discussion of analysis through IR spectroscopy is presented by Prapnnachari (*8*).

Experimental Setup

The IR experimental setup included two main units: the IR spectrometer (a Nicolet model 60SXR) and the asphalt shear deformation stage (Minimat marketed by Polymer Laboratory of Massachusetts), which fits in the sample chamber of the Nicolet IR spectrometer and which was used to shear the asphalt in a thin film. A thin-film shearing action, which is similar in concept to the shearing action induced in the thin film of asphalt coating the aggregate particles, is produced by the Minimat setup. While being sheared, the asphalt film was penetrated with an IR beam.

Selection of a proper window material was a key consideration in establishing a transmission IR spectrum. The first criterion to consider in selecting a window material was the frequency range over which the spectrum must be measured. Other important considerations included solubility, reactivity, and refractive index of the window material with respect to the sample. Mechanical and thermal characteristics of the window materials also played a major role in their consideration for this test. Hygroscopic materials such as potassium bromide (KBr) and sodium chloride (NaCl) are used most frequently, primarily because they do not react with organic compounds. Although KBr has a slightly wider spectral range than NaCl, it is too brittle to withstand significant mechanical shocks. Besides, KBr is more hygroscopic and less resistant to thermal fluctuations than NaCl. In this study, NaCl was selected as a window material.

Because of width limitations in the space available for sample holding, a 29- × 14.5- × 4-mm NaCl plate was selected for use. In sample preparation, two such rectangular NaCl plates were coated with a thin layer of asphalt and then sandwiched together. Only one end of each NaCl plate was clamped. The plates remained together under the adhesive influence of the asphalt. To ensure full adhesion to the NaCl plates, a small quantity of asphalt was smeared over one face at a temperature between 60°C and 93°C. The second NaCl plate was pressed firmly by hand over the first, still hot, NaCl plate. This sandwich arrangement was kept at a temperature between 60°C and 93°C in an oven for a few minutes to ensure uniformity. After cooling, the system was placed and clamped in sample holders. Obviously, the portion of NaCl plates under the clamp grip was not coated with asphalt. Subsequently, the entire set was mounted in the sample box of the IR spectrometer.

The maximum available overlap between the two plates through which the IR beam could pass was 13 mm. The number of reproducible IR scans per minute was not greater than six. To optimize the number of IR scans obtained during shearing, a 6-mm/min rate of shear deformation was used. The IR spectral changes below a 4-mm/min deformation rate were hardly perceptible, suggesting that the rate of deformation was slower than the asphalt's characteristic relaxation time, and the spectral changes from 4 to 6 mm/min rate of shearing were identical. The IR spectrometer was programmed so that the first IR scan collected was for the sample with no shear induced. Subsequently, Minimat movement inducing shearing within the asphalt and the IR scan were triggered simultaneously. Figures 1 and 2 show the setup of the IR experiment. Figure 1 is a view of the entire experiment setup (IR spectrometer and Minimat). Figure 2 is a view of the Minimat device, which fits within the chamber of the IR spectrometer and actually shears the asphalt between the NaCl plates while the IR spectra captured during shearing are used to analyze changes in absorbance bands. Prapnnachari (*8*) provides a much more detailed discussion of the experimental setup and the evolution of the approach used.

FIGURE 1 Minimat in Fourier transform infrared spectroscopy chamber.

Infrared Spectral Analysis

IR spectra of asphalts have nine main absorbance bands, which are summarized in Table 2. The absorbance bands are characteristic of a specific molecular structure and its mode of vibration. Absorbance is proportional to the concentration of the chemical group. Asphalt is composed of hydrocarbons, and the band assignments for hydrocarbons are well established in the literature. Primarily using the band assignments for hydrocarbons, Stewart (*13*) and Beitchman (*14*) characterized asphalt bands, as summarized in Table 2. In general, the region of the IR spectrum between 3100 and 2800 cm^{-1} indicates the nature of the hydrocarbon part of a molecule. This region was examined first, since the position of the CH stretching band suggests the structural feature of a hydrocarbon molecule. Absence of absorbance above 3000 cm^{-1} suggests that molecules are aliphatic and alicyclic with no ethylenic or aromatic structure. Figure 3, a typical IR spectrum of an asphalt, shows strong absorbance from 2950 to 2850 cm^{-1}, which suggests the dominance of aliphatic and alicyclic hydrocarbon structures in all the asphalts tested. This does not mean that aromatics are absent in the asphalt molecules. Sometimes the closer

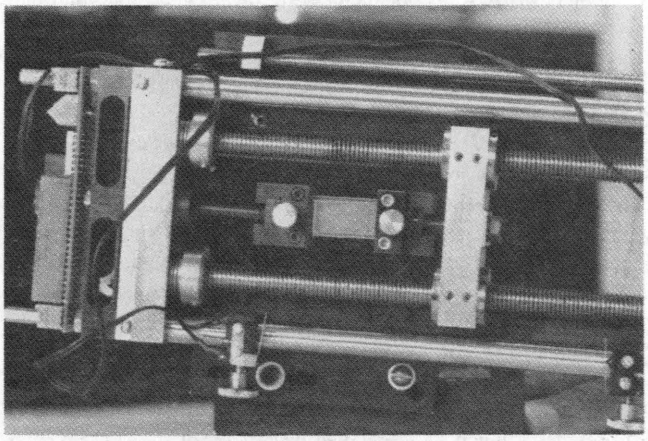

FIGURE 2 Minimat deformation stage.

frequencies develop coupled vibrations, shifting absorbance to unexpected regions of the spectrum. This might occur because of the complex structure of the asphalt molecules. Close examination of the absorbance in the 3000 to 2800 cm^{-1} region indicates the presence of two peaks for aliphatic and alicyclic CH stretching: one near 2850 cm^{-1} (alicyclic) and the other near 2925 cm^{-1} (aliphatic). The steep shoulder near the 3000 cm^{-1} peak indicates weak absorbance due to the aromatics. This peak is obscured by the very strong CH_2 and CH_3 stretching bands during shearing of the aliphatics and alicyclics. Generally, the aromatic structures in a hydrocarbon can be found (*15*) in five regions of the IR spectrum: 3100 to 3000 cm^{-1} for CH stretching, 1650 to 1430 cm^{-1} for C=C stretching, 1275 to 1000 cm^{-1} for in-plane CH bending, 900 to 690 cm^{-1} for out-of-plane CH bending, and 2000 to 1700 cm^{-1} for overtones and combinations. In the IR spectrum of an asphalt, weak absorbance near 1600 cm^{-1} suggests C=C stretching of the aromatics, and small absorbance at 863, 813, and 745 cm^{-1} is due to CH out-of-plane bending. The overtones and in-plane CH bending were not witnessed.

The region near 1460 and 1375 cm^{-1} reveals the presence of methylene and methyl groups. The band near 1460 cm^{-1} indicates the antisymmetric deformation of the HCH angle of a CH_3 molecule. The bending of methylene (CH_2) groups gives rise to a band in the same region. The symmetric CH_3 bending gives a strong, sharp band near 1376 cm^{-1}. A small band near 720 cm^{-1} is indicative of a linear chain containing four or more CH_2 groups. The relative numbers of CH_2 and CH_3 groups are evaluated by the combined study of the 1460, 1376, and 720 cm^{-1} bands. When there are more CH_2 groups than CH_3 groups present, the 1460 cm^{-1} band will be stronger (*15*) than the 1376 cm^{-1} band. A greater relative intensity of the band near 1460 cm^{-1} than 1376 cm^{-1} was found in general in the IR spectra of all the asphalts. This shows the dominance of CH_2 groups over CH_3 groups in the asphalt molecules. The relative length of CH_2 chains among asphalts can be evaluated by the study of absorbance near 720 cm^{-1}, in particular by studying the change in ratio of the CH_2 and CH_3 absorbencies.

Absorbance Peaks

The height and area of an absorbance peak indicate the concentration of a particular molecular component in the sample. For a given asphalt, the ratio of any two absorbance peaks provides the ratio of two representative molecular components present in asphalt. For an identical chemical and mechanical environment, as is noted from Beer's law, the ratio between two peaks is always reproducible irrespective of the number of IR scans and the change in thickness of the sample if the change is uniform. The spectral changes under the influence of mechanical stress on the asphalt sample can thus be quantified by study of the change in the ratio of the absorbance peaks. For a number of spectra, ratios of the peak area were also compared as suggested by Keonig (*16*). In all cases, the peak area ratios verified the results obtained from the evaluation of peak absorbance ratios.

Table 3 gives the absorbance peak ratio of all other bands of the IR spectrum of Asphalt Type A with respect to its 721 cm^{-1} peak for various stages of shearing. As shown in Figure 4, the 1376 to 1457 cm^{-1} bands ratioed with respect to the 721 cm^{-1} band changed appreciably. This is an obvious indication of the key role the chain length plays in asphalt during mechanically

TABLE 2 IR Band Assignments for Asphalt

Wave Numbers (cm^{-1}) S-Strong M-Med. W-Weak	Methyl Groups CH_3 Saturated Aliphatic	Methylene Groups CH_2 Saturated Aliphatic	Aromatic
2950 s	asymmetric stretch	asymmetric stretch	
2860 m	symmetric stretch	symmetric stretch	
1600 w			aromatic ring modes, weak for nonpolar substituents υ (c - c)
1460 m	asymmetric bending	symmetric bending	
1376 m	symmetric bending		
*866 w			1,2,3,4/5 tetra/penta substituted δ (CH)
*813 w			1,4 disubstituted (para) δ (CH)
*745 w			1,2 disubstituted (ortho) or monosubstituted δ (CH)
*720 w		rocking mode $(CH_2)_{n>4}$	monosubstituted δ (CH)

*Aromatic frequencies are more characteristic of the position of the substituents than of their nature.

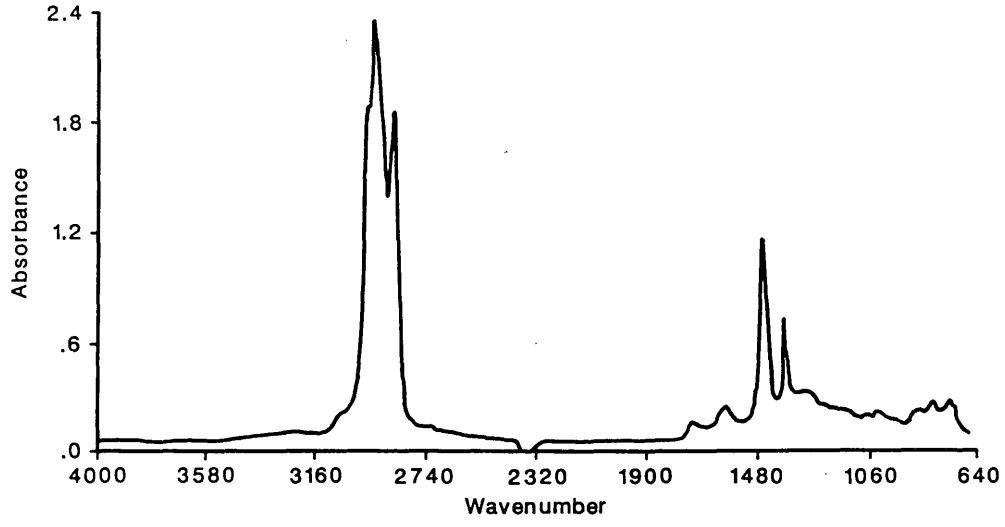

FIGURE 3 IR absorbance spectrum (650 to 4000 cm^{-1}) for unsheared Asphalt Type A.

TABLE 3 Absorbance Peak Ratios, Asphalt Type A

Stretch Stages	Peak ratio with respect to 721 cm^{-1} band				
	745 cm^{-1}	813 cm^{-1}	1376 cm^{-1}	1457 cm	1600 cm^{-1}
1	1.119	1.086	2.924	4.633	1.033
2	1.109	1.082	2.820	4.415	1.037
3	1.120	1.071	2.810	4.447	1.034
4	1.118	1.072	2.703	4.211	1.036
5	1.113	1.069	2.492	3.971	1.046
6	1.122	1.068	2.480	3.772	1.060
7	1.121	1.064	2.273	3.750	1.058
8	1.122	1.057	2.412	3.710	1.056
9	1.124	1.063	2.207	3.734	1.060
10	1.116	1.062	2.412	3.698	1.057

induced shear. Figure 5 is typical of the collective spectra obtained during the stages of shearing for an asphalt (Type K). The change in the shape of the bands and shoulders, mostly near the 745 cm^{-1} band, results from the interaction of substituent CH_2 molecules.

The studies of changes in absorbance peak ratios (Figure 4) and changes in band shapes and shoulders (Figure 5) are complementary. The most affected peak ratios, 1457 and 1376 cm^{-1} bands ratioed with respect to the 721 cm^{-1} band, indicate that CH_2 and CH_3 molecules forming the chains attached to the asphalt molecules are most active in resisting shearing. The change in band shapes and shoulders in the region of the aromatic out-of-plane CH bending absorbance suggests the interaction of the CH_2 chains with the aromatics. This suggests that the network of CH_2 chains forming the substituents to the aromatics also contributes to resisting mechanically induced stress.

WIDE-ANGLE AND SMALL-ANGLE X RAY DIFFRACTION

Principles of Diffraction

X ray diffraction is a tool for the investigation of the fine structure of matter. Early X ray use was limited to the determination of crystal structures. Today, X rays are used not only for crystal structure determination but are also applied to problems in chemical analysis, stress measurement, phase equilibrium, and the measurement of particle size.

Diffraction is produced by the interference of waves scattered by an object. When the X rays strike the object at an angle, 2θ, every electron becomes the source of a scattered wave. If an X ray beam of intensity I_0 interacts with a free electron, the intensity

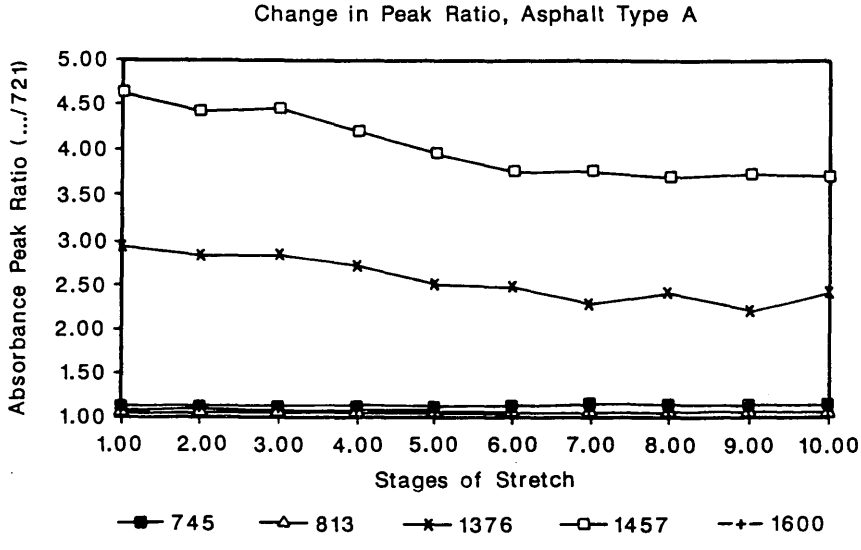

FIGURE 4 Peak ratio versus stage of shearing (mm) for Asphalt Type A.

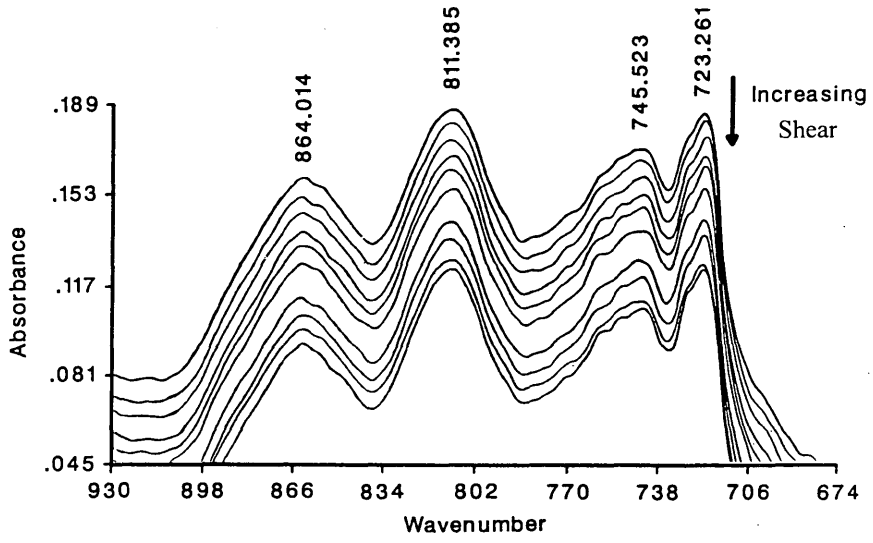

FIGURE 5 Collected IR absorbance spectra (680 to 930 cm^{-1}) for stages of shearing for Asphalt Type K.

I is expressed as

$$I = I_0 \frac{K}{R^2}\left(\frac{1 + \cos^2 2\theta}{2}\right)$$

Here the constant K is defined by e^4/m^2c^4, where e and m are charge and mass of an electron, respectively, and c is the velocity of light. R is the scattering vector.

For a noncrystalline material consisting of a single type of atom, the spatial distribution of atoms can be expressed conveniently by means of a radial distribution function ρ (r), which is described as the number density of atoms to be found at a distance r from the center of any one of the atoms.

If a material contains more than one kind of atom, its amorphous structure can be characterized in principle by a generalized radial distribution function (*17*). From the radial distribution function, the density of atoms or the frequency of separations between atoms can be obtained by analyzing the peaks in the data. This provides a quantitative information source regarding the different atoms such as carbon and hydrogen in asphalt.

X ray scattering techniques are usually categorized into wide-angle X ray scattering (WAXS) and small-angle X ray scattering (SAXS). In WAXS, the structural information is obtained on a scale of 1 nm or smaller. The angle measured is between 3 and 90 degrees. The inhomogeneities of atomic dimensions give rise to WAXS. In SAXS, fluctuations in electron density over large distances, typically 30Å to 1000Å, are determined. The inhomogeneities of colloidal dimensions generate X ray scattering and interference effects at very small angles, typically less than 2 degrees, with the wavelength of CuKα, 1.542Å.

Since WAXS probes atomic dimensions, different bands of X ray beams diffracted from the lattice planes are obtained as intensity. With knowledge of the position of peaks, quantitative information concerning crystalline and amorphous structures can be obtained. Since SAXS identifies large structures, the intensity peaks are spaced according to the distance between large areas of contrasting density. This capability provides a tool by which to determine whether asphalt is a colloid or a network structure.

Use of Fractal Analysis To Determine Asphalt Molecular Topology

Fractal analysis can be used to characterize disordered objects ranging from macromolecules to the earth's surface (*18*). These objects display "dilation symmetry," which means that they look geometrically self-similar under transformation of scale such as changing the magnification of a microscope. Complex structures such as Eden, Vold, Wittne-Sander, and so forth (*19*) can be simply characterized with the single parameter D, the fractal dimension, which is defined as the exponent that relates the mass M of an object to its size R as

$$M \propto R^D \tag{1}$$

where $\propto$ is interpreted as "proportional to" in Equations 1 through 3.

This equation also applies to simple objects such as rods, disks, and spheres, for which the exponent D is equal to 1, 2, and 3, respectively. For fractal objects, however, the exponent need not be an integer.

Polymers are described by Equation 1 and are called "mass fractals." On the contrary, colloids are "surface fractals," which are uniformly dense but have a rough surface. Surface fractals share the self-similarity property; however, if the surface is magnified, its geometric features do not change. Mathematically, surface self-similarity is represented by an analog of Equation 1:

$$S \propto R^{D_s} \tag{2}$$

where S is the surface area and D_s is the surface fractal dimension. For a smooth object, $D_s = 2$, consistent with the notion that a

smooth surface is two dimensional. For fractally rough surfaces, however, D_s varies between 2 and 3, so D_s is a measure of the surface roughness.

Fractals can be characterized by small-angle X ray scattering techniques. The asphalt sample was subjected to X rays, and the angular dependence of the scattered intensity was measured. For fractal objects, the intensity profile has a power law dependence when plotted versus the magnitude of the wave vector K (*20*):

$$I \propto S^{-2D} + D_s \tag{3}$$

The quantity $P = -2D + D_s$ is called the Porod shape. Through Bragg's law, the parameter S can be related to a characteristic length L and the scattering angle θ ($S = 2\pi/L = 4\pi\lambda^{-1}\sin\theta$), where λ is the wavelength. By scanning θ, an object on different length scales can be studied effectively. Though there are exceptions to the general rules (*20*), it is usually possible to distinguish structures by the exponent in Equation 3. Polymeric (mass fractals where $D_s = D$) systems yield scattering curves with slopes between -1 and -3, whereas smooth colloids give slopes of -4. Rough colloids give slopes of between -3 and -4 (*21*). The analysis of the Porod slopes of SAXS curves is shown in Figure 6 for polymeric and colloidal systems.

The method described above was used on four of the SHRP asphalts (AAM, AAD, AAF, and AAK). Figure 7 shows the raw data, empty cell scattering, and absorption data for asphalt AAF-1. Correction for the empty cell scattering and absorption was made as follows:

$$I_{cor} = I_{raw} - (I_{empty\ cell} - I_{abs}) \tag{4}$$

The background correction was made following the method of Ruland (*22*). Figure 8 shows the corrected intensity $I(s)$. The power law scattering, $I(s) \approx S^{-P}$ was observed in the range of -7 to -4 of ln s. The exponent P was determined to be -0.8 by the least squares method (Figure 9). This is consistent for all asphalts studied, suggesting a noncolloidal, linear system.

EVALUATION OF RELAXATION MECHANISM

The changes in the molecular structure of asphalts were observed in the collective IR absorbance spectra during shearing state; the perturbations and shoulders at random frequencies indicative of the region of substituents to the aromatics demonstrate the conformational changes to the appendages of the aromatics (Figure 5). Figure 4 shows that most of the changes occur in the peak ratio of the CH_2 and CH_3 bands (721, 1376, and 1457 cm^{-1}). The shearing of the asphalt sample in the IR beam indicates that the methylene structures, irrespective of their position in the molecule (Figure 4), are most active in resisting mechanically induced stress. The band at 721 cm^{-1} is for skeletal rocking of CH_2 molecules; the band at 1376 cm^{-1} represents the symmetrical bending mode vibration of CH_3 molecules; the band at 1457 cm^{-1} represents the combined symmetrical and asymmetrical bending modes of vibration of CH_2 and CH_3 molecules, respectively.

The length of a methylene chain structure is represented by the ratio of CH_2 and CH_3 groups. During deformation, the $[CH_3]/[CH_2]$ absorbance ratio may decrease because of an increase in $[CH_2]$ at fixed $[CH_3]$ concentration or because of a decrease in the $[CH_3]$ concentration. We cannot distinguish one mechanism from the other and therefore cannot state which occurs. But it is clear that the higher the ratio in the undeformed state, the longer the representative chain length. The changes observed in the ratio of the peaks of the absorbance bands during deformation offered qualitative information only. No fixed pattern or reproducibility was observed for each stage of shear deformation on replicates of the asphalt samples. Random changes in the peak ratio were shown that indicate high randomness in the orientation and length of asphalt chains. The observation shown in Figure 4 suggests that the changes under mechanically induced shearing are due to interactions among and within methyl and methylene molecules. The extent of these changes could not be quantified because the asphalts studied possess random orientation of the short methylene chains. The representative chain length of the asphalt molecule represented by the ratio of CH_2 (721 cm^{-1}) to CH_3 (1376 cm^{-1})

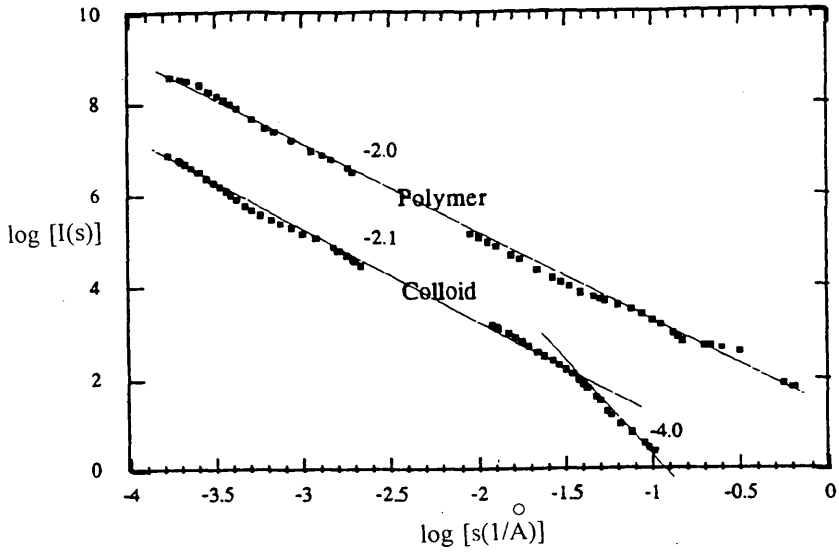

FIGURE 6 Contrasting SAXS profiles for polymeric and colloidal systems.

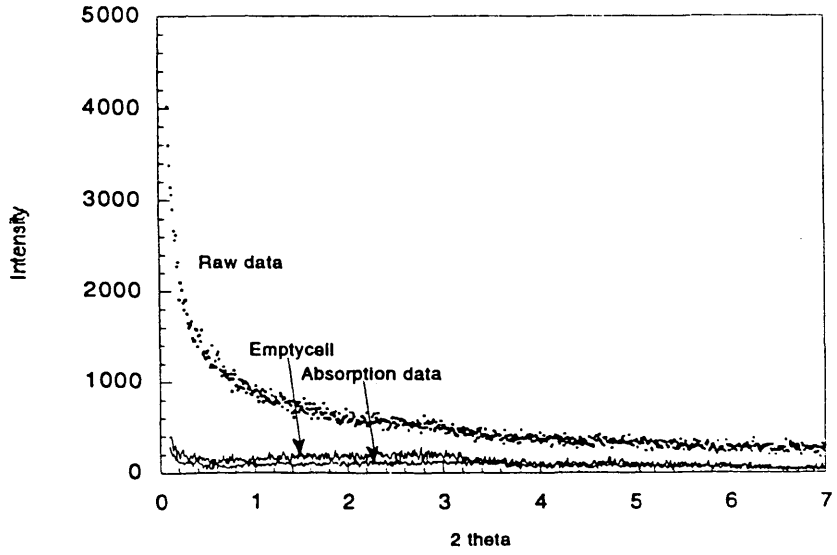

FIGURE 7 SAXS curves of AAM asphalt raw data, empty cell scattering, and absorption data.

absorbance of the undeformed sample is given in Table 4. Stewart (*13*) suggested this absorbance as indicative of the presence of bulk assemblies of aliphatic hydrocarbon chains in an asphalt molecule.

The viscoelastic characteristics of the asphalts were evaluated by the relaxation spectrum obtained from the master curves of the storage and loss moduli. The master curves were constructed from analysis of the dynamic mechanical test data explained previously. The experiment was carried out over the temperature range −25°C to 65°C, and the master curves were constructed at a reference temperature of 25°C. The absence of the rubbery plateau in the master curves of the asphalts suggests a single relaxation transition for asphalts. This indicates that the asphalts may demonstrate a polymeric solution type behavior.

Figure 10 shows the dependence of the relaxation time of asphalts on their representative chain length. The slope of the log zero shear viscosity and log CH_2/CH_3 plot is 4.2 with considerable scatter among the data. The relaxation model (*23–25*) for polymeric solutions suggests a slope of 3.45. Since these values are within statistical significance (the 95 percent confidence interval for the slope calculated between zero shear viscosity and chain length is ±0.9), we can conclude that an entangled polymerlike solution exists. Since asphalts are low-molecular-weight hydrocarbons, an explanation for this behavior is needed. A dependence

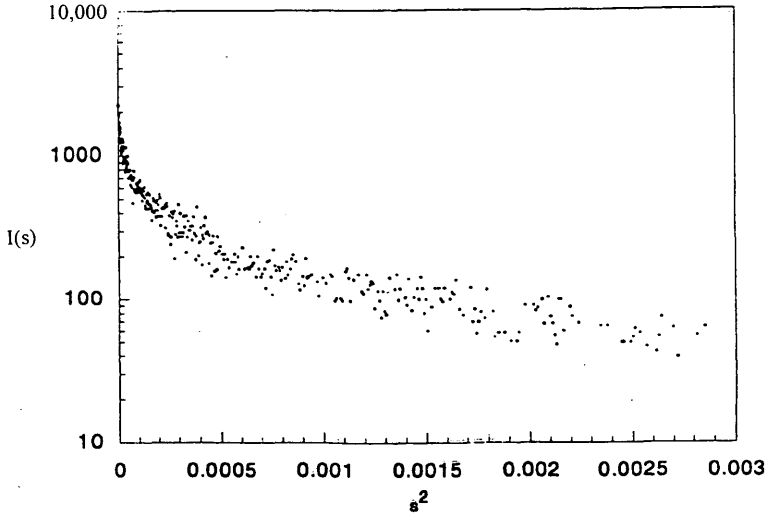

FIGURE 8 Log *I* versus s^2 plot of the SAXS curve of AAM asphalt.

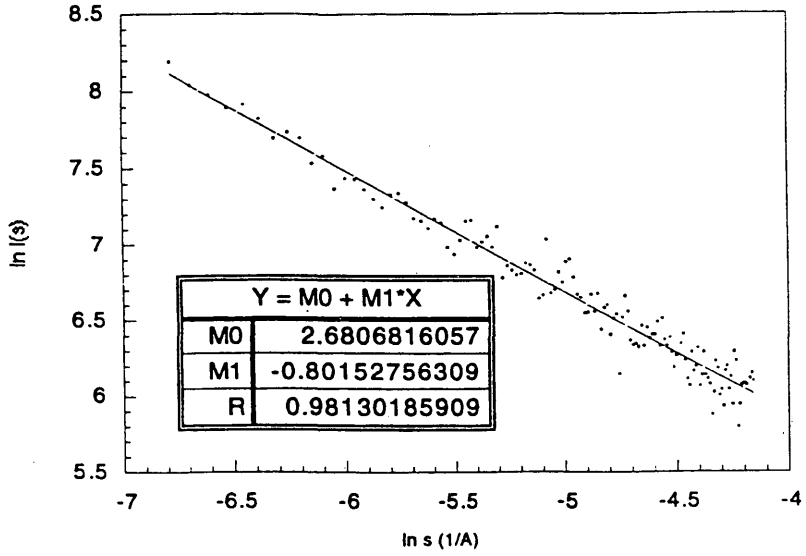

FIGURE 9 Log-log plot of the SAXS curve for AAM asphalt.

of the relaxation behavior of the asphalts on chain length was observed, suggesting a possible "virtual" network that extends linear interactions by producing virtual cross-links or entanglements. Surprisingly few of these interactions are needed to produce the observed viscoelastic behavior. The deviation from polymer solution behavior indicates that the asphalts are also strongly influenced by their dispersed structure.

The 11 asphalts previously discussed were analyzed to determine whether Corbett compositional analysis is related to the zero shear viscosity value of the asphalt. However, no component of the Corbett fraction can by itself explain the physical behavior of asphalt (Table 4). A plot of unrelaxed modulus (G_R) of the asphalts studied (unrelaxed modulus is obtained from discrete relaxation spectra at an infinitely small time common to all the asphalts) in Figure 11 demonstrates a rough correlation (except the Asphalt Type J) between representative chain lengths in the asphalt and relaxation time. Asphalt Type J, although having an abnormally high initial modulus, does not maintain the long-term resistance to flow; its initial high modulus might be due to highly polar and interactive asphaltene fractions. Table 3 indicates that Type A asphalt has the highest asphaltene percentage. But since Asphalt A has the smallest representative methylene chain length, it lacks the long-term potential of resistance to flow.

CONCLUSIONS

The objective of this study was to probe the relationship between an asphalt's structure and the viscoelastic properties observed for

TABLE 4 Values of the Ratio of Peak Absorbance of CH_2 (721 cm^{-1}) to CH_3 (1376 cm^{-1}) and Relaxation Strength of the Asphalts

Asphalt Type	Ratio of CH_2 (721 cm^{-1}) to CH_3 (1376 cm^{-1}) Absorbance	Zero Shear Viscosity (Poises)
A	0.342	2.95e+05
B	0.284	9.16e+05
C	0.624	1.78e+07
D	0.409	3.14e+06
E	0.412	4.23e+06
F	0.386	1.17e+06
G	0.406	1.19e+06
H	0.397	2.59e+06
I	0.384	1.89e+06
J	0.288	0.49e+06
K	0.376	3.76e+06

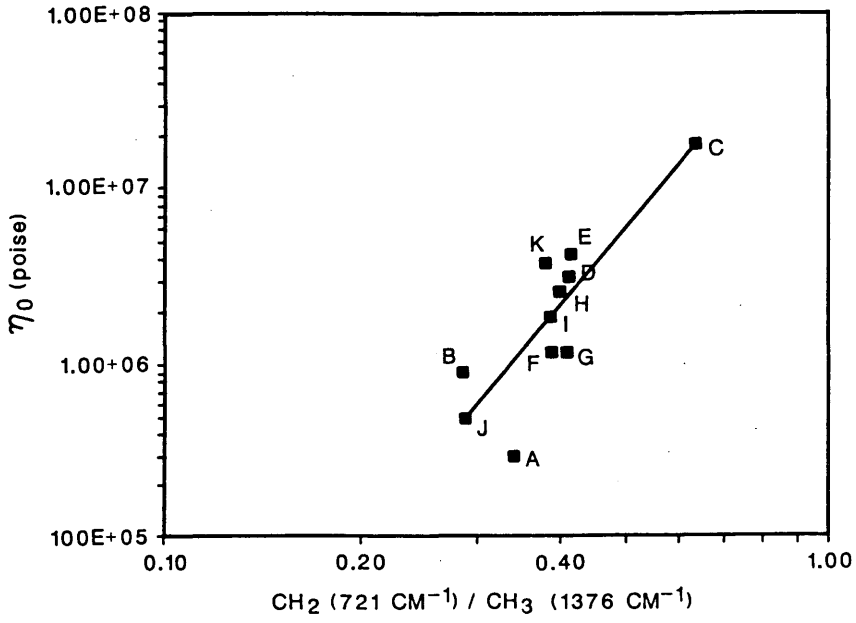

FIGURE 10 Chain length dependence of relaxation strength of the asphalts studied. η_0 is the zero shear viscosity.

the asphalt. The bulk assemblies of the methylene chains in asphalts were observed to be most active in resisting mechanically induced stress. This result is concluded from the rheo-optical studies in which specific IR bands were observed to change during shear deformation of the asphalt. The ratio of methylene to methyl absorbance in the IR spectrum offered a method of evaluating the representative length of the methylene chains in an asphalt. The methyl and methylene absorbance bands used for the study were 1376 and 721 cm^{-1}, respectively. The methylene band, 721 cm^{-1}, represents aliphatic $(CH_2)_{n>4}$ hydrocarbons in asphalts. Using this information, a correlation between the asphalt's chain "length" and the viscoelastic properties of these materials was determined. In particular, the relaxation spectrum of asphalt was used to evaluate the zero shear viscosity, which is a measure of long-term resistance to flow. The study demonstrated the dependence of the asphalt's long-term resistance to flow on the representative length of the methylene chains. It is important to note the relationship previously discovered by Benson and Little (*26*) between meth-

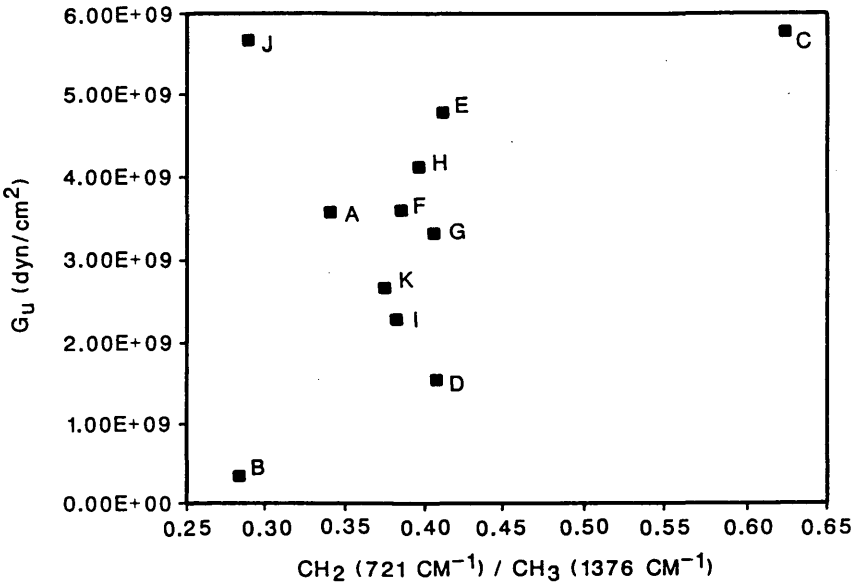

FIGURE 11 Unrelaxed relaxation strength versus chain length of the asphalts studied.

ylene chain length (methylene to methyl ratio) and microdamage healing. In the Benson and Little work, longer methylene chains resulted in superior microdamage healing.

The plot of the log of the representative length of the methylene chains versus log of the zero shear viscosity showed considerable scatter with a correlating slope of 4.2. As reported in the literature, for true polymeric solutions a slope of 3.45 should be observed. From the data, there is no ($\alpha = 0.05$) statistical difference between 4.2 and 3.45, suggesting a possible solution type behavior with chain entanglements.

These data suggest that a model supporting a colloid type structure is unlikely. The X ray data do not suggest the existence of colloid structures (in the range detectable from X ray analysis) but instead suggest the dominance of linear type structures. This is in agreement with the rheo-optical data, suggesting that "linear" structures control the viscoelastic deformation of these materials. These linear structures are interconnected through a virtual network providing the structure needed to justify the observed mechanical properties. This proposed organization is not unlike the DPF model. The polar interactions form the virtual network with a number of linear structures (appendages to the aromatic structures) thereby controlling the viscoelastic nature of the asphalt. More work is needed to further investigate this phenomenon.

REFERENCES

1. Corbett, L. W. Composition of Asphalt Based on Generic Fractionation Using Solvent Deasphaltening, Elution-Adsorption Chromatography, and Densimetric Characterization. *Analytical Chemistry*, Vol. 41, 1969, pp. 576–579.
2. Dealy, J. M. Rheological Properties of Oil Sand Bitumens. *Canadian Journal of Chemical Engineering*, Vol. 57, 1979, pp. 677–683.
3. Boduszynski, M. M., J. F. McKay, and D. R. Latham. Asphaltenes, Where Are You? *Proc., Association of Asphalt Paving Technologists*, Vol. 49, 1980, pp. 123–143.
4. Petersen, J. C. Chemical Composition of Asphalt as Related to Asphalt Durability—State of the Art. Presented at 63rd Annual Meeting of the Transportation Research Board, Washington, D.C., 1984.
5. Halstead, W. J. Relation of Asphalt Chemistry to Physical Properties and Specifications. *Proc., Association of Asphalt Paving Technologists*, Vol. 54, 1985, pp. 91–117.
6. *Binder Characterization and Evaluation.* Quarterly Report, Technical Section, SHRP A-002A. Western Research Institute, University of Wyoming Research Corporation, Laramie, June 1991.
7. Monismith, C. L. *Asphalt Paving Mixtures Properties, Design, and Performance.* Course notes, Short Course in Asphalt Paving Technology. The Institute of Transportation and Traffic Engineering, University of California, 1961.
8. Prapnnachari, S. *Investigation of Microstructural Mechanism of Relaxation in Asphalt.* Ph.D. dissertation. Texas A&M University, College Station, 1992.
9. Walters, K. *Rheometry.* John Wiley and Sons, New York, 1975.
10. Barnes, H. A., J. F. Hutton, and K. Walters. *An Introduction to Rheology.* Elsevier Science Publishing Company, New York, 1989.
11. Little, D. N., S. Prapnnachari, A. Letton, and Y. R. Kim. *Investigation of the Microstructural Mechanisms of Relaxation and Fracture Healing in Asphalt.* Final Report, Grant AFOSR-89-0520. Texas Transportation Institute, Texas A&M University, College Station, 1993.
12. Baumgaertel, M., and W. H. Winter. Determination of Discrete Relaxation and Retardation Time Spectra from Dynamic Mechanical Data. *Reologica Acta*, Vol. 18, No. 6, 1989, pp. 511–579.
13. Stewart, J. E. Infrared Spectra of Chromatographically Fractionated Asphalts. *Journal of Research of the National Bureau of Standards*, Vol. 58, No. 5, 1957, pp. 265–269.
14. Beitchman, B. D. Infrared Spectra of Asphalts. *Journal of Research of the National Bureau of Standards*, Vol. 63A, No. 2, 1959, pp. 189–193.
15. Lambert, J. B., H. F. Shurvell, D. A. Lightner, and R. G. Cooks. *Introduction to Organic Spectroscopy.* Macmillan Publishing Company, New York, 1987.
16. Keonig, J. L. *Spectroscopy of Polymers.* American Chemical Society, Washington, D.C., 1991.
17. Alexander, L. E. *X-Ray Diffraction Methods in Polymer Science.* R. E. Publishing Company, Malabar, Fla., 1985.
18. Mandelbrot, B. B. *The Fractal Geometry of Nature.* Freeman, San Francisco, Calif., 1982.
19. Schaefer, D. W. *Science*, 243, 1023, 1989.
20. Martin, J. E., and A. J. Hurd. *J. Appl. Cryst.*, 20, 61, 1987.
21. Bale, H. D., and P. W. Schmidt. *Phys. Rev. Lett.*, 53, 596, 1984.
22. Ruland, W. *Pure Appl. Chem.*, 49, 505, 1977.
23. De Gennes, P. G. *Introduction to Polymer Dynamics.* Cambridge University Press, New York, 1990.
24. Doi, M., and S. F. Edwards. *The Theory of Polymer Dynamics.* Clarendon Press, Oxford, New York, 1986.
25. Aklonis, J. J., and W. J. MacKnight. *Introduction to Polymer Viscoelasticity* (2nd edition). John Wiley and Sons, New York, 1983.
26. Benson, F. C., and D. N. Little. *Correlation Among Asphalt Concrete Mechanical Healing, Asphalt Cement Dispersion, FTIR Chemical Functional Groups and ^1H NMR Chemical Structure.* Final Report, Grant ECE-8511851. National Science Foundation, 1988.

Publication of this paper sponsored by Committee on Characteristics of Bituminous Materials.

Improved Low-Temperature Fracture Performance for Rubber-Modified Asphalt Binders

JOSEPH C. T. HUI, GEOFFREY R. MORRISON, AND SIMON A. M. HESP

The low-temperature fracture toughness was determined for rubber-modified asphalt binders. Crumb rubber tire, both plain and surface modified, and devulcanized rubber tire were investigated for their effectiveness in improving low-temperature asphalt binder performance in a notched, three-point bending beam fracture test. The increases in low-temperature fracture toughness for unmodified crumb rubber–asphalt mixtures were highest for fine ground rubber. At loading levels of 4 to 10 wt percent on the binder, the fracture toughness for 10- and 20-mesh ground rubber tire–modified samples was not significantly different from that of the unmodified binders. Reasonable increases in toughness were found for binder modification with 4 to 10 wt percent 30-, 40-, and 80-mesh rubber samples. An in situ sulfur ygrafting reaction of low-molecular-weight polybutadiene onto the crumb rubber dramatically increases the fracture performance for both coarse and fine crumb rubber–modified binders. A 9- and 15-fold increase in added fracture toughness was observed for binders containing 7 wt percent of 10- and 20-mesh cryogenically ground rubber tire. Whether these improvements will translate into a reduction in transverse thermal stress cracking remains to be investigated in further tests on binder-aggregate mixes and in field trials. The fracture toughness for a devulcanized rubber–modified asphalt was also investigated. The homogeneous sample contained as much as 10 wt percent devulcanized rubber tire but performed only marginally better than an 85-100 penetration control sample. Reaction of the devulcanized rubber–modified binder with sulfur increases its fracture toughness by 18 percent.

For more than 25 years discarded rubber tires have been used in asphalt binders to improve the low- and high-temperature performance of the road surface (*1*,*2*). During hot summer months the rubber improves the rheological performance of the asphalt binder, and this may result in a pavement with better rutting resistance and durability (*3*). The rubber tire can lower the stiffness of the binder, and as a result this reduces the brittle temperature (*4*). Advocates of this technology have often been "suggesting that this material will perform noticeably better at low temperatures, compared with standard asphalt concrete" (*5*). However, field trials to look for a possible reduction in transverse thermal stress cracking have so far been disappointing (*6*,*7*) and have been inconclusive in their judgment on the performance/cost benefits of these materials. (*8*).

The development of rubber-modified asphalt pavements has not always been driven solely by economic concerns; environmental agencies and political forces have been strong advocates for the disposal of rubber tire waste in "linear landfills" (i.e., asphalt pavements). Research in this area has often been promoted by government agencies that are concerned with reducing the estimated 2 billion to 3 billion discarded rubber tires that are believed to be stockpiled in North America alone (*9*). This number is growing by approximately 200 million tires each year, which suggests that the waste rubber tire issue will not go away easily. Moreover, it is regularly brought back to the attention of the public when a tire disposal site catches fire, resulting in significant air and water pollution and high costs associated with the cleanup.

The escalation of the scrap tire storage problem has led the United States government to pass legislation forcing the state governments to use waste rubber tire in projects supported by federal funds. The Intermodal Surface Transportation Efficiency Act of 1991 (ISTEA) (Section 1038) requires that states use waste rubber tire in asphalt pavements receiving government funding starting in 1994. The act stipulates that by 1997 all states that receive government funding should use approximately 15 percent rubber tire waste on the asphalt binder in 20 percent of their projects to remain eligible for such governmental support.

Whether this legislation will have the desired effect (i.e., increased usage of recycled rubber in asphalt pavements with an accompanying reduction in waste tire stockpiling) remains to be seen. However, the law has been a strong incentive for significant research and development efforts in this area. A recent survey conducted by Villanova University found that 38 states are currently using scrap rubber tire in their pavements (*10*). However, there are still many concerns and unanswered questions regarding the use of recycled rubber tire in large-scale paving practice.

BACKGROUND

C. H. McDonald, a materials engineer in the roads department of Phoenix, Arizona, pioneered the development of rubber-modified asphalt binders as they are now most often used throughout North America and in many other countries. Since the developments in the late 1960s by McDonald and coworkers, a number of variations on the initial technology have been developed, often with mixed results in terms of performance enhancement.

In the "wet process" as it was developed by McDonald, 14 to 20 wt percent ambiently ground rubber tire (8 to 20 mesh) is swollen in the asphalt's oily phase at high temperatures to form a gellike material after mixing for approximately 45 min at 175°C to 220°C. To this gel is added some aromatic kerosene fraction to increase its workability. This asphalt-rubber is mixed with aggregate to form the pavement. The process requires at least 20 percent more liquid asphalt than is used in a conventional hot-mix pavement. In some cases 40 to 60 percent more asphalt is used in the mix, which may in part account for the increase in both cost and performance (*11*). The thicker films of asphalt at the aggregate

Department of Chemistry, Queen's University, Kingston, Ontario, Canada K7L 3N6.

interface result in greater durability. These asphalt-rubber binders also have higher softening points, which can result in less bleeding and permanent deformation. Moreover, a 70 to 90 percent reduction in traffic noise has been observed on pavements with asphalt-rubber mix overlays compared with conventional pavements (*12*). Because of the substantially higher initial cost of the wet process, the technology has been primarily used for the control of reflective stess cracking. Asphalt-rubber has found applications in stress-absorbing membranes, in stress-absorbing membrane interlayers, as a crack and joint sealer, and to a lesser degree as a binder in thin asphalt concrete overlays (*13*).

Another method for incorporating recycled rubber crumb into asphalt pavements that has received considerable attention is the "dry process." It was originally developed in Sweden under the trade name Rubit (*14*) and subsequently registered in the United States under the trade name Plusride. It differs from the wet process in that the rubber crumb is slightly larger ($^1/_{16}$ to $^1/_4$ in.) and is directly mixed with the aggregate before the asphalt binder is added. The rubber is added at a loading of 3 to 4 wt percent of the aggregate. This process requires a special aggregate gradation to avoid any interference of the rubber crumb with the aggregate, which can lead to premature stripping. In addition, this process also calls for typically 1.5 to 3 percent more liquid asphalt than a conventional hot mix (*15,16*). The increased asphalt content is needed to achieve a voids content of less than 3 percent to prevent premature raveling of the pavement (*17*). In cold climates the Plusride technology has been used successfully to reduce the harmful effects of ice formation on roads. A 25 percent reduction in stopping distances on ice-covered roads has been recorded for pavements made by this process compared with conventional hot-mix pavements (*18,19*). Takallou (*20*) has developed a dry process that uses conventional aggregate gradations by specifying finer crumb rubber grades. The process, which is known under the Generic name, has been used in a number of paving test sections throughout the United States (*21*).

Another variation of the dry process has recently been investigated by the United States Army Corps of Engineers at the Cold Regions Research and Engineering Laboratory (CRREL) (*21*). CRREL has investigated the use of much larger quantities of a coarse rubber crumb in hot-mix pavements. The crumb rubber was added at 3 to 12 wt percent of the aggregate, compared with typically 3 wt percent for the conventional Plusride or Generic processes. The optimum binder content in the mix increases with the amount of crumb rubber added. By using such large quantities of rubber crumb in an asphalt pavement, one gets rid of a lot of scrap tire. However, the added cost of the rubber and the higher binder content of the pavement, the extra cost associated with the use of equipment to handle such large quantities of crumb rubber, and the added mix design and production complexity may increase the overall pavement cost by as much as 150 percent over that of an unmodified mix.

The fact that the cost of rubber-modified hot-mix pavements, in general, is currently anywhere from 60 to 150 percent more than the cost of a conventional asphalt pavement has deterred many municipal and state governments from using this technology. Today, asphalt-rubber is mainly used in low-volume applications such as crack and joint sealants, stress-absorbing membranes, and stress-absorbing membrane interlayers.

Concern about high initial costs combined with uncertainty about future benefits has hindered the large-scale acceptance of asphalt-rubber technology. It may be more sensible to use less crumb rubber to lower the initial cost and make the technology more affordable. If modest amounts (4 to 10 wt percent) of fine crumb rubber are applied to the asphalt binder, the pavement may be constructed with normal binder contents, which would result in only a slight overall increase in cost. This by itself may make the technology more widely acceptable, which could eventually mean that much more scrap tire will be used in hot-mix asphalt pavements.

Another concern relates to the difficulties involved with the recycling of asphalt-rubber pavements as they have been constructed until now. The high rubber content of asphalt-rubber binders may complicate the recycling of old pavements and could possibly create a serious solid waste problem in the years ahead. This would ultimately defeat the purpose of the ISTEA legislation. To facilitate hot-mix recycling of the pavement, it may be necessary to use less crumb rubber in the asphalt binder.

Recently, paving trials in Florida (*22*) and Ontario (*23*) have used binders containing only 7 to 9 percent fine crumb rubber (80 mesh) directly blended into the asphalt cement. Initial laboratory test results are promising, but it is too early to draw any conclusions from the performance of these trial pavement sections (*24*).

The work presented in this paper investigates fundamental fracture properties of a number of such recently developed asphalt binders containing only modest amounts of recycled rubber. Moreover, new products are developed by reacting the crumb rubber in situ with the asphalt phase to improve interfacial adhesion and stability.

A commercially available homogeneous asphalt binder containing devulcanized rubber tire is also investigated for its fracture performance. This binder contains 10 wt percent rubber tire and is marketed under the trade name Ecoflex. In the Ecoflex process, the crumb rubber is mixed with the asphalt and the binder is subsequently heated for up to 5 hr at 220°C to 260°C while compressed air is blown through to break down the rubber and facilitate dissolution (*25*). The company that produces this product states that its price is only 3 to 5 percent higher than conventional hot-mix asphalt binders with an increase in performance over unmodified products (*26*). If true, this may provide an incentive for the disposal of large quantities of scrap tire by devulcanizing them according to the Ecoflex process. However, it is doubtful that a process using such high temperatures and such harsh oxidative treatment will ever become acceptable.

EXPERIMENTAL

Materials

The asphalts used in this study were an 85-100 penetration grade and a 150-200 penetration grade, both from the Bow River area in Alberta, Canada. The 85-100 penetration grade control sample has been used in the U.S. Strategic Highway Research Program as a core asphalt under code AAN. Both asphalt samples were obtained from the Lake Ontario refinery of Petro-Canada in Oakville, Ontario.

The wet-ambiently ground scrap passenger car tire was obtained from Rouse Rubber, Inc., of Vicksburg, Mississippi. The 10-, 20-, 30-, and 40-mesh cryogenically ground passenger car tire samples were obtained from Recovery Technologies, Inc., of Mississauga, Ontario. The sample of 20-mesh ambiently ground tire for the preparation of the wet process asphalt-rubber binder was obtained

from Baker Rubber, Inc., of South Bend, Indiana. The Ecoflex sample containing 10 percent devulcanized scrap tire was obtained from Bitumar, Inc., of Montreal, Quebec.

The liquid polybutadiene (LPBD) was obtained from Ricon Resins, Inc., of Grand Junction, Colorado. Its conformation is 80 percent 1,4-trans and 1,4-cis and 20 percent 1,2 vinyl, and it has a number average molecular weight of 12,000 g $mole^{-1}$.

Procedures

Sample Preparation

The rubber-modified asphalt binders were prepared by slowly adding a known amount of rubber to the asphalt at 170°C ± 10°C. Additional LPBD and sulfur were added to a number of the samples. The liquid butadiene was reacted with sulfur in the hot asphalt binder to facilitate a reaction between the asphalt and the crumb rubber particles. The asphalt molecules graft onto the polybutadiene to produce an asphalt-compatible polymer (*27*). The polymer can at some point anchor itself onto the crumb rubber surface through a sulfur cross-linking reaction. This then strengthens the rubber-asphalt interface, and a much tougher asphalt binder can be obtained.

The mixtures were processed under moderate shear using a laboratory mixer (Polytron Mixer, Brinkman Instruments) for at least 2 hr, after which the samples were poured into silicone molds for fracture testing.

Low-Temperature Fracture Testing

The reacted rubber-modified binders were poured into silicone molds and subsequently left in a freezer at −20°C for a minimum of 18 hr before testing. The samples were tested using a three-point bending test based on ASTM E399-90. Testing was done in a temperature-controlled environmental chamber maintained at −20°C using a computer-interfaced Sintech 2/G testing frame. The sample bars measured 25 mm wide by 12.5 mm deep by 175 mm long and had a 90-degree starter notch 5 mm deep in their center, which was sharpened with a razor blade just before testing. The length of the loading span was 100 mm.

Brittle fracture studies were completed for all rubber-modified samples and the 85-100 and 150-200 penetration control asphalts. Measured data included the failure load and the modulus. The fracture toughness, K_{Ic}, was calculated according to Equation 1 (*28,29*).

$$K_{Ic} = \frac{P_f S}{BW^{3/2}} \times \left\{ \frac{3\left(\frac{a}{W}\right)^{1/2}\left[1.99 - \frac{a}{W}\left(1-\frac{a}{W}\right)\left(2.15 - 3.93\frac{a}{W} + 2.7\frac{a^2}{W^2}\right)\right]}{2\left(1+2\frac{a}{W}\right)\left(1-\frac{a}{W}\right)^{3/2}} \right\} \quad (1)$$

where

K_{Ic} = fracture toughness (N $m^{-3/2}$),
P_f = applied failure load, (N),
S = loading span (m),
B = specimen depth (m),
W = specimen width (m), and
a = crack length (m).

For each composition between 15 and 25 beams were fractured. At −20°C, all samples broke in a brittle mode. The standard deviation of the mean and the number of samples were used to calculate a 90 percent confidence limit according to *t*-test statistical methods (*30*).

Lee and Hesp (*31*) give a more detailed discussion of the use of linear elastic fracture toughness (K_{Ic}) measurements in modified binders to study the fundamental fracture toughening mechanisms in polyethylene-modified binders.

RESULTS AND DISCUSSION

The low-temperature fracture data for ground rubber tire–modified asphalt binders (with 90 percent confidence limit) are given in Tables 1 to 3. Various quantities of wet-ambiently and cryogenically ground rubber tire in the 80- and 40-mesh size range were added to Bow River 150-200 penetration grade asphalt. The samples were also reacted with minor amounts of LPBD and 1 wt percent sulfur. Table 4 gives the results for a series of differently sized ground rubber tire samples tested at 7 wt percent crumb rubber, with and without reactive processing with 2 wt percent LPBD and 1 wt percent sulfur.

To distinguish between the effect of the dissolved from the interfacially reacted LPBD on the fracture toughness, control samples of 150-200 Bow River asphalt containing 2, 4, and 6 wt percent LPBD were also tested. The results for the effect of dis-

TABLE 1 Fracture Toughness of 40-Mesh Cryogenically Ground Rubber Tire–Modified 150-200 Bow River Asphalt Binders

Ground Rubber (wt %)	LPBD (wt %)	Modulus (GPa)	K_{Ic} (kN $m^{-3/2}$)
0	0	0.76 ± 0.09	64.9 ± 7.1
4	0	0.79 ± 0.05	75.9 ± 3.6
7	0	0.85 ± 0.09	80.3 ± 2.1
10	0	0.79 ± 0.04	100.6 ± 2.6
4	2	0.90 ± 0.03	89.7 ± 4.3
7	2	0.88 ± 0.08	104.4 ± 3.4
10	2	1.02 ± 0.09	118.9 ± 3.3

TABLE 2 Fracture Toughness of 40-Mesh Wet-Ambiently Ground Rubber Tire–Modified 150-200 Bow River Asphalt Binders

Ground Rubber (wt %)	LPBD (wt %)	Modulus (GPa)	K_{Ic} (kN $m^{-3/2}$)
0	0	0.76 ± 0.09	64.9 ± 7.1
4	0	0.74 ± 0.05	76.6 ± 3.3
7	0	0.82 ± 0.09	81.4 ± 4.4
10	0	0.92 ± 0.10	101.5 ± 5.7
4	2	0.99 ± 0.08	85.6 ± 4.2
7	2	1.02 ± 0.17	114.1 ± 3.8
10	2	1.11 ± 0.09	140.7 ± 5.4

TABLE 3 Fracture Toughness of 80-Mesh Wet-Ambiently Ground Rubber Tire–Modified 150-200 Bow River Asphalt Binders

Ground Rubber (wt %)	LPBD (wt %)	Modulus (GPa)	K_{Ic} (kN $m^{-3/2}$)
0	0	0.76 ± 0.09	64.9 ± 7.1
4	0	0.79 ± 0.05	77.3 ± 5.2
7	0	0.68 ± 0.07	96.0 ± 4.1
10	0	0.53 ± 0.04	120.1 ± 3.2
4	2	0.85 ± 0.08	100.6 ± 5.7
7	2	0.65 ± 0.05	119.3 ± 9.6
10	2	0.62 ± 0.04	137.3 ± 6.4

solved polybutadiene on the fracture toughness of 150-200 penetration grade asphalt are given in Table 5.

From these results, it can be concluded that for each 1 percent LPBD added to the 150-200 Bow River asphalt, the fracture toughness increases by approximately 4.2 kN $m^{-3/2}$. With this information, it is now possible to show the impact that the interfacial reaction between the polybutadiene and the rubber particles has on the fracture toughness of the binders. Figure 1 shows the added benefit to the fracture toughness imparted by the crumb rubber, the LPBD, and the interfacial reaction between the polybutadiene and the rubber particles, for 10-, 20-, 30-, and 40-mesh cryogenically and 80-mesh wet-ambiently ground samples. These results show that the interfacial modification is beneficial in all samples. However, the effect is largest for the coarse crumb rubber–modified binders. The unreacted 10- and 20-mesh crumb rubber–modified binders do not show any significant improvement in fracture toughness over a 150-200 Bow River control binder. However, when the interface is strengthened, the toughness is vastly improved. The gain in fracture toughness for the interfacially modified versus the unmodified 10-mesh sample was ninefold. For the reactively processed 20-mesh sample the toughness increase due to the crumb rubber was as much as 15 times higher than for the unreacted sample. For the 30-mesh sample the added benefit in fracture toughness due to the interfacial modification was 200 percent, for the 40-mesh sample it was 100 percent, and for the 80-mesh sample it was 50 percent.

As a comparison, a 20-mesh ambiently ground rubber tire sample was mixed according to the wet process (20 wt percent rubber mixed for 45 min at 190°C). The fracture toughness for this material was determined to be 164.0 ± 4.4 kN $m^{-3/2}$, which is higher than all the samples in Tables 1 through 4. However, some of the reacted 10 percent crumb rubber samples come close to this level of toughness.

TABLE 4 Fracture Toughness of 10-, 20, 30-, and 40-Mesh Cryogenically Ground Rubber Tire–Modified 150-200 Bow River Asphalt Binders

Ground Rubber (wt %)	Mesh size	LPBD (wt %)	Modulus (GPa)	K_{Ic} (kN $m^{-3/2}$)
0	-	0	0.76 ± 0.09	64.9 ± 7.1
7	10	0	0.95 ± 0.12	66.8 ± 4.8
7	10	2	0.88 ± 0.11	93.6 ± 4.9
7	20	0	0.88 ± 0.08	67.2 ± 2.5
7	20	2	1.01 ± 0.06	105.3 ± 5.7
7	30	0	0.84 ± 0.07	81.0 ± 4.3
7	30	2	1.05 ± 0.08	107.9 ± 4.1
7	40	0	0.85 ± 0.09	80.3 ± 2.1
7	40	2	0.88 ± 0.08	104.4 ± 3.4

TABLE 5 Fracture Toughness of LPBD-Modified 150-200 Bow River Asphalt Binders

Polybutadiene (wt %)	Modulus (GPa)	K_{Ic} (kN $m^{-3/2}$)
0	0.76 ± 0.09	64.9 ± 7.1
2	0.88 ± 0.05	71.3 ± 3.8
4	1.01 ± 0.21	84.9 ± 5.1
6	0.95 ± 0.11	90.4 ± 6.2

Finally, a devulcanized rubber tire–asphalt sample was tested for its low-temperature fracture toughness. This asphalt has an 85-100 penetration grade, and since the base asphalt for this modified material was unknown, it was compared with a Bow River 85-100 penetration grade control sample. The devulcanized sample was also reacted with 1 wt percent sulfur at 170°C for 2 hr to increase the molecular weight of the devulcanized rubber. As indicated in Table 6, the fracture toughness of the devulcanized sample is only marginally better than the 85-100 Bow River control sample (or any other unmodified binder for that matter). Reacting the devulcanized rubber with sulfur increases the fracture toughness by about 18 percent, but the performance is still far below that of the (vulcanized) crumb rubber–modified binders. However, devulcanized rubber may be an ideal material to use in the interfacial reaction between crumb rubber and asphalt. The low price of this material makes it a much more attractive reactive agent than the expensive LPBD used in this work.

However, one advantage of the devulcanized rubber–asphalt systems is that they possess long-term storage stability at high temperatures. The dissolved rubber does not phase separate from the binder during storage or transport. Whether the storage stability of crumb rubber–modified binders can be improved through interfacial modification has to be investigated further.

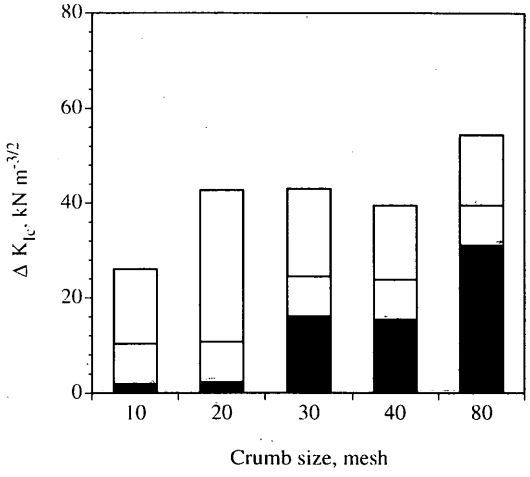

FIGURE 1 Added benefit to the low-temperature fracture toughness of crumb rubber–modified 150-200 Bow River asphalt binders (black, effect of unmodified crumb rubber; white, contribution of 2 percent LPBD; gray, effect of improved interfacial adhesion).

TABLE 6 Fracture Toughness of Devulcanized Rubber Tire–Modified Asphalt Binders

Asphalt	Additive	Modulus (GPa)	K_{Ic} (kN $m^{-3/2}$)
85-100	-	1.35 ± 0.11	44.1 ± 3.9
Ecoflex[a]	10 wt % rubber	1.14 ± 0.17	55.8 ± 6.1
Ecoflex	10 wt % rubber + 1 wt % sulfur	1.15 ± 0.12	66.4 ± 4.6

[a] Product of Bitumar Inc. of Montreal, Quebec.

CONCLUSIONS

Plain 10- or 20-mesh crumb rubber does not improve the low-temperature fracture toughness of a 150-200 penetration grade Bow River binder at additive contents as high as 10 wt percent. The gain in fracture toughness due to interfacial modification in such systems can be very significant.

Plain 30-, 40-, and 80-mesh crumb rubber tire samples increase the fracture toughness of the binder. However, in these samples, an interfacial strengthening can still give substantial improvements.

Whether the results obtained will translate into improved low-temperature thermal stress cracking resistance has to be investigated further with mix tests developed under the Strategic Highway Research Program and in field trials.

A commercially available devulcanized rubber tire–asphalt binder did not show any significant improvement in fracture toughness over that of an unmodified 85-100 Bow River control sample. However, increasing the molecular weight of the rubber through a sulfur vulcanization reaction increased the fracture toughness by 18 percent.

ACKNOWLEDGMENTS

Financial support for this research by the Ontario Ministry of the Environment, the National Science and Engineering Research Council of Canada, and the Ontario Centre for Materials Research is gratefully acknowledged.

The wet-ambiently ground rubber tire sample was provided by M. Rouse of Rouse Rubber Industries, Inc., the ambiently ground rubber sample was provided by S. Montel of Baker Rubber, Inc., and the cryogenically ground rubber samples were provided by R. Kover of Recovery Technologies, Inc. Their assistance is highly appreciated. The devulcanized rubber-asphalt sample was provided by R. Cormier of Bitumar, Inc. His assistance is also appreciated.

REFERENCES

1. McDonald, C. H. A New Patching Material for Pavement Failures. In *Highway Research Record 146*, HRB, National Research Council, Washington, D.C., 1966, pp. 1–16.
2. Schnormeier, R. H. Fifteen-Year Pavement Condition History of Asphalt-Rubber Membranes in Phoenix, Arizona. In *Transportation Research Record 1096*, TRB, National Research Council, Washington, D.C., 1987, pp. 62–67.
3. Lalwani, S., A. Abushihada, and A. Halasa. *Association of Asphalt Paving Technologists*, Vol. 51, 1982, pp. 562–579.
4. Ton, J. S., K. A. Kennedy, M. R. Piggott, and R. T. Woodhams. *Rubber Chemistry and Technology*, Vol. 53, No. 1, 1980, pp. 88–106.
5. Piggot, M. R., W. Ng, J. D. George, and R. T. Woodhams. *Proc., Association of Asphalt Paving Technologists*, Vol. 46, 1977, p. 495.
6. Woodhams, R. T. Methods of Increasing Fracture Toughness of Asphalt Concrete. In *Transportation Research Record 843*, TRB, National Research Council, Washington, D.C., 1982, pp. 21–26.
7. Schnormeier, R. H. *Cold Climate Condition Survey of Asphalt-Rubber Membranes*. Asphalt Rubber Producers Group, Phoenix, Ariz., 1988.
8. Flynn, L. Jury Remains Out on Asphalt-Rubber Use. *Roads and Bridges*, Dec. 1992, pp. 42–50.
9. Hershey, R. L. *Markets for Scrap Tires*. Report EPA/530-SW-90-074A. EPA, Office of Solid Waste, Oct. 1991.
10. Ciesielski, S. K. and R. J. Collins. Current Nationwide Status of the Use of Waste Materials in Hot Mix Asphalt Mixtures and Pavements. In *Use of Waste Materials in Hot-Mix Asphalt*, ASTM STP 1193 (H. F. Waller, ed.), American Society for Testing and Materials, Philadelphia, Pa., 1993.
11. Moore, W. Asphalt Rubber: Potential for Tougher Roads. *Construction Equipment*, Feb. 1991.
12. *Noise Reduction with Asphalt-Rubber*. Asphalt Rubber Producers Group, Phoenix, Ariz., 1988.
13. Huffman, J. E. The Use of Ground Vulcanized Rubber in Asphalt. *ASTM Special Technical Publication 724*, American Society for Testing and Materials, Philadelphia, Pa., 1980, pp. 3–12.
14. Bjorklund, A. Rubber Granules in Wearing Courses. *Proc., IVI World Road Congress*, Vienna, Austria, Sept. 1979.
15. Takallou, H. B., and R. G. Hicks. Development of Improved Mix and Construction Guidelines for Rubber-Modified Asphalt Pavements. In *Transportation Research Record 1171*, TRB, National Research Council, Washington, D.C., 1988, pp. 113–120.
16. McQuillen, J. L., J. F. Member, H. B. Takallou, R. G. Hicks, and D. Esch. Economic Analysis of Rubber Modified Asphalt Mixes. *Journal of Transportation Engineering*, Vol. 114, No. 3, 1988, pp. 259–277.
17. Narusch, F. P. *Alaska Experience with Rubberized Asphalt Concrete Pavements, 1979–1982*. Alaska Department of Transportation and Public Facilities, Juneau, Alaska.
18. Esch, D. C. *Asphalt Pavements Modified with Coarse Rubber Particles—Design, Construction and Ice Control Observations*. Report FHWA-AK-RD-85-07. Federal Highway Administration, U.S. Department of Transportation, 1985.
19. Esch, D. Construction and Benefits of Rubber-Modified Asphalt Pavements. In *Transportation Research Record 860*, TRB, National Research Council, Washington, D.C., 1982, pp. 5–13.
20. Takallou, H. B. *Evaluation of Mix Ingredients on the Performance of Rubber Modified Asphalt Mixtures*. Oregon State University, 1988.
21. Heitzman, M. An Overview of the Design and Construction of Asphalt Paving Materials with Crumb Rubber Additive. Presented at 71st Annual Meeting of the Transportation Research Board, Washington D.C., 1992.
22. Page, G. C., B. E. Ruth, and R. C. West. Florida's Approach Using Ground Tire Rubber in Asphalt Concrete Mixtures. In *Transportation Research Record 1339*, TRB, National Research Council, Washington, D.C., 1992.
23. Joseph, P. E., and G. Kennepohl. *Trial Section with Polymer-Modified Asphalts on Highway 400*. Report PAV-91-03. Ministry of Transportation of Ontario, Downsview, Ontario, Canada, 1991.
24. Joseph, P. E., J. H., Dickson, and G. Kennepohl. Evaluation of Polymer-Modified Asphalts in Ontario. *Proc., Canadian Technical Asphalt Association*, 1992, pp. 243–264.
25. Duong, Q. D. and R. Boisvert. PCT Int. Appl. WO 9317076 A2. Bitumar Inc., Montreal, Quebec, Canada, Sept. 1993.
26. *ECOFLEX, Paving the Way to a Better World*. Bitumar, Inc., Montreal, Quebec, Canada, 1993.
27. Hesp, S. A. M. Ph.D. thesis. University of Toronto, Toronto, Ontario, Canada, 1991.
28. Broek, D. *Elementary Engineering Fracture Mechanics*. Martinus Nijhoff Publishers, The Hague, Netherlands, 1982.
29. Kinloch, A. J., and R. J. Young. *Fracture Behaviour of Polymers*. Elsevier Applied Science, New York, 1983.
30. Scheaffer, R. L., and J. T. McClave. *Probability and Statistics for Engineers*. PWS-Kent Publishing Company, Boston, Mass., 1990.
31. Lee, N. K., and S. A. M. Hesp. Low-Temperature Fracture Toughness of Polyethylene-Modified Asphalt Binders. Presented at 73rd Annual Meeting of the Transportation Research Board, Washington, D.C., 1994.

Publication of this paper sponsored by Committee on Characteristics of Bituminous Materials.

Use of Rubber in Asphalt Pavements: Kansas Experience

GLENN A. FAGER

From 1990 to 1992 eight rubber hot bituminous mix projects were constructed on the Kansas Department of Transportation highway system. Four have been dry and four have been of the wet process. Two projects have been administered through normal bid procedures. Six have been constructed through change orders and negotiated prices. Approximately 616 tons of rubber was used in the hot mix overlays. Preliminary conclusions are as follows: (*a*) From the crack survey results, it is apparent that rubber may not inhibit the development of cracks in the higher-density mixes. However, even though the results are still preliminary, the gap-graded mixes show the greatest potential in reducing the amount of cracking. (*b*) Rubber in a gap-graded mix will prevent asphalt draining off the aggregates during construction. This will allow a thicker film thickness on the aggregates. (*c*) None of the rubber projects have rutted, but neither have the asphalt-only control sections. (*d*) On hot recycle projects, rubber addition rates should be based on the weight of dry virgin aggregate and recycled asphalt pavement. (*e*) Rubber absorbs a large portion of an RA-100 in a hot recycle mix. An AC-5 with rubber will reduce the asphalt absorption and improve the aggregate coating.

In response to a request of the state legislature, the Kansas Department of Transportation (KDOT) started to incorporate ground tire rubber into experimental hot mix overlays in 1990. There were three reasons why KDOT was interested in using ground tires in hot mix:

1. To determine whether it would reduce or retard reflective cracking from old portland cement concrete or bituminous pavements,
2. To determine whether it would reduce the amount of pavement rutting, and
3. To address the environmental concerns over what could be done with old tires.

Over a 2-year period (1990 to 1992), a total of eight projects were constructed. Four have been dry and four have been of the wet process. Two projects have been administered through normal bid procedures. Six have been constructed through change orders and negotiated prices. Test sections were planned on six of the eight projects. However, construction problems on two of the projects limited formal crack surveys to only four projects. Most of the projects allowed KDOT to experiment with mix variations. Standard virgin mixes, new gap-graded mixes, and even recycle mixes were tried on the projects.

The primary method of determining the amount of asphalt and rubber has been the Marshall method (*1*). This is the official mix design method for KDOT and the one most familiar to the field personnel.

Kansas Department of Transportation, 2300 Van Buren, Topeka, Kans. 66611.

Approximately 616 tons of rubber was used in the hot mix experimental overlays. A map of the project locations for the mixes is shown in Figure 1.

HISTORY

KDOT's previous experience with asphalt rubber dates back to five experimental stress-absorbing membrane interlayer (SAMI) projects constructed in 1977, 1978, and 1979. SAMI consists of an asphalt rubber seal coat followed by a hot mix overlay. Stress-absorbing membrane (SAM) is an asphalt rubber seal coat left as the wearing surface. The results of the test sections were variable. On one project the SAMI section had fewer cracks than the control section, on three sections the control section without asphalt rubber performed the best, and one project had nearly the same performance for both sections. The final report stated that none of the projects have an economic justification for the extra cost of using the asphalt rubber.

Sixteen states participated in a pooled fund study conducted by the Texas Transportation Institute (TTI) in 1986. Iowa and Kansas helped finance the study. Numerous asphalt rubber projects constructed throughout the United States were reviewed. A report issued by FHWA in September 1986 (*2*) concluded that the negative performance of some interlayer installations does not appear to be related to fundamental material properties, but to inappropriate use of the materials.

On the basis of the results of our test sections and those of the TTI study, KDOT decided not to construct any more SAM or SAMI test sections, but to continue literature reviews on asphalt rubber. KDOT then decided to construct several asphalt rubber hot mix test sections to determine whether the thicker lifts of asphalt rubber hot mix would perform better than the SAM or SAMI projects.

Two methods are used by KDOT to accomplish the introduction of rubber into the hot mixes. The first is a wet process, and the second is a new dry process.

WET PROCESS

The wet process is the already familiar MacDonald process. Crumb rubber (Type II or III) was shipped in 22.68-kg (50-lb) bags from a tire supplier or the tire grinding facility. The bags were then broken and the rubber conveyed to a mixing tank where hot asphalt at approximately 204°C (400°F) was blended with the ambient temperature rubber. A typical blending ratio of 18 percent rubber and 82 percent AC-5 was used, but a blend ratio of 16/84 was also tried. The combined asphalt-rubber was then pumped to

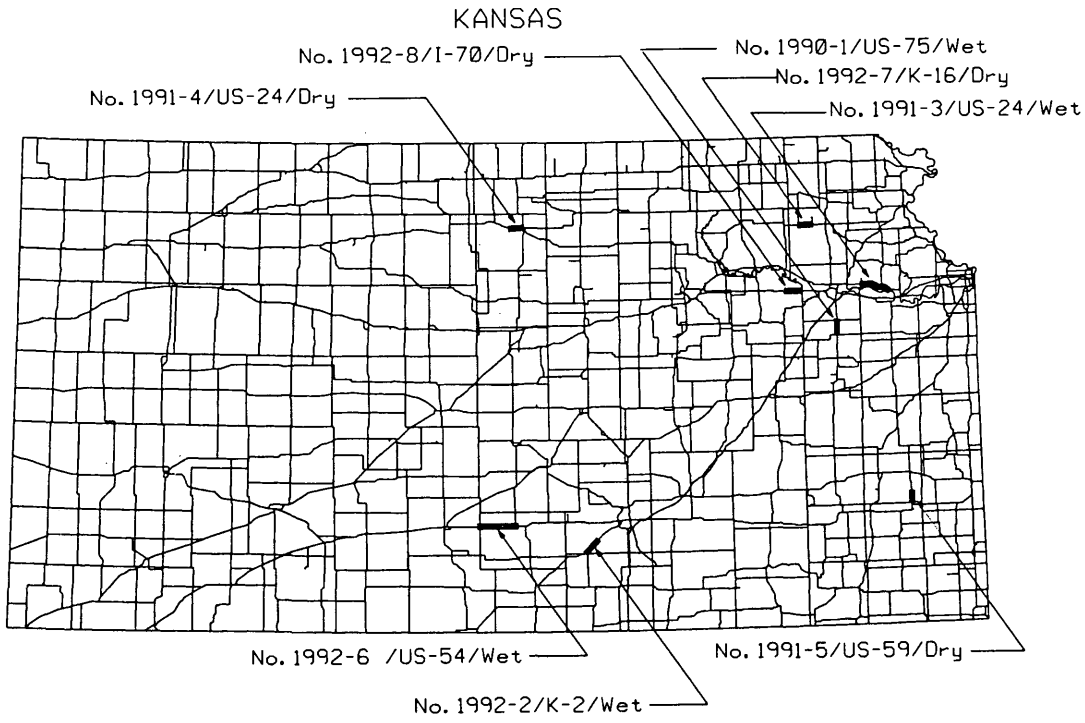

FIGURE 1 KDOT's rubber projects, 1990 to 1992.

another heated tank where the blended material was allowed to "react" for 45 to 90 min at approximately 177°C (350°F).

After the asphalt-rubber had been reacted, the material was metered into the mixing chamber of the asphalt concrete production plant at the percentage required by the job mix formula. Both a batch mix plant and drum-drier mix plant were used in KDOT projects.

Trucks used for hauling the paving mixture were tailgate discharge, dump or moving bottom (horizontal discharge) type and were compatible with the spreading equipment. At no time were bottom dump trucks used on the projects.

Paving was accomplished by a normal self-propelled, mechanical spreading and finishing paver. They were capable of distributing the material to not less than the full width of a traffic lane and to the desired depth.

Compaction equipment conisted of self-propelled rollers equipped with pads and a watering system to prevent sticking of the paving mixture to the steel-tired wheel (drums). At least two rollers were used on the projects. Usually there were three steel rollers available. Pneumatic-tire rollers were hardly ever used because of the increased adhesiveness of the asphalt-rubber binder.

DRY PROCESS

The follow dry process was the only process that KDOT tried as an alternative to the more expensive and previously described MacDonald (wet) process. It is applicable to a double drum plant mixer but was tried later on a drum mixer as well. To date, all of the projects constructed under this process used the UltraFine Rouse rubber or what is commonly referred to as GF-80 rubber.

The process involves the handling of the UltraFine GF-80 rubber in bulk form (versus bags in the wet process) through the use of pressurized truck tankers. The tanker blows the rubber into a storage silo. A gate, located at the bottom of the storage silo, discharges the rubber into a weigh chamber. The weigh chamber continuously measures the weight of the rubber where it can be monitored in the control facility. A vane feeder is also attached to the bottom of the weigh container that will meter the rubber or control the rubber feed rate. The rubber feed rate can be regulated to give the desired rubber mix content at the plant mix production rate. After the vane feeder has metered the ultrafine rubber out of the weigh container, the conveyor or auger system discharges the rubber into the outside mixing chamber of a double drum plant. The rubber is added at the same relative location as the asphalt cement and bag house fines. After hot asphalt is mixed very briefly with the superheated aggregate, the UltraFine GF-80 rubber is fed into the mix. The mix is then completely mixed in the outer barrel of the double drum plant. There is no reaction in that the rubberized asphalt is not held at elevated temperatures for 45 to 90 min.

The mix is discharged from the plant and handled in a manner similar to any other mix operation. Typically, steel rollers are used instead of pneumatic rollers because of the increased potential of rubber in the mat to stick to the rubber tires of the pneumatic rollers.

HOT MIX PROJECTS, 1990

Two 1990 projects were located on US-75 south of Topeka and on K-2 southwest of Wichita. The Topeka project (Figure 1, No. 1990-1) was constructed over an old portland cement concrete pavement, and the Wichita project (Figure 1, No. 1990-2) was

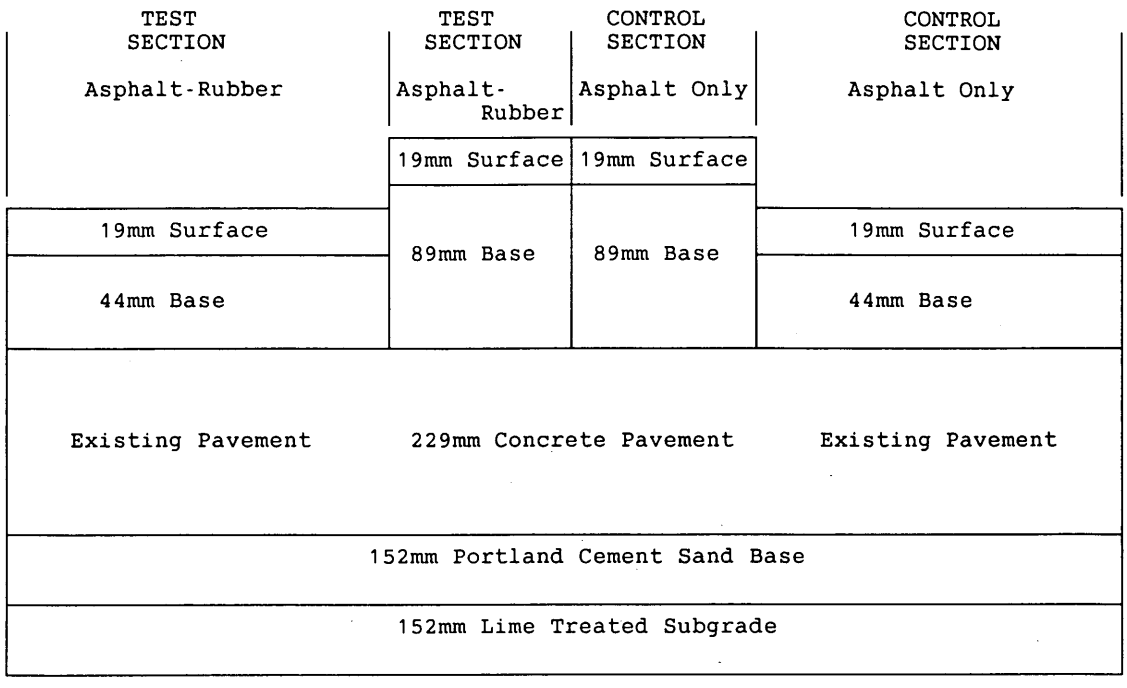

FIGURE 2 Location of test sections, US-75, Osage County (No. 1990-1).

placed over an old bituminous pavement. These were not highly experimental projects involving a great amount of testing. International Surfacing, Inc., of Phoenix, Arizona, was the subcontractor and did the preliminary mix design. The sections were constructed using their guide specifications and appropriate items from KDOT's standard specifications.

No. 1990-1, US-75, Wet

The Topeka project began about 8.1 km (5 mi) south of Topeka and continued south into Osage County. The test and control sections were located in the two northbound lanes and are shown in Figure 2. The two thicker sections were 0.8 km (0.5 mi) long and received two base course lifts of 44-mm (1.75-in.) BM-1B and one lift of a 19-mm (0.75-in.) BM-1T, for a total thickness of 108 mm (4.25 in.) over the old PCCP. The two thinner sections, each 1.61 km (1 mi), received one lift of 44-mm (1.75-in.) BM-1B and one lift of 19-mm (0.75-in.) BM-1T, a total thickness of 64 mm (2.5 in.). The rest of the project was constructed 64 mm (2.5 in.) thick as shown in the thin section. The 1989 traffic count on this four-lane roadway was 6,610 AADT.

The BM-1B base course had gradation limits as given in Table 1. This mix is predominately a crushed limestone mix that has been used for the last 2 years to reduce rutting. Most of the time the mix has been placed approximately 38 mm (1.5 in.) thick. The 19-mm (1.5-in.) BM-1T surface course is normally used for skid resistance on overlay projects for roadways with greater than 5,000 vehicles per day. It contains approximately 50 percent crushed limestone with 40 percent chat for skid resistance. Table 1 presents its gradation limits. The same two mixes were used on the Wichita project. The asphalt-rubber was placed using a drum

TABLE 1 Virgin Mix Gradations

MIX DESIGNATION	PERCENT RETAINED-SQUARE MESH SIEVES									
	19mm	12.5mm	9.5mm	4.75mm	2.36mm	1.18mm	600um	300um	150um	75um
BM-1B	0	0-10	12-26	39-56	60-76	72-87	79-92	84-95	88-98	92-98
BM-1T		0	0-14	39-56	57-72	70-85	78-91	84-94	87-97	92-98
BM-Gap Experimental		0	8-22	71-83	81-91	84-94	87-95	91-97	92-98	94-98
BM-2A	0		6-21	23-40	38-56		61-78			91-97

mix plant, in which the contractor had a new pipe installed in the drum near the existing asphalt supply line.

No. 1990-2, K-2, Wet

On the project located approximately 21 km (13 mi) southwest of Wichita, asphalt-rubber hot mix was placed near Viola. Shown in Figure 3 are the typical sections consisting of 57 mm (2.25 in.) of BM-1B and 19 mm (0.75 in.) of BM-1T, for a total of 76 mm (3.0 in.). The thinner sections consisted of 38 mm (1.5 in.) of BM-1B and 19 mm (0.75 in.) of BM-1T, for a total of 57 mm (2.25 in.).

The existing bituminous pavement had numerous transverse, longitudinal, and block cracks. Many of the transverse cracks had secondary cracks. Generally, there were slight depressions associated with the secondary cracks. Most of the roadways were on a straight alignment and flat grade.

Tables 2 and 3 present the cost data of these short experimental test sections.

HOT MIX PROJECTS, 1991

Because of the high cost of the construction of the 1990 small 2.4-km (1.5-mi) test sections, a larger and complete asphalt-rubber overlay was constructed. The principal idea was to determine whether the volume of material and the normal state competitive bidding procedures would reduce the overall cost.

No. 1991-3, US-24, Wet

The wet process was used and the design was again completed by the subcontractor (International Surfacing, Inc.). The subcontractor also accomplished the blending and reacting of the asphalt-rubber. As in the 1990 projects, a BM-1T mix was used on most of the project. However, two test sections, each 1 mi, were also designed and constructed after the total project had been awarded to the successful bidder. One of the test mixes was gap graded as indicated in Table 1. The aggregate gradation increased the voids in the mineral aggregate, which in turn allowed room for more asphalt-rubber into the mix.

The second test mix on this project was a normal BM-1T but with asphalt-rubber. This mix was also constructed on the rest of the project. A control section was constructed with a BM-1T mix using only asphalt as the binder. The location of the third project is indicated in Figure 1 (No. 1991-3). Table 4 gives a description of the aggregate, binder content, and cost data. Approximately 18.8 km (11.7 mi) of a 25-mm (1-in.) overlay was constructed on US-24 in Jefferson and Douglas counties.

As indicated in Table 4, costs still remain high, and competitive bidding on larger quantities did not appreciably reduce the cost of the overall mix. Therefore, to reduce the cost and still incorporate rubber directly into the mix, a proposal from a contractor was approved to experiment with the use of crumb rubber as an aggregate (dry process). The contractor owned a double drum counterflow hot mix plant, and the rubber could be fed so that it would not blow out with the exhaust. The ultrafine rubber was shipped from Mississippi and stored in a plant silo. When the plant was operating, the rubber was fed through a vane feeder to approximately the same location where recycled asphalt pavement (RAP) would be introduced into the plant.

No. 1991-4, US-24, Dry

Three test sections and one control section were constructed as indicated in Figure 1 (No. 1991-4). This was the fourth crumb rubber project but the first using the new dry method. Even though

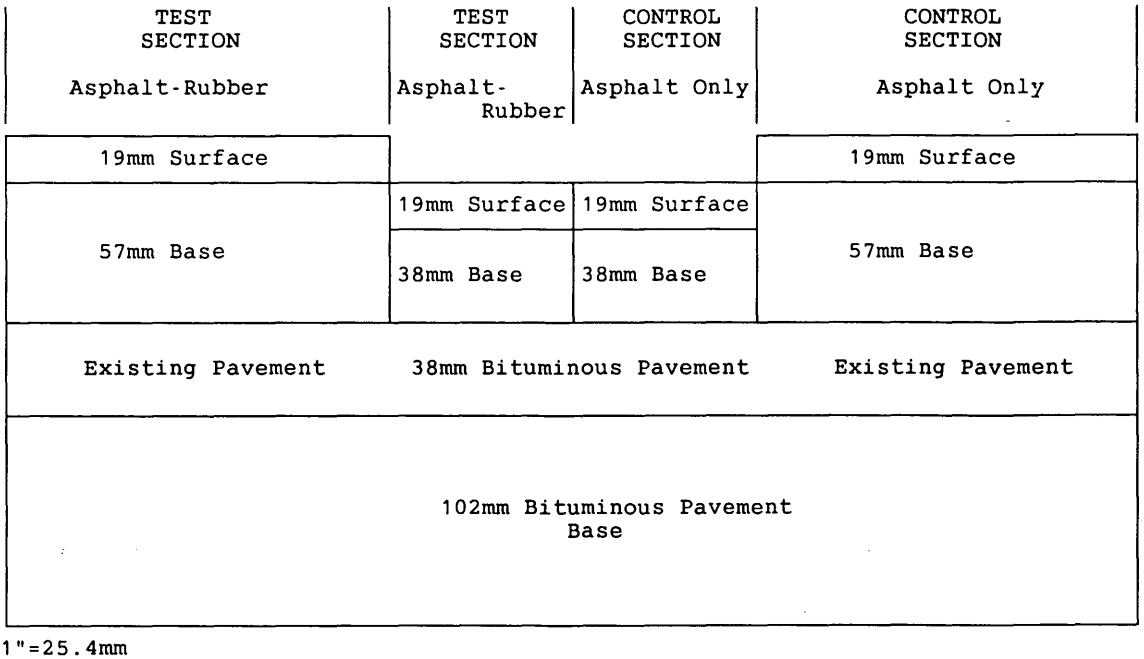

FIGURE 3 Location of test sections, K-2, Sedgwick County (No. 1990-2).

TABLE 2 Mix and Cost Data, US-75, Osage County (No. 1990-1), Wet Process

MIX	DESCRIPTION	BINDER CONTENT (AGGREGATE BASED) (%)	COST DATA (MIX) ($/TON)
BM-1B	Asphalt Only 85% Crushed Limestone 15% Sand	4.75% AC-10	17.09
BM-1B	Asphalt-Rubber 85% Crushed Limestone 15% Sand	6.16% ACR 16% Type III Rubber 84% AC-5	46.18
BM-1T	Asphalt Only 47% Crushed Limestone 40% Chat (Mine Tailings) 13% Sand	5.5% AC-10	19.97
BM-1T	Asphalt-Rubber 47% Crushed Limestone 40% Chat (Mine tailings) 13% Sand	6.3% ACR 16% Type III Rubber 84% AC-5	49.22

TABLE 3 Mix and Cost Data, K-2, Sedgwick County (No. 1990-2), Wet Process

MIX	DESCRIPTION	BINDER CONTENT (AGGREGATE BASED) (%)	COST DATA (MIX) ($/TON)
BM-1B	Asphalt Only 75% Crushed Limestone 25% Sand	5.0% AC-20	17.60
BM-1B	Asphalt-Rubber 75% Crushed Limestone 25% Sand	6.6% ACR 18% Type II Rubber 82% AC-5	44.64
BM-1T	Asphalt Only 36% Crushed Limestone 40% Chat (Mine tailings) 24% Sand	5.75% AC-20	19.64
BM-1T	Asphalt Rubber 36% Crushed Limestone 40% Chat (Mine tailings) 24% Sand	7.4% ACR 18% Type II Rubber 82% AC-5	49.45

TABLE 4 Mix and Cost Data, US-24, Jefferson County (No. 1991-3), Wet Process

MIX	DESCRIPTION	BINDER CONTENT (AGGREGATE BASED) (%)	COST DATA (MIX) ($/TON)
BM-1T	Asphalt Only 45% Crushed Limestone 40% Chat (Mine tailings) 15% Sand	5.25% AC-10	21.05
BM-1T	Asphalt-Rubber 45% Crushed Limestone 40% Chat (Mine tailings) 15% Sand	6.9 18% Type II Rubber 82% AC-5	48.97
BM-Gap Graded	Asphalt-Rubber 60% Crushed Limestone 40% Chat (Mine Tailings)	8.9% AC-10 18% Type II Rubber 82% AC-5	57.71

the rubber was added separately to the mix, it was designed as part of the liquid binder. A 10 percent asphalt-rubber mix was computed as 10 parts rubber (by weight) to 90 parts asphalt.

No major problems were encountered with the rubberized asphalt overlay. The mix was a 51-mm (2-in.) KDOT BM-2A (low traffic surface course) laid over a milled surface.

Table 5 gives the data on the cost of the asphalt mix and three rubberized asphalt mixes, excluding mobilization. Because of the relatively small quantity of rubber used on the project, the mobilization cost was a major expense. If the project had been larger with a greater utilization of rubber, the cost of mobilization would have been less significant. Also, in Table 5, the mix cost excludes

TABLE 5 Mix and Cost Data, US-24, Mitchell County (No. 1991-4), Dry Process

MIX	DESCRIPTION	BINDER CONTENT (AGGREGATE BASED) (%)	COST DATA (MIX) ($/TON)
BM-2A	Asphalt Only 66% Crushed Limestone 34% Sand	5.25% AC-10	20.22
BM-2A (3 Binder Contents)	Asphalt-Rubber 66% Crushed Limestone 34% Sand	5.5% ACR 5% Ultra Fine Rubber 95% AC-10	21.96
		5.5% ACR 7.5% Ultra Fine Rubber 92.5% AC-10	22.70
		5.5% ACR 10% Ultra Fine Rubber 90% AC-10	23.44

all other indirect costs such as tack coats, stripping, and so forth. The effect of these indirect costs would be relatively small.

No. 1991-5, US-59, Dry

The fifth project continued experimentation with the new dry process. The project was a hot mix recycle that was started in 1991 but not finished until 1992 (Figure 1, No. 1991-5). The project was the first attempt to introduce rubber into a hot recycle mix by this process. Previous KDOT products using the fine rubber involved virgin aggregates with a viscosity-graded asphalt cement.

This project was originally set to add the fine rubber to both a 30 percent RAP/70 percent virgin aggregate mix and 50 percent RAP/50 percent virgin aggregate. Both mixes would have control sections where no rubber would be added. The plan was to build a total of five test sections and two control sections.

As in the previous dry process, the rubber was added directly into the mix with no preblending or reacting with the liquid asphalt. The amount of rubber to be added was calculated as a percentage of the total liquid binder (asphalt added plus asphalt in the RAP). This calculation could also be expressed as a blend ratio. A 10 percent asphalt-rubber mix blend ratio was computed as 10 parts rubber (by weight) to 90 parts asphalt. Using this example for the asphalt-rubber recycle mixes, the 90 parts asphalt would include the asphalt added at the plant plus the asphalt in the RAP. If more asphalt was added at the plant, more rubber needed to be added to comply with the overall blend ratio.

The project was complicated further by the fact that two different additives were used for the two different mixes. An AC-5 was used in the 30/70 mix, and an RA-100 asphalt rejuvenator was added to the 50/50 mix.

Construction began during late fall 1991. The existing 3.35-m (11-ft) road was first milled to a depth of 38 mm (1.5 in.). Bituminous shoulders were extended 0.46 m (1.5 ft) at a depth of 114 mm (4-1/2 in.), which widened the total roadway to 9.1 m (30 ft). Cold weather prevented completion of the project, but a 38-mm (1.5-in.) lift of the control and test sections was finished before winter shutdown. Severe raveling occurred on the first lift, but it was uncertain whether this was due to the rubber in the mix or the cool weather at the time of construction. The surface was "smoke coated" with a diluted asphaltic emulsion by state maintenance forces. This was to control the raveling and keep the wheelpaths from "shelling out."

During the winter, a decision was made to increase the binder content to counteract the effects of the raveling. Also, construction would first be completed on other portions of the project so that the top and final lift would be constructed during warmer months of the construction season.

The 30 percent RAP/70 percent virgin test and control sections were constructed without any major problems. The rubber asphalt content was increased beyond what was originally recommended, and this appeared to help reduce the tendency of the mix to ravel. The mix appeared to be tender and was somewhat difficult to compact. The section with 10 percent rubber looked better and had better workability.

Major problems occurred in the 50/50 mix. When the rubber asphalt was increased, the rubber had to be substantially increased to maintain the overall blend ratio. The resulting mix still appeared to be dry and would not adhere to the aggregates. Apparently the additional rubber absorbed the RA-100 and prevented proper coating of the aggregates. Various percentages of additives were tried in the southbound lane, but none proved effective. Finally, a tanker load of AC-5 was ordered and used in the opposite lane the following day. This proved to be much more effective in coating the aggregates. The 50/50 mix had to use an AC-5 instead of an RA-100 to finish the test sections.

If rubber is to be added in a hot recycle project, it should not be tied to the total asphalt content as a blend ratio. It should be based on the weight of RAP and virgin aggregate (i.e., 10 lb rubber per ton of virgin aggregate and RAP). The percentage of new asphalt could then be increased or decreased without affecting the rate of rubber utilization. Estimated quantities would be more accurate and production yield rates would be more manageable.

HOT MIX PROJECTS, 1992

In 1992 the hot recycle project on US-59 in Allen County was completed. Three additional rubber projects were completed, bringing the number of KDOT rubber projects to eight. Initial crack survey results on the 1990 and 1991 projects indicated that the gap-graded mix may prove more beneficial with regard to pavement cracking. Therefore, two more rubber projects were constructed using a gap-graded mix.

No. 1992-6, US-54, Wet

The sixth project used the wet process. Competitive bids were received on a 29.8-km (18.5-mi) project on US-54 in Kingman County (Figure 1, No. 1992-6). This project did not contain any test or control sections. The mix on this project was designed and the binder reacted by International Surfacing, Inc. Costs were still high compared with a normal paving grade asphalt cement.

No. 1992-7, K-16, Dry

The seventh project (Figure 1, No. 1992-7), incorporating a gap-graded mix and a BM-1B mix, used the double-drum dry process. Prices were again negotiated and several test sections built. The method of determining rubber content on this project was changed and based on weight of dry aggregate. The asphalt cement and rubber were varied independently of each other. The three test sections and control section of the BM-1B mix were built with increased amounts of asphalt or rubber.

Three test sections and one control section were also built using the gap gradation as previously described. The 0.8-km (0.5-mi) control section contained asphalt without rubber. Severe problems were encountered with the gap-graded asphalt-only mix. The asphalt would drain down from the aggregates and stick to the truck beds. When rubber was added to the mix this "drain down" problem was substantially reduced. This mix very closely resembled a stone mastic asphalt (SMA) mix gradation. The major difference was that rubber (instead of fibers in an SMA mix) was used to control the amount of binder runoff of the aggregate. This allowed a thick asphalt-rubber film coating of the aggregates. Table 6 gives the mix and cost data of the control and test sections.

TABLE 6 Mix and Cost Data, K-16, Jackson County (No. 1992-7), Dry Process

MIX	DESCRIPTION	BINDER CONTENT (AGGREGATE BASED) (%)	COST DATA (MIX) ($/TON)
BM-1B	Asphalt Only 80% Crushed Limestone 20% Sand	5.5% AC-10	17.67
BM-1B (3 Binder Contents)	Asphalt Rubber 80% Crushed Limestone 20% Sand	5.0% AC-10 1.0% Ultra Fine Rubber	24.27
		6.0% AC-10 1.0% Ultra Fine Rubber	24.79
		7.0% AC-10 1.0% Ultra Fine Rubber	25.29
BM-Gap Graded	Asphalt Only 100% Crushed Limestone	6.0% AC-10	20.55
BM-Gap Graded (3 Binder Contents)	Asphalt-Rubber 100% Crushed Limestone	8.0% AC-10 1.0% Ultra Fine Rubber	28.30
		8.0% AC-10 1.5% Ultra Fine Rubber	31.59
		8.5% AC-10 1.5% Ultra Fine Rubber	31.80

TABLE 7 Crack Survey, US-75, Osage County (No. 1990-1)

	TRANSVERSE CRACKING (PERCENT OF ORIGINAL)			
	THIN OVERLAY		THICK OVERLAY	
SURVEY DATE (Mo/Day/Yr)	CONTROL SECTION (Asphalt Only) 19mm Surface BM-1T 44mm Base BM-1B	TEST SECTION (Asphalt-Rubber) 19mm Surface BM-1T 44mm Base BM-1B	CONTROL SECTION (Asphalt Only) 19mm Surface BM-1T 89mm Base BM-1B	TEST SECTION (Asphalt-Rubber) 19mm Surface BM-1T 89mm Base BM-1B
6-20-1990	0 (Construction)	0 (Construction)	0 (Construction)	0 (Construction)
10- 4-1990	0	0	0	0
1-17-1991	31	47	1	10
5- 2-1991	34	62	5	27
10- 3-1991	31	62	3	25
5-21-1992	50	62.3	4	39
10- 6-1992	39	58.5	3	34
4-16-1993	58	70.7	23	40

1" = 25.4mm

TABLE 8 Crack Survey, K-2, Sedgwick County (No. 1990-2)

SURVEY DATE (Mo/Day/Yr)	TOTAL CRACKING (PERCENT OF ORIGINAL)			
	THIN OVERLAY		THICK OVERLAY	
	CONTROL SECTION (Asphalt Only) 19mm Surface BM-1T 38mm Base BM-1B	TEST SECTION (Asphalt-Rubber) 19mm Surface BM-1T 38mm Base BM-1B	CONTROL SECTION (Asphalt Only) 19mm Surface BM-1T 57mm Base BM-1B	TEST SECTION (Asphalt-Rubber) 19mm Surface BM-1T 57mm Base BM-1B
8-29-1990	0 (Construction)	0 (Construction)	0 (Construction)	0 (Construction)
10-31-1990	0	0	0	0
1-18-1991	0	0	0	.4
10- 2-1991	0	0	0	.2
5- 1-1992	.4	5.6	0	1.6
12- 2-1992	3.4	6.4	.4	2.9
5- 4-1993	28.5	32.1	10.2	24.8

1" = 25.4mm

No. 1992-8, I-70, Dry

The last project was constructed on I-70 in Wabaunsee County (Figure 1, No. 1992-8). The project was built late in the construction season. The contractor was willing to try to use a normal drum mixer instead of a double drum mixer, incorporating the ultrafine rubber into the mix. Rubber was again vane fed out the silo but air blown into a coater placed at the discharge end of a drum mixer. The rubber was not introduced into the mix inside the drum dryer, where the hot gases could remove the fine rubber from the mixing chamber.

PRELIMINARY RESULTS

Even though it is too early to evaluate the final performance of the rubber projects, the following preliminary conclusions are presented:

1. Tables 7 through 10 give the crack survey results to date on several of the projects. From these results it is apparent that rubber may not inhibit the development of cracks in the higher-density mixes. Even though the results are still preliminary, the gap-graded mixes show the greatest potential in reducing the amount of cracking.

TABLE 9 Crack Survey, US-24, Jefferson County (No. 1991-3)

SURVEY DATE (Mo/Day/Yr)	TOTAL CRACKING (PERCENT OF ORIGINAL)		
	CONTROL SECTION 25mm Surface BM-1T (5.25% Asphalt Only)	TEST SECTION 25mm Surface BM-1T (6.9% Asphalt-Rubber)	TEST SECTION 25mm Surface Gap Graded (8.9% Asphalt-Rubber)
5-30-1991	0 (Construction)	0 (Construction)	0 (Construction)
10- 3-1991	.7	0	0
5-21-1992	18.7	3.0	0
10- 6-1992	15.4	2.8	.3
4-19-1993	71.3	30.9	0
10-27-1993	49.2	12.8	0

1" = 25.4mm

TABLE 10 Crack Survey, US-24, Mitchell County (No. 1991-4)

SURVEY DATE Mo/Day/Year	TOTAL CRACKING (PERCENT OF ORIGINAL)			
	CONTROL SECTION (Asphalt Only)	TEST SECTION (95% Asphalt) (5% Fine Rubber)	TEST SECTION (92.5% Asphalt) (7.5% Fine Rubber)	TEST SECTION (90% Asphalt) (10% Fine Rubber)
5-28-1991	0 (Construction)	0 (Construction)	0 (Construction)	0 (Construction)
12- 5-1991	38.5	87.8	70.4	21.3
7-30-1992	47.7	87.4	73.5	41.7
7-19-1993	91.4	131.1	99.6	86.1

1" = 25.4mm

2. Rubber in a gap-graded mix will prevent asphalt draining off the aggregates during construction. This will allow thick film on the aggregates and help retard the tendency of the mix to stick to truck beds, and so forth.

3. None of the rubber projects have rutted, but neither have the asphalt-only control sections.

4. On hot recycle projects using the dry process, rubber addition rates should be based only on the weight of dry virgin aggregates and RAP.

5. Rubber and RA-100 are very reactive in a hot recycle mix. Rubber appears to absorbed most of the RA-100, thereby causing a dryer than normal mix. An AC-5 with rubber will reduce the asphalt absorption and improve aggregate coating.

REFERENCES

1. *Mix Design Methods for Asphalt Concrete.* MS-2. The Asphalt Institute, Lexington, Ky., 1984.
2. *Investigation of Materials and Structural Properties of Asphalt-Rubber Paving Mixtures.* Final report. FHWA RD-86/027. Federal Highway Administration, U.S. Department of Transportation, Sept. 1986.

Publication of this paper sponsored by Committee on Characteristics of Nonbituminous Components of Bituminous Paving Mixtures.

Evaluation and Characterization of a Rubber-Modified Hot Mix Asphalt Pavement

DOUGLAS I. HANSON, KEE Y. FOO, ELTON RAY BROWN, AND ROBERT DENSON

The Intermodal Surface Transportation Efficiency Act of 1991 placed a minimum utilization requirement for recycled rubber in hot mix asphalt (HMA) on the state departments of transportation (DOTs). Each state DOT is required to use a minimum percentage of recycled rubber each year starting in FY 1994. As state DOTs gear toward incorporating recycled rubber materials, there is a need to evaluate the effect of the recycled rubber materials on the performance of asphalt pavement. In 1991 Mississippi placed a conventional HMA (control) along with a rubber-modified HMA (RMHMA) test section. Crumb rubber was incorporated into the pavement using a recent wet process technology known as the continuous process developed by Rouse Rubber Industries. This process blends the fine powdered crumb rubber, which passes a 236-μm (No. 80 sieve) screen and has a 75-μm (No. 200 sieve) mean particle size, with asphalt cement. The laboratory properties of the control HMA and the RMHMA were evaluated at various times for the first 2 years of the pavement's life. At the same time, the in-place performance of the two sections was also observed. The control HMA and RMHMA were subjected to a testing program that included tests to evaluate permanent deformation, indirect tensile strength, resilient modulus, gyratory properties, voids in total mix, and bulk densities. Laboratory test results indicated that the RMHMA mix has lower water susceptibility and higher tensile strength and resilient modulus. The gyratory properties and creep/permanent deformation tests indicate that the RMHMA mix should be more resistant to rutting. In-place performance was evaluated by visual observation of surface cracking and rut measurement for the first 2 years of the pavement's life. There was no cracking in either the control or the RMHMA test section. The amount of rutting was insignificant and was likely caused by densification of the mixes.

Recycling waste materials serves a much needed purpose of eliminating an expensive and environmentally unacceptable disposal problem for those products. One waste product showing promise in asphalt mixtures is processed rubber that has been retrieved from the recycling of waste passenger car and truck tires.

The environmental risks associated with land-filling tires and the possibility of incorporation of recycled rubber into asphalt pavements have brought about action at the state and national levels. By 1992, 44 states had drafted, introduced, or enacted laws or regulations to address the scrap tire problem (*1*). Section 1038 of the Intermodal Surface Transportation Efficiency Act of 1991 placed a minimum utilization requirement by stating the following:

> The minimum utilization requirement for asphalt pavement containing recycled rubber as a percentage of the total tons of asphalt laid in such State and financed in whole or part by any assistance pursuant to title 23, United States Code, shall be (*a*) 5 percent for the year 1994; (*b*) 10 percent for the year 1995; (*c*) 15 percent for the year 1996; and (*d*) 20 percent for the year 1997 and each year thereafter.

In June 1993 the Department of Transportation and the Environmental Protection Agency delivered to the Congress their report (*2*) containing guidelines on the use of rubber in hot mix asphalt (HMA). As state departments of transportation incorporate recycled rubber materials, there is a need to evaluate the laboratory properties and performance of rubber-modified HMA (RMHMA) mixes.

The primary objectives of this study were (*a*) to evaluate the properties of a control (conventional) HMA and an RMHMA immediately after construction and at various times during the first 2 years of the pavement's life and (*b*) to compare these laboratory properties with observed in-place performance.

In September 1991 a section of conventional HMA along with a section of RMHMA were placed on US-82 east of Columbus, Mississippi. At the time of construction, materials (aggregate, asphalt cement, and modified binder) were obtained for preparing laboratory specimens. Field cores were taken from the control and RMHMA pavement sections before opening to traffic and 3, 6, 9, 12, and 24 months after opening. Rutting was measured at each sampling interval. The laboratory specimens and field cores were tested to determine properties including permanent deformation, indirect tensile strength, resilient modulus, gyratory stability index (GSI), gyratory elastoplastic index (GEPI), gyratory shear (S_G), and physical properties such as voids in total mix and bulk densities.

The recycled rubber materials (CRM) were mixed with the asphalt cement using the continuous wet process developed by Rouse Rubber Industries. The CRM is finely powdered and passes a 236-μm (No. 80 sieve) screen and has a 75-μm (No. 200 sieve) mean particle size with a high surface morphology (pamphlets distributed by Rouse Rubber Industries, Inc., Vicksburg, Mississippi). Five percent of CRM by weight of asphalt cement was continuously blended with an AC-30 to produce the rubber-modified binder.

The rubber-modified binder may improve the binder and mix properties of the RMHMA mix, which should lead to better field performance. However, relationships between laboratory test results and field performance may not be accurate, especially for RMHMA, where little experience is available in correlating laboratory properties with field performance and there are many variables in the incorporation of the CRM into the asphalt.

D. I. Hanson, K. Y. Foo, and E. R. Brown, National Center for Asphalt Technology, 211 Ramsay Hall, Auburn University, Auburn, Ala. 36849-5354. R. Denson, Mississippi Department of Transportation, P.O. Box 1850, Jackson, Miss. 39215-1850.

LITERATURE REVIEW

Binder Properties

When CRM is reacted with asphalt cement, a thick, elastic, viscous, and adhesive material called rubber-modified binder is formed. The elastic quality is caused by the mechanical action of the unreacted rubber particles performing as elastic aggregate (pamphlets distributed by Rouse Rubber Industries, Inc., Vicksburg, Mississippi). The absorbing of aromatic oil from the asphalt cement into the polymer chain of the CRM increases the viscosity of rubber-modified binder, resulting in lower penetration values and higher absolute and kinematic viscosity. The rubber-modified binder produced by the traditional McDonald process also has a higher softening point and lower temperature susceptibility (*3–7*). The swelling of the CRM (when aromatic oil is absorbed) increases the adhesive property of the rubber-modified binder. Bissada and Anani (*4*) studied the adhesion properties of a rubber-modified binder on one type of aggregate using the boiling test and adding a 12-hr dynamic immersion test to intensify the moisture effect. Visual examination of the percentage stripping of the coated aggregate particles indicated that aggregates coated with rubber-modified binder retained 80 percent of their coating. Aggregates coated with asphalt cement retained only 20 percent of their coating.

Mix Properties

Marshall Design Mix Properties

The optimum binder content for an RMHMA will generally be higher than that for a conventional HMA. This is because the rubber-modified binder is more viscous, the film coating on aggregate is thicker, and the rubber-modified binder contains some unreacted solid rubber particles, which increases the binder volume. The optimum binder content of an RMHMA mixture increases with the CRM/asphalt ratio in the binder. The increase is proportional to the amount of CRM in the binder. As the CRM/asphalt cement ratio increases in the binder, the bulk densities of mixture at optimum binder content increase to a maximum and then decrease (*4*).

In general, an RMHMA has a lower Marshall stability and a higher Marshall flow than a conventional HMA (*8,9*). The Marshall stability of RMHMA mix has been shown to decrease by as much as 60 percent and the Marshall flow of RMHMA mix has been shown to increase by as much as 4.2 times the control mix. The gradation of CRM used in the rubber-modified binder also has an influence on mix stability and flow. RMHMA modified with coarse rubber particles has lower stability and higher flow than RMHMA modified with fine rubber particles. A mix modified with a coarse rubber gradation has been shown to have 49 percent lower Marshall stability and 50 percent higher Marshall flow than a mix modified with fine rubber gradation (*8*).

Fatigue Resistance

On the basis of laboratory tests, the fatigue resistance of RMHMA is better than conventional HMA. Piggott and Woodhams (*9*) concluded that adding 5 percent CRM to HMA will probably increase the fatigue resistance of a pavement to twice that of a conventional asphalt mix. Vallerga et al. (*10*) studied the fatigue resistance of one type of rubber-modified binder (77 percent asphalt cement, 3 percent oil extender, and 20 percent rubber). Specimens were fabricated at different rubber-modified binder contents: ARC-Low (4.23 percent binder), ARC-Medium (4.73 percent binder), and ARC-High (5.23 percent binder). The control specimens had 4.8 percent asphalt content. These specimens were tested at temperatures ranging from 34°F to 104°F. The researchers found that the fatigue performance of RMHMA mixes was improved at higher rubber-modified binder contents. They compared the fatigue performance of RMHMA mixes with that of the control mix and found that, at temperatures less then 60°F, all RMHMA mixes except the mix with the lowest binder content (ARC-Low with 4.23 percent binder) performed better than the control mix. At temperatures greater than 60°F, all RMHMA mixes performed better than the control mix.

Resilient Modulus

Jimenez (*11*) showed that the resilient modulus of RMHMA mixes is about 75 percent of the control mixes. Vallerga et al. (*10*) showed that the resilient modulus of RMHMA mixes is lower than that of conventional mixes but only at low temperatures (below 75°F). At temperatures higher than 75°F, the resilient modulus of RMHMA mixes is higher than that of conventional mixes.

Vallerga et al. (*10*) found that RMHMA mixes with fine CRM have higher resilient modulus values than mixes modified with coarse CRM. RMHMA mixes with higher CRM content have lower resilient modulus values (*11–13*). For the 2 percent CRM content, the resilient modulus values increased as the CRM became finer, but for the 3 percent CRM content, the resilient modulus values reached maximum at the medium CRM content. This indicates that at a low CRM content, the fine CRM may have a more significant effect on the resilient modulus of the mixes.

Jimenez (*11*) studied the effect of adding an extra 2 percent fine CRM to three RMHMA mixes whose CRM contents were 2.5, 3, and 3.5 percent. The resilient modulus of all three RMHMA mixes were increased when an extra 2 percent fine CRM was added. The greatest improvement occurred at 3.5 percent CRM content, which showed an increase of about 60 percent.

Creep and Permanent Deformation

The work by Stephens (*12*) indicates that the RMHMA mixes investigated have lower static creep resistance than conventional asphalt mixes. This difference is more pronounced at higher test temperatures. Stephens also found that mixes with fine CRM gradation have better creep resistance than mixes with a coarse CRM gradation. However, test results from dynamic creep testing indicate that RMHMA mixes have higher resistance to permanent deformation than conventional HMA mixes (*10,12*). These studies showed that under constant load the RMHMA mix deforms more than the control mix, whereas under repeated load the RMHMA mix deforms less than the control mix.

TEST PLAN

A control HMA along with an RMHMA was placed on US-82 east of Columbus, Mississippi, in September 1991. This study was

conducted to evaluate the properties of the control and RMHMA mixture during the first 2 years of traffic and compare those laboratory properties with observed in-place performance. The following test plan was established for this study.

Loose samples of materials used during the construction of the control HMA and RMHMA on US-82 east of Columbus, Mississippi, were obtained. A laboratory testing program was carried out to evaluate the materials (Figure 1).

Samples of the in-place pavement (cores) were taken at various times after construction: 0, 3, 6, 9, 12, and 24 months. The 9-month cores were taken to monitor the density of the control and RMHMA pavement sections. Only permanent deformation and gyratory recompaction testing was conducted on the 9-month cores. At the discretion of the sponsoring agency, only a limited number of 24-month cores (7 control cores and 13 RMHMA cores) were taken. Therefore, the gyratory recompaction test was not performed, and only a limited number of bulk density, indirect tensile, rice density, resilient modulus, and creep tests were conducted. In addition, the amount of rutting in the control and RMHMA pavement sections was measured at each time interval when field cores were taken.

TEST RESULTS OF LABORATORY-PREPARED SAMPLES

Mix Design Information

The mix designs for the control and the RMHMA pavement sections in Columbus, Mississippi, were performed by the Mississippi State Highway Department (MSHD). The control and RMHMA pavement sections have the same aggregate type and gradation (Table 1). Using the 4 percent air voids criteria, the optimum binder content of the control section (6.6 percent) would be higher than the optimum binder content (6.3 percent) of the RMHMA section. No reason was given for the higher optimum asphalt content for the RMHMA mix. However, MSHD indicated that both the control and RMHMA section were constructed at 6.3 percent binder content.

Loose samples of construction materials (aggregate, asphalt cement, and preblended rubber-modified binder) were obtained. The aggregate was batched according to the job mix formula (Table 1) to prepare 14 samples (7 control and 7 RMHMA samples). The

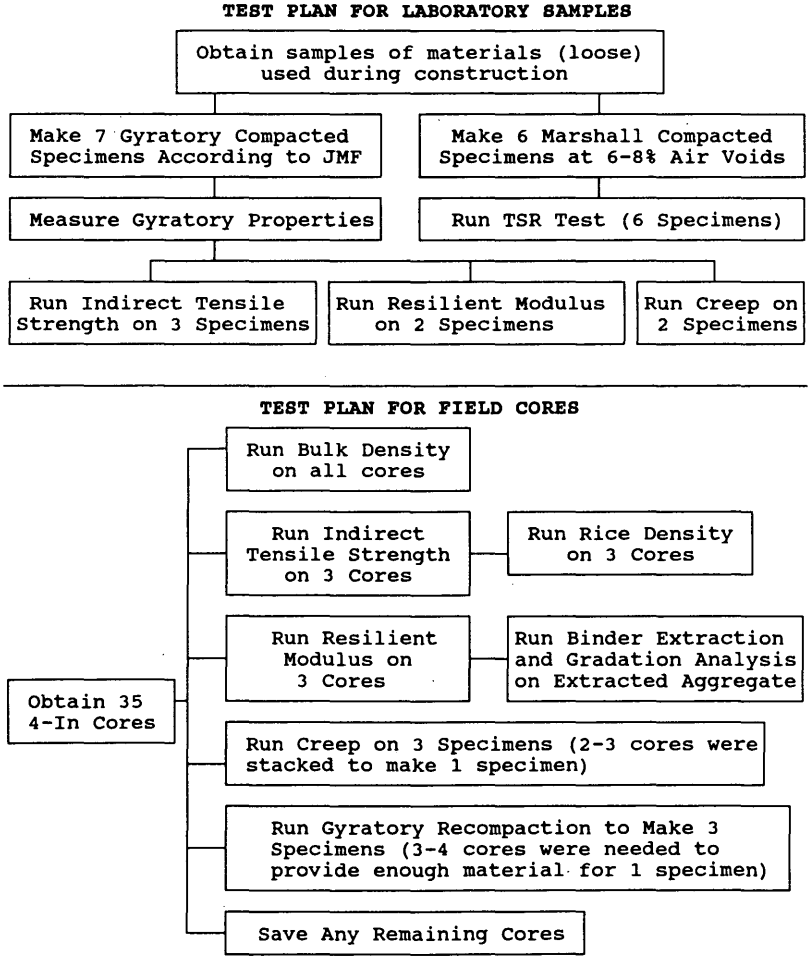

FIGURE 1 Test plan for laboratory and field (0-, 3-, 6-, 9-, 12-, and 24-month) cores.

asphalt cement and the preblended rubber-modified binder (obtained during construction) were mixed with the batched aggregate to fabricate the control and RMHMA samples, respectively. Both the control and RMHMA samples were prepared at 6.3 percent binder content because MSHD has reported that the control and RMHMA section were constructed at 6.3 percent binder content.

Gyratory Properties, VTM, and Bulk Density

The Corps of Engineers gyratory compactor, set at 1-degree angle, 120-psi normal pressure, and 300 revolutions, was used to compact the HMA specimens. The gyratory properties (S_G, GSI, and GEPI) were measured, and the compacted samples were tested for air voids and bulk density. S_G measures the shear stress required to produce a 1-degree angle during compaction. GSI is the ratio of maximum gyratory angle to the minimum gyratory angle. Asphalt mixtures with GSI values more than 1.1 have been shown to be susceptible to rutting in service, and mixtures with GSI values more than 1.3 have been shown to rut severely (*14,15*). GEPI is a reflection of the shear strain experienced by the specimen. It also reflects the internal friction in the specimen. The higher the internal friction, the lower the GEPI. The VTM and bulk density of samples compacted in the gyratory machine should reflect the in-place pavement air voids and density after traffic. HMA with voids in compacted samples below 3 percent tends to rut prematurely (*15*).

Table 2 gives the gyratory properties, VTM, and bulk density of the laboratory-fabricated samples. The gyratory properties of the control and RMHMA mix were similar. The GSI values for both mixes were less than 1.1, indicating a high probability that both mixes are not susceptible to rutting. However, the averaged laboratory compacted air voids of the control mix was 2.08 percent, whereas that of the RMHMA mix was 2.93 percent. The difference in the averaged air voids is statistically significant ($\alpha = 0.05$). According to Brown and Cross (*15*), the laboratory recompacted air voids indicated that the RMHMA mix should be more rut resistant than the control mix.

Indirect Tensile Strength and Resilient Modulus

Six of the 14 gyratory compacted samples (3 control and 3 RMHMA samples) were tested for indirect tensile strength. Table 3 shows that the RMHMA mix has a slightly higher tensile strength than the control mix, but the difference is not statistically significant ($\alpha = 0.05$).

Four of the gyratory compacted samples (two control and two RMHMA samples) were allocated for resilient modulus testing. The resilient modulus tests were not conducted for this series because of equipment problems. These four samples were kept and later tested for permanent deformation (not scheduled in the test plan).

Creep and Permanent Deformation

Four of the gyratory compacted samples (two control and two RMHMA samples) were tested for creep deformation. Creep samples were confined with 20-psi confining pressure and loaded with 120-psi total pressure for 1 hr and unloaded for 1 hr to measure creep deformation and rebound. The four samples allocated for resilient modulus test (not tested because of equipment problems) were tested for permanent deformation. The permanent deformation test results served to compare creep test results. In the permanent deformation test, samples were confined with 20-psi confining pressure and dynamically loaded with 120-psi total pressure. Dynamic loading was achieved with a cyclic rectangular

TABLE 1 Gradation Analysis of Extracted Aggregate

SIEVE SIZE	PERCENT PASSING					
	SPEC	JMF	CONTROL MIX (Averaged of two tests)		RMHMA MIX (Averaged of two tests)	
			0 Month	3 Month	0 Month	3 Month
3/4 "	100	100	100	100	100	100
1/2 "	100	100	100	99.9	99.6	99.9
3/8 "	87-100	94	91.8	94.7	92.4	94.4
No 4	53-80	61	59.7	64.2	63.2	64.4
No 8	32-63	43	40.9	43.6	42.5	42.8
No 16	-	-	30.3	31.8	31.4	31.2
No 30	12-33	22	23.3	24.6	23.7	23.1
No 50	6-20	12	15.3	14.3	13.7	12.4
No 100	-	-	8.0	7.6	7.1	5.8
No 200	2-10	4.8	6.5	5.9	4.7	3.3

Note: Gradation analysis was not conducted at 6, 9, 12, and 24 months because these tests would not yield extra information

TABLE 2 Gyratory Properties of Laboratory Specimens

	CONTROL MIX					RMHMA MIX				
	S_G (PSI)	GSI	GEPI	VTM (%)	γ_b # (PCF)	S_G (PSI)	GSI	GEPI	VTM (%)	γ_b ## (PCF)
1	36.02	1.00	1.20	2.45	141.7	37.07	1.00	1.20	3.45	141.7
2	34.91	1.04	1.20	1.33	143.7	30.79	1.04	1.20	3.10	142.2
3	35.67	1.00	1.20	1.85	142.5	36.68	1.04	1.20	2.64	142.8
4	30.00	1.04	1.15	2.24	142.0	31.79	0.96	1.20	3.53	141.5
5	32.68	1.04	1.15	2.41	141.7	30.38	1.08	1.20	2.55	143.0
6	34.86	1.04	1.20	1.25	143.4	30.64*	1.50*	0.80*	0.02*	146.0*
7	31.80	1.00	1.10	3.05	141.0	35.38	1.08	1.20	2.30	143.3
AVE	33.71	1.02	1.17	2.08	142.2	33.68	1.03	1.20	2.93	142.4

* - data was discarded because it is inconsistent, probably had error in batching materials
# - Maximum theoretical density (Control) = 145.22 pcf
- Maximum theoretical density (RMHMA) = 142.70 pcf

Statistical Test (F Test)

H_0	Mean Control voids = Mean RMHMA voids
F value for H_0	6.68
Pr > F	0.0254
Conclusion	Reject H_0: The two means are different at α = 0.05

TABLE 3 Indirect Tensile Strength of Laboratory Samples

SAMPLE	INDIRECT TENSILE STRENGTH (PSI)	
	CONTROL MIX	RMHMA MIX
1	191.0	187.8
2	188.4	198.9
3	178.9	205.3
AVERAGE	186.1	197.4

Statistical Test (F Test)

H_0	Mean Control tensile strength = Mean RMHMA tensile strength
F value for H_0	3.18
Pr > F	0.149
Conclusion	Accept H_0: The two means are equal at α = 0.05

load pulse. The loading period was 0.1 sec with a rest period of 0.9 sec. Permanent deformation samples were tested for 1 hr, and no rebound was measured since experience has shown that samples do not rebound in this test.

Like gyratory properties, creep and permanent deformation are believed to provide insight into the rut resistance of HMA mixes (*16,17*). Table 4 indicates that the averaged creep strain of the RMHMA mix (0.0067 in./in.) is higher than that of the control mix (0.0036 in./in.) and averaged permanent deformation of the RMHMA mix (0.0405 in./in.) is also higher than that of the control mix (0.0216). Although these differences appear numerically large, they are statistically insignificant ($\alpha = 0.05$) because of the small sample size ($n = 2$).

Tensile Strength Ratio

Six control and six RMHMA samples were prepared in the laboratory at approximately 7 percent voids total mix. Since there was no more preblended rubber-modified binder (obtained during construction) to prepare the six RMHMA samples, a decision was made to blend the rubber-modified binder in the laboratory. The CRM and asphalt cement were obtained from MSHD. Five percent of CRM (by weight) was added to the asphalt cement (heated in an oven to 310°F). The CRM-asphalt cement blend was kept in the oven maintained at 310°F for 45 min and stirred every 10 min.

The samples were compacted using a Marshall hammer. These samples were then conditioned using the Root-Tunnicliff procedure. Table 5 indicates that the RMHMA mix had a higher strength than the control mix before conditioning, and the difference is statistically significant ($\alpha = 0.05$). The tensile strength of the control and RMHMA mix after conditioning does not show any statistical difference ($\alpha = 0.05$). Table 5 also indicates that the RMHMA has a tensile strength ratio of 0.50 versus 0.38 for the control.

Pavement Density, Air Voids, and Rut Depth Measurements

Theoretical maximum density and bulk density tests were performed on the field cores. Average initial density for both the control and RMHMA pavement sections was approximately 90

TABLE 4 Creep and Permanent Deformation of Laboratory Samples

MIX DESCRIPTION	CREEP (IN/IN)		PERMANENT DEFORMATION (IN/IN)	
CONTROL MIX	TEST 1	0.0016	TEST 1	0.0140
	TEST 2	0.0055	TEST 2	0.0292
	AVERAGE	0.0036	AVERAGE	0.0216
RMHMA MIX	TEST 1	0.0056	TEST 1	0.0359
	TEST 2	0.0078	TEST 2	0.0450
	AVERAGE	0.0067	AVERAGE	0.0405

Statistical Test (F Test)

H_0	Mean Control creep = Mean RMHMA creep
F value for H_0	1.98
Pr > F	0.2947
Conclusion	Accept H_0: The two means are equal at $\alpha = 0.05$

Statistical Test (F Test)

H_0	Mean Control permanent deformation = Mean RMHMA permanent deformation
F value for H_0	4.53
Pr > F	0.1671
Conclusion	Accept H_0: The two means are equal at $\alpha = 0.05$

percent of maximum density (10 percent air voids) with a standard deviation of about 1.5. Table 6 gives the rut depth measurements made during the sampling of field cores and the core air voids at each sampling interval. It can be seen that the control mix is densifying faster than the rubber-modified mix and has therefore resulted in a little more "rutting" (densification). Neither of these mixes was rutting significantly after 2 years.

Extraction and Gradation

Bitumen extraction (ASTM D2172, Method A) and gradation analysis (ASTM C117 and ASTM C136) were performed on the 0- and 3-month cores only. Extraction and gradation analysis on the 6-, 9-, 12-, and 24-month cores were not conducted since these tests would not yield extra information. The average extracted binder contents for the control pavement was 5.9 percent (5.8 percent for 0-month cores and 6.0 percent for 3-month cores). The extracted asphalt content was lower than the targeted asphalt content (6.6 percent) by 0.7 percent. An increase in theoretical maximum density over time can be explained by asphalt absorption. An examination of the theoretical maximum density indicated that it remains relatively constant with time (2.352 at 0 months, 2.353 at 3 months, 2.352 at 6 months, and 2.361 at 12 months). The discrepancy between the targeted and extracted binder content was not pursued in this study because of the apparent inability to determine the binder content of the RMHMA section and, therefore, to compare the two sections. The average extracted binder content for the RMHMA pavement was 5.6 percent (5.7 percent for 0-month cores and 5.3 percent for 3-month cores). The extracted binder content was lower than the targeted binder content (6.3 percent) by 0.8 percent. The actual binder content was greater than 5.6 percent because rubber-modified binder contains solid rubber particles that are insoluble in trichloroethane. This is confirmed by visual observations of the extraction process indicating that rubber particles were contained in the aggregate mass after completion of the extraction process.

Table 1 gives the extracted aggregate gradations for the control and RMHMA pavement sections. The extracted aggregate gradations of both the control and CRM pavement sections are in close agreement with the JMF gradation.

Indirect Tensile Strength and Resilient Modulus

Table 7 gives the averaged tensile strength values of the control and RMHMA mixes. There is no significant difference between

TABLE 5 Water Susceptibility of Laboratory Compacted Samples (Measured by Tensile Strength)

SAMPLE	CONTROL MIX		RMHMA MIX LAB BLENDED BINDER	
	CONDITIONED SAMPLES (LBS)	UNCONDITIONED SAMPLES (LBS)	CONDITIONED SAMPLES (LBS)	UNCONDITIONED SAMPLES (LBS)
1	750	1950	700	2075
2	660	1875	1000	1975
3	740	1875	1425	2175
AVERAGE	717	1900	1042	2075
	TSR = 0.38		TSR = 0.50	

Statistical Test (F Test)

H_o	UNCONDITIONED Mean Control tensile strength = Mean RMHMA tensile strength
F value for H_o	7.74
Pr > |T|	0.0497
Conclusion	Reject H_o: The two means are different at α = 0.05

Statistical Test (F Test)

H_o	CONDITIONED Mean Control tensile strength = Mean RMHMA tensile strength
F value for H_o	2.34
Pr > F	0.2005
Conclusion	Accept H_o: The two means are equal at α = 0.05

TABLE 6 In-Place Air Voids and Rut Depth Measurements

TIME	CONTROL PAVEMENT SECTION		RMHMA PAVEMENT SECTION	
	VTM	RUT DEPTH (in)	VTM	RUT DEPTH (in)
0 MONTHS	10.3 %	0	9.6 %	0
3 MONTHS	9.0 %	0	8.0 %	0
6 MONTHS	6.5 %	0.128	7.9 %	0.080
9 MONTHS	6.5 %	0.133	8.0 %	0.084
12 MONTHS	6.2 %	0.142	8.0 %	0.084
24 MONTHS	6.3 %	0.136	8.3 %	0.086

TABLE 7 Indirect Tensile Strength and Resilient Modulus of Field Cores

TIME	CONTROL MIX				RMHMA MIX			
	Tensile Strength (psi)	M_r @ 40°F (ksi)	M_r @ 77°F (ksi)	M_r @ 104°F (ksi)	Tensile Strength (psi)	M_r @ 40°F (ksi)	M_r @ 77°F (ksi)	M_r @ 104°F (ksi)
0 MONTH	148.6	1125	243	94	196.5	1268	421	165
3 MONTH	153.9	1145	395	160	134.6	1394	553	252
6 MONTH	145.3	1792	891	*	162.3	2170	1086	*
12 MONTH	101.2	1327	461	161	114.5	1350	550	158.3
24 MONTH	185.3	1814	693	188	152.5	1781	860	275

Note: 9 month cores were not tested (see test plan) and * indicates sample failed during testing

the two mixes. No general trend between tensile strength and time can be established for either of the mixes. However, the tensile strength at 12 months appears to be significantly lower than the other time intervals. The reason is not known. This decrease was not observed in the resilient modulus test. Table 7 also indicates that the control mix has lower resilient modulus than the RMHMA mix. The 6-month test results were suspect and were discarded because test specimens should not be damaged during testing. Resilient modulus measured at 40°F, 77°F, and 104°F increased with time. This increase appeared to be similar for both the control and RMHMA mixes. The resilient modulus (measured at 40°F) of the control and RMHMA mixes are not significantly different. Resilient modulus (measured at 77°F and 104°F) of the control mix is significantly lower than that of the RMHMA mix. Temperature susceptibility (rate of change in M_r with temperature) for both control and RMHMA mixes were similar.

Creep and Permanent Deformation

Initially, creep tests were performed on the 0- and 3-month cores. After the 0- and 3-month tests, experience from other projects had shown that the permanent deformation test was preferred. As a result, creep tests were replaced by permanent deformation tests on and after the 3-month cores. Creep results and permanent deformation results are given in Table 8.

At 0 months, the creep deformation of the control mix is significantly greater than that of the RMHMA mix. There is no difference in creep deformation between the control and RMHMA at 3 months. Table 8 indicates that the permanent deformation of the control mix is significantly higher than that of the RMHMA mix. The permanent deformation of both the control and RMHMA mixes remains relatively constant with time. The creep and permanent deformation tests indicate that the control mix is more likely to have more rutting than the RMHMA mix.

Gyratory Recompaction

Field cores were recompacted, and the gyratory properties are given in Table 9. The S_G and GEPI values for the control mix were lower than those of the RMHMA mix at each time interval. At each time interval, the GSI values for the control mix were higher than those for the RMHMA mix. The recompacted air voids for the control mix were lower than those for the RMHMA mix. These data suggest that the RMHMA mix is more resistant to rutting than the control mix.

At 0, 3, and 12 months, the GSI values for the control mix were greater than 1.1, and the recompacted air voids were signif-

TABLE 8 Creep and Permanent Deformation of Field Cores

TIME IN MONTHS	CONTROL MIX		RMHMA MIX	
	CREEP (IN/IN)	P. DEFORMATION (IN/IN)	CREEP (IN/IN)	P.DEFORMATION (IN/IN)
0	0.0249	-	0.0110	-
3	0.0110	0.04925	0.0123	0.02995
6	-	0.04075	-	0.02824
9	-	0.03776	-	0.03128
12	-	0.03776	-	0.03128
24	-	0.04055	-	0.02731

TABLE 9 Gyratory Properties for Recompacted Field Cores

TIME IN MONTHS	CONTROL MIX					RMHMA MIX				
	S_G (PSI)	GSI	GEPI	VTM (%)	γ_b (PCF)	S_G (PSI)	GSI	GEPI	VTM (%)	γ_b (PCF)
0	22.5	1.18	1.12	2.17	143.6	28.8	1.00	1.13	3.36	142.4
3	24.9	1.31	1.20	1.64	144.7	33.4	1.09	1.13	3.21	143.0
6	27.3	1.05	1.20	2.91	142.5	34.0	1.00	1.13	5.63	139.5
9	36.6	1.03	1.13	3.77	141.4	36.5	1.03	1.10	6.03	138.8
12	25.9	1.17	1.20	1.95	143.9	32.2	1.00	1.13	5.28	140.5

Note: Gyratory properties at 24 months were not measured due to insufficient cores

icantly lower than 3 percent. These values indicate that the control mix is rut susceptible. However, the data for 6 and 9 months do not show this. The GSI values (less than 1.1) and the recompacted air voids (greater than 3 percent) for the RMHMA mix at all time intervals suggest that the RMHMA mix is not susceptible to rutting.

CONCLUSIONS

The following conclusions are obtained on the basis of the reported test results:

1. Tests on laboratory-prepared specimens indicated that the RMHMA mix has lower water susceptibility (tensile strength ratio) than the control mix.
2. The indirect tensile strength test on both laboratory samples and field cores indicated that the control and RMHMA mixes have comparable tensile strength.
3. The RMHMA field cores did not show the expected improvement in the M_r temperature susceptibility. The slopes of the M_r temperature curves for both control and RMHMA field cores were about the same. However, the curve for the RMHMA field cores was higher than (above) the control field cores. The resilient modulus of both control and RMHMA mixes increases with time.
4. In the permanent deformation test of field cores, the control mix deformed more than the RMHMA mix. Permanent deformation tests on laboratory-prepared samples indicate that there is no difference between the RMHMA and control samples, statistically.
5. The recompacted voids of the laboratory-prepared specimens suggested that the RMHMA mix is less likely to rut than the RMHMA mix. The gyratory properties of the recompacted RMHMA field cores at each sampling interval are consistently better than the control field cores. On the basis of these test results, the RMHMA mix evaluated appears to be more resistant to rutting than the control mix.
6. After 24 months of traffic, the amount of rutting in both sections is insignificant. The measured amount of rutting in the control and RMHMA pavement sections was likely due to densification of the mixes.

ACKNOWLEDGMENT

The authors acknowledge the Mississippi State Highway Department for its assistance in this research.

REFERENCES

1. Sikora, M. Third Annual Legislative Update. *Scrap Tire News,* Vol. 5, No. 1, Jan. 1991.

2. *A Study of the Use of Recycled Paving Material—Report to Congress.* Report FHWA-RD-93-147. FHWA, U.S. Department of Transportation, June 1993.
3. Bouldin, M. G., and J. H. Collins. Rheology and Microstructure of Polymer/Asphalt Blends. *Journal of Rubber Chemistry and Technology,* Sept.–Oct. 1991.
4. Bissada, A. F., and A. A. Anani. Evaluation of Rubberized Limestone Filler in Asphalt Paving Mixtures. *Journal of Rubber Chemistry and Technology,* Vol. 57, 1984.
5. Rosner, J. C., and J. G. Chehovits. Chemical and Physical Properties of Asphalt Rubber Mixtures. Report FHWA/AZ-82/159. Arizona Department of Transportation, April 1982.
6. Jimenez, R. A., and W. R. Meier. Evaluation of Structural Layer Coefficient for Asphalt-Aggregate Mixtures. *Proc., Association of Asphalt Paving Technologists,* Vol. 54, 1985.
7. Morris, G. R. *Utilization of Recycled Tire Rubber as an Additive to Asphalt Cement.* 1978.
8. Roberts, F. L., P. S. Kandhal, E. R. Brown, and R. L. Dunning. *Investigation and Evaluation of Ground Tire Rubber in Hot Mix Asphalt.* National Center for Asphalt Technology, Auburn University, Auburn, Ala., Aug. 1984.
9. Piggot, M. R., and R. T. Woodhams. Improved Hot Mix Asphalts Containing Reclaimed Rubbers. *Proc., Association of Asphalt Paving Technologists,* Vol. 46, 1977.
10. Vallerga, W. B., G. R. Morris, J. E. Huffman, and B. J. Huff. Applicability of Asphalt-Rubber Membrane in Reducing Reflection Cracking. *Proc., Association of Asphalt Paving Technologists,* Vol. 49, 1980.
11. Jimenez, R. A. Behavior of Asphaltic Concrete Diaphragms to Repetitive Loads. International Conference on Structural Design of Asphalt Pavements, Aug. 1962.
12. Stephens, J. E. Field Evaluation of Rubber Modified Bituminous Concrete. In *Transportation Research Record 843,* TRB, National Research Council, Washington, D.C., 1982.
13. Esch, D. C. Construction and Benefits of Rubber Modified Asphalt Pavements. In *Transportation Research Record 860,* TRB, National Research Council, Washington, D.C., 1982.
14. Kandhal, P., S. A. Cross, and E. R. Brown. Evaluation of Bituminous Pavements for High Pressure Truck Tires. Report FHWA-PA-90-008-87-01. Pennsylvania Department of Transportation, Dec. 1990.
15. Brown, E. R., and S. A. Cross. A Study of In-Place Rutting of Asphalt Pavements. *Proc., Association of Asphalt Paving Technologists,* Vol. 59, 1990.
16. Gabrielson, J. R. *Evaluation of Hot Mix Asphalt (HMA) Static Creep and Repeated Load Test.* Ph.D. dissertation. Auburn University, Auburn, Ala., Dec. 1992.
17. Foo, K. Y. *Predicting Rutting in HMA.* Ph.D. dissertation. Auburn University, Auburn, Ala., March 1994.

Publication of this paper sponsored by Committee on Characteristics of Nonbituminous Components of Bituminous Paving Mixtures.

Effect of Antistrip Additives on the Properties of Polymer-Modified Asphalt Binders and Mixtures

MOON C. WON AND MICHAEL K. HO

The effect of liquid antistrip additives on the properties of polymer-modified asphalt binders and mixtures as related to rutting and moisture damage was investigated. The use of polymer-modified asphalts has increased in recent years because of their ability to resist rutting at high temperatures and improve fatigue resistance at low temperatures. In the Houston area liquid antistrip additives are used for almost all the mixtures to mitigate moisture damage. Liquid antistrip additives have been shown to soften certain asphalts. Whether liquid antistrip additives soften polymer-modified asphalts, thus degrading the rut resistant capability of polymer-modified asphalt, has become a concern to highway engineers. Asphalt binder properties known to have a bearing on rutting were evaluated on polymer-modified asphalts with three commercial liquid antistrip additives. Moisture damage of the mixture was evaluated using the conditioned-unconditioned indirect tensile test. In general, the liquid antistrip additives reduced the viscosity and softening point of polymer-modified asphalts, especially at high dosage. This will make polymer-modified asphalt binders more rut susceptible. For polymer-modified asphalt mixtures, increasing the dosage of liquid antistrip additives did not improve resistance to moisture susceptibility. On the basis of the investigation, lower dosages of liquid antistrip additives are recommended for polymer-modified asphalts than would be required for straight asphalts.

Moisture damage of asphalt concrete pavement has been a serious problem throughout the country. Extensive research has been conducted to identify its mechanisms and to develop methodologies for evaluating moisture susceptibility of mixtures. In 1985 Hazlett (*1*), after evaluating a number of moisture damage testing procedures for their effectiveness, selected the Lottman test and modified it for Texas Department of Transportation's (TxDOT's) use. The test uses the tensile strength ratio (TSR) of conditioned to unconditioned specimens as an indicator of the mixture's resistance to moisture damage. In TxDOT's Houston district the test is routinely conducted to ensure that the mixtures are not moisture susceptible.

Figure 1 shows TSR distributions of 103 surface mixtures evaluated in 1992 at the district laboratory. Ratios of 1 or more were obtained for more than 20 percent of the mixtures tested. Given the level of damage induced in the conditioned specimens, it is not expected that conditioned strengths are greater than unconditioned in more than 20 percent of the mixtures. There are several probable reasons for conditioned strengths being greater than unconditioned. One may be the softening of asphalt by liquid antistrip additives even though it is not known whether the asphalt softening has a more significant effect on the tensile strengths of unconditioned specimens than on those of the conditioned. Anderson et al. (*2*) found that the addition of liquid antistrip additives softened certain asphalts. They attributed this to the reactions between polar components in liquid antistrip additives and functional groups in asphalts.

In addition to moisture damage, rutting has been a major distress in the Houston area because of high temperatures, heavy traffic, and increasing tire pressures. Although such variables as proper gradation and binder content have a more significant effect on rutting, binder properties also affect a mixture's resistance to rutting. This is manifested by the creep test results, which increase rapidly with temperature. King et al. (*3*) found that for straight soft asphalts a relatively small amount of polymer can reduce rut depths significantly. The Houston district has increased the use of polymer-modified asphalts in recent years because of their ability to resist rutting. Liquid antistrip additives are used for almost all mixtures in the Houston area to meet the required minimum TSR value of 0.7. However, whether they soften the polymer-modified asphalts as they do the straight asphalts has become a concern to highway engineers. Figure 2 shows the unconditioned tensile strengths of the polymer-modified asphalt mixtures with and without liquid antistrip additives. The polymer used was ethylene-vinyl-acetate at 3.5 percent, and the base asphalt was AC-10. The mixtures were obtained from a drum mix plant where the contractor produced both mixtures to determine whether liquid antistrip additives were needed to meet the minimum TSR requirement. In Figure 2 hollow dots represent tensile strengths of asphalt concrete mixtures without antistrip additives. Solid dots represent those with antistrip additives. The figure indicates that adding liquid antistrip additive resulted in the decrease of tensile strength by more than 30 percent. The decrease appears to be due solely to the use of 1.0 percent liquid antistrip additive since all the other variables such as aggregates, gradation, and asphalt content were kept the same.

OBJECTIVES

The objectives of the study are (*a*) to investigate the effect of liquid antistrip additives on the properties of polymer-modified asphalt binders as related to rutting and (*b*) to evaluate the effectiveness of liquid antistrip additives mixed with polymer-modified asphalts on the resistance of asphalt mixtures to moisture damage.

TEST PROGRAM

Asphalt binder properties were evaluated to investigate the effect of liquid antistrip additives. The properties include viscosities,

Texas Department of Transportation, P.O. Box 1386, Houston, Tex. 77251-1386.

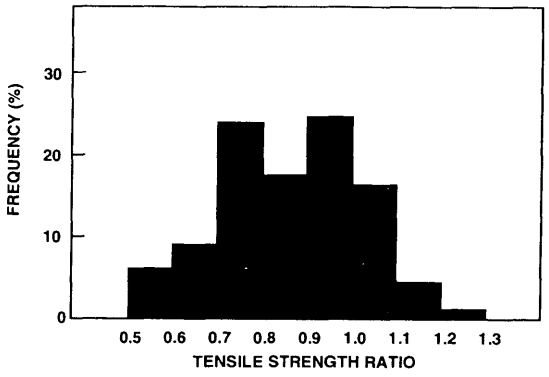

FIGURE 1 Distribution of tensile strength ratios.

softening points, ductility, and flash point. Moisture damages of asphalt mixtures were evaluated by measuring indirect tensile strengths of conditioned and unconditioned specimens.

Materials

- Two grades of straight asphalts, AC-10 and AC-20, and their modified asphalts by styrene-butadiene-styrene (SBS) polymers, AC-30P and AC-45P, all meeting TxDOT specifications, were obtained from KOCH Materials, Baytown, Texas. AC-30P is a blend of AC-10 with 3 percent SBS, and AC-45P is a blend of AC-20 with 3 percent SBS.
- Sandstone, limestone, limestone screenings, and field sand were obtained and combined to produce mixes that met the TxDOT specification requirements for the surface courses.
- Four antistrip additives were selected: hydrated lime and three proprietary liquid antistrip additives. Liquid I is amine based with a recommended dosage of 0.25 to 1.0 percent, and the specific gravity ranges from 0.94 to 0.97. Liquid II is a highly concentrated reacted polyamine with significantly increased molecular weight. Its specific gravity is 1.04 at 25°C, and it is much stickier than Liquids I and III at room temperature. It is a low-odor product, and the recommended dosage ranges from 0.5 to 1.0 percent. Liquid III is amine based with a recommended dosage of 0.5 to 1.0 percent with an approximate specific gravity of 1.04 at room temperature. The liquid antistrip additives were blended with asphalt cement by pouring metered amounts into heated asphalt.

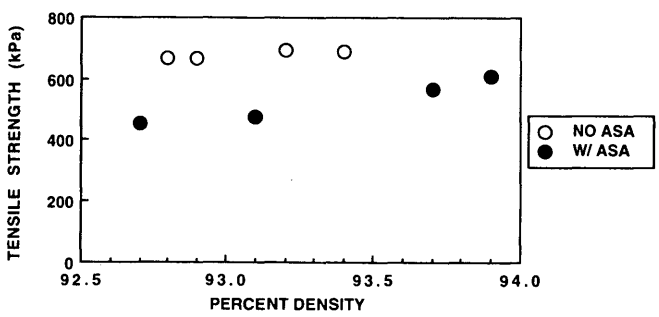

FIGURE 2 Effect of antistrip additives on unconditioned strength of polymer-modified asphalt mixtures.

TABLE 1 Aggregate Gradations Selected for Study

sieve size	gradation	master grading
1/2 "	100	100
3/8 "	94.4	85-100
No. 4	65.4	50-70
No. 10	39.2	32-42
No. 40	25.0	11-26
No. 80	9.8	4-14
No. 200	3.0	1-6

Mixture Design

The job mix formula was developed following the procedures in Construction Bulletin C-14 of TxDOT. The aggregate gradation of the mixture is given in Table 1. The master gradation is for fine surface course, designated as Type D surface in Item 340 of TxDOT *Standard Specifications* (*4*). The optimum asphalt content was 5.0 percent.

Test Procedures

A partial list of binder tests conducted on polymer-modified asphalts and test methods followed is as follows: absolute viscosity at 60°C, ASTM D2171; kinematic viscosity at 135°C, ASTM D2170; penetration at 25°C, ASTM D5; softening point, Tex-505-C; ductility, Tex-503-C.

Moisture susceptibility of the mixtures was evaluated according to TxDOT Procedure (*5*) Tex-531-C test method. The mixing of aggregates with asphalt binders was done using a mechanical mixer following TxDOT Procedure Tex-205-F. Specimens 10.16 cm in diameter and 5.08 cm high were molded in a motorized gyratory-shear molding press. The number of gyrations applied was determined by trial and error so that the air voids in the specimens were within 6 to 8 percent. Eight specimens were prepared for each testing. The specimens were divided into two groups of four specimens in such a way that the average void content in each group was approximately the same. One group of specimens was stored in a desiccator (unconditioned), and the other group underwent a conditioning process that induced moisture damage (conditioned). The conditioning process consisted of saturating the voids with water and freezing and thawing of the specimens as follows. The specimens were placed in a vacuum chamber filled with enough distilled water to submerge them. Vacuum was applied at the appropriate level and duration to fill the voids in the specimens with water at 60 to 80 percent. These four specimens were then placed in a freezer at −17.8°C for a minimum of 15 hr. They were removed from the freezer and placed in a 60°C water bath for 24 hr. The conditioned and unconditioned specimens were placed in a 25°C water bath for 3 to 4 hr and tested for indirect tensile strength at a 5.08 cm/min deformation rate until sample failure occurred.

TABLE 2 Factorial Experiment

Dosage	ASA	Unconditioned				Conditioned			
		10		20		10		20	
		no	yes	no	yes	no	yes	no	yes
0	none								
0.5	I								
	II								
	III								
	L								
1.0	I								
	II								
	III								
	L								

Cond – Conditioning
Asp Grad – Asphalt Grade
SBS – Styrene Butadiene Styrene
ASA – Antistrip Additives
L – Lime

Factorial Experiment

For polymer-modified asphalt binders three liquid antistrip additives were added to each binder at two concentrations (0.5 and 1.0 percent by asphalt weight), resulting in 12 combinations. In addition, the tests were conducted on polymer-modified and straight asphalt binders without liquid additives as control.

For evaluation of moisture susceptibility, a factorial experiment was set up to investigate the significance of variables. Table 2 gives the experimental design for this study. It is a balanced design, and each cell represents a specific combination of treatments. Since eight specimens are required for each cell, a total of 288 specimens were made.

DISCUSSION OF TEST RESULTS

Effect of Antistrip Additives on Asphalt Binder Properties

Measurements of polymer-modified asphalt binder properties as affected by liquid antistrip additives are given in Table 3. Blending straight asphalts with 3 percent SBS changes certain physical characteristics of the binders significantly. Changes include increases in absolute and kinematic viscosity, ring and ball softening points, and ductility. Polymer modification increased absolute viscosity of AC-10 asphalt by 400 percent, whereas a slightly smaller increase (360 percent) is observed for AC-20 asphalt. The same trend is observed for kinematic viscosity, with less magnitude. The softening point also increased by 12.2°C (AC-10) and by 8.8°C (AC-20). However, these data are merely for reference, since the purpose of the study is to determine the effect of the liquid antistrip additives on the characteristics of polymer-modified binders and mixtures, not the effect of polymer modification of straight asphalt.

Figure 3 shows the changes in absolute viscosity at 60°C due to liquid antistrip additives.

Results for AC-30P asphalts include the following:

1. At 0.5 percent liquid dosage the viscosity increased, whereas the viscosity decreased for all liquids at 1.0 percent.
2. The effect on viscosity is antistrip additive specific. Liquid I has the most pronounced effect, and Liquid III exhibits least effect; Liquid I at 0.5 percent increased viscosity by 20 percent whereas at 1.0 percent it decreased by 34 percent. The decrease at 1.0 percent is so great that it barely meets the minimum viscosity required for AC-30P by TxDOT specification.
3. For liquids with significant effect (I and II) the effect is highly sensitive to their dosage. Liquid III is least sensitive to dosage.

The following were observed for AC-45P asphalts:

1. Viscosity decreased at both dosages for all liquids. Decreases are more pronounced at 1.0 percent except for Liquid III.

TABLE 3 Test Results for Polymer-Modified Asphalt Binder Properties as Affected by Liquid Antistrip Additives

Grade	Liquid ASA		Viscosity 60 C,Poises	Viscosity 135 C,cSt	Penetration, 25 C	Softening Point, C	Flash Point, C	Ductility at 4 C	Polymer Con., %	Specific Grav., 25C
AC-10	none		1175	366	100	47.2	315+	13	none	1.027
AC-20	none		2296	510	70	50.6	315+	6	none	1.030
AC-30P	none		4674	932	84	59.4	315.6	37	3.06	1.024
	0.5 %	I	5635	890	83	59.4	307.2	33	2.96	1.024
		II	5025	871	85	54.4	298.9	41	3.10	1.023
		III	4574	880	82	54.4	296.1	45	3.20	1.022
	1.0 %	I	3081	818	83	52.8	287.8	54	3.10	1.024
		II	3570	836	82	53.9	298.9	44	3.10	1.026
		III	3828	912	89	54.4	293.3	47	3.10	1.023
AC-45P	none		8289	1080	69	59.4	307.2	33	3.10	1.023
	0.5 %	I	6511	1025	73	58.9	304.4	39	3.07	1.025
		II	7494	1024	75	60.0	296.1	46	3.29	1.026
		III	5516	995	76	58.9	298.9	45	3.25	1.024
	1.0 %	I	5120	1079	75	60.0	285.0	40	3.31	1.024
		II	6878	922	70	57.8	285.0	41	3.30	1.024
		III	5653	963	76	57.2	287.8	29	3.10	1.025

2. As in AC-30P, the effect on viscosity is antistrip additive specific. At 1.0 percent dosage the largest decrease is obtained with Liquid I, followed by Liquids III and II. A similar trend is observed at 0.5 percent.

The changes in softening points due to liquid antistrip additives are shown in Figure 4. The decreases on AC-30P are significant, ranging from 5°C to 6.6°C, except for Liquid I at 0.5 percent. This amount of decrease is much more than the values reported by Anderson et al. (*2*) on straight asphalts. The decreases on AC-45P are not significant.

King et al. (*3*) investigated the influence of asphalt grade and polymer concentration on the resistance of polymer-modified asphalt mixtures to rutting using the French rutting simulator. They found that for polymer-modified soft asphalts a good correlation was obtained between rut depths and such variables as absolute viscosity and softening point. Figures 3 and 4 indicate that a 1.0 percent liquid dosage will reduce the resistance of AC-30P mixtures to rutting.

Effect of Antistrip Additives on Moisture Damage

An analysis of variance algorithm was applied to the moisture susceptibility test results. The variables investigated, which included asphalt grade, the use of polymer, antistrip additive type, and its dosage, were all significant except for antistrip additive type. The coefficient of variation of four strength values for each combination of treatments, which corresponds to each cell in Ta-

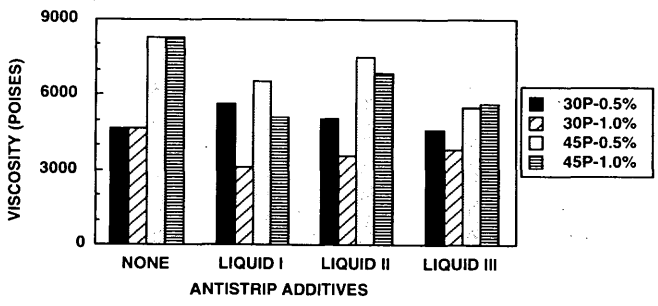

FIGURE 3 Effect of liquid antistrip additives on absolute viscosity.

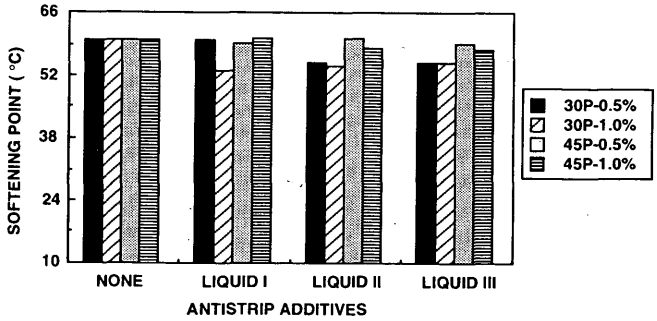

FIGURE 4 Effect of liquid antistrip additives on softening point.

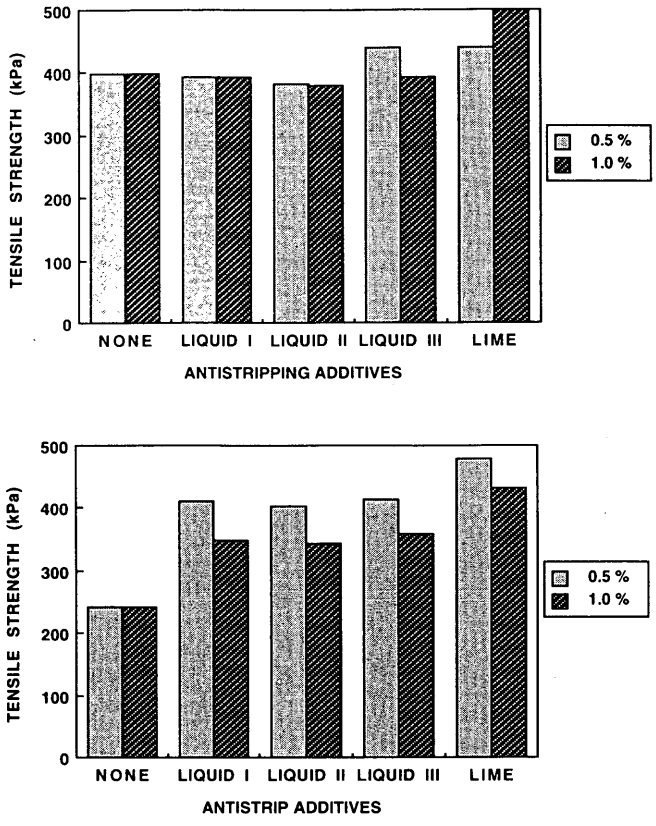

FIGURE 5 Indirect tensile strengths of AC-10 mixtures: unconditioned (*top*) and conditioned (*bottom*).

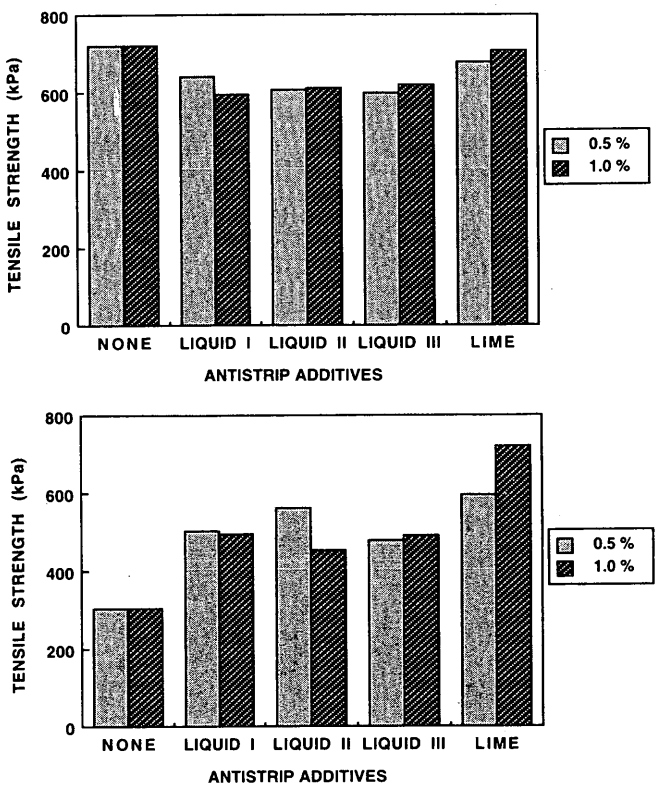

FIGURE 6 Indirect tensile strengths of AC-20 mixtures: unconditioned (*top*) and conditioned (*bottom*).

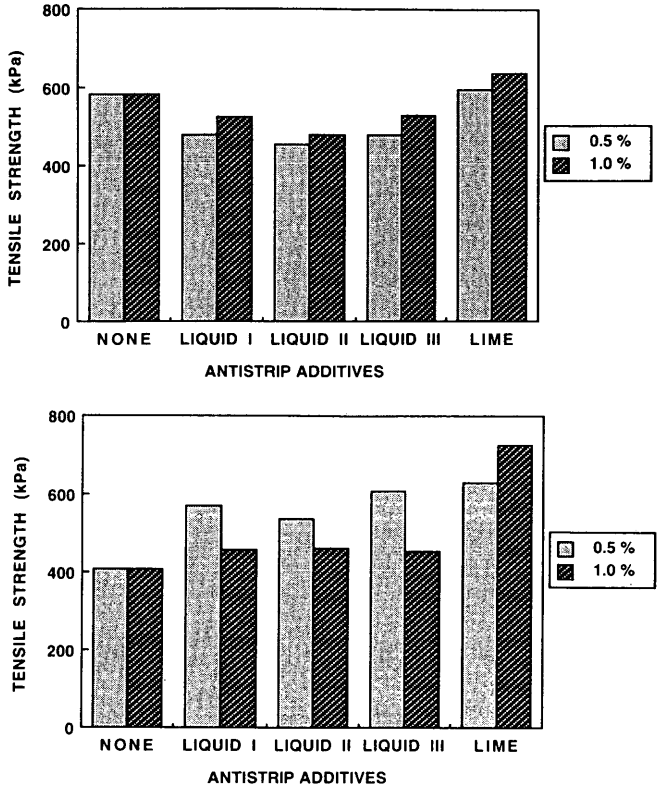

FIGURE 7 Indirect tensile strengths of AC-30P mixtures: unconditioned (*top*) and conditioned (*bottom*).

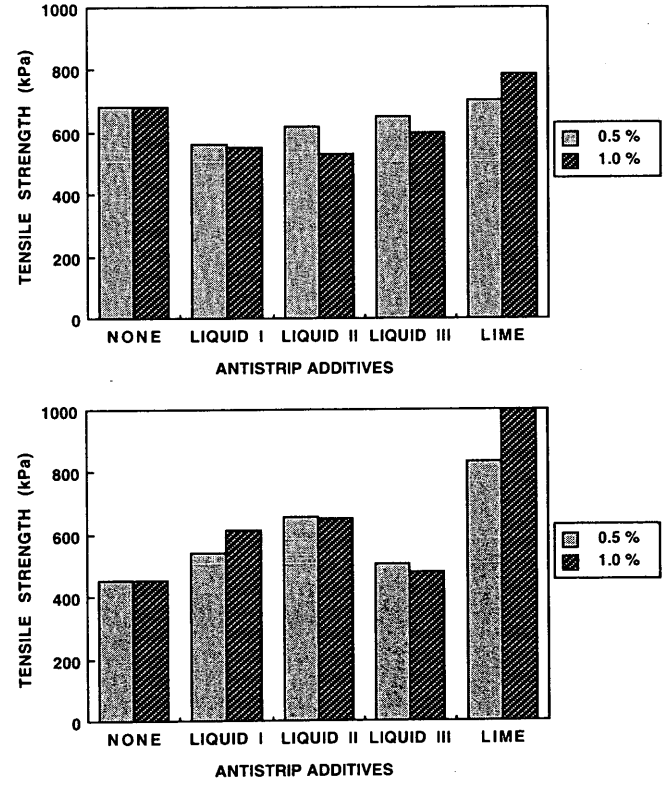

FIGURE 8 Indirect tensile strengths of AC-45P mixtures: unconditioned (*top*) and conditioned (*bottom*).

ble 2, ranged from 1.01 to 9.9 percent; the average was 3.8 percent. Moisture susceptibility test results are summarized as follows:

- AC-10 mixtures: The strengths of unconditioned and conditioned specimens are shown in Figure 5. Whereas antistrip additives do not have a significant effect on unconditioned strengths, with the exception of lime, they improve conditioned strengths over control. The three liquids have almost identical effects on conditioned strengths. At 0.5 percent dosage the increase over control is approximately 70 percent with liquid additives and 100 percent with lime. Note that the strengths at 1.0 percent dosage are lower than those at 0.5 percent. Anderson et al. (*2*) found that each asphalt has a certain demand for the antistrip additive. On the other hand, Dybalski (*6*) states that excessive dosage of liquid antistrip additives can create a mechanically weak, water-susceptible, shear plane. It appears that the particular AC-10 asphalt binder used in this study has little demand for the liquid antistrip additives. Lime improves both conditioned and unconditioned strengths more than liquids.
- AC-20 mixtures: Figure 6 (*top*) shows a decrease in unconditioned strengths due to additives. The three liquids reduce the strengths by approximately 20 percent over the control. This can be an indication of asphalt softening by liquid additives. Lime also decreased the strengths, but by a small proportion. The improved strengths of specimens conditioned by antistrip additives are shown in Figure 6 (*bottom*). At both dosages all the liquids improve in strength by the same amount except for Liquid II at 0.5 percent. As far as conditioned strengths are concerned, lime is more efficient than the three liquids included in this study.
- AC-30P mixtures: Figure 7 (*top*) shows the effect of additives on unconditioned strengths. Strength reduction by almost identical amounts is produced by three liquids at 0.5 percent dosage. At 1.0 percent dosage the strengths are higher than those at 0.5 percent but still lower than control. Lime enhances unconditioned strengths at both dosages. The improved conditioned strengths over control are shown in Figure 7 (*bottom*). At 1.0 percent the increase is small and almost the same for the three liquids, whereas at 0.5 percent the increase is significant. From this figure it appears that the AC-30P asphalt binders have little demand for antistrip additives. Note that the same observation was made for AC-10 mixtures.
- AC-45P mixtures: A decrease in unconditioned strengths as affected by liquid antistrip additives is shown in Figure 8 (*top*). The effect is more pronounced at 1.0 percent for Liquids II and III. In the case of Liquid I the decrease is not affected by dosage. As with AC-30P mixtures, lime increases strength over control. Conditioned strengths are shown in Figure 8 (*bottom*). Whereas Liquids I and II increase conditioned strength moderately, the increase for Liquid III at both dosages is insignificant. Lime improves conditioned strengths significantly, especially at 1.0 percent dosage.

Tensile strength ratios of all the mixtures investigated in this study are summarized in Figure 9. Polymer-modification itself increases TSR values over straight asphalts. For AC-10 asphalt binders, polymerization made the mixtures exceed the required TSR ratio of 0.7. For AC-20 asphalt binders, polymerization increased TSR values by more than 60 percent. Figure 9 also shows that the effectiveness of additives in mitigating moisture damage is specific to asphalt grade and dosage.

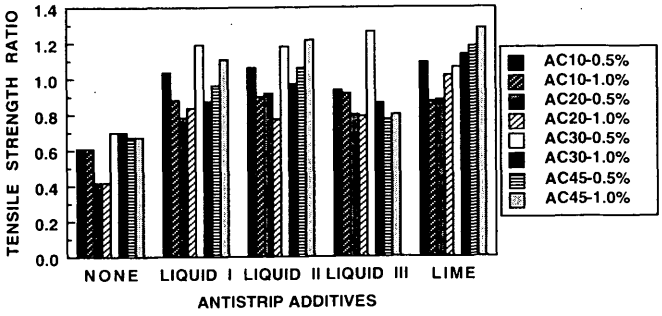

FIGURE 9 Effect of antistrip additives on TSRs.

CONCLUSIONS

A limited study has been conducted to determine the effect of liquid antistrip additives on polymer-modified asphalt binder properties. The effectiveness of antistrip additives on the moisture damage of straight and polymer-modified asphalt mixtures was also investigated. On the basis of the data presented, the following conclusions can be drawn:

1. Liquid antistrip additives affect the viscosity and softening point of polymer-modified asphalts. Adding 1.0 percent of all three liquid antistrip additives included in this study significantly reduced viscosity. Softening point was also decreased with the addition of liquid antistrip additives. The effect is more pronounced for AC-30P than for AC-45P. It may be inferred that the effectiveness of polymer modification of soft straight asphalts on the rut resistance decreases by the addition of 1.0 percent of liquid antistrip additives.
2. In almost every case, liquid antistrip additives reduced unconditioned tensile strength of the polymer-modified asphalt concrete mixtures while increasing conditioned tensile strength. This resulted in tensile strength ratios of some mixtures greater than 1.0.
3. Polymerization of asphalt alone improves the TSR by increasing conditioned strength more than unconditioned strength over control. Lower dosages of liquid antistrip additives than would be required for straight asphalts are recommended for polymer-modified asphalts.
4. Lime is effective in preserving unconditioned and conditioned tensile strengths of the mixtures.

ACKNOWLEDGMENT

The authors wish to thank Gene Coward of Materials and Tests Division of TxDOT and Houston District Laboratory personnel for their support.

REFERENCES

1. Hazlett, D. G. *Evaluation of Moisture Susceptibility Tests for Asphalt Concrete.* Report 3C2102. Texas Department of Transportation, 1985.

2. Anderson, D. A., E. L. Dukatz, and J. C. Petersen. The Effect of Antistrip Additives on the Properties of Asphalt Cement. *Proc., Association of Asphalt Paving Technologists,* Vol. 51, 1982, pp. 298–317.
3. King, G. N., H. W. King, O. Harders, P. Chavenot, and J. P. Planche. Influence of Asphalt Grade and Polymer Concentration on the High Temperature Performance of Polymer Modified Asphalt. *Proc., Association of Asphalt Paving Technologists,* Vol. 61, 1992, pp. 29–61.
4. *Standard Specifications for Construction of Highways, Streets, and Bridges.* Texas Department of Transportation, 1993.
5. *Manual of Testing Procedures* (Vol. 2). Texas Department of Transportation, 1991.
6. Dybalski, J. Cationic Surfactants in Asphalt Adhesion. *Proc., Association of Asphalt Paving Technologists,* Vol. 51, 1982, pp. 293–297.

Publication of this paper sponsored by Committee on Characteristics of Nonbituminous Components of Bituminous Paving Mixtures.

Evaluation of Natural Sands Used in Asphalt Mixtures

KEVIN D. STUART AND WALAA S. MOGAWER

Five tests for sands were studied to determine whether they could distinguish good-performing from poor-performing natural sands. Performance was based on the effects of the sands on asphalt pavement rutting. The methods were National Aggregate Association Method A, direct shear, ASTM Method D3398, Michigan Department of Transportation Method MTM 118-90, and a flow rate method. The best methods for predicting how the sands would perform in pavements were the flow rate method and ASTM Method D3398. The combined effect of shape, texture, gradation, and quantity of sand on the susceptibility of an asphalt mixture to rutting was evaluated using Marshall stability and flow, the U.S. Army Corps of Engineers gyratory testing machine, Georgia loaded-wheel tester, and the French pavement rutting tester. None of these tests differentiated the poor- from the good-quality sands in the particular mixture tested.

Asphalt paving mixtures containing natural sands are generally more susceptible to rutting, shoving, and bleeding than mixtures containing 100 percent manufactured (crushed) fine aggregates. However, some natural sands have performed as well as manufactured fine aggregates. Natural sands range in shape from very round to angular, depending on their mineralogy and geologic history. The performance of an asphalt mixture can also depend on the quantity of sand used.

The Federal Highway Administration's (FHWA's) Technical Advisory T5040.27 provides the following recommendations regarding natural sands:

> The quality of natural sand varies considerably from one location to another. Since most natural sands are rounded and often contain some undesirable materials, the amount of natural sand as a general rule, should be limited to 15 to 20 percent for high volume pavements and 20 to 25 percent for medium and low volume pavements. These percentages may increase or decrease depending on the quality of the natural sand and the types of traffic to which the pavement will be subjected. (*1*)

This recommendation is somewhat vague, but tests that can predict the pavement performances of mixtures containing natural sands and set maximum allowable percentages for these sands are not available.

OBJECTIVES

The primary objective of this study was to evaluate the ability of methods that measure the particle shape and texture of sands to distinguish good- from poor-performing sands. Performance was based on the effects of the sands on pavement rutting. By using these tests, poor-quality sands could be rejected or only low percentages used in a mixture. Five methods were evaluated:

- National Aggregate Association (NAA) Method A,
- Direct shear,
- ASTM Method D3398,
- Michigan Department of Transportation Method (MTM) 118-90, and
- Flow rate.

A second objective was to examine the combined effect of shape, texture, gradation, and quantity of sand on the susceptibility of an asphalt mixture to rutting using Marshall stability and flow, the U.S. Army Corps of Engineers gyratory testing machine (GTM), Georgia loaded-wheel tester (GLWT), and the French Laboratoires des Ponts et Chaussées (LPC) pavement rutting tester. Part of this objective was to learn whether the GTM can be used to determine how much natural sand can be incorporated into a mixture.

EVALUATION OF SAND TESTS

Types of Sands

Four good- and five poor-quality natural sands and three good-quality manufactured fine aggregates were tested in this study. (All these materials are called sands in this paper for convenience.) The sands were tested for gradation and specific gravity, washed through a 0.075-mm sieve to remove most of the dust, dried at 110°C, and sieved into the size fractions needed for the methods. Gradations are given in Table 1.

The pavement performances of the Virginia and Maryland manufactured sands, the poor-quality New Jersey and Wisconsin sands, and the good-quality White Marsh and Fredericksburg sands were determined through previous studies conducted by FHWA. The performances of the other sands were based on the experiences of the state highway agencies. These sands consistently performed either poorly or well when used in mixtures subjected to high traffic volumes. This requirement was important because only one coarse aggregate was to be used in the mixture evaluation. The two poor-quality sands received from the Georgia Department of Transportation (GDOT) are no longer used in pavements that carry more than 2,000 vehicles per day. Up to 20 percent sand is allowed when the traffic is 1,000 to 2,000 vehicles per day. The Arkansas State Highway and Transportation Department allows up to 15 percent natural sand in mixtures subjected to high traffic volumes.

K. D. Stuart, Federal Highway Administration, Turner-Fairbank Highway Research Center, 6300 Georgetown Pike, McLean, Va. 22101-2296. W. S. Mogawer, Department of Civil Engineering, University of Massachusetts Dartmouth, North Dartmouth, Mass. 02747.

TABLE 1 Gradations of the Sands

	Percent Passing (mm)								
	12.5	9.5	4.75	2.36	1.18	0.600	0.300	0.150	0.075
Poor Quality Natural Sand									
Rheinhart, GA	100.0	100.0	100.0	99.9	99.7	92.2	40.6	4.1	0.6
A. N. Adcock, GA	100.0	100.0	99.3	99.0	98.3	91.2	56.6	12.8	4.8
New Jersey	100.0	100.0	100.0	98.1	89.2	64.5	25.8	5.2	0.6
Wisconsin	100.0	100.0	98.8	84.2	67.9	51.0	22.1	6.4	3.1
Graham Pit, AR	100.0	100.0	100.0	100.0	100.0	100.0	93.4	24.5	11.2
Good Quality Natural Sand									
Anthony Dairy, GA	100.0	100.0	99.0	95.6	85.1	64.5	37.7	20.8	11.0
Oxford Gray, GA	100.0	100.0	99.8	98.5	90.9	68.0	35.9	18.5	10.7
White Marsh, MD	100.0	100.0	97.2	86.8	73.2	52.2	19.0	3.9	1.5
Fredericksburg, VA	100.0	100.0	98.7	93.6	81.7	56.8	21.7	5.4	1.8
Manufactured Sand									
Manassas Traprock, VA	100.0	100.0	96.8	75.5	52.4	38.0	27.4	19.5	13.3
Texas Marble, MD	99.4	98.6	97.1	94.0	86.3	66.1	32.9	15.0	7.0
Donnafill, AR	100.0	100.0	100.0	100.0	99.7	95.3	64.8	40.4	23.6

Microscopic analyses showed that all good-quality sands were angular, whereas all poor-quality sands were rounded, subangular, or subangular to angular.

Size fractions between the 2.36- and 0.150-mm sieves were tested. The variable performances of natural sands are associated with sizes within this range. The NAA method also specifies this range.

The Michigan method was also performed on the 2.36- to 0.600-mm size fraction because the method specifies this fraction. As reported elsewhere, this size fraction did not provide data that agreed with pavement performance (*2*). One reason for this may be that several sands had very little material retained on the 0.600-mm sieve, and thus the data may not have been representative of the entire sand. The Michigan method discussed in this paper is a modified method because size fractions between 2.36 mm and 0.150 mm were tested.

Data were generated for both as-received and NAA gradations. "As-received gradation" means that the sands were proportioned according to the as-received gradations after removing the plus 2.36-mm and minus 0.150-mm size fractions. "NAA gradation" means that the sands were proportioned as specified by NAA Method A. In this method, a 190-g sample of sand is graded as follows: 44 g of 2.36 to 1.18 mm, 57 g of 1.18 to 0.600 mm, 72 g of 0.600 to 0.300 mm, and 17 g of 0.300 to 0.150 mm. A standard gradation is needed because this method relates shape and texture to void contents. These void contents would be a function of gradation and shape and texture if different gradations were used.

The data for as-received gradations are reported elsewhere (*2,3*). These gradations provided similar results for the ASTM D3398 and direct shear methods but poorer results in the NAA Method A, Michigan, and flow rate methods. A standard gradation should be used in the latter three methods.

Some sands did not contain sufficient material for testing the size fraction above 1.18 or 0.600 mm. NAA Method A does not include an approach for testing sands that do not have all four size fractions. When any of the size fractions were missing, the required masses for these missing fractions were eliminated. The sand was then proportioned according to the masses specified for the remaining fractions. Therefore, all of the sands did not have the same gradation.

The volume of each sand must be determined for the NAA, ASTM D3398, and flow rate methods by dividing the mass of the sand by its bulk-dry specific gravity. The specific gravity of each individual size fraction present in amounts of 10 percent or more by mass was measured as required by ASTM D3398. This is very time-consuming, but it is specified because individual size fractions are tested in this method; the specific gravities of some materials, such as slags, can vary significantly from size fraction to size fraction.

Methods Used To Measure Sand Shape and Texture

NAA Method A

This method evaluates shape and texture in terms of the percentage of voids in a dry, uncompacted sample (*4*). High voids usually indicate high angularity and a rough texture. Low voids usually indicate the sand is rounded and smooth. (NAA Method B, which tests individual size fractions, was not evaluated.)

The blend of sand is poured through a funnel into a weighed, 100-cm^3 calibrated cylinder. Excess sand on top of the cylinder is struck off, and the mass of the collected sand is determined. The volume of the collected sand is calculated by dividing this mass by the bulk-dry specific gravity. The uncompacted void content is the difference between the volume of the cylinder and the volume of the collected sand. The percent uncompacted voids is then calculated on the basis of the volume of the cylinder.

Direct Shear

The resistances of compacted sands to displacement can be measured by the internal friction angle ϕ using the direct shear appa-

ratus (*5,6*). The blend of sand is placed in the apparatus and a normal stress is applied to consolidate it. A shear stress is then gradually applied until it reaches a maximum. Three different normal stresses are used. A graph of normal stress versus maximum shear stress is constructed, and the slope of the plot represents ϕ.

ASTM Method D3398

ASTM Method D3398 calculates a particle index called I_a for each size fraction (*7*). Each fraction is compacted in a calibrated mold in three layers using 10 drops of a standard tamping rod. The percentage of voids in each fraction is the difference between the volume of the mold and the volume of the sand. The volume of the sand is the mass of the sand in the mold divided by the bulk-dry specific gravity. The method is then repeated using 50 drops per layer. The I_a for each size fraction is calculated as follows, using both the percentage of voids at 10 drops (V_{10}) and the percentage of voids at 50 drops (V_{50}):

$$I_a = 1.25V_{10} - 0.25V_{50} - 32.0$$

A weighted average I_a is then calculated on the basis of the percentages of the sand fractions in the grading.

This method uses the same concept as NAA Method A in that shape and texture are based on uncompacted void contents. The equation calculates the voids for an uncompacted state and subtracts the voids for polished, single-sized spheres, which is 32.0 percent (*7*). Testing each size fraction eliminates the need for a standard gradation but makes the method time-consuming.

Michigan Test Method

MTM 118-90 provides an angularity index (AI) (*8*). The concept of determining shape and texture on the basis of uncompacted voids is also used by this method.

The method places 100 mL of distilled water into a 250-mL-capacity graduated cylinder and pours 250 g of sand into it. The volume of the sample in water (solids plus voids filled with water) and the total volume (volume at the water level) are measured to the nearest 1 mL. The volume of the solids is equal to the total volume minus the 100 mL of water. The volume of voids is equal to the volume of the sample in water minus the volume of the solids. The angularity void ratio is the ratio of the volume of voids to the volume of solids. The AI is then calculated as follows:

$$AI = (10.0)(\text{angularity void ratio} - 0.6)$$

This method has an advantage over the NAA, ASTM, and flow rate methods in that the bulk-dry specific gravity of the sand is not needed. The volume of the sand is determined through the displacement of water. However, the volume of any absorbed water will be included in the volume of the voids.

Flow Rate Method

This method was developed by the Bureau of Public Roads (now FHWA) but was later modified (*9–11*). It provides a shape-texture index (STI).

The method was performed according to the NAA procedure using the NAA apparatus with the exceptions that 500 g of sand was used instead of 190 g and the time the sand needed to flow out of the funnel was recorded instead of determining its uncompacted void content (*11*).

The flow rate of the sand is calculated by dividing the volume of the sand (cm^3) by the flow time (sec), which is the time needed by the sand to flow out of the funnel. The volume of the sand is calculated by dividing its 500-g mass by the bulk-dry specific gravity. An STI is calculated by dividing the flow rate for a standard set of round balls by the flow rate for the sand. Therefore, the STI of a sand is proportional to its flow rate. The flow rate for the standard set of balls used in this study was 13.70 (*11*).

Both the STIs and the flow times were used to evaluate the sands. Using the flow time does not account for the variations in the volumes of the sands.

Both individual size fractions and the blends of sands were tested, but testing individual size fractions did not affect the conclusions, required more sand, and was more time-consuming. The data using individual size fractions are reported elsewhere (*2*).

Results and Discussion

The sands were ranked from 1 to 12 according to the average value. A ranking of 1 indicates that the sand was most angular or rough textured according to the method. An analysis of variance and Fisher's least significant difference statistical procedures were used to determine whether any of the poor-quality natural sands ranked better than or equal to any of the good-quality natural or manufactured sands at a 95 percent confidence level. The test results are given in Table 2.

NAA Method A

The poor-quality Graham Pit sand ranked the same as the good-quality White Marsh sand. Thus, NAA Method A was slightly deficient in its ability to determine quality. The Graham Pit sand lacked both size fractions above 0.600 mm. Poor- and good-quality sands will divide at an uncompacted void content around 44.7 percent.

Direct Shear

The poor-quality Wisconsin sand ranked higher than all good-quality natural sands. There was also no significant difference between the poor-quality New Jersey sand and the good-quality Oxford Gray sand. The ability of this method to quantify shape and texture was not as good as the other methods evaluated in this study. This method was also time-consuming.

No reason for the high ranking for the Wisconsin sand was known. This sand had highly rounded particles and was well graded. It was hypothesized that the sand compacted to a high degree during the procedure, causing it to resist shear. Size fractions may have to be tested individually using this method.

ASTM Method D3398

All of the poor-quality sands statistically ranked lower than all of the good-quality sands. Poor- and good-quality sands will divide at a weighted average I_a between 11.7 and 13.9.

TABLE 2 Results of Sand Tests and Rankings

	NAA Method A, Percent Uncompacted Voids		Direct Shear, Internal Friction Angle ϕ		ASTM D 3398, Weighted Average Particle Index I_a		Michigan Angularity Index		Flow Rate Method: Shape-Texture Index (STI)		Flow Rate Method: Flow Time	
Poor Quality Natural Sand												
Rheinhart	43.6	8	47.0	10	11.7	8	0.4	11	0.99	9	13.8	9
A. N. Adcock	42.7	9	44.5	11	10.7	11	1.2	8	0.98	10	13.6	10
New Jersey	41.5	10	47.2	9	11.6	9	0.8	9	1.04	7	14.4	8
Wisconsin	40.4	11	51.6	3	10.8	10	0.7	10	1.01	8	13.8	9
Graham Pit	44.7	7	47.2	9	10.1	12	1.6	6	0.79	11	12.5	11
Good Quality Natural Sand												
Anthony Dairy	45.0	6	49.9	5	13.9	7	1.6	6	1.12	5	16.2	4
Oxford Gray	45.5	5	48.8	8	14.0	6	2.1	3	1.06	6	15.9	5
White Marsh	44.7	7	49.8	6	14.5	4	1.4	7	1.12	5	15.5	7
Fredericksburg	46.3	3	49.6	7	15.8	3	1.8	5	1.15	4	16.5	3
Manufactured Sand												
Manassas Traprock	47.9	2	59.3	1	17.5	2	2.8	2	1.34	1	17.0	1
Texas Marble	45.8	4	54.7	2	14.3	5	1.9	4	1.21	3	15.6	6
Donnafill	50.6	1	51.5	4	18.9	1	3.5	1	1.22	2	16.8	2

Michigan Test Method

The poor-quality Graham Pit sand ranked higher than the good-quality White Marsh sand and was statistically equal to the good-quality Anthony Dairy sand. This method was not as accurate as the ASTM D3398 and the flow rate methods. The Graham Pit sand lacked both size fractions above 0.600 mm.

Flow Rate Method

All of the poor-quality sands statistically ranked lower than all of the good-quality sands according to the STIs and flow times. Poor- and good-quality sands will divide at an STI around 1.05 and at some flow time between 14.4 and 15.5.

Obtaining the flow times is less time-consuming than obtaining STIs because the bulk-dry specific gravities of the sands are not needed. Even though the flow times do not account for the variations in the volumes of the sands, they differentiated the poor- from the good-quality sands better than the STIs. A reason for this was not apparent.

MIXTURE STUDY

Types of Mixtures

The good-quality Fredericksburg and Oxford Gray sands and the poor-quality A. N. Adcock and Wisconsin sands were tested in mixtures. The A. N. Adcock sand consistently provided poor rankings according to the sand tests, and the Wisconsin sand was the most rounded sand. Each sand was blended with No. 10 traprock screenings and an 11.1-mm traprock coarse aggregate. This aggregate was used in pavements tested by the accelerated loading facility (ALF) machine located at the FHWA Turner-Fairbank Highway Research Center. The No. 10 traprock screenings are the Manassas traprock material that was tested for shape and texture.

Twelve aggregate blends for the four natural sands were prepared by using 10, 20, or 30 percent natural sand by total aggregate mass. These percentages provided natural sand contents of 28, 56, and 77 percent in the 2.36- to 0.150-mm size fraction using the poor-quality A. N. Adcock sand and contents of 27, 50, and 75 percent using the poor-quality Wisconsin sand. One control aggregate blend having no natural sand was also prepared. The gradations of the blends are given in Table 3.

The aggregates were blended by adjusting the percentages of coarse aggregate and screenings according to the percentage of natural sand. This duplicates what is done in practice. However, this provided different gradations, including different dust contents. This could confound the experimental design. For example, the decrease in dust content with increasing natural sand content could itself increase rutting potential. It was assumed that the effects of the natural sands would still be apparent, but if the data were difficult to interpret, other approaches for blending the aggregates would be tried. (Alternative approaches would be to equalize the dust contents or the entire gradation.) The asphalt was an AC-20.

Mixture Tests

Mixture Design

The mixtures were designed by the 75-blow Marshall method. Specimens tested for rutting were prepared at the asphalt contents corresponding to a 4 percent air void level.

GTM

The rutting susceptibilities of the 13 mixtures were evaluated by measuring the gyratory stability index (GSI) and the gyratory elas-

TABLE 3 Aggregate Gradations (Percent Passing) for the Mixtures

Sieve Size (mm)	0 %	A. N. Adcock Sand 10 %	A. N. Adcock Sand 20 %	A. N. Adcock Sand 30 %	Fredericksburg Sand 10 %	Fredericksburg Sand 20 %	Fredericksburg Sand 30 %	Wisconsin Sand 10 %	Wisconsin Sand 20 %	Wisconsin Sand 30 %	Oxford Gray Sand 10 %	Oxford Gray Sand 20 %	Oxford Gray Sand 30 %
12.5	100.0	100.0	100.0	100.0	100.0	100.0	100.0	100.0	100.0	100.0	100.0	100.0	100.0
9.5	94.2	94.7	94.2	94.2	95.9	95.7	95.4	94.5	94.6	95.0	94.5	94.3	94.2
4.75	55.3	59.0	55.8	56.0	67.2	66.0	64.2	57.6	58.4	61.4	57.7	56.6	56.2
2.36	34.9	40.6	39.6	41.9	48.2	48.7	48.4	37.8	39.3	42.9	39.2	40.2	41.8
1.18	24.3	31.2	33.4	38.0	35.2	37.2	38.7	27.2	29.2	32.7	29.5	32.4	35.8
0.600	18.1	25.1	28.8	34.1	25.6	26.9	27.8	20.4	22.1	24.7	22.1	24.5	27.1
0.300	13.7	17.7	19.5	22.4	17.0	16.0	14.7	13.8	13.5	13.9	15.2	15.6	16.2
0.150	10.2	10.3	8.9	8.2	11.4	9.7	7.8	9.4	8.2	7.5	10.6	10.2	9.9
0.075	7.2	6.9	5.5	4.7	7.8	6.5	5.0	6.5	5.6	5.0	7.3	6.8	6.5
NAA Method A, Percent Voids (Min = 44.7)		45.6 Pass	43.5 Fail	42.2 Fail				46.1 Pass	44.8 Pass	42.2 Fail			
STI (Min = 1.05)		1.23 Pass	1.17 Pass	1.09 Pass				1.24 Pass	1.17 Pass	1.09 Pass			
Flow Time, s (Min Between 14.4 and 15.5)		16.1 Pass	15.7 Pass	14.8 **				15.8 Pass	15.0 **	14.5 **			

Min = Minimum criterion established in this study.
** = Pass/fail could not be established.

toplastic index (GEPI) using the U.S. Army Corps of Engineers GTM, Model 6B4C. The GTM is a combination compaction and plane strain shear testing machine that applies stresses simulating pavement conditions. The GTM provides a gyratory angle that is a measure of shear strain.

The GSI is the ratio of the maximum angle that occurs at the end of the test to the minimum intermediate angle. It is a measure of shear susceptibility at the refusal, or ultimate, density. The GSI at 300 revolutions is close to 1.00 for a stable mixture and is significantly above 1.10 for an unstable mixture (*12*).

The GEPI is the ratio of the minimum intermediate angle to the initial angle. A GEPI of 1.00 indicates high internal friction. A GEPI significantly above 1.00 indicates lower internal friction due to rounded aggregates. (The manufacturer suggests using an acceptable range of 1.00 to 1.50 and a marginal range of 1.51 to 1.65.) A GEPI below 1.00 indicates that the aggregate is deteriorating.

The GTM was operated in accordance with the National Cooperative Highway Research Program's Asphalt-Aggregate Mixture Analysis System (*13*). The diameter of each specimen was 101.6 mm, and the heights after compaction were approximately 63.5 mm. A vertical pressure of 0.827 MPa, a 0.035-radian gyratory angle, and the oil-filled roller were used.

Specimens were initially compacted to a 6 percent air void level at 143°C. The specimens in their molds were then placed in an oven at 60°C for 3 hr. They were then compacted to refusal density at 60°C using 300 revolutions. A trace of the gyratory angle versus revolutions was obtained to determine the maximum and minimum intermediate angles.

GLWT

Rutting susceptibilities were also evaluated by the GLWT, shown in Figure 1. The control mixture and the four mixtures containing 20 percent natural sand were tested. Twenty percent is the limit recommended for mixtures subjected to heavy traffic by the FHWA advisory (*1*).

The GLWT tests a beam for permanent deformation at 40.6°C. Each beam is 76.2 mm in width and thickness and 381 mm in length. The air voids of the beams ranged from 4.4 to 5.1 percent. These voids were slightly above the target level of 4.0 percent, but the densities were within 97 percent of the Marshall design densities as recommended by GDOT.

The beams were cured for 7 days at room temperature and for 24 hr at 40.6°C. The sides of a beam are confined by steel plates during the test except for the top 12.7 mm. A 690-kPa, pressurized, stiff rubber hose is positioned across the top of the beam and a loaded steel wheel runs back and forth on top of this hose for 8,000 cycles to create a rut. One cycle is two passes of the wheel.

The load was found to vary with the direction of travel. When the wheel was moving from right to left, the load was approximately 740 N at the center of the beam, whereas it was 630 N when moving left to right. Across the central region of the beam

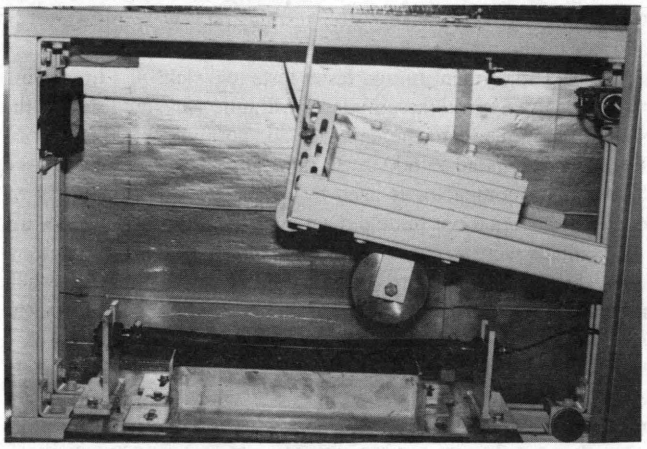

FIGURE 1 GLWT.

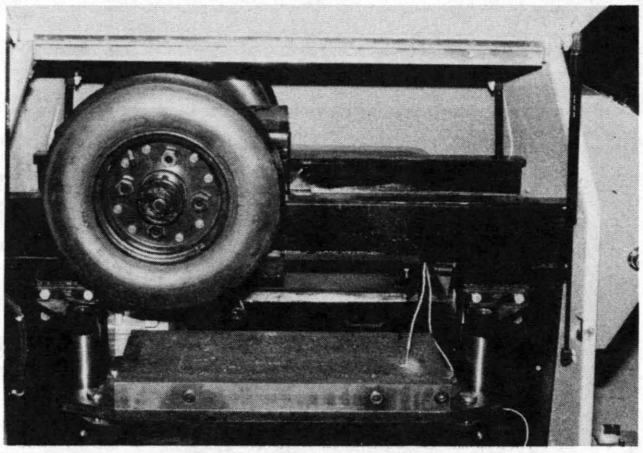

FIGURE 2 LPC pavement rutting tester.

where the deformations are recorded, each of these loads had a variation of less than 5 percent.

Deformations are measured at the center of the beam, 51 mm left of the center, and 51 mm right of the center. The data are averaged. If the average rut depth for three replicate beams exceeds 7.6 mm, the mixture is considered susceptible to rutting (*14*). Testing one beam requires 4 hr.

LPC Pavement Rutting Tester

Rutting susceptibilities were also evaluated by the LPC pavement rutting tester, shown in Figure 2. The machine tests a slab for permanent deformation at 60°C. Each slab had a length of 500 mm, a width of 180 mm, and a thickness of 50 mm.

The slabs were fabricated using the LPC plate compactor. Each slab is compacted in a steel mold using a smooth, reciprocating, pneumatic rubber tire that has a diameter of 415 mm and a width of 109 mm. Various sequences of different compactive efforts, tire pressures, and positions of the tire relative to the width of a slab are used to compact a slab. These parameters depend on the thickness of the slab and the desired air-void level. The manufacturer verbally stated that the sequence used in this study should provide a uniformly distributed air-void level of around 5 to 6 percent for dense-graded mixtures. Air-void levels before testing were measured using the entire slab. After testing, they were measured in and out of the wheelpath after sawing.

The LPC pavement rutting tester tests two slabs at a time using two reciprocating tire assemblies. Hydraulic jacks underneath the slabs push upward to create the load, normally 5000 ± 50 N. Each tire is inflated to 600 ± 30 kPa. The same type of tire used by the plate compactor is used by this tester. Approximately 67 cycles are applied per minute. One cycle is two passes of the tire.

The slabs were cured at room temperature in their molds for 4 days, then placed in the pavement rutting tester and tested in their molds. Initially, 1,000 cycles are applied at 25°C to densify the mixture and to provide a smoother surface. The height of each slab is then calculated by averaging measurements taken at 15 specified positions using a depth gauge with a resolution of 0.1 mm. This average height is considered the initial height, or point of zero rut depth. The slabs were then heated to 60°C for 6 hr. The tester was started, and the average rut depths at 30, 100, 300, 1,000, and 3,000 cycles were measured. To apply 3,000 cycles, 2 to 2.5 hr is needed.

A mixture is acceptable if the average rut depths at 1,000 and 3,000 cycles are less than or equal to 10 and 20 percent of the thickness of the slab, respectively. Slopes for different mixtures taken from log rut depth versus log cycles plots can also be compared. Rut-susceptible mixtures generally have higher slopes.

Results and Discussion

Mixture Design

Mixture design properties are given in Table 4. The Marshall stabilities of 12 out of 13 mixtures were above the minimum stability of 8006 N required for heavy traffic levels (*15*). The mixture containing the poor quality A. N. Adcock sand at a 30 percent level was slightly below 8006 N. (State highway specifications use either a minimum stability of 8006 N or 6670 N.) All flows met the required limits of 8 to 14 (*15*). There was a slight trend of decreasing flow with increasing natural sand content. An opposite trend would be expected, especially since the dust contents also decreased with increasing natural sand content. This anomaly could not be explained from the data collected.

GTM

The GTM results are given in Table 5. The variation in GEPI from mixture to mixture was small, and all GEPIs were less than 1.50. The GSIs were slightly more variable, but the differences were also low. It was expected that the GSIs or GEPIs for the poor-quality sands would be significantly higher than for the good-quality sands and that they would increase with increasing sand content. This did not occur. The GSI and GEPI did not differentiate the poor- from the good-quality sands. No trends in the refusal air-void levels were found.

The GSIs for the good-quality Fredericksburg sand and the poor-quality A. N. Adcock and Wisconsin sands at a 20 percent level were statistically equal. These mixtures should perform similarly. However, the mixture with the 20 percent Fredericksburg sand did not rut in pavements tested by the ALF machine.

The GSI for the good-quality Fredericksburg sand at a 30 percent level was statistically higher than the GSIs for the poor-quality A. N. Adcock and Wisconsin sands. The higher GSI and the low refusal air-void level of 1.3 percent could be due to the higher asphalt content of this mixture, as shown in Table 4.

GLWT

The GLWT results are given in Table 5. The average rut depths did not correlate with the quality of the sand, and none of the rut depths exceeded the specification level of 7.6 mm. All rut depths were statistically equal.

LPC Pavement Rutting Tester

The LPC pavement rutting tester results are given in Table 6. The percent rut depths did not correlate with the quality of sand, and

TABLE 4 Marshall Mixture Design Properties

	Optimum Asphalt Content (%)	MSG	Density (kg/m³)	Stability (N)	Flow (0.25-mm)	VMA (%)	VFA (%)
0 % Natural Sand	5.0	2.648	2541	14 230	13	14.8	72.9
Poor Quality							
10 % A. N. Adcock	4.4	2.649	2542	11 530	10	13.5	70.4
20 % A. N. Adcock	4.5	2.618	2512	9 820	9	14.2	71.9
30 % A. N. Adcock	4.9	2.578	2474	7 890	8	15.8	74.7
10 % Wisconsin	4.4	2.653	2528	14 670	12	14.3	67.2
20 % Wisconsin	4.5	2.632	2523	15 050	10	14.2	71.3
30 % Wisconsin	4.6	2.616	2506	13 150	10	14.5	71.1
Good Quality							
10 % Fredericksburg	5.1	2.624	2518	12 600	11	14.4	72.2
20 % Fredericksburg	5.5	2.582	2480	12 720	10	15.5	74.2
30 % Fredericksburg	6.3	2.528	2427	10 920	10	17.5	77.1
10 % Oxford Gray	4.3	2.650	2539	17 020	13	13.3	68.9
20 % Oxford Gray	4.2	2.627	2517	15 610	13	13.1	68.6
30 % Oxford Gray	4.3	2.601	2492	14 600	10	13.3	68.9

Marshall Design Blows = 75
Mixing Temperature = 154 °C
Compaction Temperature = 143 °C

MSG = Maximum Specific Gravity of the Mixture
VMA = Voids in the Mineral Aggregate
VFA = Voids Filled with Asphalt

none of them exceeded 10 percent at 1,000 cycles or 20 percent at 3,000 cycles. The poor-quality sands did not have higher slopes.

The initial air voids of the slabs before testing are also given in Table 6. These levels were higher than expected since the compaction procedure used in this study reportedly provides an air-void level around 5 to 6 percent. All levels were above 6 percent.

The data in Table 6 appear to indicate that the air voids in the wheelpath decreased during testing. However, by evaluating the air voids in and out of the wheelpath after testing and by sawing additional untested slabs, it was found that the air voids were lower in the middle of the slabs than at the edges before testing. The air voids decreased very little, if at all, from testing.

Additional Sand Tests

The lack of significant differences in rutting potential was not expected. The differences in gradation, binder content, and sand

TABLE 5 GTM and GLWT Results

	GTM, Average GEPI	GTM, Average GSI	GTM, Average Refusal Air Voids (%)	GLWT, Average Rut Depth (mm)
0 % Natural Sand	1.00	1.00	3.6	3.3
Poor Quality				
10 % A. N. Adcock	1.05	1.15	2.2	
20 % A. N. Adcock	1.05	1.10	1.9	5.2
30 % A. N. Adcock	1.10	1.05	2.0	
10 % Wisconsin	1.05	1.20	2.3	
20 % Wisconsin	1.05	1.20	1.7	3.3
30 % Wisconsin	1.05	1.10	2.8	
Good Quality				
10 % Fredericksburg	1.10	1.10	2.6	
20 % Fredericksburg	1.05	1.10	2.8	4.4
30 % Fredericksburg	1.10	1.20	1.3	
10 % Oxford Gray	1.05	1.10	2.8	
20 % Oxford Gray	1.05	1.05	3.1	3.7
30 % Oxford Gray	1.10	1.10	3.0	

TABLE 6 LPC Pavement Rutting Tester Results

	Percent Rut Depth			Initial Specimen Air Voids (%)	Air Voids In Wheel-Path After Testing (%)	Air Voids Outside of Wheel-Path (%)
	1000 Cycles	3000 Cycles	Slope			
0 % Natural Sand	5.1	6.7	0.27	8.8	7.2	10.5
Poor Quality						
20 % A. N. Adcock	4.6	6.0	0.22	6.1	3.5	7.6
20 % Wisconsin	3.3	4.3	0.23	6.2	4.0	7.7
Good Quality						
20 % Fredericksburg	5.2	7.3	0.32	7.5	5.4	9.0
20 % Oxford Gray	4.2	5.9	0.24	7.5	4.6	8.8

content should more likely produce differences in the data that would be difficult to relate to the percentage of natural sand alone. Possible reasons for the lack of differences were that the characteristics of the poor-quality natural sands were masked by the other aggregates, the mixture tests are not sensitive enough for measuring the effects of natural sands, or a combination of the two.

NAA Method A and the flow rate method were performed on the 2.36- to 0.150-mm size fractions of the aggregate combinations containing the two poor-quality natural sands to determine the quality of the blend of materials. These data are included in Table 3. The results are mixed, but they do not clearly show that the 20 percent level used in the wheel-tracking devices, which provided approximately 53 percent natural sand in the 2.36- to 0.150-mm size fraction, should lead to rutting. However, the data, especially the STIs, introduce a problem with testing blends of sands. The criteria developed in this study were based on testing individual poor- and good-quality sands. Any poor-quality sand with a value slightly under the minimum criterion will pass the method when blended with only a small amount of good-quality material. Some poor-quality sands may always provide a passing value when blended. However, this blend could fail another method. The different methods do not provide the same ranking for poor-quality sands, and field performance data are insufficient to develop a true ranking. Therefore, these methods should only be performed on unblended sands.

CONCLUSIONS

Methods Used To Measure Sand Shape and Texture

1. ASTM Method D3398 differentiated all of the poor-quality sands from all of the good-quality sands. Poor- and good-quality sands will divide at some weighted average particle index (I_a) between 11.7 and 13.9. (All criteria are for heavy traffic pavements.)

2. The STIs and the flow times from the flow rate method differentiated all of the poor-quality sands from all of the good-quality sands. Poor- and good-quality sands will divide at an STI around 1.05 and at some flow time between 14.4 and 15.5.

3. NAA Method A did not differentiate the sands perfectly. One poor-quality sand ranked the same as one good-quality sand. Poor- and good-quality sands will divide at an uncompacted void content around 44.7.

4. The Michigan method did not differentiate the sands perfectly. One poor-quality sand ranked better than one good-quality sand and equal to another good-quality sand.

5. The direct shear method was not as good as other methods evaluated in this study. This test is also time-consuming.

6. The best method was the flow time. The flow times matched the qualities of the sands and was the easiest parameter to obtain.

7. Methods for measuring shape and texture can only be expected to group sands into generalized performance categories, such as high or low potential for rutting. The performance of a sand depends on its quality, the quantity used, the qualities of the other aggregates, and traffic level.

8. Each sand should be tested to determine its rutting potential. The methods are not sensitive enough to evaluate the blend of materials found in a job-mix formula gradation.

9. The discrepancies provided by the NAA and the Michigan methods may be related to gradation. A single, standard gradation should be used in these methods so that the voids they provide are only a function of shape and texture. However, natural sands have widely different maximum particle sizes. Thus, specifying a standard gradation will mean that some sands cannot be tested. Theoretically, a standard gradation should also be used in the flow rate method, even though there were no discrepancies in this study.

Mixture Tests

The Marshall design data, GSI and GEPI from the GTM, and the rut depths from the GLWT and LPC pavement rutting tester did not differentiate the poor- from the good-quality sands. How much natural sand can be incorporated into a mixture could not be established using the GTM data. Reasons for this lack of differentiation could not be established from the information collected.

RECOMMENDATIONS

1. Highway agencies should try both the flow rate method and NAA Method A for evaluating their natural sands using the gradation and apparatus specified by the NAA method.

2. ASTM Method D3398 can also be used. However, this method has not been widely used in the past because it is very time-consuming.

3. The Michigan method is quick and easy to perform. However, this method should only be performed on sands where a single, standardized gradation can be used. This recommendation may also apply to NAA Method A. NAA Method B, which tests individual size fractions, may have to be used when size fractions are missing.

4. Additional mixtures should be tested to determine the validity of the mixture tests used in this study. Other mixture tests, or variations of the tests used in this study, may be needed.

REFERENCES

1. *Asphalt Concrete Mix Design and Field Control.* FHWA Technical Advisory T5040.27. FHWA, U.S. Department of Transportation, March 1988.
2. Stuart, K. D., and W. S. Mogawer. *Evaluation of Natural Sands Used in Asphalt Mixtures.* FHWA-RD-93-070. Federal Highway Administration, U.S. Department of Transportation, McLean, Va., June 1993.
3. Mogawer, W. S., and K. D. Stuart. Evaluation of Test Methods Used To Quantify Sand Shape and Texture. In *Transportation Research Record 1362*, TRB, National Research Council, Washington, D.C., 1992, pp. 28–37.
4. Meininger, R. C. *Proposed Method of Test for Particle Shape and Texture of Fine Aggregate Using Uncompacted Void Content.* National Aggregates Association, Silver Spring, Md., 1990.
5. Das, B. M. *Soil Mechanics Laboratory Manual* (3rd edition). Engineering Press, Inc., 1989.
6. *1990 Annual Book of ASTM Standards.* Section 4, Volume 04.08. ASTM, Philadelphia, Pa., March 1990.
7. *1991 Annual Book of ASTM Standards.* Section 4, Volume 04.03. ASTM, Philadelphia, Pa., April 1991.
8. *Test Method for Measuring Fine Aggregate Angularity.* Michigan Test Method 118-90. Michigan Department of Transportation, Lansing, 1990.
9. Rex, H. M., and R. A. Peck. A Laboratory Test To Evaluate the Shape and Texture of Fine Aggregate Particles. *Public Roads*, Vol. 29, No. 5, Dec. 1956, pp. 118–120.
10. Meier, W. R., Jr., E. J. Elnicky, and B. R. Schuster. *Fine Aggregate Shape and Surface Texture.* FHWA-AZ88-229. Arizona Department of Transportation, Phoenix, 1989.
11. Jimenez, R. A. Flow Rate as an Index of Shape and Texture of Sands. In *Transportation Research Record 1259*, TRB, National Research Council, Washington, D.C., 1990.
12. Roberts, F. L., P. S. Kandhal, E. R. Brown, D. Y. Lee, and T. W. Kennedy. *Hot Mix Asphalt Materials, Mixture Design, and Construction.* National Asphalt Pavement Association Education Foundation, Lanham, Md., 1991.
13. Von Quintus, H. L., J. A. Scherocman, C. S. Hughes, and T. W. Kennedy. *NCHRP Report 338: Asphalt-Aggregate Mixture Analysis System.* TRB, National Research Council, Washington, D.C., 1991.
14. Lai, J. S. *Development of a Laboratory Rutting Resistance Testing Method for Asphalt Mixtures.* FHWA/GA/89/8717. Georgia Department of Transportation, Atlanta, Aug. 1989.
15. *Mix Design Methods for Asphalt Concrete and Other Hot-Mix Types.* Manual Series No. 2, Asphalt Institute, Lexington, Ky., 1988.

Publication of this paper sponsored by Committee on Characteristics of Nonbituminous Components of Bituminous Paving Mixtures.

Empirical Evaluation of Olive Husk in Asphalt Cement Binder and Bituminous Concrete

HASHEM R. AL-MASAEID, MOHAMMAD M. HAMED, AND TAISIR S. KHEDAYWI

The results of an experimental study undertaken to evaluate quantitatively the effects of olive husk material on the properties of both asphalt cement binder and bituminous concrete mixtures are summarized. Olive husk material was added to asphalt cement at four levels, ranging from 0 to 15 percent by total weight of binder. For each husk-asphalt binder, physical behaviors of binder, including penetration at different temperatures, softening point, and ductility tests, were investigated. The previous husk-asphalt binders were used to prepare husk-asphalt mixtures. Three types of aggregate, including limestone, basalt, and granite, were used in this study. For each level of husk-asphalt and aggregate type, Marshall, stripping, Marshall immersion, and indirect tensile tests were performed on the laboratory-made specimens with 50 blows on each face. The results indicated that the addition of olive husk material up to 10 percent by total weight of binder would reduce the binder stiffness at low temperatures, increase the stiffness at high temperatures, and help reduce brittleness and temperature sensitivity of binders. For all types of aggregate mixtures, the addition of olive husk material improved workability and stability and reduced the optimum binder content compared with asphalt mixtures without olive husk. The inclusion of olive husk, up to 10 percent, in bituminous concrete mixtures improved stripping resistance, durability, water and temperature resistance, and resistance to both moisture and repeated freeze-thaw induced damage.

In the Mediterranean region, the climate and soil characteristics encourage farmers to plant olive trees on a large scale. Olive oil is obtained through a pressing process in an olive mill. One problem associated with this process is the formation of hundreds of tonnes of solid olive husk. The use of olive husk material is very limited, and it is adversely affecting vegetation and creating environmental problems, at least in Third World countries. In this paper attention is focused on the potential benefits of using olive husk material in asphalt mixtures.

The purpose of this study is to investigate the efficiency of using olive husk material as an additive and partial substitute for asphalt cement under both normal and freeze-thaw conditions. The physical behaviors of the husk-asphalt binder, including penetration, softening point, and ductility, were examined. Stripping resistances of husk-asphalt mixtures were determined by using Texas boiling and Scandinavian rolling tests. The basic engineering strength properties of the mixtures, including Marshall stability, Marshall immersion stability, and tensile strength under normal and freeze-thaw conditions, was investigated. Three types of aggregate, including limestone, basalt, and granite, and four levels of husk material were used in the study.

Civil Engineering Department, Jordan University of Science and Technology, P.O. Box 3030, Irbid, Jordan.

LITERATURE REVIEW

Several studies have investigated asphalt chemical composition (*1–4*) and the influence of different additives and modifiers on the physical properties of binders (*5–6*) and asphalt mixtures (*6–8*). Other studies have focused on the effects of filler materials on the properties of asphalt binder and on such basic properties of the asphalt mixtures as stability, durability, flexibility, optimum asphalt content, and workability (*9–11*).

Asphalt is a homogeneous mix of many different molecules, which may be differentiated into asphaltenes, resins, and oils. Conversion of oils to resins and resins to asphaltenes takes place inside asphalt through chemical reactions when asphalt is exposed to heat, air, light, or other environmental physical actions (*1*). The conversion process increases the asphaltenes content and produces a more viscous asphalt. In addition, Epps et al. (*2*) indicated that mineral aggregate might absorb the oil fraction and may result in more hardening of the asphalt binder. Accordingly, Noureldin (*3*) suggested a range of oil, resin, and asphaltenes contents for some types of asphalt. Violations of these ranges have some detrimental effect on pavement mixtures. David and Thomas (*4*) pointed that asphalt that has too much asphaltenes content would result in a mixture with potential brittleness and thermal cracking, whereas low asphaltenes would result in moisture sensitivity and rutting problems. To avoid these problems, additives or modifiers are used to bring the asphalt to a suitable chemical composition for consistency and durability.

Additives/modifiers are known to react differently with asphalt, and they produce considerable changes in the physical properties of the binder. Epps (*5*) stated that the ideal modified asphalt binder would contribute to higher stiffness at high temperatures, lower stiffness at cold temperatures, and increase stripping resistance. Fernando and Guirguis (*6*) concluded that the addition of natural rubber to asphalt not only increased the stiffness modulus of asphalt at high temperatures but also reduced the stiffness modulus at low temperatures.

In addition to the role of additives/modifiers in improving the physical properties of binders, other additives are incorporated in asphalt mixtures to improve stripping resistance. The stripping of asphalt from aggregate is defined as the loss of the adhesion strength in the presence of water and has been recognized as a major cause of pavement distress (*7*). Pablo (*8*) indicated that the addition of hydrated lime improved the bonding properties of quartzite and dolomite sands, whereas the addition of amine additive was necessary to maintain good bonding in natural rounded gravel.

The role of mineral fillers has been investigated by many studies. Puzinauskas (*9*) stated that the mineral fillers fill the voids and provide contact points between coarser aggregate particles in the mixtures. Moreover, because of their fineness and surface characteristics, fillers may serve as active materials. Joseph et al. (*10*) investigated the physicochemical effect of the filler on the behavior of filler-asphalt systems and asphalt mixtures. They indicated that the most important filler asphalt interface property is the selective sorption (adsorption and absorption), which is influenced by the complex group composition of asphalt, the physical-chemical properties of the filler surface, and the internal pore structure of the filler particles. Also, they stated that because of the capillary effect of micropores, the filler particles absorb first the low-viscosity components of asphalt with lower molecular weight (oils fraction). The amount of asphalt absorbed is lost asphalt, which does not affect the mechanical behavior of mixtures.

Recently, interest has focused on the use of by-products to provide the benefits of recycling, reduce associated environmental problems, and act as an asphalt extender or as a partial substitute for the asphalt in asphalt mixtures. In a study by Al-Masaeid et al. (*11*), it was found that the substitution of oil shale ash, a by-product of the oil shale rock industry, up to 10 percent by volume of asphalt would improve the performance of mixtures under normal and freeze-thaw conditions. Peltonen (*12*), on the other hand, indicated that the addition of tall oil pitch, a by-product of the sulfate cellulose industry, improves the adhesion and water resistance of pavement mixtures. He also indicated that the addition of selected cellulose fibers from old newspaper materials improves the properties of asphalt mixtures.

In summary, several studies on the performance of different additives, minerals, and by-products have been carried out, but no information is available on the role played by olive husk material in bituminous mixtures. The olive husk particles have a sub-angular geometry with oily texture; they contain traces of oils. It is believed that this material might play a beneficial role in bituminous binder and mixture characteristics. Therefore, this study explored the possible permanent applications of olive husk material in bituminous binders and mixtures.

MATERIALS USED

One asphalt cement (80/100) penetration grade asphalt typically used in pavement construction in Jordan was used in the study. Table 1 presents the properties of the asphalt cement used.

Three types of aggregate were used in the study: crushed limestone, crushed basalt, and crushed granite. These are the major types of aggregate used in pavement construction in Jordan. Their gradations conformed to the Ministry of Public Works and Housing specifications in Jordan. The aggregate gradation is given in Table 2.

The husk material was obtained from Al-Nu'aemh's olive mill. The husk was piled in open space and was about 1 year old. Results of the pyrolysis test carried out at laboratories of the

TABLE 1 Properties of Asphalt Cement Used in Study

Properties	ASTM Test Designation	Test Result
Specific Gravity at 25°C	D 70	1.010
Penetration, (0.1 mm), 100 gm, 5sec	D 5	83.0
Softening Point (°C) Ring and Ball	D 36	47.5
Ductility (cm) at 25°C	D 113	130

TABLE 2 Aggregate Gradations Used in Study

Sieve Size	% Passing	Specification[a]
3/4 in.	100	100
1/2 in.	95	90-100
3/8 in.	85	75-90
# 4	60	45-70
# 8	45	33-53
# 30	25	15-33
# 50	15	10-20
# 100	7	4-16
# 200	5	2-9

[a] Jordan Specification Limits.

TABLE 3 Olive Husk Gradations[a] Used in Study

Size, Micron[b]	Percent Finer
75	100
55	95
45	90
35	83
25	68
15	55
10	50
7	47
3.5	45
1	36

[a] Hydrometer Analysis
[b] 1 μm = 1* 10^{-6} m

Natural Resources Authority, Jordan, indicated that the olive husk material contains about 12 percent oils by total weight. Naturally, olive husk contains fatty amines. The husk fraction passing sieve No. 200 was used in the study. Table 3 gives its gradation by hydrometer analysis on selected samples.

TEST PROCEDURE AND PHASES OF INVESTIGATION

Physical behavior and stripping characteristics of husk asphalt binder were investigated. A Marshall test (ASTM D1559), a Marshall immersion test, and an indirect tensile test were performed on the laboratory-made specimens with 50 blows on each face. The specimen was 4 in. in diameter and 2.5 in. high. To achieve the objectives of this study, five phases of investigation were undertaken.

Phase 1: Physical Behavior of Husk-Asphalt Binder

The objective of this phase was to evaluate quantitatively the effect of husk level on the behaviour of husk-asphalt binder using penetration, softening point, and ductility. The variables in this phase were percent husk by total weight of binder (asphalt + husk) (0, 5, 10, and 15) and penetration 100 g and 5 sec (at 0°C, 10°C, 17.5°C, 5°C, and 35°C).

Asphalt was heated in an oven at 145°C. The required amount of husk was weighed and added slowly in small quantities to the asphalt and stirred into the asphalt at 145°C. Once the required quantity of husk had been added to the asphalt in this manner, mixing was continued for a further 10 min at 1,600 rpm to achieve a homogeneous binder mix.

Results of penetration at the specified temperature levels are presented in Table 4, and Table 5 gives the results of ring-and-ball softening point and ductility tests.

Phase 2: Optimum Husk-Asphalt Binder Content

The objectives of this phase were to determine the optimum husk-asphalt binder content by weight of total mix (conventional bituminous mix) and to evaluate the effect of husk level on the

TABLE 4 Penetration[a] of Husk-Asphalt Binder at Different Temperatures and Percentages of Husk (Results of Phase 1)

Temperature (°C)	Husk Percent[b]			
	0	5	10	15
0.0	3	21	33	29
10.0	13	30	44	38
17.5	27	40	52	47
25	83	101	110	108
35	195	192	198	196

[a] Penetration, 0.1mm, 100gm, 5 Sec.
[b] Husk percent by total weight of binder (Husk Plus Asphalt).

TABLE 5 Softening Point and Ductility of Husk-Asphalt Binder (Results of Phase 1)

Test	Husk Percent			
	0	5	10	15
Softening Point (°C) Ring and Ball	47.5	46.2	47.7	47.9
Ductility (cm) at 25°C	130	118	115	69

optimum binder content. The Marshall test (ASTM D1559) was carried out to determine the optimum binder content. The variables in this phase of study were as follows:

1. Aggregate type (limestone, basalt, and granite),
2. Percent husk by total weight of binder (asphalt + husk) (0, 5, 10, and 15), and
3. Percent binder by total weight of mix (3.5, 4.0, 4.5, 5, 5.5, 6.0, and 6.5).

The procedure used in preparing the bituminous mixtures and testing Marshall specimens is that outlined in Asphalt Institute Manual MS-2 (*13*). In the case of husk-asphalt binder, the binder prepared as explained in Phase 1 was directly added to the heated aggregate. During the course of the work, it was found that control mixtures (mixes with zero husk level) produced unworkable mixes at 3.5 percent binder content. Therefore, all control mixtures were started with 4.0 percent of binder instead of 3.5 percent. Three specimens were prepared for each combination of aggregate, husk, and binder level. Therefore, 81 specimens for each type of aggregate were made. Results of this phase, including optimum binder content and the associated mixture properties for each husk-aggregate combination level, are presented in Table 6.

Phase 3: Moisture Sensitivity of Husk-Asphalt Mixtures

The objective of this phase was to investigate the effect of husk level on moisture resistance of husk-asphalt mixtures. Moisture sensitivity of mixtures, often attributable to stripping, was evaluated by using the Texas boiling test (*14*) and the Scandinavian rolling test. The Scandinavian rolling test is used by the Ministry of Public Works and Housing in Jordan. One hundred g of large aggregate ($^3/_8$- to 4-in. mesh size) was used in preparing each sample. Variables in this phase were as follows:

1. Test type (Texas boiling test and rolling test),
2. Aggregate type (as in Phase 2), and
3. For each husk level, the optimum husk-asphalt binder content obtained in Phase 2 was used to prepare the stripping samples.

TABLE 6 Optimum Husk-Asphalt Binders for Different Aggregate Types and Husk Levels and Their Associated Mixture Properties (Marshall Results, Phase 2)

Agg. Type	Husk Percent	Optimum[a] Binder Content	Marshall Stability lb, 60°C	Flow (0.01 in.)	V.T.M[b] (%)
Limestone	0	5.30	3695	12.1	3.8
	5	4.75	3804	11.0	3.2
	10	4.60	4100	12.0	3.1
	15	4.80	3855	13.5	3.0
Basalt	0	5.00	3660	15.7	4.5
	5	4.50	3780	11.5	4.2
	10	4.75	4338	13.5	4.2
	15	4.80	4220	13.0	4.0
Granite	0	5.00	3117	16.2	4.8
	5	4.50	3220	14.5	4.6
	10	4.66	3228	15.0	4.5
	15	5.00	3205	13.5	4.1

[a] Binder Content: percent by total weight of the mix.
[b] V.T.M: Air voids in the mix, percent by total volume.

For each type of test, 12 samples were prepared. The resultant amount of stripping resistance was determined by five observers and reported in terms of the observed percentage of asphalt coating retained on the aggregate. The results of this phase are given in Table 7.

Phase 4: Durability of Husk-Asphalt Mixtures

The objective of this phase was to evaluate quantitatively the effect of husk on the durability of bituminous mixtures using the Marshall immersion test. This test is recognized as a durability criterion for hot bituminous mixtures (*15*), and it evaluates the combined damaging effects of water and temperature on asphalt mixtures.

Type of aggregate and optimum husk-asphalt binder content were the same as in Phase 3. Marshall specimens were set into two groups. The first group of specimens was cured in air at room temperature for 24 hr. The second group was cured in a 60°C water bath for 24 hr.

For each aggregate type and husk percent in binder, three specimens were prepared. Therefore, 36 specimens for each group were prepared. Results of the Marshall test, which was performed at 60°C, are presented in Table 8.

Phase 5: Tensile Strength of Husk-Asphalt Mixtures

The objective of this phase was to evaluate quantitatively the effect of husk on the behavior of bituminous mixtures using an indirect tensile test, under dry conditions (normal) and under wet conditions after 10 cycles of freezing and thawing. The test was used to evaluate the mixture's resistance to moisture damage and repeated freeze-thaw-induced damage, specifically low-temperature cracking.

The indirect tensile test involved loading a cylindrical specimen with compressive loads that act parallel and along the vertical diametrical plan. Marshall specimens measuring 4 in. in diameter and 2.5 in. high were used in the study. To distribute the load and maintain a constant loading area, the compressive load was applied through a 0.5-in.-wide steel loading strip that was curved at the interface with the specimen and had a radius equal to that of the specimen. In this study, Marshall apparatus was used to apply load.

The theoretical relationship used in calculating the specimen tensile strength [TS (psi)] is as follows (*16*):

$$TS = 0.156PF/h \quad (1)$$

where PF is total load at failure (lb) and h is height of the specimen (in.).

Type of aggregate, optimum husk-asphalt binder content, and the number of specimens were the same as in Phase 4. Marshall specimens were set into two groups. The first group of specimens was cured in air at room temperature for 10 days. The second group was subjected to 10 cycles of freezing and thawing. They were put in plastic freezing bags, and about 10 mL of water was added to each bag; they were kept in a freezer at −18°C for 16 hr followed by 8 hr of thawing at 25°C (*11*). All specimens were kept at a constant temperature of 25°C for 24 hr before the indirect tensile test, which was performed at 25°C. Results of this phase are presented in Table 9.

TEST RESULTS AND DISCUSSION

In Phase 1, the effect of husk level on the behavior of husk-asphalt binder was evaluated using penetration, softening, and ductility. Results of penetration indicated that the relationship between the logarithm of penetration (log P) and temperature (T) is linear, as shown in Figure 1. That is,

$$\log P = A + BT \quad (2)$$

where A is the constant of the regression line and B indicates the temperature sensitivity of the logarithm of the penetration. Values of A and B as a function of husk level in the husk-asphalt binder are given in Table 10. It can be seen in Table 10 and Figure 1 that penetration increases with increasing husk level up to 10 percent at relatively low-temperature conditions, whereas penetration decreases with increasing husk level up to 10 percent for temperatures higher than 30°C. This result suggests that husk may be used as an additive or softening agent for asphalt. It contributes

TABLE 7 Stripping Resistance of Husk-Asphalt Binders (Results of Phase 3)

Test Type	% Husk	% Asphalt Coating Retained on Aggregate		
		Limestone	Basalt	Granite
Texas Boiling Test	0	95	82	54
	5	95	88	56
	10	97	93	65
	15	99	94	79
Scandinavian Rolling Test	0	78	65	30
	5	82	74	35
	10	90	80	50
	15	93	86	52

TABLE 8 Marshall Stabilities for Husk-Asphalt Mixtures (Results of Phase 4)

Agg. Type	Husk Percent	Marshall Stability (lb)		Index of Retained Marshall Stability (Wet/Dry)
		Dry[a]	Wet[b]	
Limestone	0	3692	2936	0.795
	5	3812	3318	0.870
	10	4088	3589	0.878
	15	3850	3268	0.849
Basalt	0	3660	3360	0.918
	5	3750	3402	0.907
	10	4245	3876	0.892
	15	4222	3695	0.875
Granite	0	3120	2837	0.909
	5	3218	3040	0.945
	10	3225	2877	0.892
	15	3198	2446	0.765

[a] Specimens were cured in air at room temperature for 24hr.
[b] Specimens were cured in a 60°C water bath for 24hr.

TABLE 9 Indirect Tensile Strength at 25°C (Results of Phase 5)

Agg. Type	Husk Percent	Marshall Stability (lb)		Index of Retained Marshall Stability (Wet/Dry)
		Dry[a]	Wet[b]	
Limestone	0	103.60	84.74	0.818
	5	113.51	96.30	0.848
	10	132.20	119.56	0.904
	15	119.30	106.39	0.892
Basalt	0	86.11	73.13	0.849
	5	90.48	77.50	0.857
	10	102.21	89.11	0.872
	15	95.53	82.12	0.860
Granite	0	62.40	50.05	0.802
	5	63.46	51.04	0.804
	10	69.76	58.60	0.840
	15	68.64	54.66	0.796

[a] Specimens were cured in air at room temperature for 11 days and tested at 25°C.
[b] Specimens were subjected to 10 cycles of freeze-thaw and tested at 25°C after 24 hours at 25°C.

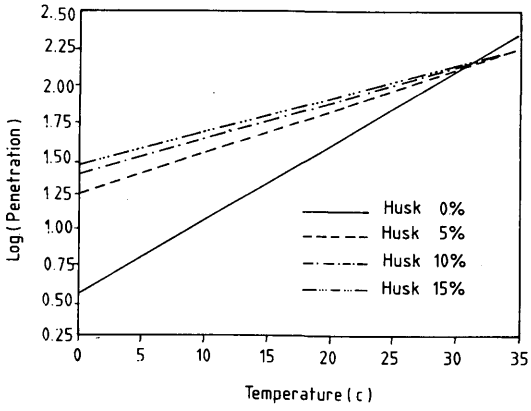

FIGURE 1 Relationship between log (penetration) and temperature at different olive husk levels.

to lower stiffness at relatively low temperatures and higher stiffness at higher temperatures. Moreover, the addition of husk material to asphalt cement reduces the temperature sensitivity of binder (*B* values).

Pfeiffer and Van Doormaal (*17*) defined the penetration index, PI, as

$$PI = (20 - 500B)/(1 + 50B) \quad (3)$$

where B is the temperature sensitivity of the logarithm of the penetration. Values of PI as a function of husk level are included in Table 10. The results presented in Table 10 indicate that penetration index increases with increasing husk level up to 10 percent. Except for the control level (binder with zero husk level), all binders (5, 10, and 15 percent husk levels) exhibit substantially non-Newtonian flow behavior (PI more than +2). Therefore, it can be said that the addition of husk material reduces the brittleness of asphalt cement at low temperatures.

Results of softening point using the ring-and-ball test and ductility test are given in Table 5. Table 5 indicates that there is a slight improvement in softening point associated with higher husk levels. In contrast, a substantial reduction in ductility was associated with higher husk levels. Typical pavement asphalt required a ductility of 1 m or more; therefore, addition of up to 10 percent of husk would not violate the ductility specifications.

In Phase 2, mixes were made with husk-asphalt binder to determine optimum binder content and to evaluate the effect of husk material on mechanical and strength properties of husk asphalt mixtures. For each type of aggregate, asphalt mixtures with zero percent husk represent the control mix. Optimum binder content was computed as the average of values resulting in maximum unit weight, maximum stability, and 4 percent air voids in the total mix. Results of this phase are presented in Table 6.

For each type of aggregate, optimum binder contents as a function of husk level are shown in Figure 2. The results indicate that husk material has a considerable effect in reducing the optimum binder content compared with the pure asphalt binder (binder with zero husk level). As shown in Figure 2, a minimum optimum binder content is achieved at 10 percent husk in the case of limestone aggregate and at 5 percent husk in the case of basalt or granite. However, as indicated in Table 6, maximum stability at optimum binder content is associated with 10 percent husk in all types of aggregate mixtures.

Results of this phase suggest that the addition of husk material not only improves the workability and stability properties of bituminous mixtures but also reduces the optimum binder content. In the case of limestone mixtures with 10 percent husk level, the potential saving in the amount of asphalt was about 15 percent compared with mixtures with 0 percent husk level (pure asphalt binder).

Results of the Texas boiling test and Scandinavian rolling test (Phase 3) are given in Table 7. Stripping resistance increases with the increase in husk level for all types of aggregate. The same trend is observed in the results of both tests. In fact, olive husk has an oily texture and some traces of oils and resins. These chemical components might bring the asphalt to a suitable chemical composition for durability and consequently provide better bonding properties between the binder and aggregate even in the presence of water.

Results of the Marshall immersion test (Phase 4) are presented in Table 8. The retained stability of limestone mixtures increases with the increase in husk level up to 10 percent, that of basalt mixtures slightly decreases with the increase in husk level, and that of granite mixtures slightly increases at 5 percent husk level. Furthermore, for all types of aggregate and husk levels in this study, Marshall immersion results comply with the durability criteria for hot bituminous mixtures (75 percent retained strength is recommended as a criterion in many studies). Therefore, it can be said that the addition of husk material improves bonding properties between the binder and aggregate and results in a high water and temperature resistance. In addition, husk particles constitute part of the mineral aggregate. They fill space and improve the interlocking bond between larger aggregate particles.

TABLE 10 Regression Coefficients and Penetration Index

Husk Percent[a]	Regression Coefficient		Penetration Index
	A	B	
0	0.5346	0.0521	-1.678
5	1.2362	0.0287	+2.320
10	1.4425	0.0229	+3.986
15	1.3754	0.0247	+3.423

[a] Husk Percent by total weight of binder (Husk Plus asphalt).

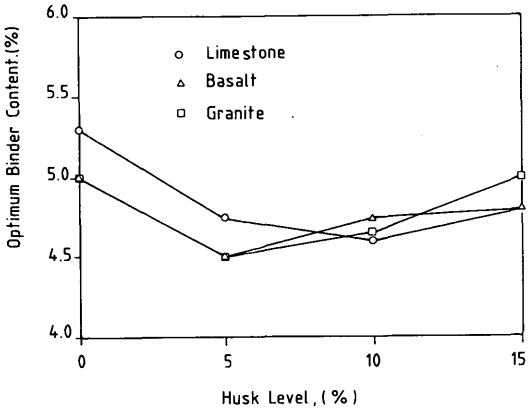

FIGURE 2 Relationship between optimum binder content and olive husk level for limestone, basalt, and granite mixes.

The indirect tensile test results (Phase 5) are presented in Table 9. They indicate that the addition of husk material resulted in a substantial increase in tensile strength up to 10 percent husk and a slight decrease at the 15 percent level. The same trend is observed for the retained tensile strength. These trends are observed for all types of aggregate in this study. For limestone and basalt mixtures, the tensile strength value (Table 9) at 10 percent husk in freeze-thaw conditions is still higher than that for the control mix (0 percent husk level) with no husk in dry conditions.

The results of this phase indicate that husk material has a significant effect in improving a mixture's resistance to moisture damage and repeated freeze-thaw-induced damage, and the beneficial effects were associated with 10 percent husk level in both dry and freeze-thaw conditions.

In summary, results of this study supported the belief that olive husk material has a beneficial role in bituminous technology. The study gave numerical values for husk asphalt binder and mixture characteristics at different husk levels—0, 5, 10, and 15 percent. On the basis of physical test results, the addition of husk material was found to reduce stiffness of binder at low temperatures, improve stiffness at higher temperatures, and reduce the temperature sensitivity of binder. Also, the basic engineering properties of asphalt mixtures were investigated using stripping tests, the Marshall stability test, the Marshall immersion test, and the indirect tensile test under freezing and thawing conditions. The results suggested that the addition of husk material improves stripping resistance, water and temperature damage resistance, freeze-thaw damage resistance, and the strength properties of mixtures. Furthermore, the addition of husk material was found to be effective in improving workability and reducing the optimum binder content. The optimum olive husk level is 10 percent, which fulfills the design criteria of strength, durability, flexibility, and workability of bituminous mixtures made from limestone, basalt, and granite aggregates.

CONCLUSIONS

The study evaluated the effect of olive husk material on binder and bituminous mixtures. On the basis of the results, the following conclusions are drawn:

1. The addition of up to 10 percent olive husk material to asphalt results in an increase in penetration values at low temperatures and a decrease in penetration values at high temperatures. This indicates that olive husk material reduces the binder stiffness at low temperatures and increases the stiffness at high temperatures.
2. The penetration index of husk-asphalt binder increases with the increase in husk level up to 10 percent. This suggests that the addition of olive husk material contributes to reduction in the brittleness and temperature sensitivity of the binder.
3. Slight changes in the ring-and-ball softening point were observed with high husk levels. In contrast, ductility was found to reduce substantially with increase in husk level. Up to 10 percent husk level, ductility values of more than 1 m were found.
4. The addition of olive husk material results in an appreciable improvement in both workability and strength properties. Moreover, the olive husk material reduces the optimum binder content for all types of aggregate mixtures.
5. For all types of aggregate mixtures, stripping resistance was found to increase with increase in olive husk level. This indicates that olive husk material has antistripping characteristics.
6. Similarly, olive husk material improves durability of mixtures. The results of the Marshall immersion test indicated that the retained stability of husk-asphalt limestone mixtures increases with the increase in husk level up to 10 percent, whereas slight changes in the retained stability of basalt and granite mixtures was observed up to 10 percent husk level. However, for all types of aggregate mixtures, the peak values of Marshall immersion stability were observed at 10 percent husk level. These results suggest that the inclusion of olive husk material in bituminous mixtures would reduce the combined damaging effects of water and temperature.
7. In evaluating the effects of olive husk on the mixture's resistance to both moisture and repeated freeze-thaw-induced damage, it was observed that the tensile strength of mixtures increases as the husk level increases, up to a husk level of 10 percent, and then decreases under dry as well as wet conditions after 10 cycles of freezing and thawing. For all types of aggregate mixtures, the same trend was observed for the retained tensile strength.

REFERENCES

1. Rostler, F. S., and R. M. White. Composition and Changes in Composition of Highway Asphalt, 85-100 Penetration Grade. *Proc., Association of Asphalt Paving Technologists,* Vol. 31, 1962, pp. 35–89.
2. Epps, J. A., D. N. Little, R. J. O'Neal, and B. M. Gallaway. Mixture Properties of Recycled Central Plant Materials. *STP 662,* ASTM (L. E. Wood, ed.), Nov. 1978.
3. Noureldin, A. S. *Experimental and Statistical Evaluation and Improvements of Local 60/70 Asphalt Cement.* M.S. thesis. Cairo University, 1982.
4. David, R., and W. Thomas. The Asphalt Model: Results of the SHRP Asphalt Research Program. VTI rapport, 372A, Part 5, Swedish Road and Traffic Research Institute, 1991, pp. 1–13.
5. Epps, J. Asphalt Pavement Modifiers. *Civil Engineering,* ASCE, April 1986, pp. 57–59.
6. Fernando, M. J., and H. R. Guirguis. Natural Rubber for Improved Surfacing. *Proc.,* ARRB, Vol. 12, Part 2, 1984, pp. 121–130.
7. Curtis, C. W., and C. J. Brannan. An Investigation of Asphalt-Aggregate Interactions and Their Sensitivity to Water. VTI rapport, 372A, Part 5, Swedish Road and Traffic Research Institute, 1991, pp. 36–51.
8. Pablo, E. B. Moisture Susceptibility Behavior of Asphalt Concrete and Emulsified Asphalt Mixtures Using the Freeze-Thaw Pedestal Test. In

Transportation Research Record 1228, TRB, National Research Council, Washington, D.C., 1989, pp. 9–16.
9. Puzinauskas, V. P. Filler in Asphalt Mixtures. *Proc.,* Canada Technical Asphalt Association, Vol. 13, 1986.
10. Joseph, C., I. Ilan, and S. Arieh. Some Physico-Chemical Aspects of the Effect and the Role of the Filler in Bituminous Paving Mixtures. *Proc., Association of Asphalt Paving Technologists,* Vol. 47, 1978, pp. 558–588.
11. Al-Masaeid, H., T. Khedaywi, and M. Smadi. Properties of Asphalt-Oil Shale Ash Bituminous Mixtures Under Normal and Freeze-Thaw Conditions. In *Transportation Research Record 1228,* TRB, National Research Council, Washington, D.C., 1989, pp. 54–62.
12. Peltonen, P. *Asphalt Mixtures Modified with Tall Oil Pitches and Cellulose Fibers.* Ph.D. thesis. Technical Research Center of Finland, Espoo, Finland, 1992.
13. *Mix Design Method for Asphalt Concrete and Other Hot-Mix Types.* Asphalt Institute, MS-2, 1976, pp. 17–32.
14. Kennedy, T. W., F. L. Roberts, and K. W. Lee. Evaluating Moisture Susceptibility of Asphalt Mixtures Using the Texas Boiling Test. In *Transportation Research Record 968,* TRB, National Research Council, Washington, D.C., 1984, pp. 45–53.
15. Goode, J. F. Use of the Immersion Compression Test in Evaluation and Designing Bituminous Paving Mixtures. *ASTM SPT 252,* 1959, pp. 113–125.
16. Kandhal, P. S. Evaluation of Sulphur Extended Asphalt Binder in Bituminous Paving Mixtures. *Proc., Association of Asphalt Paving Technologists,* Vol. 51, 1982, pp. 189–221.
17. Pfeiffer, J. P., and P. M. Van Doormaal. The Rheological Properties of Asphalt Bituminous. *J. Inst. Petroleum Technology,* Vol. 22, 1936, pp. 414–440.

Publication of this paper sponsored by Committee on Characteristics of Nonbituminous Components of Bituminous Paving Mixtures.